HEAT TRANSFER INVESTIGATIONS FOR THE FLOW

OF SUPERHEATED STEAM AT VELOCITIES RANGING UP

TO THE SONIC

BY

R.M.G. MEEK B.Sc.

THESIS SUBMITTED TO THE UNIVERSITY OF GLASGOW

FOR THE DEGREE OF DOCTOR OF PHILOSOPHY

1954.

<p style="text-align:center">CONTENTS.</p>

- - - - - - - - - - - - -

INTRODUCTION.

- - - - - - - - - - - - -

PART I - REVIEW OF PREVIOUS WORK.

1. EXPERIMENTAL WORK.

- - - - - - - - - - - -

PART II - AN INVESTIGATION ON THE FLOW OF STEAM

IN A SHORT CONVERGENT DIVERGENT NOZZLE YIELDING

VALUES FOR THE RECOVERY FACTOR AND DATA RELATING

TO THE SUPERSATURATED CONDITION

THE PRELIMINARY INVESTIGATION.

- - - - - - - - - - - - - -

PART III - THE MEASUREMENT OF RECOVERY FACTORS FOR STEAM

FLOWING IN A SIX INCH LONG ANNULAR DUCT

BIBLIOGRAPHY.

APPENDIX.

SUMMARY.

The thesis, together with the introduction, is presented

in four Parts:

    Part I   -   Review of Previous Works.

    Part II   -   An Investigation on the Flow of Steam in a
                  Short Convergent - Divergent Nozzle Yielding
                  Values for the Recovery Factor.

    Part III -   The Measurement of Recovery Factors for Steam
                  Flowing in a Six-inch long Annular Duct.

    Part IV   -   The Measurement of Heat Transfer Coefficients
                  for Flow in an Annular Duct and the Analogy
                  with Friction.

INTRODUCTION.

1. Historical.

The influence of high fluid speeds on convective heat transfer

is a subject of both academic and practical interest, which has increased

in importance with the advent of high speed flight and the development of

the gas turbine.   Typical of the practical aspects of the problem is the

design of oil coolers on aircraft under near sonic speed conditions.

Since an insulated surface in high speed flow assumes a

temperature greater than the surrounding fluid, the normal concept that

the rate of heat transfer is proportional to the difference between the

surface and ambient fluid temperatures becomes absurd.   The failure of

the usual equations when applied to heat transfer in these conditions was

found to be mainly due to the effects of frictional heating.   This

difficulty was overcome by the use of a redefined heat transfer coefficient

based on the difference between the actual wall temperature and an

adiabatic wall temperature.   Theoretical investigations showed that such

a coefficient was independent of the temperature difference and had the same value as that for low velocity flow under similar conditions. The concept of recovery factor was introduced to obtain a relationship between the adiabatic wall temperature and the free stream temperature.

2. Purpose of Present Research Work.

Previous experimental data relating to this field of heat transfer had been gained by the use of air as the working fluid. The decision was taken to explore the possibility of using superheated steam in place of air in the present investigation. The purpose of this was twofold. The considerable expense involved in the compression and drying of the air stream was avoided and secondly it was considered desirable to extend experimental data to a second fluid.

It was also intended to study the effect of frictional heating more fully by keeping the difference between the wall and the stream temperatures small. It was found convenient to study heat transfer under these conditions by observing the heat exchange at the inner surface of an annular duct.

Measurements of recovery factor and friction coefficients were also to be made.

Part I. Review of Previous Work.

1. Experimental Work.

Investigators have carried out experiments for the flow of air through paralled ducts and divergent nozzles at both subsonic and supersonic speeds, over a flat plate placed in a wind tunnel and over the conical head of a flying V-2 rocket. The results of these researches indicate that the modified heat transfer coefficient is independent of the temperature difference, though the temperature differences were so

great in many cases as to obscure the effect of frictional heating.

Measurements of recovery factor have been made in most of the
investigations on heat transfer at high fluid speeds. Values of the
same order as the theoretical were obtained, though slight variations
were sometimes observed, especially in the case of turbulent flow.

Previous attempts to measure the temperature of steam expanding
through nozzles mostly failed, since the importance of frictional heating
was not realised.

2. Theoretical Considerations.

In this section the theoretical analyses are reviewed, starting
from the basic equations for convective heat transfer. The solutions
applicable to high speed flow are emphasised.

A discussion is presented on the influence which the boundary
layer has on heat transfer, an influence which is not always realised
in the examination of experimental data, particularly for starting
regions in pipes.

Part II - The Flow of Steam through a Simple Nozzle.

Preliminary experiments were undertaken to assess the suitability
of steam as the working fluid for such investigations. Steam was
expanded through a simple convergent divergent nozzle, and the temperature
was recorded by thermocouple on the surface of a search tube or probe
constructed of insulating material and placed along the axis of the nozzle.
Recovery factors computed from these observations were those for a laminar
boundary layer which developed along the walls of the nozzle until
recompression. It was found that the temperature recovery in the
boundary layer was similar to that for air. The measured values of r were

somewhat lower than the theoretical, which is unity for superheated
steam, but the variations were not sufficient to justify departure
from the intended programme of research.

Supersaturated Steam.

Values of recovery factor obtained for supersaturated steam of
the first type in these tests were the same as those for superheated
steam, but the presence of water droplets in suspension was found to
cause considerably lower temperatures to be recorded.

Part III - The Measurement of Recovery Factors for Steam
flowing in a Six-inch Long Annular Duct.

In this part of the thesis are described experiments carried
out to obtain values of recovery factor for steam flowing in apparatus
designed for the study of heat transfer.   This consisted of a six-inch
long annular duct .413 in. o.d. and .1875 in. i.d.   The surface
temperature of the inner tube was again recorded when this was constructed
of insulating material.

The recovery factor was again found to be lower than the
theoretical and to be dependent on the superheat.

Part IV - The Measurement of Heat Transfer Coefficients
and the Analogy with Friction.

The heat exchange between the flowing steam and the inner
surface of the annulus was studied by passing air at suitable temperatures
through the inner tube.   The rise in air temperature and the wall
temperature were recorded by thermocouple.   Local heat transfer
coefficients were calculated from these readings and the adiabatic wall
temperature obtained from values of recovery factor known from the results
of the investigation described in Part III.

The effect of flow conditions on heat transfer coefficients were analysed. A laminar boundary layer existed for only a short distance at the entrance of the duct. Thereafter there was a gradual transition to turbulence which occupied a considerable length of the test section. The turbulent boundary layer did not completely fill the cross-section at the exit, and for a short distance before this point, in the mid-stream region, supersonic velocities were attained.

The values of the re-defined heat transfer coefficients were the same as those for low velocity flow under similar conditions. For the turbulent region they were compared with those for the entrance regions of an equivalent pipe. In making the comparison a correction must be applied to allow for the method whereby the heat transfer coefficients for low speed pipe flow are based on the bulk temperature of the fluid instead of the more logical temperature at the axis. Previous investigators had failed to apply this correction when comparing heat transfer results for high speed flow in pipes with data for low velocities. Neglect of this results in apparently low values for the coefficients.

Friction coefficients were computed from observations of the static pressure. These could be compared with the heat transfer coefficients on account of the analogy between momentum and heat transfer. Since the Prandtl number for steam is 1, the simple equation derived by Reynolds was found to hold for sections where the apparent friction coefficients calculated from the pressure distribution were sufficiently near the true values.

It was the original intention to pass into the supersonic field, when the effect of compressibility at high Mach numbers could be studied.

Experimental difficulties, however, precluded the carrying out of this part of the programme. The design of a suitable nozzle to yield shock free expansion for Mach numbers much in excess of unity could not be covered in the time available.

LIST OF ILLUSTRATIONS.

LIST OF TABLES.

APPENDIX.

NOMENCLATURE.

a	Cross-sectional area of stream, ft.^{2}.
A	Surface area for heat transfer, ft.^{2}.
b	Breadth, ft.
c	Circumference or perimeter, ft.
Cp	Specific heat at constant pressure, B.T.U./lb.^{o}F.
Cv	Specific heat at constant volume, B.T.U./lb.^{o}F.
D	Diameter, ft.
f	Coefficient of friction, dimensionless.
F	Frictional force, lb.
g	Acceleration due to gravity, ft./sec.^{2}.
g	Conversion factor, lb.$_m$ ft./lb.$_f$ sec.^{2}.
G	Mass velocity, lb.$_m$/sec.ft.^{2}.
h	Coefficient of heat transfer, B.T.U./hr.ft.^{2} ^{o}F.
H	Enthalpy B.T.U./lb.
J	Mechanical equivalent of heat, 778.26 ft.lb./B.T.U.
k	Thermal conductivity B.T.U./hr.ft.^{o}F.
l, L	Representative linear dimension, ft.
L	Effective beam length, ft.
m	Mass rate of flow, lb.$_m$/sec.
p	Pressure lb./ft.^{2}.
p$_s$	Partial pressure of water vapour lb./ft.^{2}.
q	Rate of heat flow B.T.U./hr.
Q	Heat transferred per lb. of fluid B.T.U./lb.
r	Recovery factor, dimensionless.
r	Radius, ft.

NOMENCLATURE (Contd.)

R   Gas law constant, ft. $lb._f/lb._m$ $^\circ$F abs.

S   Entropy, B.T.U./$^\circ$F.

t   Temperature $^\circ$F.

t*   Reference temperature for property values, $^\circ$F.

T   Absolute temperature, $^\circ$F abs.

u   Internal energy in absence of motion, gravity, electricity, etc., B.T.U./lb.

u   Velocity in direction of x - co-ordinate, ft./sec.

v   Specific volume, $ft.^3/lb._m$

v   Velocity in direction of y co-ordinate, ft./sec.

V   Velocity, ft./sec.

W   Frictional resistance or drag, lb.

x, y, z   Co-ordinates.

x   Distance in direction of flow, ft.

y   Distance from wall, ft.

Greek Letter Symbols.

$\propto$ Radiation absorptivity, dimensionless.

γ Specific weight, $lb._m/ft.^3$

γ Ratio of the specific heats, dimensionless.

δ Thickness of the boundary layer, ft.

δ Pohlhausen's function of the Prandtl Number, dimensionless.

ϵ Radiation emissivity, dimensionless.

ϵ' Effective emissivity, dimensionless.

ϵ Maxwell's constant, dimensionless.

ς Ratio of thermal and flow boundary layer thicknesses.

η Viscosity, poises.

NOMENCLATURE (Contd.)

θ Temperature difference, °F.

θ Temperature ratio, $t_w - t$ $/t_w - t_s$.

λ Thermal conductivity, I.T. calories/sec. cm. °C.

μ Viscosity, lb. sec./ft.^{2}

ν Kinematic viscosity, ft.^{2}/sec.

ρ Density, lb. sec.^{2}/ft.^{4}

σ Surface tension, lb./ft.

τ Time, hr.

τ Shearing stress, lb./ft.^{2}

τ Reciprocal of absolute temperature, °F^{-1}

ϕ Velocity ratio, U_m/U_s

ψ Stream function, ft.^{2}/hr.

ω Supersaturation ratio.

Δt Temperature difference, °F.

$\dfrac{d}{dx}$ Differential operator.

$\dfrac{\partial}{\partial x}$ Partial differential operator.

Dimensionless Groups.

j   Heat transfer factor, $St\,(Pr)^{2/3}$

M   Mach number V/Va

Nu   Nusselt Number hD/k.

Pr   Prandtl number, $C_p\,\mu\,/k$.

Re$_l$ Reynolds number (length), $\rho\,xV/\mu$

Re$_d$ Reynolds number (diameter), $\rho\,DV/\mu$

St   Stanton number, $h/C_p G$.

Subscripts.

a   Acoustic

NOMENCLATURE (Contd.)

a	Air.
ad	Adiabatic.
aw	Adiabatic wall.
b	Boundary between laminar sub-layer and turbulent zone.
B	Bulk.
c	Convective.
e	Equivalent.
e	Natural.
f	Film.
g	Gas.
l	Local.
m	Mean.
m	Minimum area.
m	Maximum velocity.
o	Initial or supply.
o	Free stream.
r	Radiant.
s	At axis or outside the boundary layer.
s	Maximum entropy.
s	At saturation for same temperature.
sat	At saturation for same pressure.
t	Total or stagnation.
w	Wall.
w	Wetted.
1	Inner wall of annulus.
2	Outer wall of annulus.

1. Historical.

It is only within comparatively recent years that attention has been paid to the field of heat transfer at high fluid velocities. The need to explore this field arose with the development of the gas turbine and with the increasing speeds of modern aircraft. In the gas turbine problems arose in the heat exchange between the turbine blades and the working fluid as well as those arising from the high velocity of the gases across the heat exchange surfaces. The surface temperatures of aircraft approaching or exceeding the speed of sound rise to such a degree by the aerodynamic heating effect that cooling has to be provided for the cabin and sometimes for the structural parts. The problem is more acute in the case of rockets and at low altitudes cooling becomes critical. An interesting example of heat transfer at high velocities is the Velox steam boiler. Here the heating surface can be made much smaller by using gas velocities of some hundred feet per second.

As these developments have taken place the problem has been investigated experimentally within the last few years. The number of these investigations has now increased considerably yet so large is the variation of both thermal and hydrodynamic conditions that much more experimental work must yet be undertaken before the effect of all the parameters concerned can be clearly understood

Previous theoretical and experimental investigations for the case of low speed flow resulted in showing that for forced convection,

the heat transfer coefficient when presented in dimensionless form,
e.g. the Nusselt Number, is dependent only on the Reynolds and the
Prandtl numbers.   These terms represent the conditions of the flow
and the properties of the fluid respectively.   The important point
is that the coefficient h is independent of the temperature difference.
Otherwise the coefficient would have no utility and it would not be
practicable to use Newtons Law for the heat transfer calculations.

Failure of the Normal Relationships at High Velocities.

With higher velocities, however, the application of those
relationships becomes distinctly erroneous.   The value of this
coefficient is no longer independent of temperature difference,
particularly for small temperature differences e.g. when heat transfer
is zero (adiabatic flow) the temperature of the surface may be greatly
in excess of the mean temperature of the adjacent stream and the
coefficient in question is therefore zero.   It has been observed that
such frictional heating in air can cause adiabatic surface temperatures
to rise $57°$ F. above the ambient air temperature at flight speeds of
600 m.p.h., and $1940°$F. for 3,600 m.p.h. (from tests on a V-2 rocket).

If the temperature of the wall is increased so as to cause
heat transfer to the fluid, the coefficient becomes greater than zero.
If the wall temperature was decreased sufficiently to invert the
direction of heat transfer but not sufficiently to invert the difference
between wall and mean-stream temperatures, the coefficient would then
become less than zero, which is, of course, absurd.

There are two reasons why the theoretical relationships no

longer hold for high velocity flows:- (a) the properties of the fluid are no longer constant but vary considerably with, and normally to, the direction of flow, and (b) frictional heating has an increasing influence.

As regards (a), the properties of fluids are dependent both on the temperature and the pressure. If the properties are independent of temperature, then it can be deduced from the differential equations controlling fluid flow and heat transfer that the velocity field is not influenced by heat transfer. The development of the boundary layer is then a pure fluid mechanics problem. In most cases the temperature dependency is not so great that it would affect fluid-flow processes decisively. The effect of pressure is most noticeable, in the case of gases, on the density of the fluid. Below a certain velocity, approximately one third the sonic velocity, the pressure dependency of density may be neglected and the value of this property considered constant. It is with the assumptions of constant property values that the theoretical relations have been derived. As soon as the velocities become comparable with the velocity of sound, it can thus be seen that the equations are no longer immediately applicable since the property values can in no way be considered constant. A new dimensionless value appears in the dimensionless equations the Mach number - $M = V_0/V_a$, the ratio of the reference velocity V_0 to the sound velocity V_a. The flow is influenced as soon as M reaches values of 0.6 to 0.7. Also, (b), in the boundary layers the velocities are decreased by shearing stresses. The lost kinetic energy is transformed into heat and this
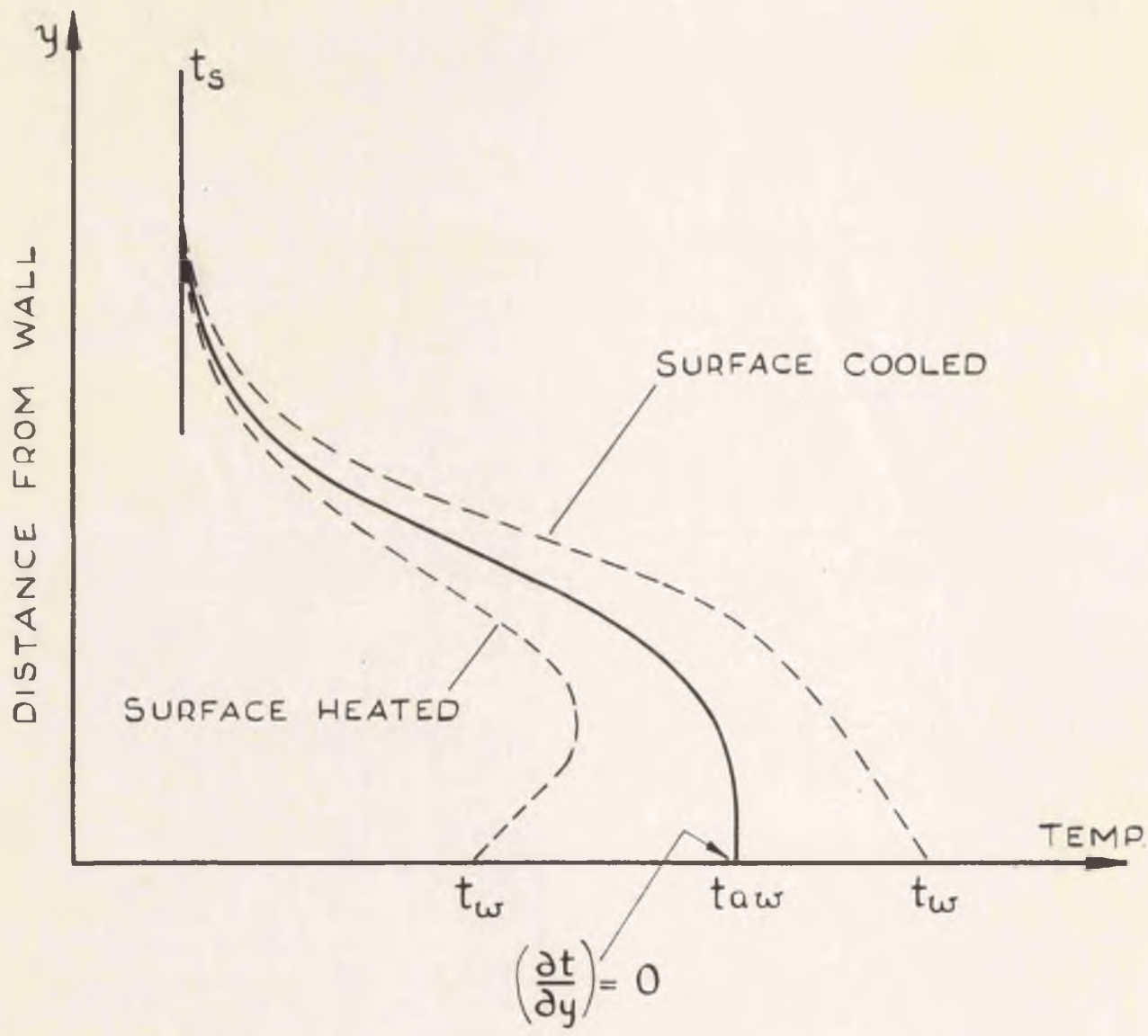
FIG. 1. TEMPERATURE DISTRIBUTION

heat influences the temperature field in the boundary layer and therefore the heat transfer. At low velocities the effect of this heating may be neglected, but cannot be neglected at higher velocities. The dependence of the heat transfer coefficient on temperature difference and Mach number may be demonstrated by dimensional analysis as will be shown later.

The Re-defined Heat Transfer Coefficient.

It is therefore necessary to derive a heat transfer equation in which the temperature potential and heat transfer coefficient are independent of each other. The deduction of such an equation is based on the following considerations. Suppose that a thermally insulated plate is placed parallel to the direction of flow in a high speed fluid stream. The viscous forces cause a flow boundary layer to be built up. The effects of damming, work done by friction, and heat conduction through the fluid tend to create a temperature distribution in the thermal boundary layer. Fig. 1 shows a typical temperature distribution obtained analytically by Pohlhausen for a laminar boundary layer. Since the plate is thermally insulated, the heat transfer at the wall, and therefore the temperature gradient there, is zero. The temperature which the plate, and the fluid in contact with it, assume is designated as the adiabatic surface temperature t_{aw}.

If the plate is heated so that its surface temperature t_w is greater than t_{aw}, then the temperature gradient with respect to the normal is no longer zero and heat is transferred to the fluid. The

converse is true if t_w were less than t_{aw}.   The dotted lines in Fig. 1
indicate the modified temperature distribution under these conditions.

It is therefore postulated that the convective heat transfer
with frictional heating can be expressed as

$$q = hA (t_w - t_{aw})$$

where h is the new coefficient with frictional heating.   Such a
coefficient was first suggested by Brun and Jumpy in 1936, and has been
investigated in several theoretical analyses.   These investigations
showed that h is both independent of the modified temperature potential
and is identical with that for low speeds as evaluated for the same
Reynolds and Prandtl moduli.

The Recovery Factor.

In employing the equation $q = hA (t_w - t_{aw})$, the wall
temperature t_w may be measured while heat transfer takes place.   The
adiabatic wall temperature is, however, unobtainable under these
conditions and it is convenient to express this value in terms of an
obtainable temperature i.e. the stream temperature.   This may usually
be obtained from a knowledge of the initial conditions, the flow
characteristics and the heat transferred.

The adiabatic wall temperature is then expressed in terms of
the free stream temperature and the recovery factor r.   This is
defined as the ratio of the difference between adiabatic wall temperature
and stream temperature to the difference between the total temperature
and stream temperature.   By dimensional analysis it can be shown to be
a function of the Reynolds, Prandtl and Mach numbers.

A knowledge of r is therefore a prerequisite to a determination of the modified temperature potential and is treated independently of the heat transfer.

Again experimental work in the determination of values of recovery factor is inadequate, perhaps even more so than in the case of heat transfer coefficients for high velocities. Especially for turbulent flow, agreement in the values obtained for r is not satisfactory and the Mach number effect in supersonic flows is not yet determined.

2. Purpose of Present Research Work.

Available data referring to heat transfer in this field have
been obtained mostly by aerodynamicists using, of course, air as the
working fluid. The first stage in the present programme of research
comprised an examination of the suitability of superheated steam as a
working fluid in place of air. The need for a high powered compressor
and elaborate equipment for purifying and drying the air is eliminated.
Further, advantages are obtained in the use of a gas having different
property values. The fact that the Prandtl number for steam is unity
for the range of conditions encountered in the tests makes the results
obtained of interest since most of the theoretical solutions for heat
transfer are simplified when the value of this dimensionless group is 1.

When measurements of the recovery factor demonstrated that
superheated steam was a suitable medium, the second stage of the
investigation was undertaken. This comprised the measurement of heat
transfer coefficients and friction factors. The initial superheat was
always sufficiently high to ensure that the steam remained superheated
throughout the expansion.

Investigations of this nature involving high velocities may be
carried out either by studying the flow over a flat plate or body of
revolution or by studying the flow through a tube or duct. To study
heat transfer with flat plate flow involves the use of a wind tunnel,
while the cost of experimenting with flow in a duct is very much less
for similar dimensions of the heat transfer surface. The results of
the latter type of investigation are applicable both to tube flow and

to flat plate flow for low length Reynolds numbers. On account of these considerations and since a laboratory nozzle testing apparatus could readily be adapted for such a purpose, it was decided to carry out experiments on heat transfer for the flow of superheated steam through an annular duct.

At velocities at or near the sonic value, transition from laminar to turbulent flow occurs at a very short distance from the leading edge of a flat plate or from the entrance of a pipe. As the mechanisms of heat transfer for laminar and turbulent flow are quite different, it is necessary to measure coefficients for both conditions separately. Further, the coefficient is dependent on the thickness of the boundary layer, which constantly increases in the entry region of a pipe. It is important therefore that local coefficients of heat transfer be recorded. In many previous investigations mean coefficients have been measured, while in others so-called local coefficients were obtained which were really mean coefficients over a short length. In the present investigation it was found simple to measure true local coefficients. This was facilitated by the arrangement of the apparatus, the heat transfer being studied for the inner surface of the annulus. The growth of the boundary layer along this surface could also be examined.

In most of the previously published experimental work on heat transfer for high speed flow, the temperature differences were relatively large. This means that heat is transferred mainly by the normal means of convection, and frictional heating plays a proportionately small part.

It was intended in the present research to study heat transfer for cases in which a large proportion of the heat involved was caused by friction. This meant abstracting small amounts of heat so that the actual wall temperature did not differ greatly from the "natural" temperature. The temperature profile is then similar to that under adiabatic conditions, whereas, when the temperature difference is large, the profile is not greatly different from that for the case where frictional heating plays no part. Also the use of large temperature differences obscures the dependence of the heat transfer coefficients on the temperature difference, and it is more difficult to determine the reference temperature on which the difference should be based.

As well as measurements of heat transfer coefficients being carried out, values were obtained for the recovery factor and also for friction coefficients, since a close analogy exists between friction and heat transfer. The conditions existing in the expansion of steam in nozzles were also examined and data gained relating to the super-saturated condition.

Work commenced in October, 1950. The investigation described in Part II of the thesis occupied the first year. By then new apparatus had been designed and built and work continued on the measurement of recovery factors, heat transfer coefficients, and friction factors for flow in a parallel annular duct.

PART I

REVIEW OF PREVIOUS WORK.

1. EXPERIMENTAL WORK.

In this section the work of previous investigations on heat transfer at high velocities, recovery factors, and also friction at high fluid speeds is presented.

Also reviewed are various experimental data relevant to the present research. In a discussion on the use of steam as the working fluid, previous attempts at the measurement of the temperature of flowing steam are reviewed, and the properties of steam which enter into heat transfer relationships are considered. Various empirical equations for heat transfer in annuli are presented. There is also a discussion on the temperature at which property values should be evaluated.

Investigations on Heat Transfer at High Velocities.

One of the most comprehensive programmes of research on heat transfer at high velocities has been undertaken at the Massachusetts Institute of Technology, U.S.A. This has been concerned with the transfer of heat to air flowing in tubes. The results of experiments on subsonic flow are presented by McAdams, Nicolai and Keenan (74). Air at sub atmospheric pressures was passed through a tube of 0.281 in. diam. at velocities corresponding to Mach numbers of 0.1 to 1.0. The total length was 127 in. while the heated section at the downstream end was 15 in. long, the flow thus being fully developed while heat transfer takes place.

Heat transfer data showed that the coefficients based on the difference between wall and adiabatic wall temperatures were independent
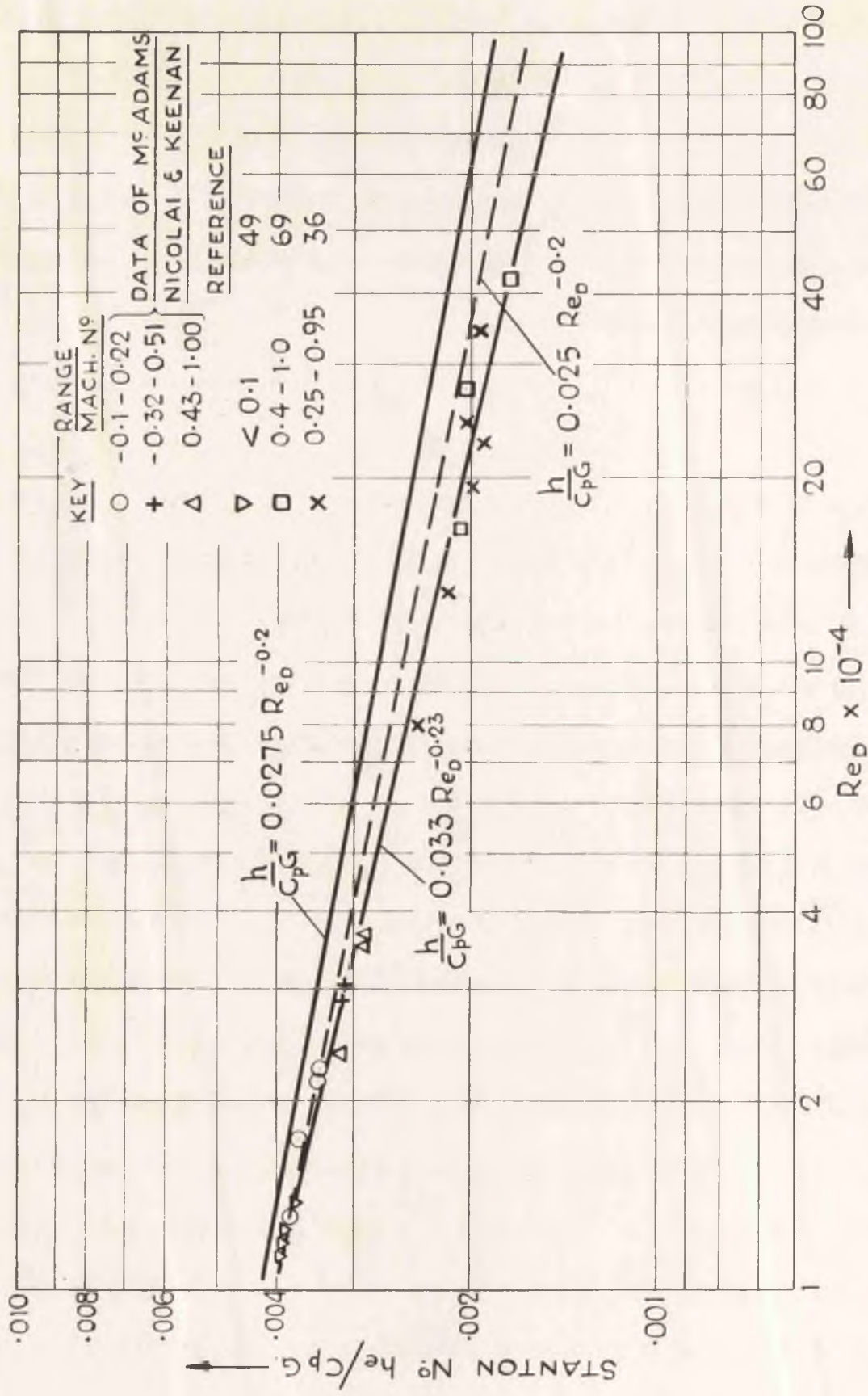
FIG. 2. HEAT TRANFER DATA OF McADAMS NICOLAI AND KEENAN
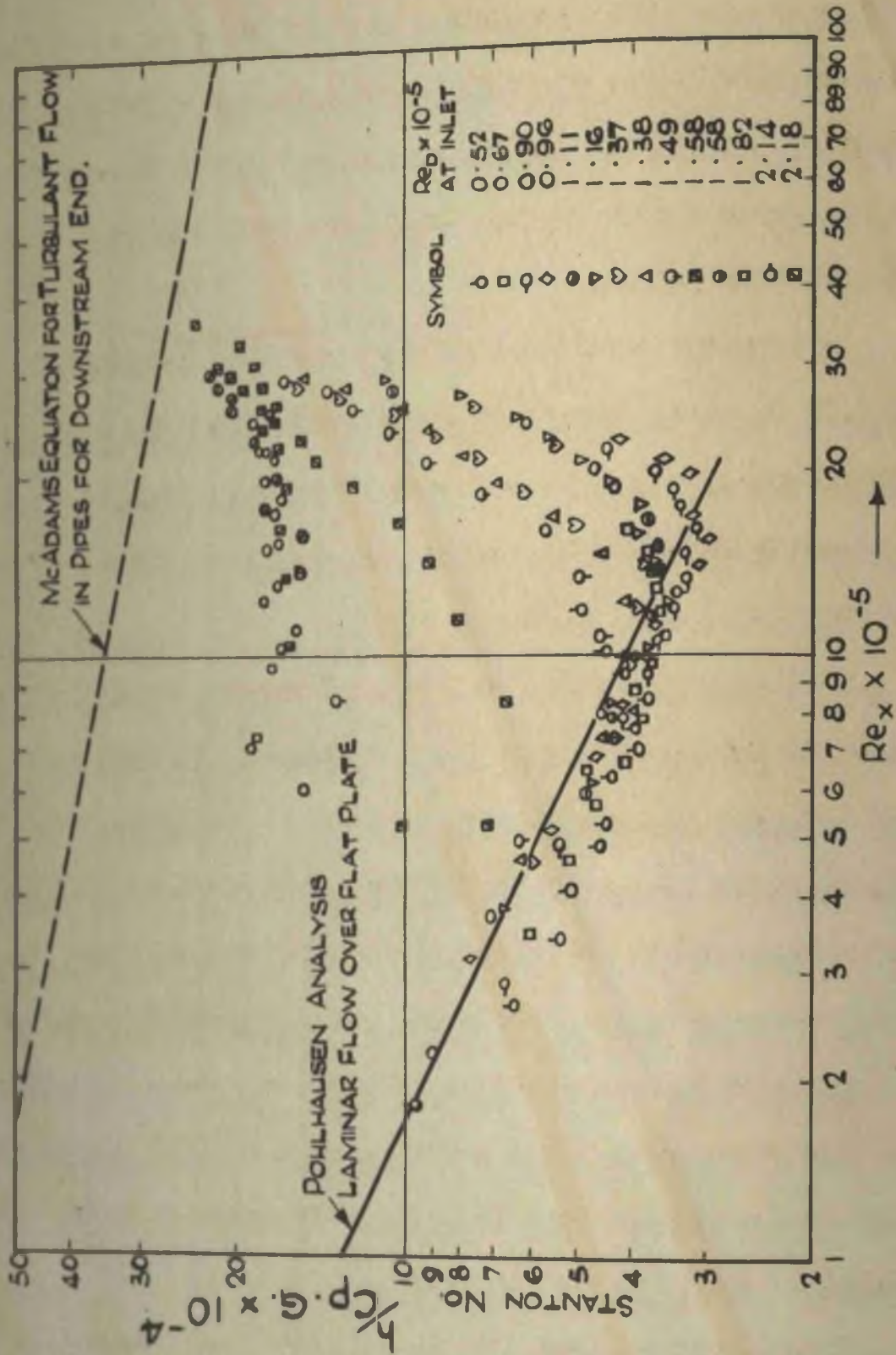
FIG 3. HEAT TRANSFER DATA FOR SUPERSONIC FLOW
OF KAYE, KEENAN AND McADAMS.

Stanton numbers against length Reynolds numbers (Fig. 3). Values of
the upstream portion of the tube agree with values for laminar flow
over a flat plate. The considerable scatter of points corresponding
to turbulent flow in the downstream portion is due to the plotting of
all points on one diagram against the length Reynolds number only,
whereas the coefficients for this region are dependent more on the
diameter Reynolds number.

An improved correlation of the results in the laminar region
was obtained by Brown (8) by introducing corrections for pressure
gradient effects. The corrected data are shown in Fig. 4 and are seen
to lie close to the line representing the Pohlhausen equation for
laminar flow over a flat plate.

The above papers give some idea of the elaborate apparatus
necessary for the preparation of the air stream. As well as a high
capacity compressor, equipment must be provided for purification of
the air, since the properties of the fluid must be known accurately.
Also it is important to reduce the moisture content to a very low value
otherwise condensation shock waves may affect the static pressure.

In these tests heat was added to the air stream by condensing
steam on the outer wall. This ensured a constant wall temperature,
while the amount of heat transferred could be obtained directly from the
measurement of the weight of condensate.

Johnson and Monaghan (46) investigated heat transfer at super-
sonic velocities for flow over a flat plate. At first they introduced
a thin sharp-edged plate into a supersonic wind tunnel, but found
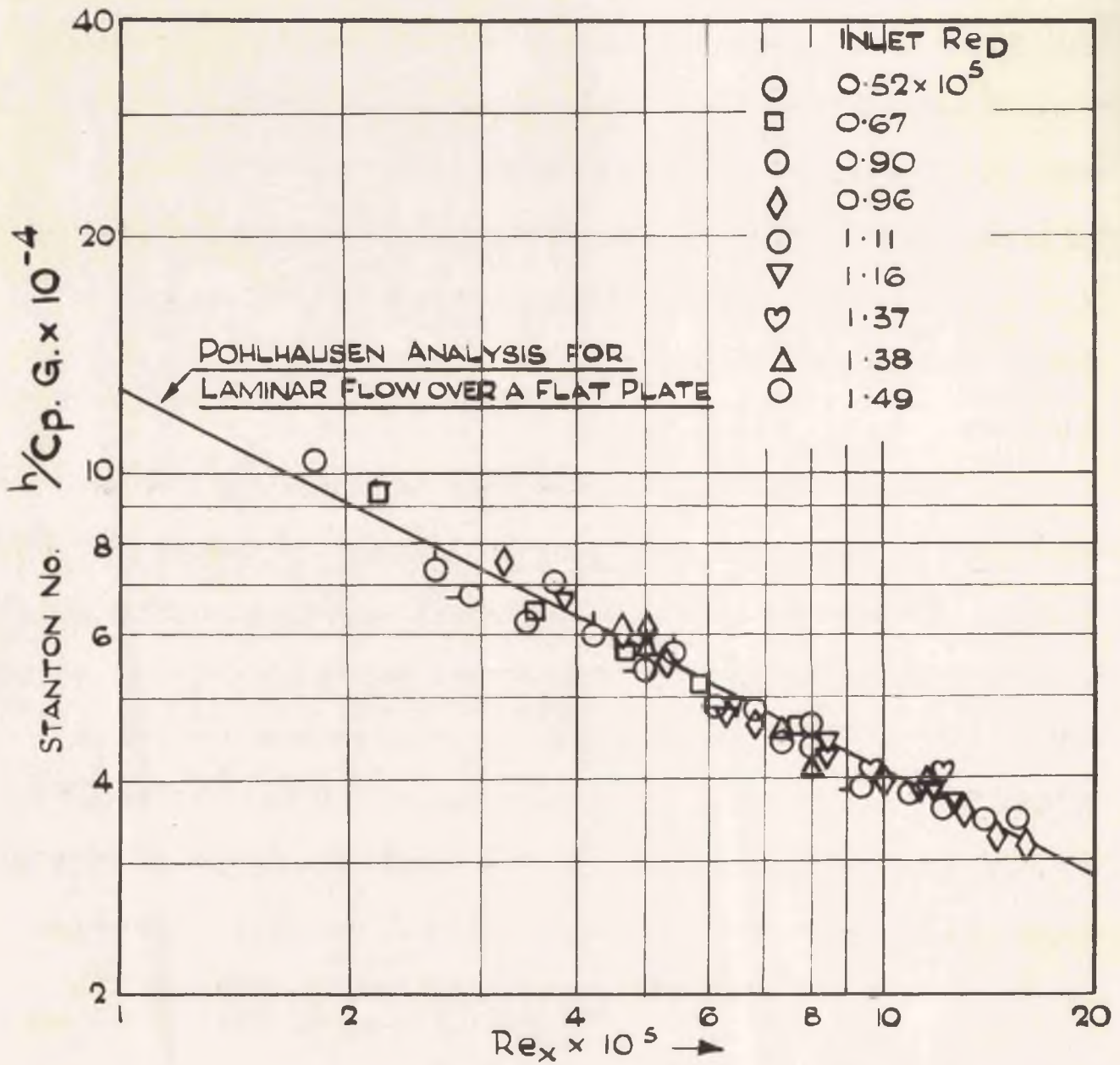
FIG. 4. DATA OF KAYE, KEENAN AND McADAMS
CORRECTED FOR PRESSURE DROP BY BROWN.

difficulty in obtaining a thin enough heater inside the plate. They then used a heated plate forming part of the tunnel wall, and started a new velocity boundary layer at the upstream edge of the plate by means of a suction slot. Their results showed transition taking place at length Reynolds numbers between 4×10^5 and 8×10^5 and the heat transfer values agreed with those deduced from turbulent flow theory using the Prandtl-Karman analogy between heat transfer and skin friction.

A programme of experimental work on heat transfer at supersonic velocities in nozzles and ducts has been initiated at Imperial College, London. Saunders and Calder (89) presented results for heat transfer in water cooled nozzles, using high temperature combustion gases as the working fluid. The total or stagnation temperature of the gases, instead of the adiabatic wall temperature, was employed in calculating the heat transfer coefficients. Little error was introduced by doing so, as the difference between wall temperature and fluid temperature was large. It was found that heat transfer coefficients could be represented by the law.

$$\frac{h}{c_p G} = 0.0285 \ Re^{0.2} \quad \ldots\ldots\ldots\ldots\ldots\ldots(2)$$

which is the theoretical expression for flat plate heat transfer at low velocities derived by Latzko (67, also p 482 reference 45). This law can only be considered approximate since no allowance was made by Latzko for the laminar sub-layer of the turbulent boundary layer. Further, this equation yields the value of the local coefficient, while,

for the first section of the nozzle at least, the mean coefficient
would be observed, which is of higher value than the local coefficient.
That the values obtained corresponded to turbulent flow was surprising
as transition from laminar flow would not be expected for the length
Reynolds numbers. No variation with Mach number was observed.

In the second series of experiments, straight and conical
heated pipes were used, fed with air from a sufficient length of inlet
pipe to establish an equilibrium velocity distribution at the entrance
to the heated section. Heating was obtained by means of an electric
current. In a report by Bialokoz (3) it is stated that heat transfer
coefficients were found to vary with the Mach number to a much larger
extent than had previously been observed, the values being much lower
than those for low velocity flow at the same Reynolds numbers.

Fischer and Norris carried out experiments on the conical
head of a flying V-2 rocket, and obtained values for heat transfer
coefficients at supersonic velocities (31). Values for these
coefficients were found to agree well with values calculated from
formulae for low velocities. For small Reynolds numbers the law for
laminar boundary layers held, whilst at the higher Reynolds numbers
the coefficients corresponded to turbulent flow. The transition from
laminar to turbulent flow was found to depend, however, on some
characteristic other than the Reynolds number. To obtain the adiabatic
wall temperatures necessary to calculate the heat transfer coefficients
allowing for skin friction, Fischer and Norris assumed the values of the
recovery factor to be $\sqrt{Pr}$ for laminar flow and $\sqrt[3]{Pr}$ for turbulent flow.
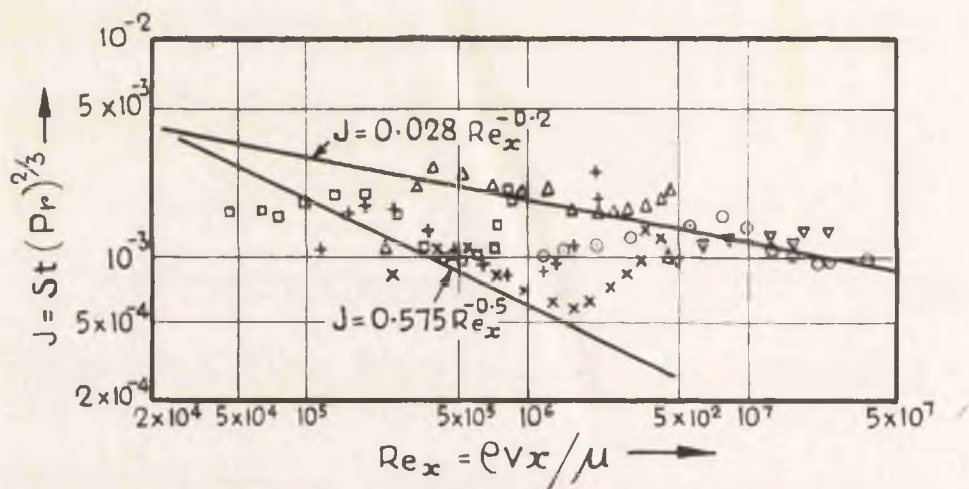
FIG. 5. HEAT TRANSFER MEASUREMENTS BY
FISCHER AND NORRIS ON A V-2 ROCKET

Fig. 5 shows the results of those experiments compared with the values obtained for formulae for low velocities.

The investigations of Joukowsky (49), Lelchuck (69) and Guchman, Iljuchin, Taasowa and Warschawksi (36) carried out in the U.S.S.R. may also be mentioned. These, however, had such large temperature differences that the effect of frictional heating could be neglected. Hot air flowed at super-atmospheric pressure inside a water cooled tube. McAdams, Nicolai & Keenan used this data to extend the conclusions of their own work on subsonic flow of air to higher Reynolds numbers and temperature differences and arrived at the equation

$$\frac{h}{c_p G} = 0.033 \left(\frac{DG}{\mu_m} \right)^{-0.23} \quad \ldots\ldots\ldots\ldots(3)$$

These data are also shown in Fig. 2 where the full line represents equation 3.

Humble, Lowdermilk and Grele (43) carried out similar experiments with air flowing in electrically heated tubes. Data were obtained for a range of Reynolds numbers from 1×10^3 to 5×10^5 and tube-exit Mach numbers up to about 1·1. Again large temperature differences were employed, with average surface temperatures of up to $2060^\circ R$, so that the total temperature instead of the adiabatic wall temperature was used in the calculations. The authors found the results agreed closely with the formulae for low velocities when the Nusselt, Reynolds and Prandtl numbers were defined as follows:-

$$Nu = \frac{hD}{k_w} \; ; \quad Re = \frac{\rho_w V_b D}{u_w} \; ; \quad Pr = \frac{C_p u_w}{k_w}$$

The subscripts w and b refer to air properties evaluated at the wall temperature and the bulk temperature respectively.

The problems of heat transfer at high velocities arising in the cooling of gas turbine blades are dealt with in reference (24) by Eckert.

It can be concluded from the foregoing review that the theoretical deduction that the coefficient of heat transfer at high velocities should be based on the temperature difference defined as that between the actual wall and the adiabatic wall temperatures is confirmed by the experimental evidence. The temperature potential and the heat transfer coefficient are then independent of each other, though in many of the investigations the temperature differences were so great that the effect of frictional heating could be neglected. The values obtained for this coefficient were substantially the same as that for low velocity flow under similar conditions.

Investigations on the Recovery Factor.

Measurements of recovery factor were made in most of the investigations mentioned above. In the investigation at M.I.T., this was accomplished by carrying out runs under adiabatic conditions. In the case of the supersonic experiments, the test section for this purpose was constructed of the insulating material lucite in order to ensure no heat transfer took place.

For subsonic flows, McAdam, Nicolai and Keenan found r to be
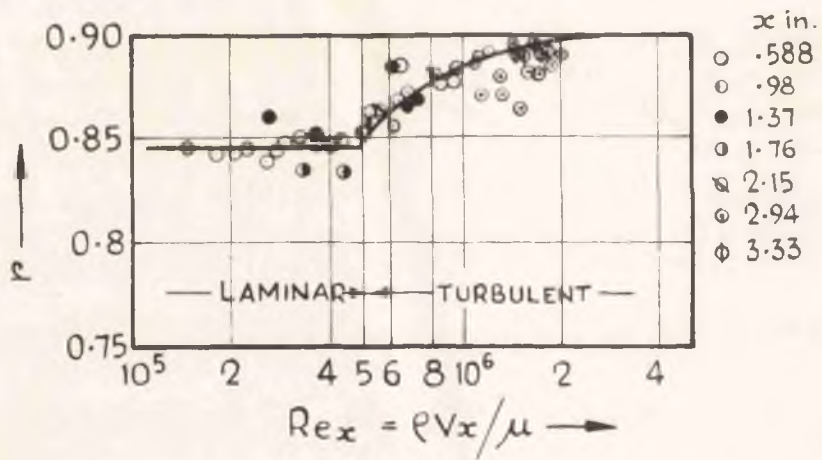
FIG. 6. RECOVERY FACTORS MEASURED

BY ECKERT AND WEISE

substantially independent of Mach number in the range 0.2 to 1 and to vary from 0.875 to 0.901 (the square and the cube root of the Prandtl number for air are 0.86 and 0.904 respectively).

Recent reports (55, 52 and 53) of progress in the investigation for supersonic flow state that values for the recovery factor in the laminar region agree well with theoretical values for flat plate flow. In the turbulent region agreement is not so good, no doubt due to the fact that with the thickening of the boundary layer, the simple flat plate theory can no longer hold, while the velocity profile is not fully developed and pipe flow formulae cannot be applied.

In the investigation by Bialokoz (3) for turbulent flow in conical pipes for Mach numbers greater than 1, values for the recovery factor were found to be closer to the value $(Pr)^{\frac{1}{2}}$ than to $(Pr)^{\frac{1}{3}}$.

As well as those found in the investigations on heat transfer coefficients mentioned above, measurements of recovery factor have also been made separately. Eckert and Weise (26, 27) experimented with flow over flat plates and axial flow along cylindrical probes. Fig. 6 shows results obtained from experiments with the cylindrical probe in subsonic and supersonic nozzles. This shows r to be 0.85 for laminar and increasing to 0.90 for turbulent flow, corresponding to $(Pr)^{\frac{1}{2}}$ and $(Pr)^{\frac{1}{3}}$ respectively. In these tests the probe was constructed entirely of metal. In view of the resulting conduction of heat along the length, it is doubtful if the temperature could be regarded as the true adiabatic wall temperature.

Hilton (41) measured the surface temperature on a flat plate
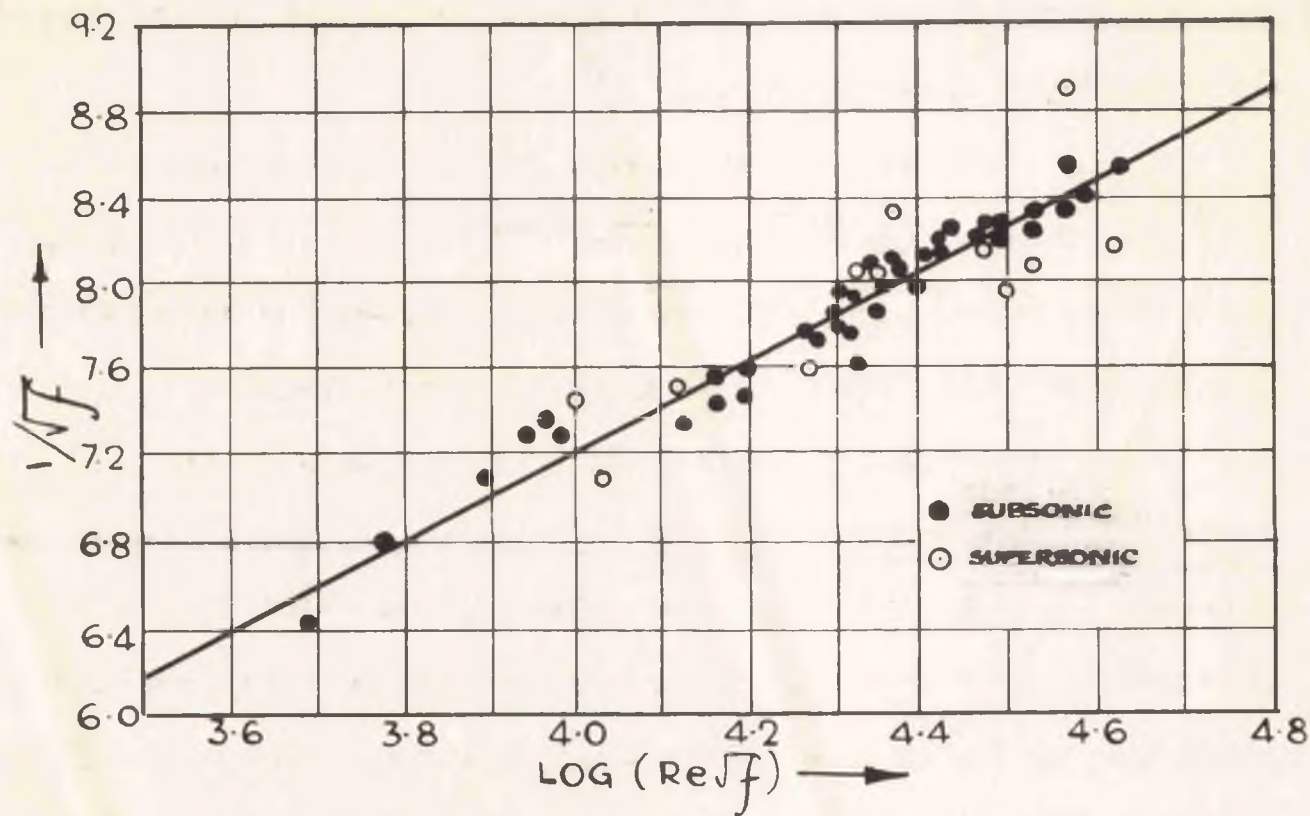
FIG.7   FRICTION COEFFICIENTS MEASURED
BY FROSSEL

constructed of Tufnol, a poorly conducting material, placed in a wind
tunnel and verified the equation giving r as the square root of the
Prandtl modulus for subsonic laminar flow.

At supersonic velocities this value has also been substantiated
somewhat by the data of Eber (23) who performed experiments for flow in
the transition region over cones.

For turbulent boundary layers, Hilton obtained values near
$(Pr)^{\frac{1}{3}}$ for subsonic velocities. Kraus (65) however reported values
about 7% higher for supersonic velocities, suggesting a Mach number
effect as well as Reynolds and Prandtl moduli dependence.

In conclusion, therefore, for laminar subsonic flow experimental
results appear to indicate $r = (Pr)^{\frac{1}{2}}$ but there is considerable variation
in values for turbulent flow. The effect of compressibility is also
yet uncertain. Thus in reference (54) the authors attributed low
values of r to the varying Mach number, while Kraus (65) suggested high
values of r were owing to a Mach number effect. The need for further
research is therefore apparent.

Investigations on Friction at High Velocities.

In 1936 Frossel (32) published the first extensive measurements
of friction coefficients for the flow of air through a smooth tube with
velocities above and below the velocity of sound. These indicated that
the computed mean coefficients are the same as for an incompressible
fluid with the corresponding Reynolds number. Fig. 7 shows Frossel's
results. In the case of the supersonic region, the accuracy of these
results must be called in question. As far as can be ascertained

suitable nozzles to develop shock-free expansion were not developed, while the existence of an oblique shock would considerably affect the results obtained.

Keenan (58) investigated friction for flow of steam at subsonic velocities. This confirmed that the coefficients correspond to those for incompressible flow for the same Reynolds number. Further experiments confirming this were carried out by Iljuchin (44) and Humble, Lowdermilk and Grele (43). Keenan and Neumann (60) published results of measurements of friction in a pipe for subsonic and supersonic flow of air. For subsonic flow the conclusions were confirmed, that for large values of L/D the apparent friction coefficient is essentially independent of Mach number and is the same function of Reynolds number as the friction factor for incompressible fluids.

For supersonic flow, the investigation indicated that the apparent friction coefficient is a function of L/D as well as Reynolds number over the attainable range of L/D, and that the effect of Mach number is to limit the range of values of L/D. The Authors suggested that incompressible values of f are reached for L/D $\geqslant$ 50, and that at low Mach numbers, the Mach number effects are negligible. Friction for supersonic air flows in tubes was further investigated at M.I.T., together with the measurement of recovery factors and heat transfer coefficients and the results published in references 52, 53, 54 and 55. In these papers, the friction coefficients are shown to be dependent on the growth of the boundary layer and on the transition from laminar flow

to turbulent flow. The value was found to correspond to that for flow over a flat plate, the agreement being best in the laminar range. In references 55 and 52 the results were based on a one-dimensional flow model, while in reference 53 a simple two-dimensional flow model was employed, whereby the boundary layer and the unaffected core were treated separately. The results of previous tests were recalculated following this method and plotted versus the length Reynolds number. The points were found to lie close to the lines representing the boundary layer equations for incompressible flow past a flat plate.

The Use of Steam as the Working Fluid in
Investigations on Heat Transfer at High Velocities.

All the experimental results mentioned in the foregoing review have been obtained using air as the working fluid - largely because air is the medium in which frictional heating has the greatest application, viz. high speed flight.

It was considered that by the use of superheated steam instead of air as the working fluid an experimental investigation could be simplified. The need for elaborate equipment for purification and the removal of moisture is avoided. Steam can be readily supplied and there is no need for a compressor of high capacity as used in the experiments with air. The measurement of the mass flow of steam is easy and absolute since the exhaust can be condensed and the condensate weighed directly.

The physical properties of steam are well established. An interesting property is that the Prandtl number for moderate pressures and temperatures is substantially unity. This is of much importance in a fundamental investigation on heat transfer as the Prandtl number has a large bearing on the process of heat transfer.

The results of a previous investigation (92) on supersaturation in nozzle flow however raised doubts as to the validity of the normal recovery factor for steam. Since the ability to measure the adiabatic wall temperature and so obtain recovery factors is a prerequisite to the measurement of heat transfer at high velocities, it is necessary to examine the problem more closely. In the light of the present

programme of research the results of previous attempts to measure
steam temperatures attain a new significance.   A review is therefore
given here.

Steam Temperature Measurements.

Attempts made to measure the temperature of steam expanding
through nozzles mostly failed in that the importance of frictional
heating was not realised.   Because of this Stodola stated that "no
method is known that will determine the true temperature in flowing
fluids" (reference 93 p.73).

Many of these investigations were concerned with the
supersaturated state of steam and with the measurement of temperatures
below that of saturation.

Batho (2) attempted to measure the temperature of initially
dry saturated steam expanding through a De Laval nozzle by means of a
movable thermocouple with the wires stretched along the nozzle axis.
The majority of his searches produced temperatures greater than the
expected (saturation) temperatures, although in one case temperatures
lower than the saturation values were recorded.

Martin (70) recorded temperature measurements with an ordinary
mercury thermometer shielded by hygroscopic substances fitted at the
exhaust flange of a steam turbine.   These temperatures were lower than
the saturation values, in some cases by as much as 10°F.

Stodola (p.73 reference 93) recorded temperatures indicated by
a thermocouple stretched along the axis of a nozzle.   With steam
remaining superheated throughout the expansion, and a total adiabatic

temperature drop of about 100°F., he recorded a temperature almost constant and equal to the supply temperature along the nozzle axis. This he attributed to the result of friction. With greater expansions the recorded temperature tended to fall slightly along the length and he obtained curves of measured temperature and calculated steam temperature which exhibit similar characteristics to those obtained in the present investigation (e.g. Fig. 23).

The experimental results of Muller (78) are even more revealing. He obtained characteristics similar to those of Stodola, and found an unstable temperature variation after the point of expansion where condensation was estimated to occur. He also made a device which consisted of a magnesia search tube containing thermocouple wires able to be moved along the nozzle axis as desired. With initially dry saturated steam he obtained temperatures which compared closely with the saturated temperatures, being sometimes above and sometimes below these values. He then measured the outlet steam temperature with this thermocouple and compared them with the expected outlet temperature which was judged to be about 100°F. below the supply temperature. He found that, as soon as the initial state was increased above the dry condition, the final temperature jumped from near the saturation value to only 30°F. below the supply temperature. As the supply temperature was raised further the final temperature rose also, tending to become closer to the initial temperature as it was increased.

Sorour (92) in attempting to measure the temperature of steam expanding in the supersaturated region, used a temperature measuring

device shown in detail in Fig. 13a and described later. In an extensive series of tests he obtained at certain points of the expansion temperatures varying from 2°F. to 15°F. below the saturation values corresponding to the pressure.

When these tests were carried out it was thought necessary to explain why the readings were so much higher than the estimated steam temperature. The reason commonly given was that condensation took place on the surface of the temperature measuring device and that the saturation temperature was recorded. So long, however, as condensation is absent, any temperature measuring device inserted into a high speed steam flow will register a temperature near the total or stagnation temperature, a temperature recovery factor of approximately unity being expected for a gas. It is then necessary to explain why low temperatures were recorded in many of these investigations. That these were owing to the presence of water droplets will be demonstrated later.

The results of measurements of temperature in the high velocity flow of steam were published recently by Murdoch and Fioch (79). The investigation was concerned with the design of suitable temperature measuring devices for industrial applications. Here the total temperature is required, so the sensing element was placed in a suitable well surrounded by almost stagnant steam. Recovery factors for the most satisfactory of these devices were of the order of 0.9. Instruments similar to the cup type for total temperature measurement, but not suitable for industrial use, gave a recovery factor equal to 1. Unity would also be expected for r since Pr $=$ 1. Low values may have been

owing to conduction effects.

A preliminary investigation which was undertaken to clarify the position as to steam temperature measurement is described in Part 11 of the thesis.

The Properties of Steam - particularly the Prandtl Number.

Water and water vapour are perhaps more commonly employed in engineering and experimental work and the properties known with precision over a wider range than any other substance. These properties have been tabulated in detail in steam tables.

Yet the true value of the Prandtl number has long remained in doubt, and the assumptions made as to this have been many and varied. This dimensionless number is composed of the properties c_p, μ and k and it is a basic function in the determination of heat transfer by convection.

McAdams (72) gives the value of Pr for steam as 0.78. This value is due to Eucken, who developed it from Maxwell's theoretical work on gases.

Maxwell (71) found that the thermal conductivity of any gas was related to the viscosity and specific heat by the equation

$$k = \epsilon \, c_v / \mu \quad \dots \dots \dots \dots \dots \dots \dots (4)$$

where ϵ is a constant for any one gas. He predicted a value of 2.5 for ϵ, which has been found to be nearly correct for monatomic gases. For diatomic gases ϵ is about 1.90 and for triatomic gases 1.72. Eucken (30) suggested the emperical velation

$$\epsilon = 0.25 \, (9 \gamma - 5) \dots \dots \dots \dots \dots \dots (5)$$

where γ is the ratio of specific heats. By substituting in equation

4, the Prandtl number can be obtained in terms of the adiabatic index.

$$\frac{c_p \mu}{k} = \frac{6}{9 - 5/\gamma} \qquad \dots\dots\dots\dots\dots(6)$$

If the value of γ for steam is taken as $1\cdot3$, then $Pr = 0.78$.

The true value of the Prandtl number to be employed in heat transfer equations, must be obtained from the values of the component properties. The experimental difficulties in measuring the viscosity μ and the thermal conductivity k are, however, great. On account of these difficulties the value of Pr computed in this way was not accepted as reliable and the lower value of 0.78 was assumed in the development of heat transfer equations.

Later and reliable measurements of viscosity and thermal conductivity confirmed, however, that the true value of the Prandtl number is nearly unity for low pressures.

For viscosity the values of Hawkins, Solberg and Potter (39) as given by Leib (68) are recommended as being the most accurate. Keyes (62) derived equations to represent these data. These are

$$10^4 \, (\eta \text{ poises}) = 10^4 \left[\eta_0 + \tau_p (6.364 - 2.307.10^{-3} \times 10^{1340}) + (3.89.10^{-2} \times p^2.10^{-5.476.10^{-3}} T) \right] \dots\dots(7)$$

$$10^4 \, (\eta_0 \text{ poises}) = 0.1501 \, \sqrt{T}/(1 + 444.7)$$

η is in kg. per cm^2 $\qquad \tau = T^{-1} = (273.16 + t^{\circ}C)^{-1}$

η_0 - viscosity at zero pressure.

These data have been incorporated into Table 6 of the 21st printing (1950) of Thermodynamic Properties of Steam (59).
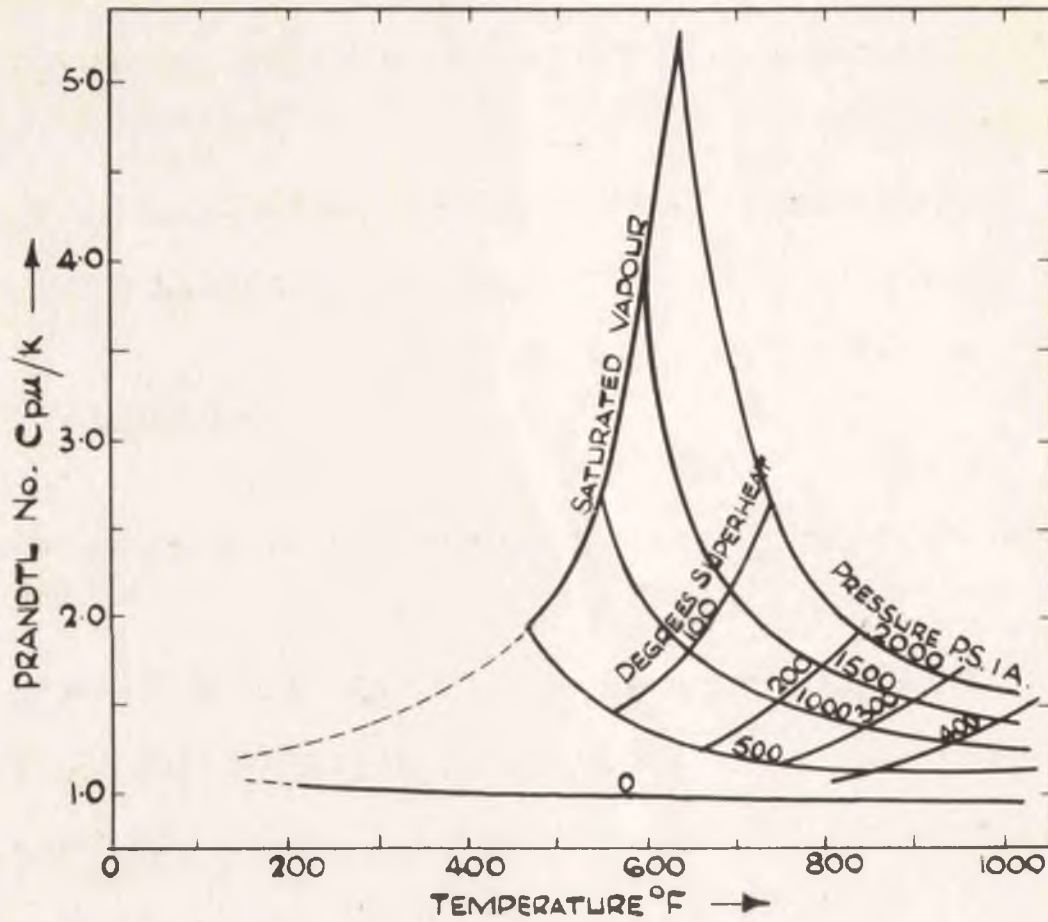
FIG. 8. VARIATION OF PRANDTL NUMBER WITH
PRESSURE AND TEMPERATURE.

These values were employed in the calculation of Reynolds numbers in analysing the results of the present investigation. A chart was drawn of viscosity versus temperature for various pressures, and the viscosity could easily be picked off for the appropriate conditions.

The latest measurements of heat conductivity are those of Keyes and Sandell (63). The results can be represented by

$$10^5 \lambda_o = 1.3456 \sqrt{T}/(1 + 1737.3 \tau/10^{12\tau})$$

$$\ldots\ldots\ldots\ldots\ldots(8)$$

$$10^5 \lambda = 10^5 \lambda_o + 1.096 (10^{0.934.10^9 T^4 p} -1)$$

p is in atmospheres, λ in I.T. calories per sec. per cm. per °C.

λ_o = conductivity at zero pressure.

From these data, Keyes (62) showed that the "Maxwell Constant" ϵ for near zero pressure for steam is of the order of 1.2 and independent of temperature. Using this value and substituting in equation 4, and taking $\gamma = 1.3$, the Prandtl number is obtained as $c_p u/k = 1.08$.

In fact the Prandtl number varies from 1.06 to 1.08 for zero pressure. This was substantially the case for the conditions under which the present investigation was carried out, and for the range of temperatures encountered Pr could be taken as 1.06.

In Fig. 8 is shown the variation of Pr with temperature and pressure as presented by Rubin (88). For high pressures it is seen that the variation with temperature is much greater than at low pressures.

When new determinations of thermodynamic properties are made
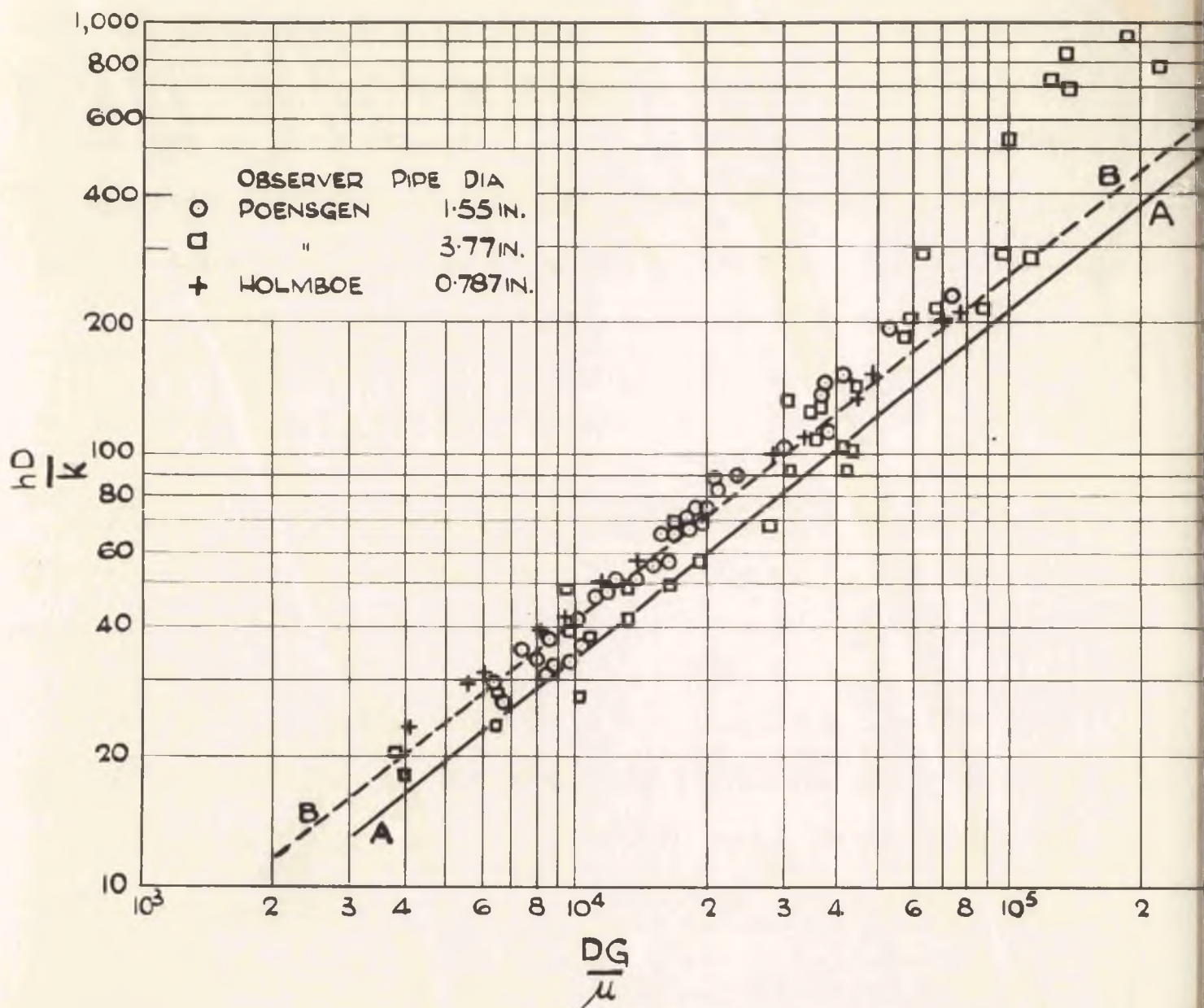
FIG. 9. DATA ON COOLING OF SUPERHEATED STEAM COMPARED WITH MᶜADAMS EQUATION WHEN Pr = 0·78 AND 1·06.

available, they cannot be used in conjunction with the heat transfer relationships and equations made prior to the existence of the new data. Previous results should be recorrelated using the new physical properties and a new equation obtained.   An interesting result of the new value of Prandtl number is in the revised interpretation of Poensgen's and Holmboe's data on superheated steam.   Fig. 9 is a reproduction of Fig. 77 of reference 72 showing values obtained by these observers.   Line AA is equation 4i of that reference

$$\frac{hD}{k} = 0.021 \left(\frac{DG}{\mu} \right)^{0.8} \qquad \dots\dots\dots\dots\dots(9)$$

This equation is obtained by assuming that $c_p \mu / k = 0.78$ and substituting in the McAdams equation for pipe flow

$$\frac{hD}{k} = 0.023 \left(\frac{DG}{\mu} \right)^{0.8} \left(\frac{c_p \mu}{k} \right)^{0.4} \qquad \dots\dots\dots\dots(10)$$

Line BB on the same figure is obtained by substituting $c_p \mu / k = 1.06$ in this same equation.   It can be seen that the points on the graph follow this equation more closely than that corresponding to Line AA.

Heat Transfer in Annuli.

The cylindrical tube is the most convenient for theoretical treatment. For other shapes the calculations become difficult. To evade such difficulties the concept of an equivalent circular tube is used i.e. a tube which would represent the same resistance against flow or would secure the same heat transfer as the duct actually used under comparable conditions. The diameter of such a tube is termed the equivalent diameter De. This is usually defined by

$$De = \frac{4a}{C} \quad \dots\dots\dots\dots\dots\dots\dots\dots\dots\dots\dots\dots(11)$$

where a is the cross-sectional area and c the perimeter of the cross-section. Equal values of this ratio ensure dynamical similarity since this represents the ratio of inertia forces which are proportional to a and frictional forces which are proportional to c. For a circular tube of diameter D, according to the above definition, De = D.

The above reasoning holds when evaluating the pressure drop, but because of the existing similarity between momentum transfer and heat transfer, it is also used in problems of heat transfer by convection.

For an annulus, the above formula for equivalent diameter gives De = D_2 - D_1 where D_2 and D_1 are the outer and inner diameters respectively. The generally accepted equation for heat transfer in a circular tube for fully developed turbulent flow is of the form

$$\frac{hD}{k} = a \left(\frac{DG}{\mu} \right)^n \cdot \left(\frac{c_p \mu}{k} \right)^m \quad \dots\dots\dots\dots(12)$$

For an annulus, h would then be found by substituting De = D_2 - D_1 for

D in this equation. A difference is often made between the heated and unheated part of the circumference when evaluating the equivalent diameter. The value of C is restricted to the portion through which heat is transferred. It has been found, however, that to use the wetted part of the circumference C_w usually gives better results than the use of the heated part C_h when these are not the same.

Besides the equations obtained by straight substitution of De in the normal formulae for circular tubes, a number of more complicated formulae have been presented in the literature. These have been based on experimental data covering limited ranges of test conditions and are of many forms relating individual coefficients to fluid properties and apparatus dimensions.

For turbulent flow, Monrad and Pelton (77) obtained from experiments the emperical equation

$$\frac{h_1 D_e}{k} = 0.020 \left(\frac{\rho V D_e}{\mu}\right)^{0.8} \left(\frac{c_p \mu}{k}\right)^{1/3} \left(\frac{D_2}{D_1}\right)^{0.53} \quad \ldots\ldots\ldots(13)$$

where h_1 is the coefficient of heat transfer for the inner surface of the annulus.

Davis (20) represented the experimental results of different investigators in the form

$$\frac{h_1 D_1}{k} = 0.031 \left(\frac{\rho V D_1}{\mu}\right)^{0.8} \left(\frac{c_p \mu}{k}\right)^{1/3} \left(\frac{\mu}{\mu_1}\right)^{0.14} \left(\frac{D_2}{D_1}\right)^{0.15} \quad \ldots\ldots(14)$$

(The constant is erroneously printed as 0.038 in the original paper.) μ_1 is taken at the temperature of the surface 1.

It can be seen that for small values of D_2/D_1, Davis' formula gives higher values of h_1 than Monrad and Pelton's formula and vice

versa for large values of D_2/D_1.

Wiegand (96) recommended the correlation for the inner wall:-

$$\frac{h_i D_e}{k} = 0.023 \left(\frac{\rho V D_e}{\mu_f}\right)^{0.8} \left(\frac{c_p \mu}{k}\right)_f^{1/3} \left(\frac{D_2}{D_1}\right)^{0.45} \qquad \ldots\ldots\ldots\ldots(15)$$

where the subscript f refers to the film temperature.

Mizushina (76), in discussing the analogy between fluid friction and heat transfer in annuli, points out the considerable variation in value of the heat transfer coefficient obtained from these and similar equations, all the values being higher than his own experimental values for air. From the analogy between heat transfer and friction he obtained a semi-theoretical equation which correlated his data for air and agreed with Monrad and Pelton's equation for higher values of Prandtl number.

Since the values of heat transfer coefficient from these specialised formulae differ considerably, it would appear best to follow the procedure of substituting the equivalent diameter in the usual equations for cylindrical tubes. Carpenter, Colburn, Schoenborn and Wurster (11) obtained data which at high Reynolds numbers approached correlation of results for circular tubes. They obtained the equation

$$\frac{h D_e}{k} = 0.023 \left(\frac{\rho V D_e}{\mu}\right)^{0.8} \left(\frac{c_p \mu}{k}\right)^{1/3} \left(\frac{\mu}{\mu_w}\right)^{0.14} \qquad \ldots\ldots(16)$$

Further support for the use of De is given by the results of reference 16 for rectangular passages.

An investigation of considerable interest on account of the

similarity of the conditions to those in the experiments described
in the thesis is that of McAdams, Kennel and Addoms (73). Local
coefficients of heat transfer from a 12 in. length of 0.252 in.
tubing to steam flowing upward in a vertical annulus were measured
for high pressures and temperatures.

The correlation involving local coefficients at four
different values of L/D_e is given by

$$\frac{h D_e}{k} = 0.0126 \left(\frac{\rho V D_e}{\mu_f}\right)^{0.89} \left(\frac{c_p \mu}{k}\right)^{1/3}_f \left(\frac{D_e}{L}\right)^{0.13} \quad \ldots\ldots\ldots(17)$$

The physical properties are all evaluated at the film temperature.
When new data on the thermal conductivity of steam became available,
the calculations were revised and an improved correlation obtained.
The final equation is:-

$$\frac{h D_e}{k} = 0.0214 \left(1 + \frac{2.3}{L/D_e}\right) \left(\frac{\rho V D_e}{\mu_f}\right)^{0.8} \left(\frac{c_p \mu}{k}\right)^{1/3}_f \quad \ldots\ldots\ldots(18)$$

These equations will be used as a basis of comparison between heat
transfer at high and low velocities of steam.

The Temperature at which Property Values should be Evaluated.

It is usual to introduce the property values at the mean temperature which results in the best correlation of available data. To determine this reference temperature, Humble, Lowdermilk and Grele (43) carried out an investigation on heat transfer to air with large temperature differences. They found that their results could be made to agree closely with the conventional formulae when the density, the thermal conductivity and the viscosity were evaluated at the wall temperature and the velocity was that of the bulk of the fluid.

Crocco (18) carried out calculations on the problem for laminar flow and from these Rubesin and Johnson (87) found that the calculations based on property values independent of temperature give the same result as those based on variable properties when the values are introduced at a reference temperature t determined by the equation.

$$t - t_s = 0.58 \ (t_w - t \ ) \quad \dots\dots\dots\dots\dots\dots\dots(19)$$

Exact measurements on this type of heat transfer were made by Jakob and Dow (46), who summarise in their paper all previous experiments.

Hoffmann (42) investigated the influence of the variability of the property values for turbulent flow. He found that the equations based on constant property values hold true when the property values are inserted at the reference temperature:

$$t = t_s - \frac{0.1 Pr + 40}{Pr + 72} \ (t_s - t_w) \quad \dots\dots\dots\dots(20)$$

For gases where Pr is nearly 1, this gives approximately the

arithmetic mean between fluid and wall temperature and is almost the same as that given by equation 19 for laminar flow.

In the case of flow at high velocities, Johnson and Rubesin (87) showed by an analysis of values calculated by different authors for laminar boundary layer flow on a flat plate that the reference temperature t for the property values in the heat transfer equation is given by:

$$t - t_s = 0.58 (t - t_s) + 0.17(t_{aw} - t_s) \dots\dots\dots\dots\dots(21)$$

Deissler (21) investigated the effects of variable properties on heat transfer for fully developed turbulent flow through pipes at Mach numbers up to 0.5. From this study and also the results of Desmond and Sams (22) for higher velocities he found that the effects of variable properties on the Nusselt number and friction coefficient correlations for both heating and cooling can be eliminated by evaluating the fluid properties at a temperature close to the average of the wall and the bulk temperatures.

In computing the Stanton and Reynolds numbers, the above investigations point to the insertion of the properties at the average of the wall and bulk temperatures.

2. THEORETICAL CONSIDERATIONS.

In this section it was thought advantageous to state the basic equations for forced convection heat transfer and to review very briefly the method of solution for a few particular cases. The main points of interest may then be noted and the application of the solutions examined. The results of the application of dimensional analysis to the problem of heat transfer are then presented.

Though heat transfer is considered to be a boundary layer phenomenon, the influence of the boundary layer is often not recognised while analysing experimental data. A discussion is therefore given on the effect of the boundary layer thickness, the hydrodynamic and thermal boundary layers and local and average values of heat transfer coefficients. Emphasis is made on the bearing which these factors have on heat transfer in the present investigation.

Finally the method of calculating the stream conditions during expansion of the stream through the ducts used in the experiments is presented.

The Theoretical Analyses.

The theoretical analyses have been confined mainly to laminar flow over a flat plate, and depend upon the solution of a number of differential equations, often by special methods. Assuming the plate to be infinite perpendicular to the direction of flow, a co-ordinate system is fixed, the x axis in the stream direction and the y axis perpendicular to the plate. The equations for the boundary layer are then as follows:

(i) The equation of motion derived from Newton's fundamental

equation and considerations of dynamical and frictional forces.

$$\frac{\partial u}{\partial \tau} + u \frac{\partial u}{\partial x} + v \frac{\partial u}{\partial y} = -\frac{1}{\rho} \frac{\partial p}{\partial x} + \frac{1}{\rho}\left[\frac{\partial}{\partial x}\left(\mu \frac{\partial u}{\partial x}\right) + \frac{\partial}{\partial y}\left(\mu \frac{\partial u}{\partial y}\right)\right]$$

.....................(22)

For steady flow, no pressure drop, and since $\frac{\partial^2 u}{\partial x^2}$ may be neglected in comparison with $\frac{\partial^2 u}{\partial y^2}$, this reduces to:-

$$u \frac{\partial u}{\partial x} + v \frac{\partial u}{\partial y} = \frac{1}{\rho}\left[\frac{\partial}{\partial y}\left(\mu \frac{\partial u}{\partial y}\right)\right]$$ ....(22a)

(ii)   The equation of continuity

$$\frac{\partial(\rho u)}{\partial x} + \frac{\partial(\rho v)}{\partial y} = 0$$ ....(23)

(iii)   The energy equation, which accounts for heat conduction extended to the case of a moving fluid

$$\rho \frac{\partial}{\partial \tau}(c_p t) + \rho u \frac{\partial}{\partial x}(c_p t) + \rho v \frac{\partial}{\partial x}(c_p t) - \left(\frac{\partial p}{\partial \tau} - u \frac{\partial p}{\partial x}\right)$$

$$= \frac{\partial}{\partial x}\left(k \frac{\partial t}{\partial x}\right) + \mu\left(\frac{\partial u}{\partial y}\right)^2$$ ....(24)

The last term represents the energy per unit volume converted to heat by friction.   Again, for no pressure drop and steady flow, this reduces to

$$\rho u \frac{\partial}{\partial x}(c_p t) + \rho v \frac{\partial}{\partial y}(c_p t) = \frac{\partial}{\partial x}\left(k \frac{\partial t}{\partial x}\right) + \mu\left(\frac{\partial u}{\partial y}\right)^2$$

.....................(24a)

Prandtl's boundary layer hypothesis also shows that the pressure throughout the boundary layer and hence in the entire field is constant.   The

material quantities therefore only depend on the temperature. At
airspeeds up to the velocity of sound, the temperature rise is
relatively small and the material values and density may be regarded
as constant. The continuity equation may therefore be written:

$$\frac{\partial u}{\partial x} + \frac{\partial v}{\partial y} = 0 \qquad \dots\dots\dots\dots\dots\dots\dots(23a)$$

The boundary conditions are $\quad u = 0, \quad v = 0 \quad$ for $y = 0$
$$\qquad\qquad\qquad\qquad\qquad\quad u = u_0 \qquad\qquad\quad \text{for } y = \infty$$

u_0 is the velocity of undisturbed flow.

Pohlhausen's Solution.

Direct solutions of these equations are due to Pohlhausen
(84) who dealt with two cases:-

      a.   Uniform surface temperature of plate.
      b.   external perfect heat insulation of the plane plate.

In the solution of the equations for the first case, the last term of
equation 24a was neglected, since the rate of frictional heating is
generally small compared with the heat flow perpendicular to the
surface. This leads to the well known equation for the coefficient
of heat transfer for flow over a flat plate:

$$\frac{hL}{k} = 0.664 \left(\frac{c_p \mu}{k}\right)^{1/3} \left(\frac{\rho u_0 L}{\mu}\right)^{1/2} \qquad \dots\dots\dots\dots(25)$$

For case b, the result of the solution yields the value of the recovery
factor r, for laminar flow over a plate. Here the last term of
equation 24a cannot be neglected, since friction is the only source of
heat. The additional boundary conditions are

$$\partial t/\partial y = 0 \quad \text{for } y = 0$$
$$t = t_0 \quad \text{for } y = \infty$$

By introducing the stream function ψ, and the variables

$$\xi = \frac{1}{2} y \sqrt{\frac{u_0}{\nu x}} \qquad\qquad \theta = t - t_w$$

$$S(\xi) = \frac{\psi}{\sqrt{\nu u_0 x}} \qquad\qquad \theta_0 = t_0 - t_w$$

and $\quad X(\xi) = \frac{2 c_p (\theta - \theta_0)}{u_0^2}$

the partial differential equations convert into ordinary differential equations. S was solved from the respective differential equations in a calculation by Blasius (4), and the values tabulated. Using these values, X may be calculated numerically. The temperature of the surface t_w may be expressed by

$$t_w = t_0 + \frac{u_0^2}{2 c_p} \cdot \delta \qquad\qquad \dots\dots\dots\dots\dots\dots(26)$$

where δ is a function of $c_p \mu / k$ only. Values of δ, which is of course equal to the recovery factor r, were calculated by Pohlhausen. These are shown tabulated below. The last two values for very viscous liquids were obtained by Eckert and Weise.

Table 1.

Pr	$(Pr)^{\frac{1}{3}}$	δ
.6	.774	.77
.7	.836	.835
.8	.894	.895
.9	.949	.95
1.0	1.0	1.0
1.1	1.049	1.05
7.0	2.646	2.515
10.0	3.162	2.965
15.0	3.874	3.535

This shows that r is very nearly equal to $(Pr)^{\frac{1}{2}}$ for the range of Pr for gases.

The Solution of Eckert and Drewitz.

Eckert and Drewitz (25) obtained a solution for the general case of heat transfer for flow at high velocities over a plane plate by solving equations 22 to 24. The frictional heating term in equation 24a was not neglected, while the boundary conditions are the same as in case (a) of Pohlhausen's solution.

The stream function ψ, and the variables ξ and ζ are again introduced, values of ζ being given by the Blasius solution. With these variables, and inserting the Prandtl number, equation 24a transforms to

$$\frac{d^2\theta}{d\xi^2} + Pr\,\zeta\,\frac{d\theta}{d\xi} = -\frac{Pr}{2}\cdot\frac{u_0^2}{2gc_p}\cdot\left(\frac{d^2\zeta}{d\xi^2}\right)^2 = f(\xi) \quad\cdots\cdots(27)$$

By putting the term $f(\xi) = 0$, which is equivalent to neglecting the heat introduced by the internal friction, Eckert obtained a solution for the case of low speed flow identical with that given in a slightly different form by Pohlhausen.

The general solution of the inhomogeneous differential equation 27 is obtained from the solution of the homogeneous equation where $f(\xi) = 0$ by "variation of the constants". The equation for this solution, and the equation for heat removal from the plate at point x; $-q = -k\,(\partial\theta/\partial y)_{y\,=\,0}$, can be transformed if the gas temperature in the undisturbed flow is replaced by the temperature that the unheated wall assumes in the gas stream. This is termed the "natural temperature" t_e by the authors. They obtained an

equation giving this temperature which is also in agreement with the solution by Pohlhausen for the plate thermometer.

Subsequent to the introduction of t_e into the solution, the temperature field can be written in a form representing the sum of the temperature field resulting from an increase of plate temperature and that due to frictional heating. This results from the linear construction of equation 24a.

When the heat transfer coefficient is defined by

$$q = h (t_w = t_e) \qquad \ldots\ldots\ldots\ldots\ldots\ldots(28)$$

then the Nusselt number $h x /k$ is given by

$$Nu = 0.332 (Pr)^{\frac{1}{3}} (Re)^{\frac{1}{2}} \qquad \ldots\ldots\ldots\ldots\ldots\ldots(29)$$

and formed with the mean heat transfer from the beginning of the plate is

$$Nu_m = 0.664 (Pr)^{\frac{1}{3}} (Re)^{\frac{1}{2}} \qquad \ldots\ldots\ldots\ldots\ldots\ldots(30)$$

The coefficient formed in this way therefore follows the same relationship as at low velocities and is independent of temperature difference.

The authors then rechecked the derived formula for the case of $Pr = 1$. These calculations showed that the allowance for the variability of the properties does not alter the heat transfer coefficient by more than 3% when the Mach number varies from 0 to 2. At other Pr not far from unity the error is of the same order of magnitude. Also for $Pr = 1$, Reynolds formula holds. At low speeds this is

$$\frac{q}{W} \qquad g \frac{c_p (t_o - t_w)}{u_o} \qquad \ldots\ldots\ldots\ldots\ldots\ldots(31)$$

At high velocities the ratio is then given by

$$\frac{q}{W} = g \frac{c_p (t_o - t_w)}{u_o} \qquad \ldots\ldots\ldots\ldots\ldots\ldots(32)$$

Turbulent Boundary Layer.

In this same paper, the authors also considered the case of turbulent flow. They state that the linear super-position of the temperature fields, as it occurs in the laminar boundary layer, remains also in the turbulent so long as the material values can be regarded as constant. This is manifested by the general differential equation for the heat flow in a mass particle

$$g \rho c_p \frac{D\theta}{d\tau} = \lambda \Delta^2 + \mu \text{ (diss. fct } (\underline{\omega})) \ldots \ldots (33)$$

Where $D/d\tau$ is the substantial differential quotient w.r.t. time and diss. fct $(\underline{\omega})$ is the dissipation function for the velocity vector $\underline{\omega}$. Even this equation is already linear in θ exactly as equation 24a. The field of flow is completely independent of the temperature field assuming ρ is a constant, and therefore also the heat developed by internal friction - $(\mu$ diss. fct. $(\underline{\omega}))$, a quantity defined by the velocity field.

The temperature field without these sources of heat is known from measurements at low speeds, and the theory of similitude affords the aspect of the temperature at high speeds in the absence of internal friction. The resultant field may then be obtained by superposition. From the linear superposition of the temperature fields it follows that in turbulent as in laminar boundary layer, the characteristic relation

$$Nu = f \text{ (Re, Pr)} \ldots \ldots (34)$$

established for heat transfer at low speeds must be equally applicable at high speeds, if the heat transfer coefficient is referred to the

difference between the wall temperature and the natural temperature.

There are no turbulent boundary layer solutions which give values for the recovery factor comparable to the Pohlhausen analysis, but some estimates have been made which include frictional dissipation. Notable are those of Shirokov (90) giving

$$r = 1 - 4.55 (1 - Pr) . (Re)^{-0.2} \quad \dots\dots\dots\dots\dots\dots(35)$$

which gives rather high values; and Ackermann (1) giving

$$r = (Pr)^{\frac{1}{3}} \quad \dots\dots\dots\dots\dots\dots\dots\dots\dots(36)$$

Solutions allowing for Variable Properties.

In the foregoing solutions the variation of fluid properties in the boundary layer was neglected. As this left some doubt as to their applicability to high velocity cases with large temperature ranges, several analysis were undertaken to rectify this matter.

In 1935 Busemann (10) set forth the procedure for integrating equations 38 to 40 for the conditions that Pr = 1, and that viscosity and thermal conductivity vary with the square root of the absolute temperature. Only the case of an insulated plate and $M = 8.8$ was integrated however.

Von Karman and Tsien (51) considered the case of viscosity and thermal conductivity varying with the 0.765 power of the absolute temperature and Pr = 1, for Mach numbers ranging from 0 to 10.

Crocco (19) performed an analysis for Pr = 1 and the exponent for variation of viscosity and thermal conductivity, $n = 1.25, 0.75$ and 0.5. Numerical integrations were carried out for Mach numbers

ranging from 0 to 5.

The solution of Brainerd and Emmons (29), restricted to the case of an insulated plate, yielded values for the recovery factor. Using a differential analyser for the solution of the differential equations, they obtained a more general form for equation 26 as follows:

$$r = \eta \, (Pr)^{\frac{1}{2}} + (1 - \eta) \, Pr \quad \dots\dots\dots\dots\dots(37)$$

where $\eta = 1 - 0.1 \log_{10} (2\sigma + 0.4)$

and $\sigma = (\gamma - 1) M^2$

All these solutions confirm that the effect of frictional heating is to modify the temperature potential in the Newton equation while leaving the heat transfer coefficient approximately that of low speed flow. The temperature potential is modified in that the free stream temperature is replaced by the adiabatic wall temperature. For the insulated plate, these analyses show that the recovery factor is dependent solely on the Prandtl modulus and is approximately equal to $(Pr)^{\frac{1}{2}}$.

Dimensional Analysis (reference 26).

At low speeds the term with the dissipation function in equation 33 can be discounted. If the values ρ, μ, Cp and k are treated as constant, similarity of speed, temperature and pressure is afforded for two processes when the boundaries of the problem are geometrically similar, when the temperature and velocity fields are similar at the boundaries, and the two constants $Re = \rho \, u_0 \, l / \mu$ and $Pr = Cp \, \mu / k$ each have the same magnitude.

At high speeds the term with the dissipation function may
not be neglected. Even though the material values are treated as
constant, the above conditions must be supplemented by a further
constant which, after multiplying by the Reynolds number, takes the
form $c_p\, g\; \theta_0/u_0^2$, where θ_0 is a representative high temperature
taken from the boundary conditions. The temperature rise caused by
adiabatic damming of the gas flow at speed u_0 is $\theta_{ad} = u_0^2/2g\, c_p$.
So the above constant can equally be employed in the form θ_0/θ_{ad}.
In the temperature field the excess temperatures θ above the chosen
reference point at similarly located points can then be non-dimensionally
written:

$$\frac{\theta}{\theta_0} = f\left(Re,\ Pr,\ \frac{\theta_0}{\theta_{ad}}\right) \dots\dots\dots\dots\dots\dots\dots(38)$$

The dimensionless heat transfer coefficient Nu is then found from the
temperature gradient at the wall.

$$Nu = \frac{hl}{k} = \left(\frac{\partial\frac{\theta}{\theta_0}}{\partial\frac{y}{l}}\right)_w = f\left(Re,\ Pr,\ \frac{\theta_0}{\theta_{ad}}\right) \dots\dots\dots(39)$$

In the case of variable density, the above equations must be supplemented
by the equation of state. Besides similarity of temperature and
pressure fields, the density fields must also be similar. This can be
reconciled with the equation of state only in the presence of similitude
of absolute temperature and pressure, and not merely the excess
temperatures and pressures. The fields of absolute temperature maintain
similitude only if θ_0/T_g is constant, where T_g is the representative
absolute gas temperature. Equation 38 is then:

$$\theta/\theta_o = f (Re, Pr, \theta o/\theta ad, \theta o/T_g) \dots\dots\dots\dots\dots(40)$$

The constant $\theta o/\theta$ ad can be transformed by multiplication with the reciprocal value of the temperature ratio $\theta o/T_g$.

$$\frac{\theta_o}{\theta ad} \cdot \frac{T_g}{\theta_o} = \frac{2gC_p \theta_o}{U_o^2} \cdot \frac{T_g}{\theta_o} = \frac{2gC_pT_g}{U_o^2}$$

The sonic velocity of the gas is given by $a = \sqrt{g(\gamma-1)C_pT_g}$

$$\therefore \frac{\theta_o}{\theta ad} \cdot \frac{T_g}{\theta_o} = \left(\frac{a}{U_o}\right)^2 \cdot \frac{2}{\gamma-1} = M_o^2 \cdot \frac{2}{\gamma-1}$$

$$\therefore \frac{\theta}{\theta_o} = f_1 (Re, Pr, M, \frac{\theta_o}{T_g}) \dots\dots\dots\dots\dots\dots\dots\dots\dots(41)$$

It is thus seen that, with frictional heating, the heat transfer coefficient is a function of the Reynolds and Prandtl numbers and the ratio $\theta o/\theta ad$. With variable density, the heat transfer coefficient is also a function of the Mach number as well as the above. Only Re and Pr normally appear for heat transfer since the other dimensionless variables are substantially zero for low speed flow.

The natural temperature follows by putting the temperature gradient at the surface equal to zero. Then

$$\frac{\theta_o}{T_g} = f_2 (Re, Pr, M) \dots\dots\dots\dots\dots\dots\dots\dots(42)$$

or by dividing the equation by the Mach number the recovery factor is obtained as

$$r = f_3 (Re, Pr, M) \dots\dots\dots\dots\dots\dots\dots\dots(43)$$

For heat transfer at high velocity, the coefficient is defined by

$$q = h \ (T_s - T_w) = k \left(\frac{\partial \theta}{\partial y} \right)_w \quad \dots\dots\dots\dots\dots\dots(44)$$

This is the only way in which the heat transfer coefficient can be made independent of the temperature difference. Defined in the conventional manner this is not the case as can be seen from equation 39.

THE INFLUENCE OF THE BOUNDARY LAYER ON HEAT TRANSFER.

The Effect of Thickness of the Boundary Layer.

It can be readily shown that the heat transfer coefficient is dependent on the thickness of the boundary layer. In the ideal case of flow over a flat plate, the heat transfer coefficient as included in the Nusselt number is given as a function of the Prandtl number and the length Reynolds number. The thickness of the boundary layer is also directly dependent on the length Reynolds number, therefore the variation of heat transfer coefficient with boundary layer thickness can be found exactly.

In other cases where the boundary layer growth cannot be predicted, it can be shown as follows that the coefficient varies with the thickness.

The heat flow may be expressed either by using a coefficient of heat transfer or as thermal conduction through a thin film on the surface. Thus

$$q = hA (t_s - t_w) = k . \left(\frac{\partial t}{\partial y} \right)_{y = o} . A \dots\dots\dots\dots(45)$$

where t = the temperature at distance y from the wall.

Then
$$h = \frac{k . \left(\frac{\partial t}{\partial y} \right)_{y = o}}{t_s - t_w} \dots\dots\dots\dots\dots\dots\dots(46)$$

When the boundary layer is thin, the temperature gradients throughout the thickness will be greater for the same overall temperature difference. It can be seen therefore from the above expression for h that the heat transfer coefficient will be larger in these circumstances and will

decrease as the thickness of the boundary layer increases.

In the case of high velocity flow, the adiabatic wall temperature taw must be substituted for the temperature of the free stream ts.   The above reasoning will still apply, however, since the temperature gradients will still be greater for a thin boundary layer resulting in a greater value of h for the same value of taw - tw.

The Hydrodynamic and Thermal Boundary Layers.

In the previous section reference has been made to temperature gradients and it is obvious that the boundary layers which are mentioned are thermal boundary layers.   The concept of the thermal boundary layer and the influence that it has on heat transfer has evidently not been understood in interpreting the results of many experimental investigations. The growth of this type of boundary layer may be quite separate from that of the hydrodynamic boundary layer.

The thermal boundary layer may be defined as the region round a body in which the temperature field is altered from that under adiabatic conditions by the addition or abstraction of heat at the surface of the body.   This definition will also apply to high velocity flow, the temperature field under adiabatic conditions being already influenced by frictional heating.

Some of the results of theoretical analyses bearing on the present investigation are reviewed here.

The Flat Plate in Laminar Flow.

Assuming that the first part of the plate of length Xo is unheated, the hydrodynamic boundary layer then begins at the leading edge while the thermal boundary layer starts at the edge of the heated

section.   At a section x from leading edge δ and δ_t are the thicknesses of the hydrodynamic and the thermal boundary layers respectively.   The ratio $\delta t / \delta$ is equal to ς.   By drawing up a heat balance of a volume element and assuming a temperature distribution for the boundary layer, formulae for the heat transfer coefficient h and the ratio ς may be derived.   These are:

$$\frac{h}{k} = 0.331 \sqrt[3]{Pr} \sqrt{\frac{u_s x}{\nu}} \cdot 3\sqrt{\frac{1}{1 - \left(\frac{x_0}{x}\right)^{\frac{3}{4}}}} \quad \dots\dots\dots\dots(47)$$

and $$\varsigma = \sqrt[3]{\frac{1}{Pr}} \sqrt[3]{1 - \left(\frac{x_0}{x}\right)^{\frac{3}{4}}} \quad \dots\dots\dots\dots\dots(48)$$

It can be seen that at the point where the thermal boundary layer starts, where $x = x_0$, the heat transfer coefficient will have an infinite value.

When the plate is heated over the whole length the above equations reduce to:

$$\frac{hx}{k} = 0.331 \sqrt[3]{Pr} \cdot \sqrt{Re_x} \quad \dots\dots\dots\dots\dots\dots(49)$$

and $$\varsigma = \sqrt[3]{\frac{1}{Pr}} \quad \dots\dots\dots\dots\dots\dots(50)$$

From equation 50 it can be seen that when the Prandtl number equals 1, the hydrodynamic and the thermal boundary layers have the same thickness. Such will be the case for the present investigation, where heat was abstracted from the start of the test length and since Pr = 1 for steam.

Laminar Flow through a Tube.

For fully developed flow in a tube, theory shows the Nusselt

number to be a constant. Graetz (35) and Nusselt (80) found that

$$\frac{hD}{k} = 3.65 \qquad \dots\dots\dots\dots\dots\dots\dots\dots\dots\dots\dots(51)$$

In the entrance regions, the growth of the boundary layers causes a varying heat transfer coefficient. For the case where the thermal and hydrodynamic boundary layers develop simultaneously no thorough investigation seems to exist, though as long as the boundary layers are thin the formulae for a flat plate may be applied. The case where heating begins at a section where the velocity profile is already fully developed was calculated by Graetz (35) in 1889 and later by Nusselt (80). The results of these calculations showed that the Nusselt number depends only on the value of $\left(\frac{1}{Re\ Pr}\right)\left(\frac{x}{d}\right)$

These results are not applicable to the conditions of flow encountered in the experiments since transition to turbulence occurs before the flow becomes fully developed.

Turbulent Flow through a Tube.

Latzko (67) devoted to this subject a thorough theoretical investigation. Starting from Prandtl's and Von Karman's equations on shearing stress, velocity distribution in turbulent flow, and "turbulent conductivity", he obtained the equation for the local heat transfer coefficient:

$$h = 0.0346 \, V_m \rho c_p \cdot \left(\frac{\nu}{V_m D}\right)^{\frac{1}{4}} \cdot \frac{1.078e^{-m_1 x} + 0.134e^{-m_2 x} + 0.98e^{-m_3 x}}{0.970e^{-m_1 x} + 0.024e^{-m_2 x} + 0.006e^{-m_3 x}} \dots(52$$

where V_m = the mean velocity

x = distance of section considered from the inlet

$$m_n = \beta_n \cdot \frac{1}{D} \cdot \sqrt[4]{\frac{\nu}{V_m D}}$$

$$\beta_1 = 0.1510 ; \quad \beta_2 = 2.844 \text{ and } \quad \beta_3 = 29.42$$

Because of the finite temperature difference between the surface and entering fluid, h starts with an infinitely great value, though this cannot be seen from the approximate equation 52 with three terms only. As x becomes finite, the fast increase of the exponents with n causes a rapid decrease of h.

Latzko also considered the heat transfer in a starting section in which turbulence is not fully established. For a starting section in which turbulence is only partly established the equation he derived is:

$$h_p = B \ V_m . \rho . c_p \left(\frac{\nu}{V_m \ D} \right)^{\frac{1}{4}} = B \ V_m . \rho . c_p \ (Re)^{\frac{1}{4}} \quad \ldots \ldots \ldots (53)$$

B is a function of ξ , the ratio of boundary layer thickness to tube radius, and ξ is a function of Reynolds number and length to diameter ratio. Values of B and ξ were presented in graphical form in the original paper.

For the range of fully established turbulence the equation is:

$$h_f = 0.03461 \ V_m . \rho . c_p \left(\frac{\nu}{V_m \ D} \right)^{\frac{1}{4}} . \frac{0.969 e^{-m_1 x} + 0.038 e^{-m_2 x}}{0.873 e^{-m_1 x} + 0.0068 e^{-m_2 x}} \ldots (54)$$

The heat transfer coefficient as given by equations 53 and 54 is somewhat slower in approaching the minimum value of $0.0384 \ V_m . \rho . c_p \left(\frac{\nu}{V_m \ D} \right)^{\frac{1}{4}}$ than when the hydrodynamic state is fully established.

It is probable that Latzko's analysis may be improved since his work was based on Von Karman's "seventh-root rule" of velocity distribution.

Major differences in the experimental results of different reliable observers are due to different starting conditions which had not been recognised and considered before Latzko's analysis. Even yet the importance of distinguishing between the different cases sometimes does not seem to be realised. In some recent investigations it is found for instance, that heat transfer coefficients obtained from a section with hydrodynamic state fully established but thermal state unestablished are compared with theoretical values for both states fully established.

The above sections demonstrate that it is necessary in comparing experimental results with theoretical values to consider not only the growth and nature of the hydrodynamic boundary layer, but also the growth of the thermal boundary layer. In the flow through the annular duct used in the present investigation, heat is abstracted from the start of the section. Both the thermal and hydrodynamic boundary layers will therefore develop simultaneously. For the laminar flow, since the Prandtl number is unity, both types of boundary layer will increase at the same rate from equation 50. No such relationship for the ratio of the thicknesses of the two types of boundary layer exists for turbulent flow. It is probable, however, that in this range also the thermal boundary layer will continue to increase at the same rate as the hydrodynamic.

Local and Average Values of Heat Transfer Coefficient.

In the brief review of the theoretical solutions in the previous section it can be observed that local coefficients of heat transfer are obtained, that is coefficients based on the values of

temperature and heat transferred at the point considered. In practice
and in experimental investigations it is, however, usually much easier
to measure average coefficients of heat transfer. These coefficients
are based on the heat transferred over a finite length and a mean
temperature difference over this length. In comparing experimental
and theoretical values it is important therefore to distinguish between
the two types of coefficient, since they will in general be different.

It is often possible, starting from the formula for the local
heat transfer coefficient, to obtain an equation for the average
coefficient. The average coefficient h_m is defined by the equation :

$$q = h_m \, A. \, \Delta t \quad \dots\dots\dots\dots\dots\dots(55)$$

while the local coefficient h_θ is given by :

$$\partial q = h_1 \, \partial A. \, \Delta t \quad \dots\dots\dots\dots\dots\dots(56)$$

where ∂q and ∂A are small.

If a relationship exists for h_1 the amount of heat transferred
over the whole area A may be obtained by integrating equation 56 and so
the mean coefficient found.

In the case of flow over a flat plate, the average coefficient
can be easily derived. The local coefficient is a function of the
length Reynolds number, and is given by an equation of the form :

$$\frac{h_\theta}{c_p \, G} = C \, (Pr)^m \, (Re_1)^n \quad \dots\dots\dots\dots\dots(57)$$

$$= C \, (Pr)^m \left(\frac{\rho Vx}{\mu}\right)^n$$

c_p, G, C, $(Pr)^m$ and $\left(\frac{\rho V}{\mu}\right)$ are all constant for any one case and the
equation may be written :

$$h_1 = K \, x^n$$

where in the constant K are combined all values not dependent on x.

The local rate of heat transfer is then

$$\partial q = h_1 . \partial A . \Delta t$$
$$= K x^n b. \partial x . \Delta t \ldots\ldots\ldots\ldots\ldots\ldots\ldots\ldots\ldots(58)$$

For flat plate flow, the surface temperature and the temperature outside the thermal boundary layer are assumed constant. The difference between these temperatures is represented by Δt, which is therefore also constant.

Equation 58 may therefore be integrated giving:

$$q = K \frac{1}{n+1} x^{n+1} b. \Delta t$$

$$= K x^n . \frac{1}{n+1} bx . \Delta t$$

$$= h_1 . \frac{1}{n+1} . A . \Delta t = h_m . A . \Delta t$$

$$\therefore \quad h_m = \frac{1}{n+1} h_1 \quad\ldots\ldots\ldots\ldots\ldots\ldots\ldots\ldots\ldots\ldots(59)$$

For laminar flow, $n = -1/2$, therefore the average coefficient is twice the local coefficient at the end of the section.

For turbulent flow over a flat plate, $n = -0.2$ according to Latzko's analysis (67). Then $h_m = 1.25 h_1$.

For fully developed flow in a pipe, there is of course no variation of the heat transfer with length and the average coefficient is the same as the local value.

In the starting region of pipe flow, owing to the falling heat

transfer coefficient with build up of the boundary layer, there is again a difference between the average and local values of the coefficient. In this case there are considerable difficulties in deriving the average value from the local coefficient. The first difficulty is in obtaining a suitable equation for the local coefficient in terms of length from the entrance. Both the equations for laminar flow, and the analysis of Latzko for entry conditions with turbulent flow would cause considerable difficulty in integration when finding the total heat transfer rate.

In order to correlate experimental values of average coefficients of heat transfer for a tube of length L, it has become the practice to include in the dimensionless equations a length to diameter ratio. Thus the equation usually has the form:

$$St_m = C \ (Pr)^m \ (Re_D)^n \ (\frac{D}{L})^i \quad \ldots\ldots\ldots\ldots\ldots\ldots(60)$$

It is likely, therefore, that such a term should be included in the equation for local heat transfer coefficients, and this would result in a simpler form than Latzko's analysis. It has already been noted that McAdams (73) obtained a correlation of results for local coefficients by including the term $(1 + \frac{k}{x/D})$.

The second difficulty is that the temperature difference between fluid and wall is no longer constant. If the fluid temperature were a function of the heat transferred, it would then be possible to solve the problem in a way similar to that adopted for obtaining a mean temperature difference with constant heat transfer coefficient. So long as the coefficient is independent of temperature and only dependent

on the length from start of heating section, this procedure could
result in the formula

$$Q = h_m . A . \Delta t_m \dots\dots\dots\dots\dots\dots\dots(61)$$

where Δt_m is the usual logarithmic mean temperature difference and

equals $\dfrac{\Delta t_i - \Delta t_e}{\log(\Delta t_i/\Delta t_e)}$, and the mean coefficient h_m bears a simple
relationship to the local coefficient.

The theoretical heat transfer coefficient is, however, based
on the equation in which the temperature difference is that between the
wall and the fluid outside the boundary layer. This fluid temperature
is therefore unaffected by the heat transferred from the definition of
the thermal boundary layer and the above assumption is invalid. The
fluid temperature on which the heat transfer calculations are based is
quite independent of heat transferred in the starting region. For an
incompressible fluid it will remain constant but in the case of a gas
this will vary according to the pressure conditions. If an equation
for the local heat transfer is assumed as:

$$St_1 = C(Pr)^m . (Re_D)^n . (D/x)^i \dots\dots\dots\dots\dots\dots(62)$$

Then the coefficient

$$h_1 = Kx^{-i} \dots\dots\dots\dots\dots\dots\dots\dots\dots\dots\dots(63)$$

where K is a constant combining all the other constants in the above
equation for the starting length.

Then the local heat transfer rate

$$\delta q = h_1 . \delta A . \Delta t$$

$$= Kx^{-i} . \pi D . \Delta t . \delta x \dots\dots\dots\dots\dots\dots(64)$$

This may be integrated graphically if the variation of Δt is known.

Boelter, Young and Iverson (5) in an experimental investigation carried out to check Latzko's theoretical equations, derived an emperical relationship between the local and average coefficients. If h_1 is the local coefficient at a point where the temperature distribution is fully developed, then the average coefficient

$$h_m = h_1 \left(1 + \frac{KD}{x}\right) \quad \dots\dots\dots\dots\dots\dots\dots\dots\dots\dots\dots(65)$$

where $K = 1.4$ if the velocity distribution is fully developed at the entrance, and $K = 0.7$ for initially uniform velocity distribution.

The above discussion shows the importance of distinguishing between local and average values of heat transfer coefficient when comparing experimental and theoretical results and would indicate the advantage of obtaining the local coefficient for starting sections of pipe flow, as being of more fundamental character. Once the local coefficient is known, the average value can be derived if the variation of temperature difference is known. The fact that average coefficients have been measured in most experimental investigations has disguised the variation of the value in the entrance region and the dependence on the growth of the thermal boundary layer and on the transition from laminar to turbulent flow in this section. It is possible also that these considerations would explain why two separate equations are often given for heating and cooling.

It will be demonstrated that the experimental technique employed to obtain the data described in the thesis results in the local value of heat transfer coefficient being obtained. Though so-called local heat transfer coefficients have been measured in a few other
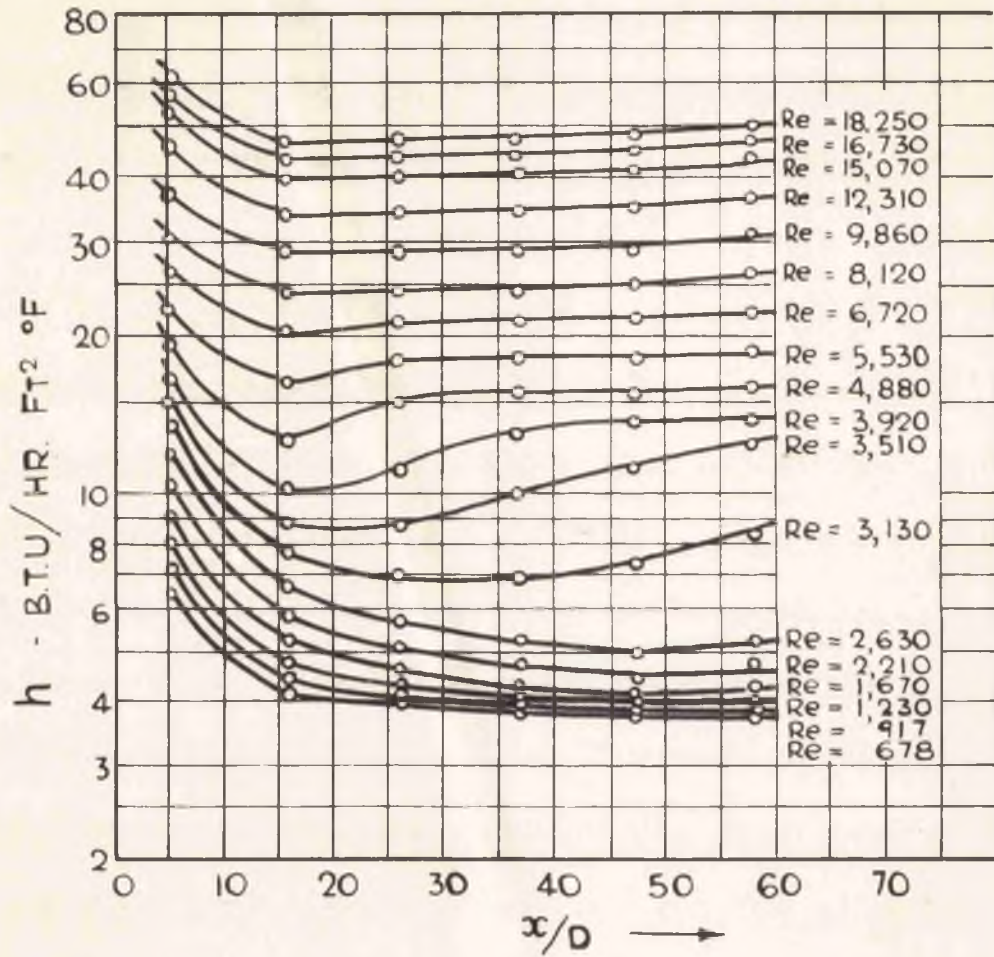
FIG. 10. VARIATION OF LOCAL COEFFICIENT WITH POSITION - CHOLETTE

investigations, these usually have been average values over short
sections of the flow, while the measurements presented here can be
claimed to be true local values for a particular section and are thus
of greater significance for the reasons mentioned above.

An investigation by Cholette (12) is of interest in that the
heat transfer coefficient was found for short sections of the length,
and the influence of the factors discussed above is shown in the
variation of the local heat transfer coefficient.

The apparatus used in this investigation was essentially a
tubular heat exchanger. Air passed through tubes which were of 0.19 in.
i.d. and 12 in. long. The heat added to sections each of 2 in. length
was measured and the average coefficient for these lengths calculated.
Such coefficients are called local coefficients in the paper.

Fig. 10 is reproduced from Cholette's paper and shows the
variation of the local coefficient with length for various diameter
Reynolds numbers. The curves for Re_D below 2,000 correspond to
purely laminar flow, and for Re_D above 8,000, to turbulent flow. The
significance of the curves for Re_D between these values is not however
realised in the paper, and it is stated that the minimum and slight
increase thereafter in the curves is "perhaps on account of the change
in physical properties as the air is being heated". The reason for the
increase of coefficient is, of course, owing to the transition of the
boundary layer from laminar to turbulent flow before the velocity
distribution becomes fully developed. The transition is, of course,
dependent on the length Reynolds number rather than on the diameter
Reynolds number and therefore the portion of the curve with increasing

values of the coefficient which corresponds to the transition region, moves towards the entrance with increasing Re_D.

That there is always a portion near the entrance where a laminar boundary layer starts to build up is not often realised, and it is often thought that the diameter Reynolds number will indicate whether the entire flow is turbulent or laminar.

The Method of Calculating the Stream Conditions
During Expansion in a Duct.

In analysing the results of the experiments which are
described later in the thesis it is essential that the condition of
the steam in expanding through the nozzle or duct be known. The only
property which can be observed directly at any point along the length
is the static pressure. To determine the state it is necessary to
calculate one other property and then the conditions of the flow, such
as velocity and other properties dependent on the state can be readily
deduced.

The calculation is based on a simple one-dimensional flow
model, i.e. the properties are assumed constant across the cross-section
at any point. This is not actually the case, since it is known that a
boundary layer is established at the walls of the duct, the flow within
this being affected by viscosity. Thus the velocity is less near the
boundaries of the flow than in the central region. It will be shown
later, however, that the errors involved are small.

Since the one-dimensional flow is affected by friction the
expansion is irreversible and the equations for isentropic expansion
are no longer applicable. An approximate method of solution is to
assume isentropic expansion and apply a loss factor. The entropy can
indeed be assumed constant for the central core of the fluid which is
unaffected by viscosity, and the temperature and velocity in this core
calculated on this basis. It is difficult, however, to estimate for
how long this core exists and the point at which the flow becomes fully
developed. The calculations were therefore based on the following

considerations:-

The equations which are applicable at any section to the one dinensional flow are

(i) The energy equation

$$H + \frac{v^2}{2gJ} = Ho \quad \dots\dots\dots\dots\dots\dots\dots\dots(66)$$

(ii) The equation of continuity

$$V = \frac{mv}{a} \quad \dots\dots\dots\dots\dots\dots\dots\dots(67)$$

(iii) The equation of state

$$H = A + Bpv \quad \dots\dots\dots\dots\dots\dots\dots\dots(68)$$

The values taken for the constants A and B in equation 68 were those given by Keenan in reference 58 as

A = 851 B.T.U./lb. or 662, 400 ft.lb./lb. and B = 4.117. This equation represents the relationship for water vapour superheated for pressures under 100 lb./sq.in.

In these three equations, there are three unknowns - H, V and v. The other terms are all known from measurement and conditions of the test, therefore the equations may be solved simultaneously. All the unknowns except v may be eliminated and there results the quadratic equation.

$$\frac{m^2}{a^2. 2gJ} . v^2 + Bpv + (A - Ho) = 0 \quad \dots\dots\dots\dots\dots\dots(69)$$

This may be solved in the usual manner. By substituting the values of A and B and suitably adjusting the constants for the units in which the various terms are measured, the specific volume is given by:-

$$v = \frac{-.7619p \overset{+}{-} \sqrt{(.7619p)^2 - 4\left[\frac{m^2}{a^2} \cdot \frac{1}{2gJ}\right]\left[851-Ho\right]}}{2\left[\frac{m^2}{a^2} \cdot \frac{1}{2gJ}\right]}$$

$$\cdots\cdots\cdots(70)$$

where v is in $ft^3/lb.$ m is in lb/sec.

    p is in lb./sec.   a is in $ft^2.$

    H is in B.T.U./lb.

In tests carried out with heat transfer, the stream temperature may still be calculated if the amount of heat abstracted is known. Letting Qx equal the amount of heat transferred per lb. of steam up to the section considered, then equation (58) will be modified to:

$$H + \frac{V^2}{2gJ} + Qx = Ho \cdots\cdots\cdots\cdots\cdots(71)$$

and the specific volume is then:

$$v = \frac{.7619p \overset{+}{-} \sqrt{(.7619p)^2 - 4\left[-\frac{m^2}{a^2} \cdot \frac{1}{2gJ}\right]\left[851 + Qx - Ho\right]}}{2\left[\frac{m^2}{a^2} \cdot \frac{1}{2gJ}\right]}$$

$$\cdots\cdots\cdots(72)$$

Once the specific volume is obtained, and since the pressure is known, the temperature may be found by interpolation in the steam tables (59). The velocity may then be obtained from the continuity equation

$$V = \frac{m}{a} v = Gv$$

Other properties of the flow may then be readily obtained.

A difficulty exists, however, in estimating the stream temperature from values of pressure and specific volume when the expansion proceeds beyond the saturation point into the supersaturated zone. No tables of stream properties are available for this region. Goudie (34) provides alignment charts which give the relationship between

the properties for supersaturated steam and an "H - ∅" chart has been prepared by Stodola (93). It was found that the Goudie charts gave distinctly erroneous results and were therefore discarded while the Stodola chart was of such a small scale that accurate estimation of the properties was difficult.

The approximate equation of state which applies for low pressures and high temperatures, $pv = RT$, where $R = 85.8$ gives a guide as to what the temperature should be. The generalised equation of state which applies to steam under all conditions is usually given in the form

$$\frac{pv}{RT} = 1 + \alpha_1 p + \sum \alpha_i p^i \quad \dots\dots\dots\dots\dots\dots\dots(73)$$

where each α is a function of temperature and $\sum \alpha_i p^i$ denotes a series of terms for each of which the exponent i is greater than 1. It is therefore impossible to obtain T directly from such an equation knowing only p and v.

An equation which may readily be solved for temperature and which represents completely the variations of the vapour and gaseous states is that proposed by Van der Waals. It is usually written as:

$$p = \frac{RT}{v - b} - \frac{a}{v^2} \quad \dots\dots\dots\dots\dots\dots\dots\dots\dots\dots\dots(74)$$

where a and b are constants for any one substance. These constants may be taken so as to accord best with the measured values of these properties in a selected region. In carrying out the calculations for the tests, values of a and b were found by substituting values of p, v and T obtained from steam tables for two points of the expansion in the super-heat field immediately above the saturation line. It is, of course, a

property or rather a definition of the supersaturated field that the same laws and equation of state will apply as for the superheated field.

The temperature could therefore be easily obtained from this equation, and this method was latterly employed for evaluating the state for all points in the supersaturated zone.

The assumption of constant properties across the cross-section has already been noted above. If, however, the mean value of a property were to be greatly different from the maximum value, then errors might become appreciable when analysing the results of heat transfer and recovery factor tests.

The velocity is retarded at the boundaries of the flow by friction. The variation of the other properties across the flow then corresponds to that of the velocity. It is therefore only necessary to examine the velocity profile.

For fully developed turbulent flow, the profile is well established, the velocity being nearly constant across the middle sections and falling rapidly near the walls. The one-dimensional flow model is therefore justified for such flow.

In fully developed laminar flow, on the other hand, the profile is much more curved, and the mean velocity differs appreciably from the maximum. There is evidence to show, however, that the boundary layer undergoes a transition from laminar to turbulent flow while it is still thin and therefore the greater area of the cross-section has a constant velocity unaffected by viscosity. The thickness of the boundary layer at transition may be obtained from the equation

$$\delta = 5.2 \, L/\sqrt{Re_1} \qquad \dots\dots\dots\dots\dots\dots\dots (75)$$

The critical Reynolds number was found to be approximately 15×10 .
Taking L as 4 in. which was about the maximum distance at which
transition occurred for the longer duct, then

$$\delta = 5.2 \times 1/3 / \sqrt{15 \times 10} \text{ ft.} = 0.0167 \text{ in.}$$

The distance between the walls of this annulus is .1128 in. The
thickness of the boundary layer is therefore only 15% of this distance.
The one-dimensional basis of calculation is therefore sufficiently
accurate for the purposes of analysing the results for any section of
the duct.

PART II

AN INVESTIGATION ON THE FLOW OF STEAM IN A SHORT

CONVERGENT DIVERGENT NOZZLE YIELDING VALUES FOR THE RECOVERY

FACTOR AND DATA RELATING TO THE SUPERSATURATED CONDITION.

K

ARRANGEMENT OF END
FOR PRESSURE SEARCH

THERMOCO
LEADS
POTENTIO

R

S

CONDENSER

J

TANK

SUPERHEATER 2

H

M

N

TO POT.

C

G

D

T
P
L

E

DRAINS

F

a

SUPERHEATER 1

TO POT.

B

A

FROM BOILER SUPPLY
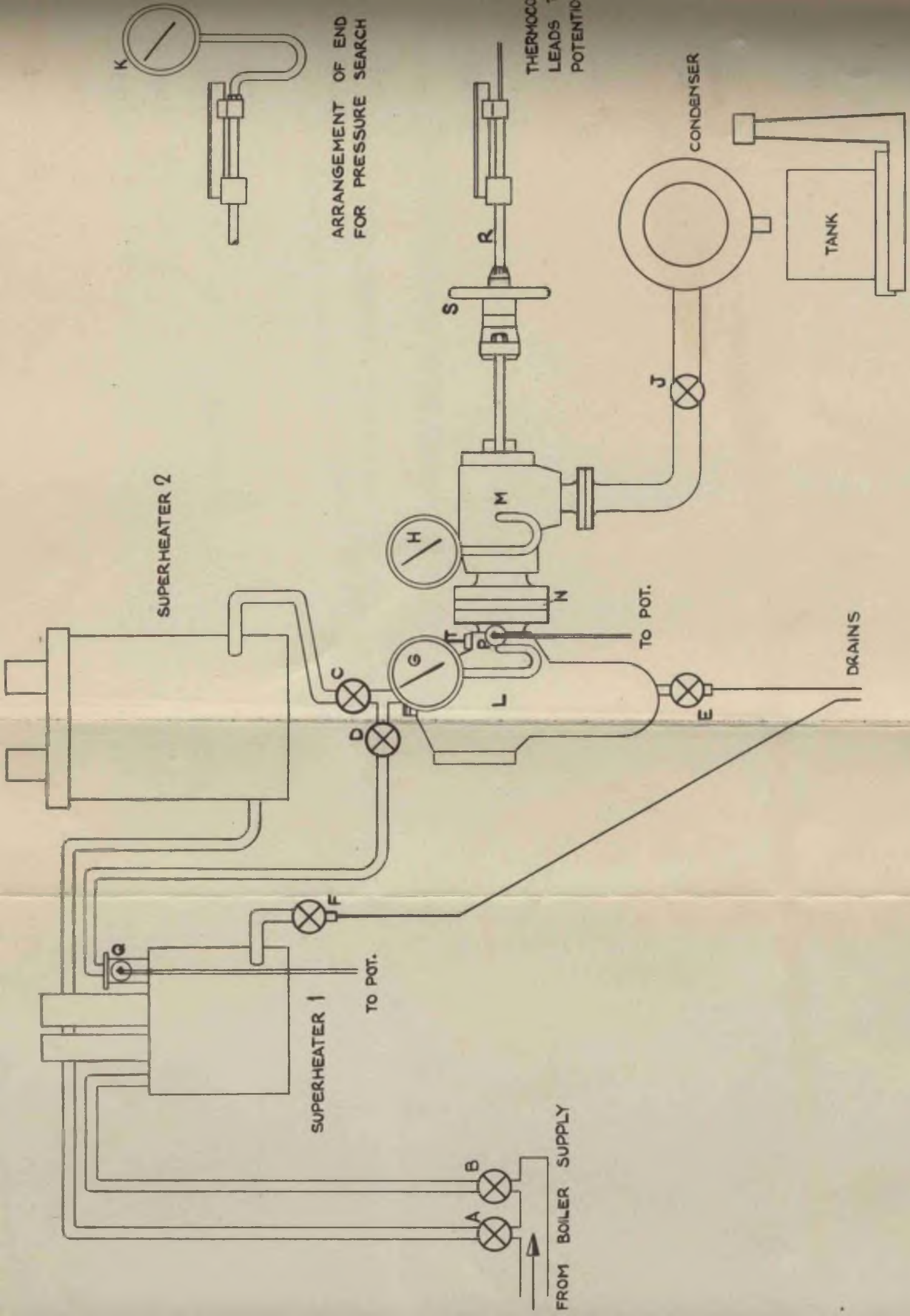
Fig. 11   GENERAL ARRANGEMENT OF APPARATUS.

THE PRELIMINARY INVESTIGATION.

On account of the varied results obtained by investigators in their efforts to measure steam temperatures, it was thought well to carry out a preliminary investigation which would show whether reliable values could be obtained for the recovery factor for steam. The temperatures measured in many of these previous investigations would indicate very low values of recovery factor - much lower than those indicated by theory which would be around unity.

It has already been noted that many of these measurements were recorded while studying the phenomenon of supersaturation. In this preliminary investigation described here it was intended to gain more light regarding the limit of supersaturation and the conditions for which the normal concept of recovery factor would hold.

For carrying out this investigation the nozzle testing apparatus in the heat engines laboratory was adapted and the temperatures recorded on the surface of a search tube or probe inserted longitudinally along the axis of a convergent divergent nozzle. In this way adiabatic wall temperatures could be measured and recovery factors calculated.

APPARATUS.

The general arrangement of the nozzle testing apparatus is shown diagrammatically in Fig. 11 while Fig. 12 shows the details of the receiver, nozzle and search tube fittings.

Steam from the boiler is admitted to the system through either of the valves A and B on the distribution chest in the laboratory. It is then passed through the superheaters, which consist of double helical

FROM CONTROL VALVE
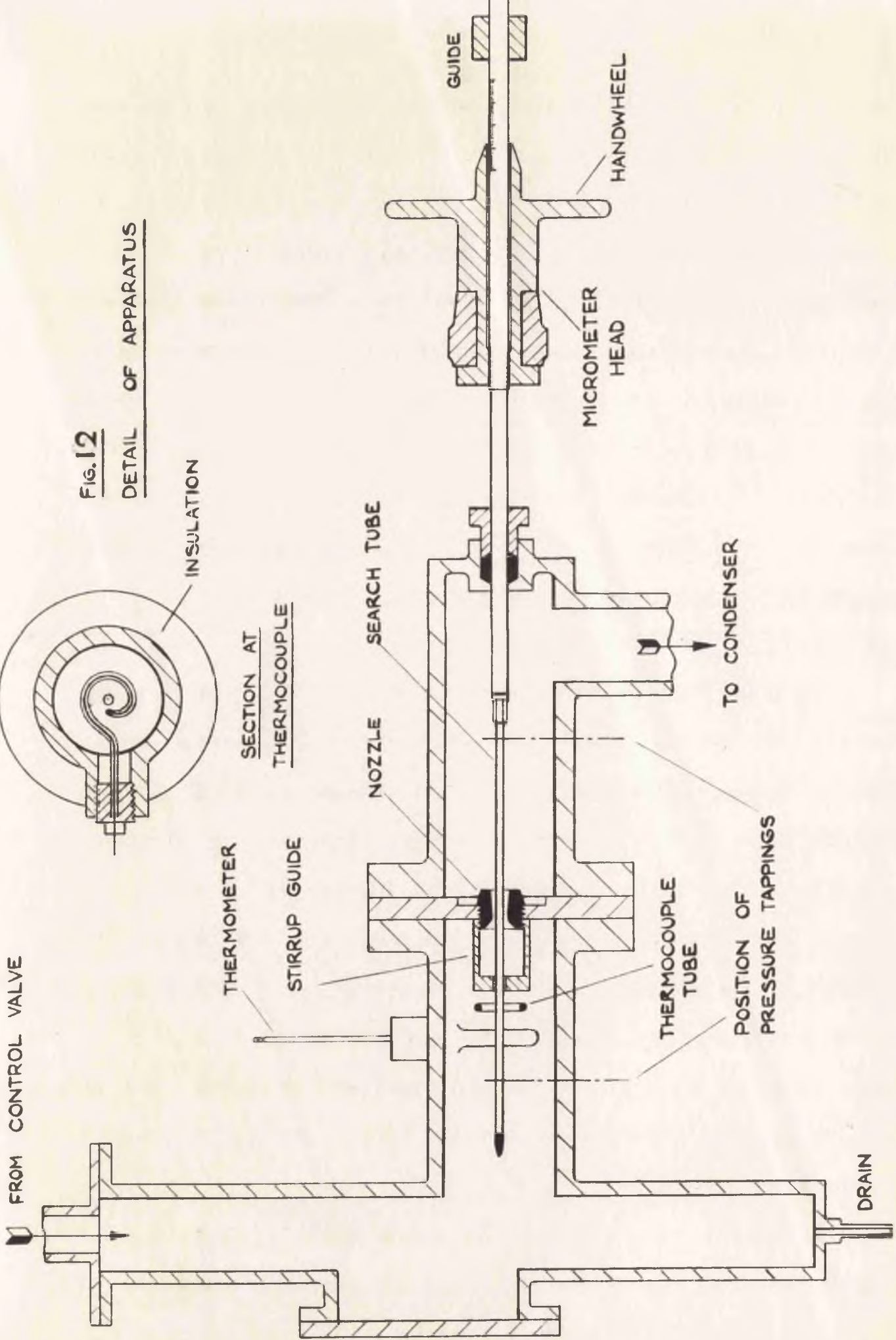
FIG. 12

DETAIL OF APPARATUS

INSULATION

SECTION AT
THERMOCOUPLE

THERMOMETER

STIRRUP GUIDE

NOZZLE   SEARCH TUBE

GUIDE

HANDWHEEL

MICROMETER HEAD

TO CONDENSER

THERMOCOUPLE TUBE

POSITION OF PRESSURE TAPPINGS

DRAIN

coils of 1 in. diam. pipe, directly heated by double ring gas burners.
After leaving the superheaters the steam is admitted through the control
valves C and D to the receiver L.   In this way either No. 1 or No. 2
superheater could be used for raising the supply steam to the desired
temperature.   Superheater 2 was found to produce very steady conditions,
but only moderate superheats whereas superheater 1 could produce much
higher superheats but with relatively unstable conditions.   The greater
length of pipe between this superheater and the apparatus meant a delay
in any change in temperature becoming apparent and for this reason a
thermocouple Q was fitted in the steam pipe at the superheater outlet.
This gave much earlier warning of variations, though control still
proved more difficult than with superheater 2.

The receiver L is fitted with a drain and drain valve E while
the part of the receiver immediately before the nozzle is fitted with a
calibrated Bourdon type pressure gauge G, a thermometer T, and a copper-
constantan thermocouple P.   The thermocouple is carried in a spiral
copper tube 1/8 in. o.d.   The glass fibre insulated copper and
constantan wires are passed up through the length and soldered to the
closed end forming the hot junction.   The length of copper tube prevents
heat conduction affecting the reading.   The mercury thermometer is
retained only as a check on the temperature.   As it was found that with
the higher superheats conduction along the wall of the pocket resulted in
low thermometer readings.

The nozzle is screwed into the nozzle plate N, and carries on
the inlet side a stirrup with a guide hole for centering the search tube.

The nozzle is of brass, of convergent divergent form.   Details are
shown in Fig. 15.

After expanding through the nozzle, the steam enters the
exhaust chamber M, and from thence passes to an atmospheric condenser.
The pressure in the exhaust chamber is controlled by the valve J and is
recorded on the gauge H.   The condensate is collected in a tank
mounted on a platform balance, where it can be weighed.

The search tube is screwed into the end of pipe R which passes
through a stuffing box at the rear of the exhaust chamber.   This tube
has an external screw threaded portion and a graduated length forming
part of the micrometer head, the location being adjusted by the
handwheel S.   The zero reading on the micrometer is determined by
aligning the search portion with the nozzle inlet.

Setting up operations are facilitated by the whole assembly
from the nozzle back (excluding the exhaust pipe) being mounted on
horizontal slides and moved by a screw and handwheel.

The pressure search tube is of brass, 1/4" outside diameter.
It is closed at the leading end and connected through the tube R to a
calibrated Bourdon gauge K.   At a point near the middle of the tube a
0.03125 in. diam. hole is drilled diametrically through the tube walls.
The static pressure at any section occupied by this exploring hole is
consequently indicated on the gauge K.

The Temperature Search Tube.

The search tube used in this investigation was developed from
that used by Sorour (92) which is shown in Fig. 13a.   This consisted of
a 1/4" o.d. copper tube with a small length of Sindanyo inserted near the

1/4" DIA.

1/4"

a. ORIGINAL ARRANGEMENT

BRASS PLUG, SCWD. 6 B.A.

1/16" DIA. HOLE

4 1/2"

1/4" DIA.

SCREWED 1 B.A.
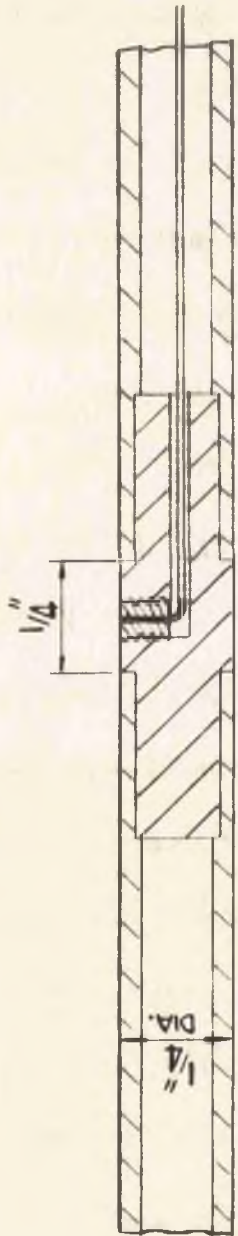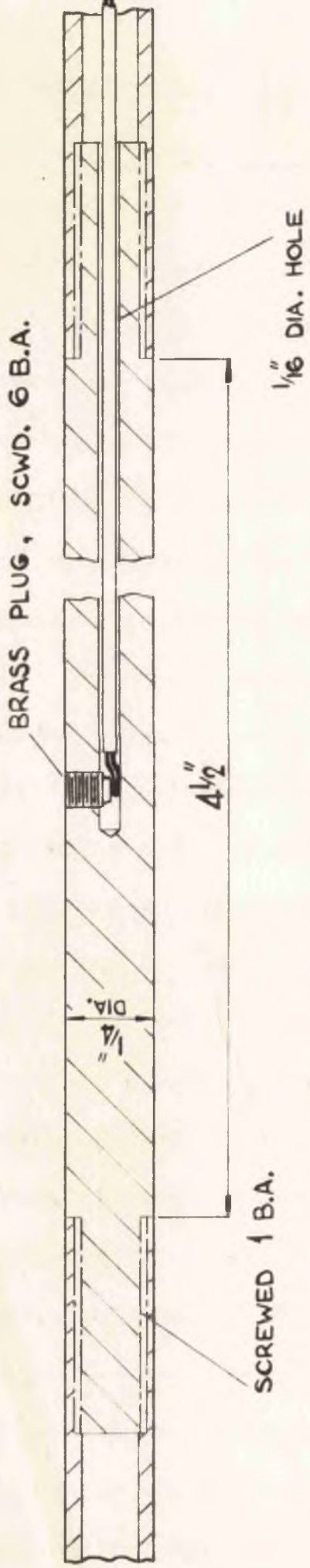
b. IMPROVED SEARCH TUBE

FIG. 13. SEARCH TUBE DETAILS.

middle of the tube. Copper and constantan thermocouple wires were led up the tube, through the Sindanyo into a small copper pin inserted radially in this material, the wires being joined to the pin by silver solder. The Sindanyo is an asbestos bonded insulating material, and thus the temperature recorded by the pin is unaffected by conduction of heat away from the pin, that along the wires being negligible.

The improved form of search tube as used in the tests is shown in Fig. 13b. It is made from 1/4" o.d. brass tube with a similar arrangement of Sindanyo, although this part is made considerably longer than in the tube used by Sorour. A minimum of 4.1/2 in. for the insulating portion was decided upon for the following reasons. The friable nature of the Sindanyo and the bonding grain running transversely across the tube make the achievement of a perfectly continuous surface at the junctions between the Sindanyo and brass tube impossible. The length prescribed above ensured that at all positions of the search tube the joint portions were at no time less than 1" outside the nozzle ends, and in this way any disturbing effects eliminated which might otherwise occur in the flow owing to a discontinuity on the surface. Moreover, these junctions are subject to great erosion when exposed to a high velocity stream. Secondly, the after junction is a source of steam leakage into the tube and so to the thermocouple insulation when subjected to steam pressures above atmospheric. When this junction is always beyond the nozzle exit it is subjected only to the back pressure for any particular test, which was in most cases atmospheric pressure. Also the effects of heat transmission along the tube wall on the temperature of the boundary layer is minimised by having the entire

length of the boundary layer adjacent to the insulating material.

The thermojunction is formed by welding the ends of the copper and constantan wires and the brass plug is screwed down on this junction as shown. Any change of temperature on the surface of the plug was found to be indicated on the reading of the E.M.F. almost instantaneously. The thermocouple wires were insulated with a normal commercial woven covering of glass fibre. As a further protection the whole length of lead within the search tube and pipe R up to the junction was coated with an insulating varnish capable of withstanding high temperatures. This prevented any moisture present affecting the E.M.F. reading.

All the screw threads and joints were coated when assembling with "Stag" brand jointing paste, which was allowed to harden before the exterior surface was finished. This was found to give efficient steam-tight joints, except that frequent renewal was necessary at parts exposed to the high speed stream. The brass plug was filed flush with the tube surface and finished with No. 0 emery cloth. The whole assembly was then polished with No. 000 emery paper and no tube was put into service unless the surface was completely free from irregularities or marks of any kind.

This procedure usually sufficed for two days working in the nozzle stream. At the end of that time a small crevice had usually been created around the plug owing to the removal of the "Stag" paste by the stream action. If left in this state the crevice became larger through erosion of the Sindanyo at the crack edge. Accordingly the crevice was immediately filled by a new application of paste and the surface refinished when this had dried and hardened. This latter
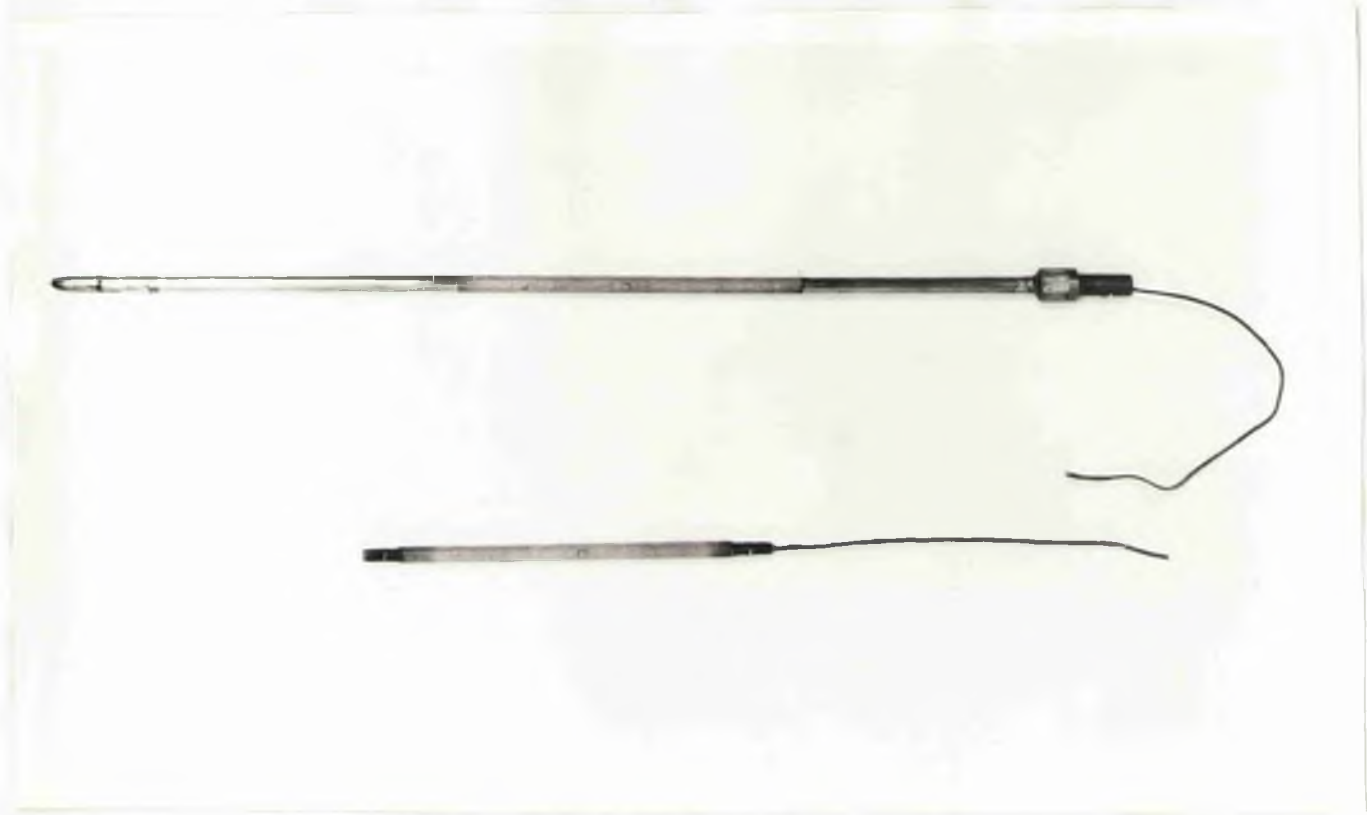
Fig 13c   PHOTOGRAPH   OF   SEARCH   TUBE

AND   SINDANYO   PORTION

procedure was then repeated after each subsequent day's working. The total life of a search tube with these precautions was about six working days. At the end of this time the whole surface of the Sindanyo portion began to show signs of erosion, especially at the ends of the boundary fibres which ran transversely across the tube. It was also found that the material became porous if used beyond this time, and water entered the tube, with consequent effects on the temperature recorded. A photograph of a complete search tube and a Sindanyo portion removed from the brass tube may be seen in Fig. 13c (both pieces having undergone a normal period of service). The brass plugs can be seen in each case, about the middle of the Sindanyo portions. The good degree of surface finish produced by continuous polishing can be seen and it will be observed that the whole assembly presents a smooth uninterrupted surface to the flow of the fluid.

The thermocouple wires were led to a selector switch along with those for couple P (and also couple Q for superheater 1) and thence to a cold junction. The cold junctions were immersed in a test tube full of oil and surrounded by melting ice, the whole, together with a thermometer being enclosed in a thermos flask. A portable potentiometer connected to the switch leads enabled the e.m.f. generated to be measured in millivolts to an accuracy of one hundredth part of a millivolt. The temperatures were obtained from a calibration chart prepared for these copper constantan thermocouples.

Five search tubes of this type were used in the present tests, while a greater number was discarded during manufacture on account of various faults.

SOLDERED JOINT
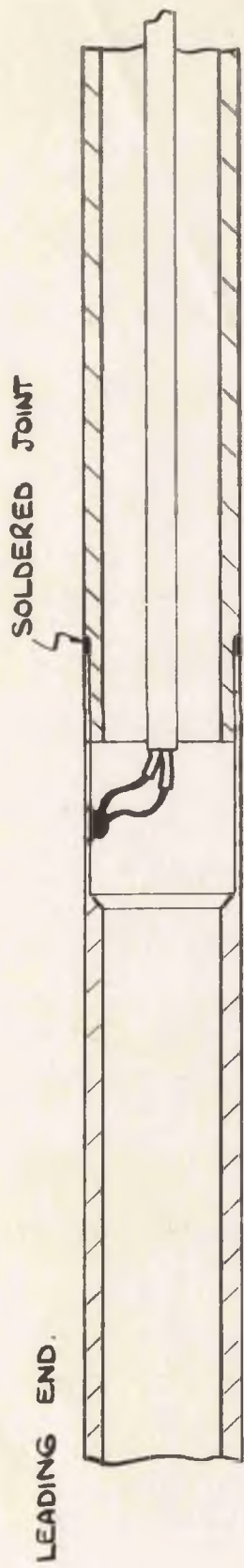
LEADING END.

FIG. 14   DETAIL OF BRASS SEARCH TUBE.

The Brass Temperature Search Tube.

A second type of search tube was also constructed as shown in Fig. 14. A brass tube 1/4" outside diameter and 3/16" inside diameter, with a sealed leading end was carefully machined on the inner diameter for about 5/8" length until the wall thickness was reduced to about .012". A welded copper constantan thermo-junction was then silver soldered to the inside of this thin-walled portion. On a second length of tube, with the usual type of screwed end for attachment to pipe R (Fig. 11), a small landing was machined to fit this new diameter. The thermocouple leads were threaded through this second brass portion and the parts mated. The junction was completed by silver soldering, during which operation extreme care had to be taken not to disturb the soldered thermocouple. The exterior was then smoothed and polished in the usual fashion with emery cloth. The above construction resulted in the outer join of the brass tube being behind the thermocouple when in use, and so there were no potential sources of disturbance to the flow. The zero position of the search tube was determined by aligning the tube join with the nozzle inlet and adding the distance between this and the thermojunction as measured from an X-ray photograph taken of the assembly.

It was thought that the extreme thinness of the wall would ensure that the actual local surface temperature would be recorded by the thermocouple and that longitudinal heat conduction would be reduced to a negligible minimum.

1¹⁄₃₂″

5⁄16″ R.

·344″ DIA.

·380″ DIA.

THROAT

a b   c d e f g h j

·113″   ·1″ ·1″ ·1″ ·1″ ·1″ ·1″ ·1″ ·1″ ·1″   ·018″
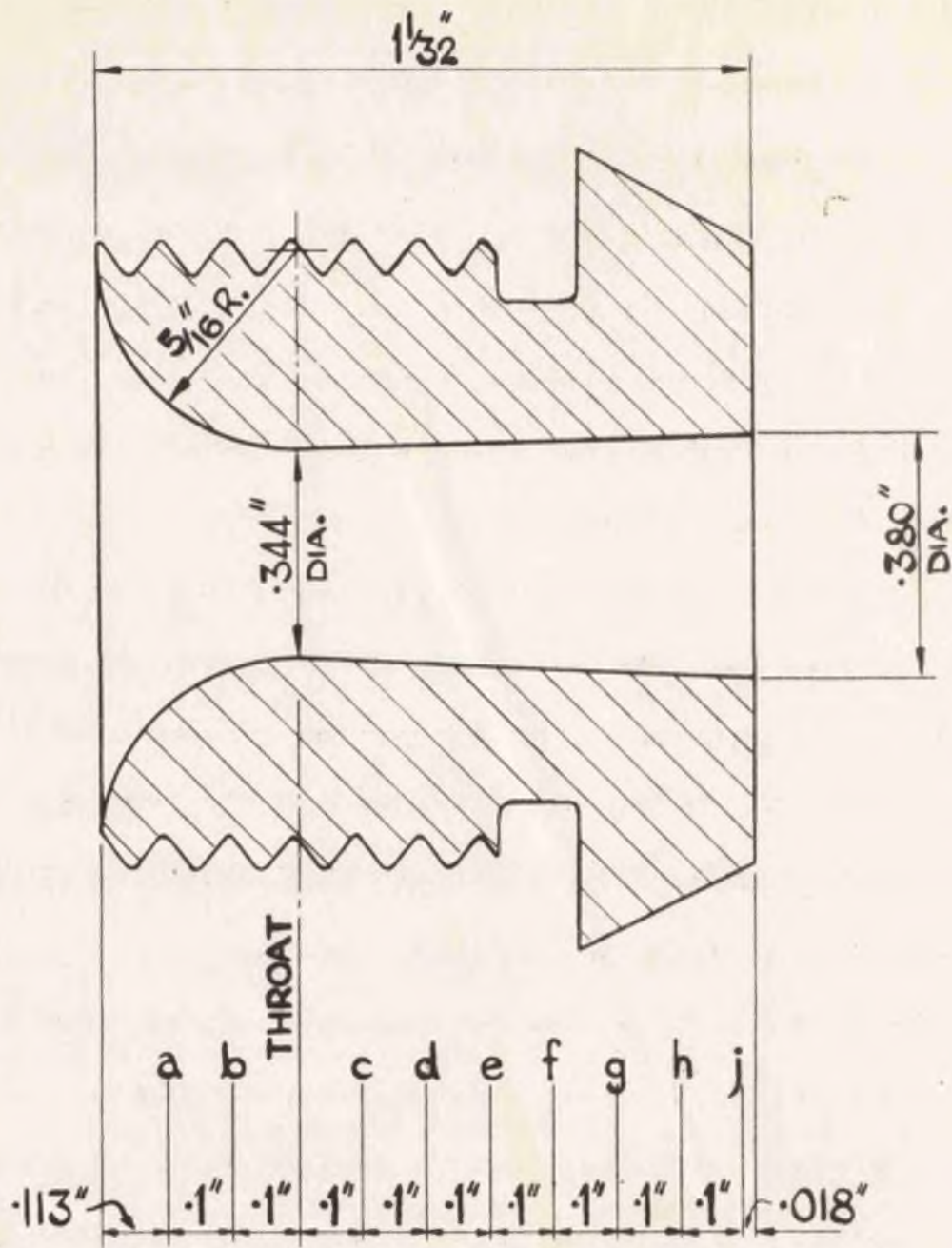
FIG 15.   NOZZLE DETAIL.

Procedure and Results of Pressure Searches.

The system was first drained, the appropriate valves opened and the steam allowed to circulate. The system was heated up by passing steam through at the desired pressure conditions and with the gas taps of the superheater fully open until the supply temperature was slightly above the required value. Then the temperature was reduced to this level by adjusting the flow of gas. This procedure could be completed for the pressure searches in about two hours. The pressure and temperature conditions were maintained throughout a test by constant attention to the various controls.

The search hole was set in a position about 1/4" in front of the nozzle entrance and the test commenced by reading the pressure registered on the gauge K. This was repeated at intervals of .05" until a point about 1/4" behind the nozzle exit was reached. Time was allowed at each position for a stable pressure reading to be reached, and the complete search lasted about four hours.

The probable reason for the time taken by the pressure to reach a steady value is seen from the following considerations. The pressure from the 1/32" diameter search hole is transmitted to the pressure gauge through a medium, formed partly of water and partly of steam according to the surrounding temperature which fills the tube R. A change in position of the search hole will alter the temperature distribution along tube R and thus upset the equilibrium between steam and water. Either a quantity of water will evaporate or a quantity of steam condense. A change in pressure is thus caused within the system and this altered pressure may or may not be equal to the pressure in the stream at the
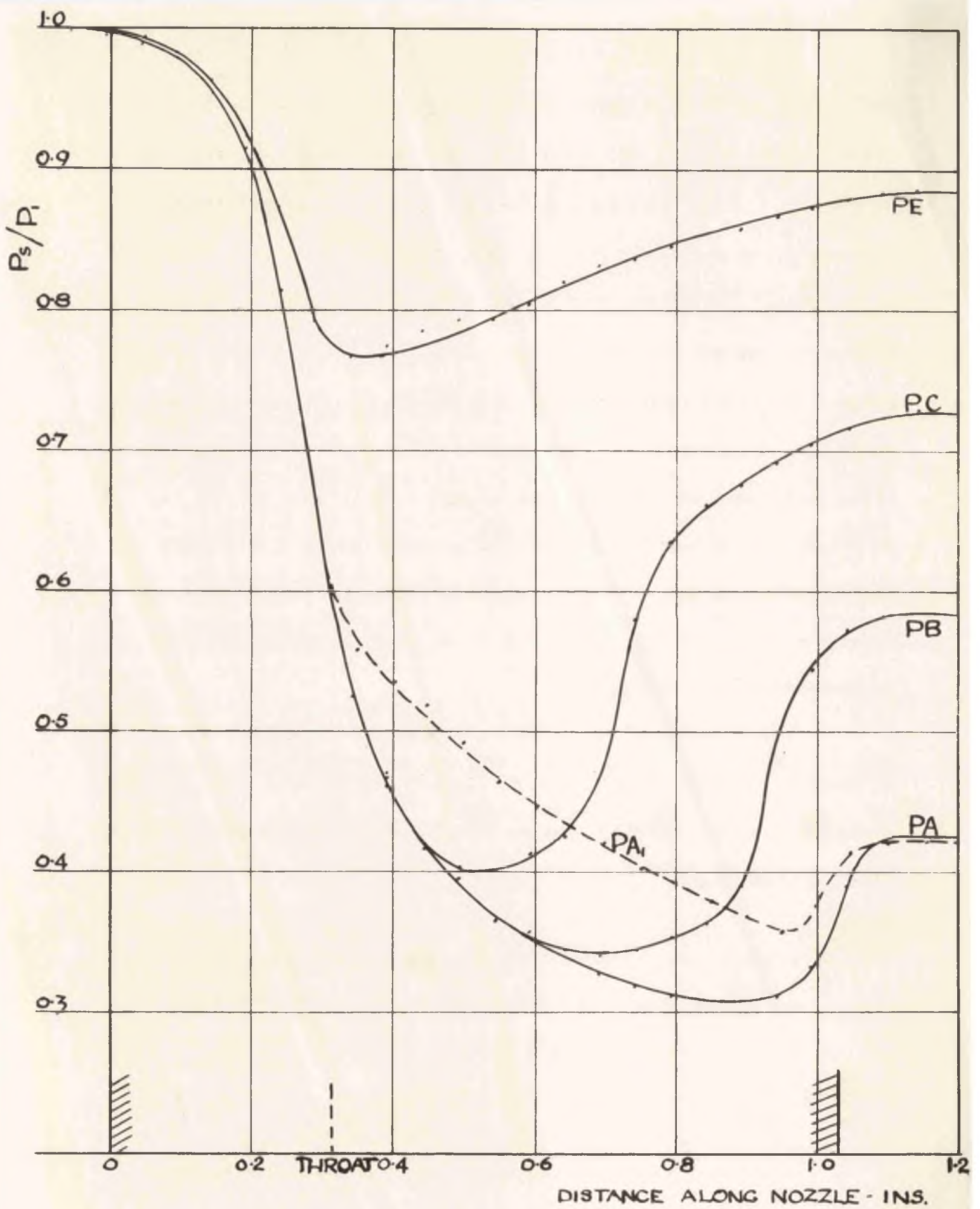
Fig. 16 PRESSURE RATIO P_s/P_1, SERIES PA, PB & PC.

position of the search hole. If unequal, equilibrium is attained by steam passing through the 1/32" diameter hole until the pressures are equalised. Since this hole is small and the pressure difference is also small, considerable time is taken for the final steady state to be reached. It was found when the search hole was moved rapidly from a position behind the nozzle to a position in front, the reading on gauge K was considerably higher than the supply pressure as read by gauge G. This was doubtless caused by the greater length of tube R being surrounded by steam in the exhaust chamber causing the water to evaporate and so result in a rise of pressure until steam escaped sufficiently for equilibrium to be established. A period of about 10 minutes was found in most cases to be sufficient for the pressure to reach the final value.

The results of the pressure searches are plotted in the form of pressure ratios along the nozzle length in Figs. 16 and 17. The curves are marked with the serial letters which denote conditions as shown in Table 2.

Table 2.

Letter	Supply Pressure lb./sq.in. Gauge.	Back Pressure lb./sq.in. Gauge.
PA	20	0
PB	20	5
PC	20	10
PD	30	0
PE	20	15

The results shown were obtained with initial superheats of 120°F., which ensured that the entire expansion took place in the

FIG.17. PRESSURE RATIO P_s/P_1, SERIES P.D.

THROAT

DISTANCE ALONG NOZZLE - INS.
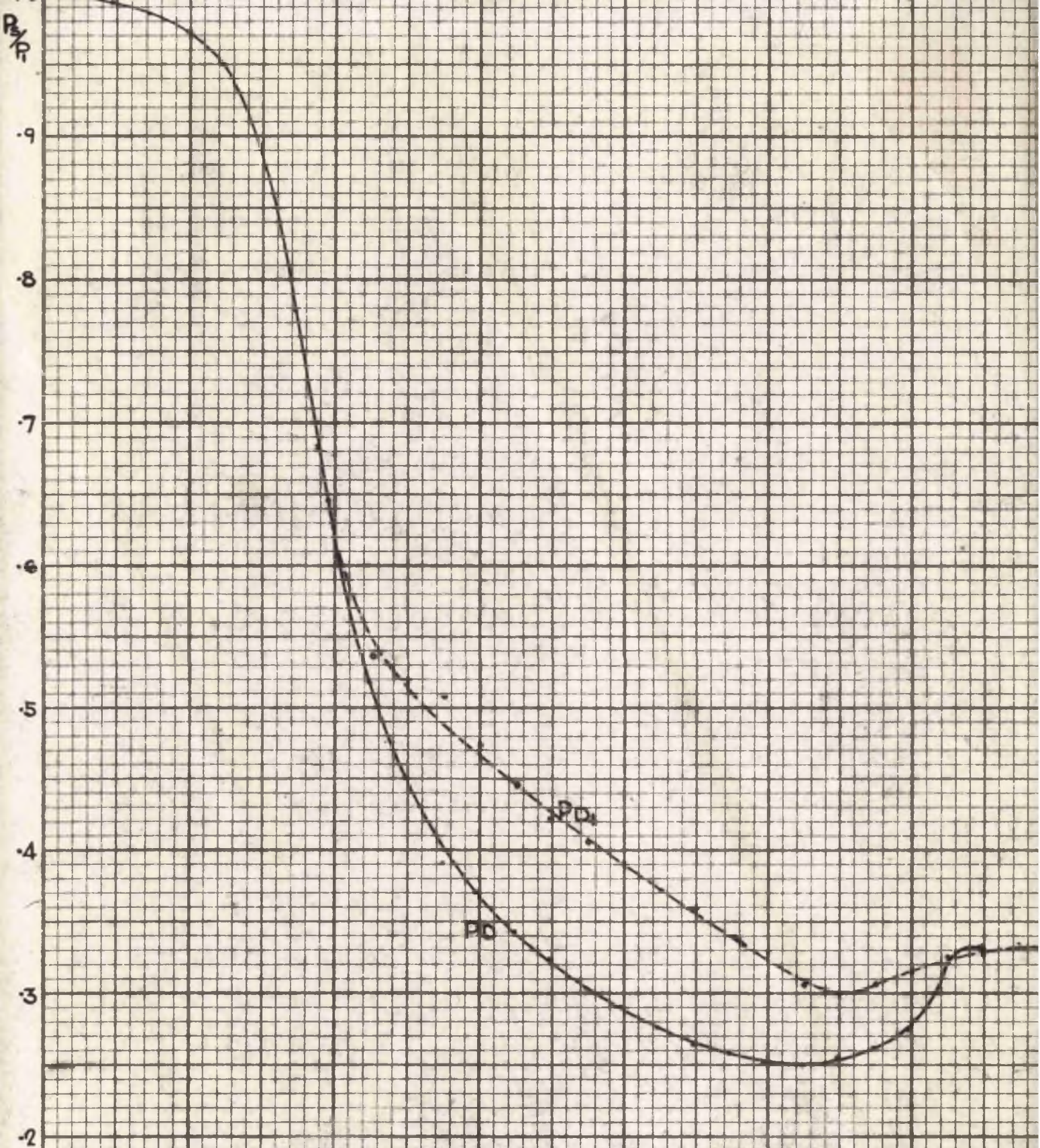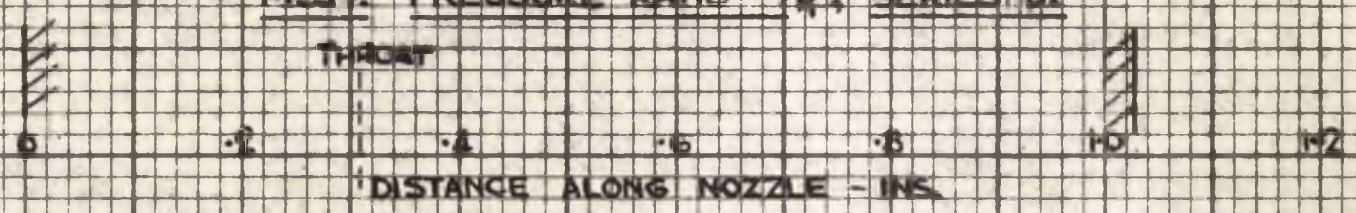
superheated field. When these results were checked using different
initial superheats (low enough in some cases for part of the expansion
to be supersaturated), no appreciable differences were found in the
pressures. This is in agreement with the findings of Mellanby and
Kerr (75) who showed that little or no pressure changes were apparent
over a temperature range of 150°F.

The only pressure differences recorded were with initially
wet steam. In these cases the bottom of the pressure ratio curve was
found to be much flatter and the expansion never attained such low
pressures as in the first cases. The divergence for wet steam is shown
for cases PA and PD by the broken lines marked PA, and PD respectively.
The significance of these results is discussed later.

The curves are of a well established form in each case. The
tests at 20 lb./sq.in. supply pressure show recompression occuring
progressively earlier as the back pressure is increased, while in case
PD only a small recompression occurs just before the nozzle exit. Curve
PE, Fig. 16, for 15 lb./sq.in. back pressure shows a condition at which
the critical pressure ratio is never attained during the expansion and
the pressure ratio curve is of a rather different form from the others
shown.

Procedure and Results of Temperature Searches.

The initial stages were similar to those in the pressure
searches. It was important, however, to ensure that the supply
temperature was perfectly steady whereas in the pressure tests it was
not important if the temperature varied by a few degrees. For this
reason much more time and care had to be given to the establishment of

a steady supply temperature, the time required usually being about three hours. Afterwards a limit of $\pm$ 1/2°F. was maintained by constant checking and adjustment of the control valves and gas taps. The maintenance of a steady supply temperature was much more difficult than the maintenance of a steady supply pressure. While any variation of pressure could be noticed immediately on the pressure gauge G and at once checked by adjustment of the valve causing an immediate return of the correct pressure throughout the system, a variation of heat supplied to the steam did not immediately become apparent at the thermocouple P, and an adjustment of the gas took some time to have the desired effect on the temperature of the supply steam.

Temperature readings were again taken at intervals of .05 in. and over the same range, except that in some cases readings were started 1 in. in front of the nozzle entrance to investigate irregularities in the initial readings. The average time taken to make a temperature search was about three hours, after attainment of steady conditions. Before a search tube reading was taken, the stagnation thermocouple was checked to ensure that the supply temperature was remaining constant at the correct value. With supply temperatures of less than 350°F. and using superheater 2 the establishment and maintenance of a steady temperature was achieved by time and care. With higher temperatures and superheater 1, chance variations were much greater and more frequent. The use of thermocouple Q helped, but though the temperature of the steam immediately after the superheater could then be maintained constant, the effects of variable losses in the pipe between the superheater and the control valve still remained. These troubles increased with increasing

FIG.18. TEMP. READINGS (T.w.) SERIES A.
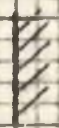
supply temperature, and tests attempted with greater superheats than those recorded had to be discontinued because of the large variations encountered in the supply temperature.

During each temperature search, the flow quantity was measured, at least three separate measurements being made, each lasting for about thirty minutes. The procedure was to measure the time taken for a known weight of condensate to collect in the tank. Timing commenced as the balance arm of the weighing machine swung gently upwards through the central position when set for the first weight and stopped as it swung upwards when set at the second weight. The flow quantities thus obtained are given for each test in Table 4.

The temperatures obtained, being those of an adiabatic wall, are shown in Figs. 18 - 21, plotted against the distance from the nozzle inlet. The tests represented are listed in Table 3.

Table 3. - Temperature Searches.

Pressure Conditions.	Test.	Supply Temp. °F.	Search Tube No.
PA	1	394.5	1
	2	381.75	5
	3	339.0	1
	4	306.0	3
	5	260.0	5
	6	260.5	2
PB	1	394.0	1
	2	367.0	2
	3	340.0	2
	4	306.0	3
PC	1	397.5	2
	1	427.5	3
	2	374.5	3
	3	347.0	3
	4	311.25	4
	5	276.0	4
	6	274.0	4
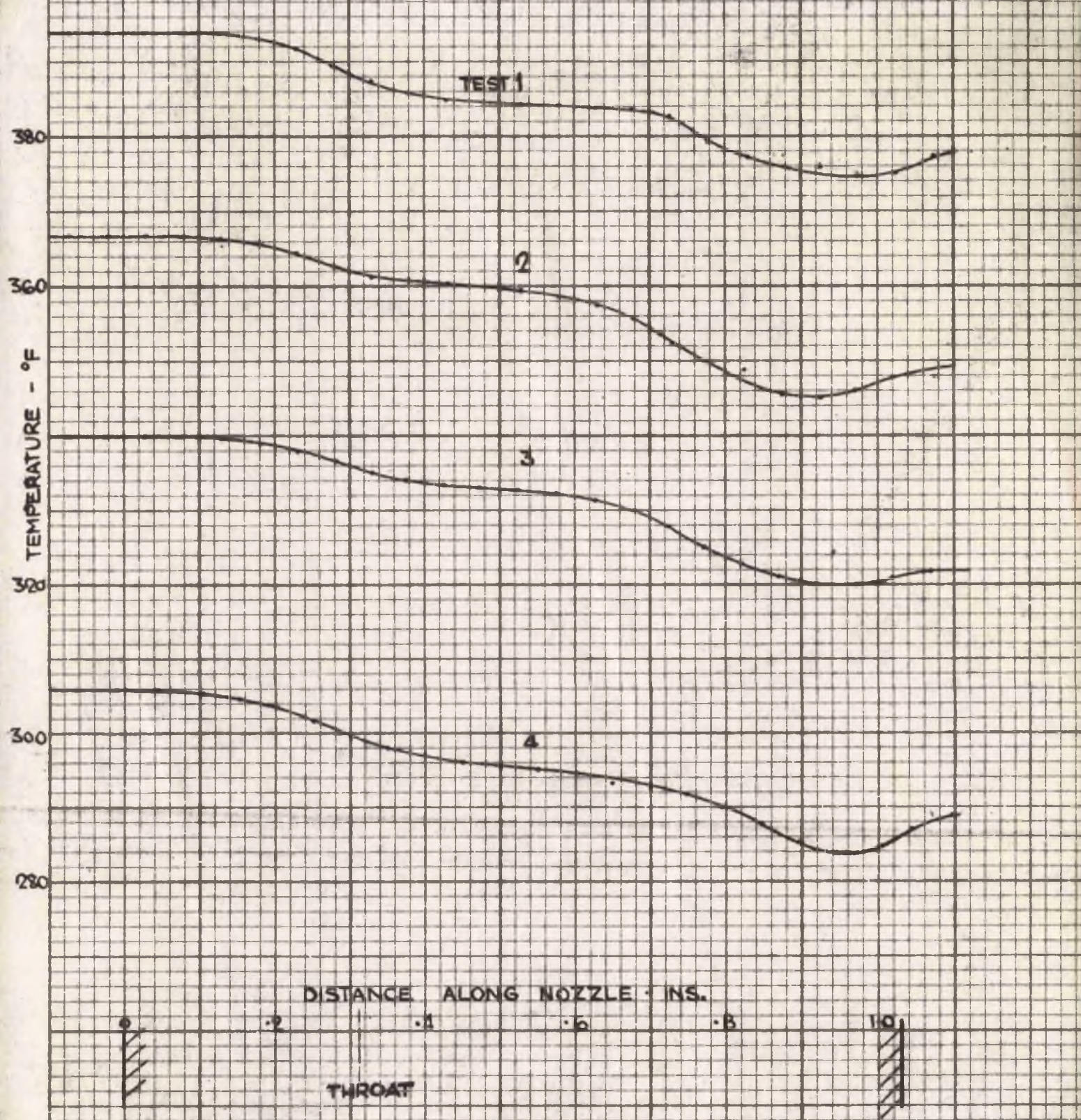
FIG. 19. TEMP. READINGS (tₐw) SERIES PB.

FIG 20. TEMP READINGS (t max)
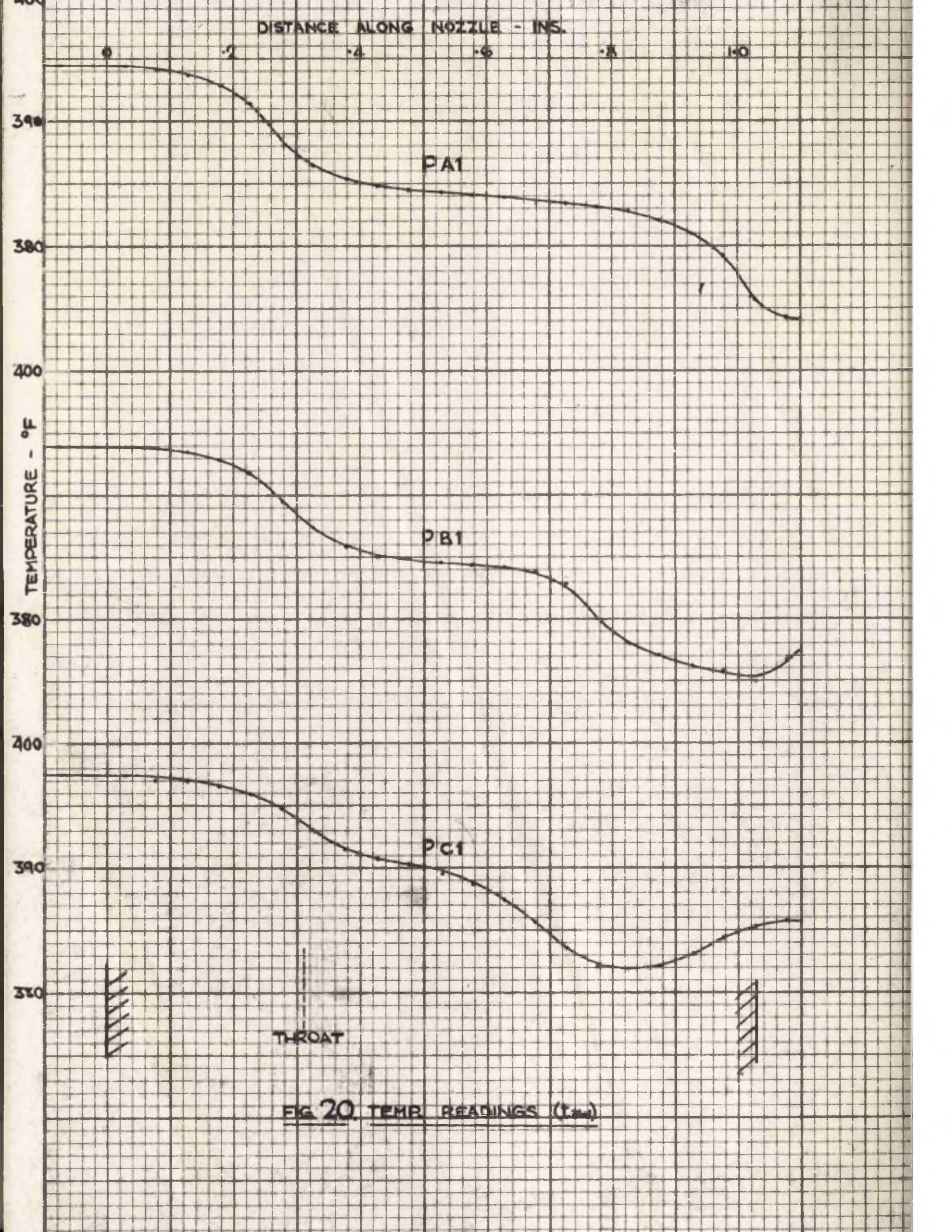
In Fig. 18 are shown the temperature variations for tests of the series PA. Tests 1, 2, 3 and 4 exhibit similar characteristics. The temperature drops from the stagnation value at the nozzle inlet gradually at first, more steeply in the throat region and then more gradually again in the divergent portion of the nozzle. Some distance before the nozzle exit the temperature again drops steeply and then gradually levels out at the exit. The general shape up to the second large gradient is as may be expected from consideration of the stream temperature variation (see Fig. 24). This large drop, however, occurs as the stream temperature begins to rise as a result of recompression. It can be seen to start in these four cases between 0.9 and 0.95" from the nozzle entrance. Reference to the pressure ratio curve PA, Fig. 15, 16/ shows that recompression commences in this region i.e. about 0.93" from the nozzle inlet.

Fig. 19 shows the readings for the four tests of series PB. Here the temperature variation is the same as in series PA up to between 0.65" and 0.7" from the nozzle inlet, where a second large drop of the same form as noted above occurs. After this earlier reduction in temperature the curves tend to rise once more. From Fig. 16 it is seen that recompression commences in case PB at a point distant 0.69" from the nozzle inlet, again corresponding closely with comparatively large temperature drops.

Fig. 20 shows the only test in series PC along with tests PA1 and PB1 plotted to a larger scale. In this case the second temperature drop starts at 0.52" from the nozzle inlet, corresponding to recompression at 0.54". The temperature curve makes a partial recovery after the
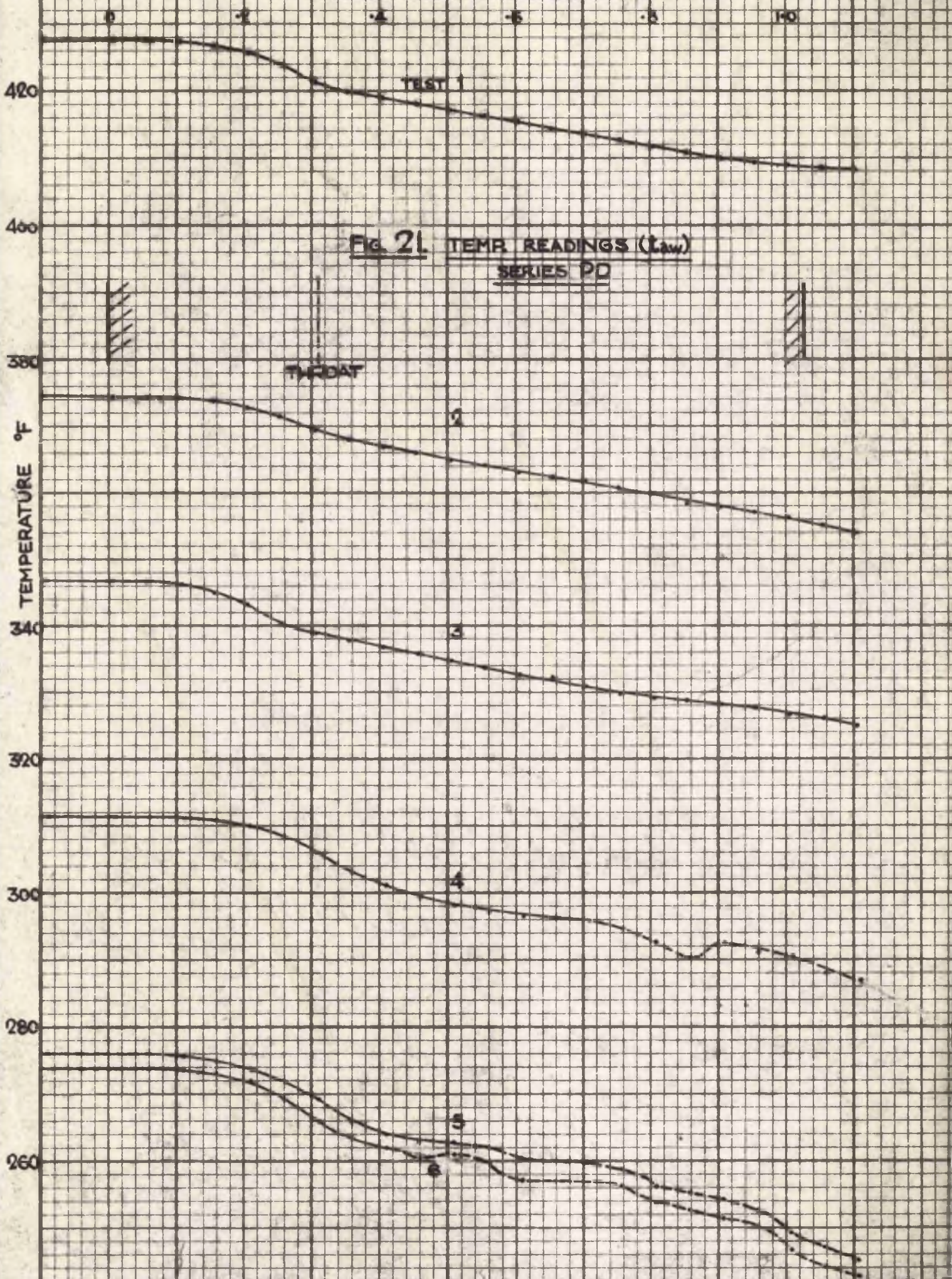
FIG 21 TEMP READINGS (t.a.w.)
SERIES PD

recompression drop, becoming almost horizontal at the nozzle exit. These three tests, which have the same supply pressure and approximately the same temperature, show clearly the effects of varying the back pressure on the adiabatic wall temperature. In addition to the progressively earlier breakdown of normal temperatures, all the temperature gradients are lessened with increase in back pressure.

Fig. 21 shows the tests in series PD. Here, with only a very small amount of recompression just before the nozzle exit, no effect is visible in the adiabatic wall temperature curves of tests 1, 2 and 3 and the moderate temperature gradient of the divergent part of the nozzle is nearly constant over this whole length.

Temperature measurements were also attempted at pressure condition PE. In this case the changes in temperature recorded were very small and it was difficult to distinguish the smaller gradients with the method of measurement used. In addition the temperatures were relatively unsteady from the region of the throat onwards. Experiments with this pressure distribution were therefore discontinued.

Tests PA5, PA6, PD4, PD5 and PD6 were all made with steam initially dry or only slightly superheated. They all exhibit peculiarities of adiabatic wall temperature variation. In all cases except PA5, the temperature begins to drop more rapidly than usual after a part of the nozzle beyond the throat is reached, with incidental variations in temperature of a size not encountered in the tests previously discussed. Up to this point, which varies from 0.43" to 0.70" from the nozzle inlet the curves are precisely the same as for the tests already discussed. The portions of the curves thus affected are

DISTANCE ALONG NOZZLE - INS.

a.

b.

c.

THROAT
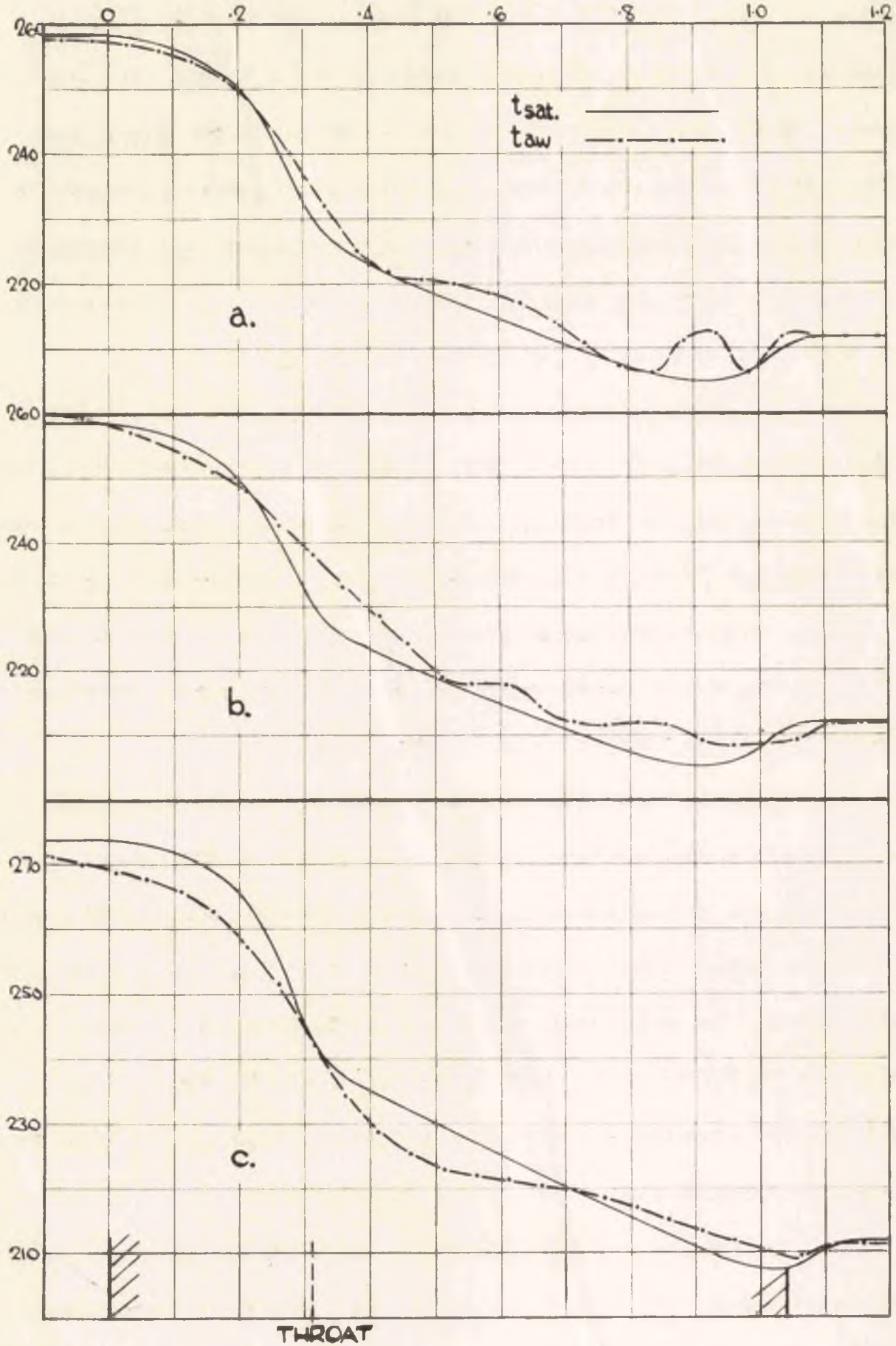
FIG. 22. WET STEAM TESTS.

shown in Figs. 18 and 21 by broken lines. In test PA5, the temperature, after a normal variation up to 0.44" from the nozzle inlet, rises above the usual type of curve until the stagnation temperature is almost reached. At this point, having reached the region of recompression, the temperature falls steeply through the remaining part of the nozzle. The reasons for these phenomena depend on the interpretation of the stream conditions.

In order to study the effects of suspended water particles in the steam stream, some tests were made in which initially wet steam was expanded through the nozzle. In these tests the superheaters were not used, and the pressure was reduced to a large extent by throttling at valve A. The steam becomes gradually wetter in the system owing to heat losses, and the small pressure drop across valve C necessary for control does not dry the steam excessively.

Fig. 22 shows the results of three such tests. a and b were both tests at 20 lb./sq.in. gauge supply pressure and atmospheric back pressure, the former made with a Sindanyo search tube and the latter using the brass tube. Test c was made at 30 lb./sq.in. gauge pressure and atmospheric back pressure using a Sindanyo search tube. In each case the adiabatic wall temperatures are shown joined by a broken line and the corresponding saturated steam temperatures (calculated from pressure searches PA_1 and PD_1) by a full line.

In all cases the temperatures recorded in the inlet portion of the nozzle were below the saturation values corresponding to the pressures previously obtained. This difference is as much as 7°F. in case C and persists until more than halfway through the nozzle. In the

DISTANCE ALONG NOZZLE - INS.

TEMPERATURE - °F

BRASS TUBE

TEST PB3

THROAT
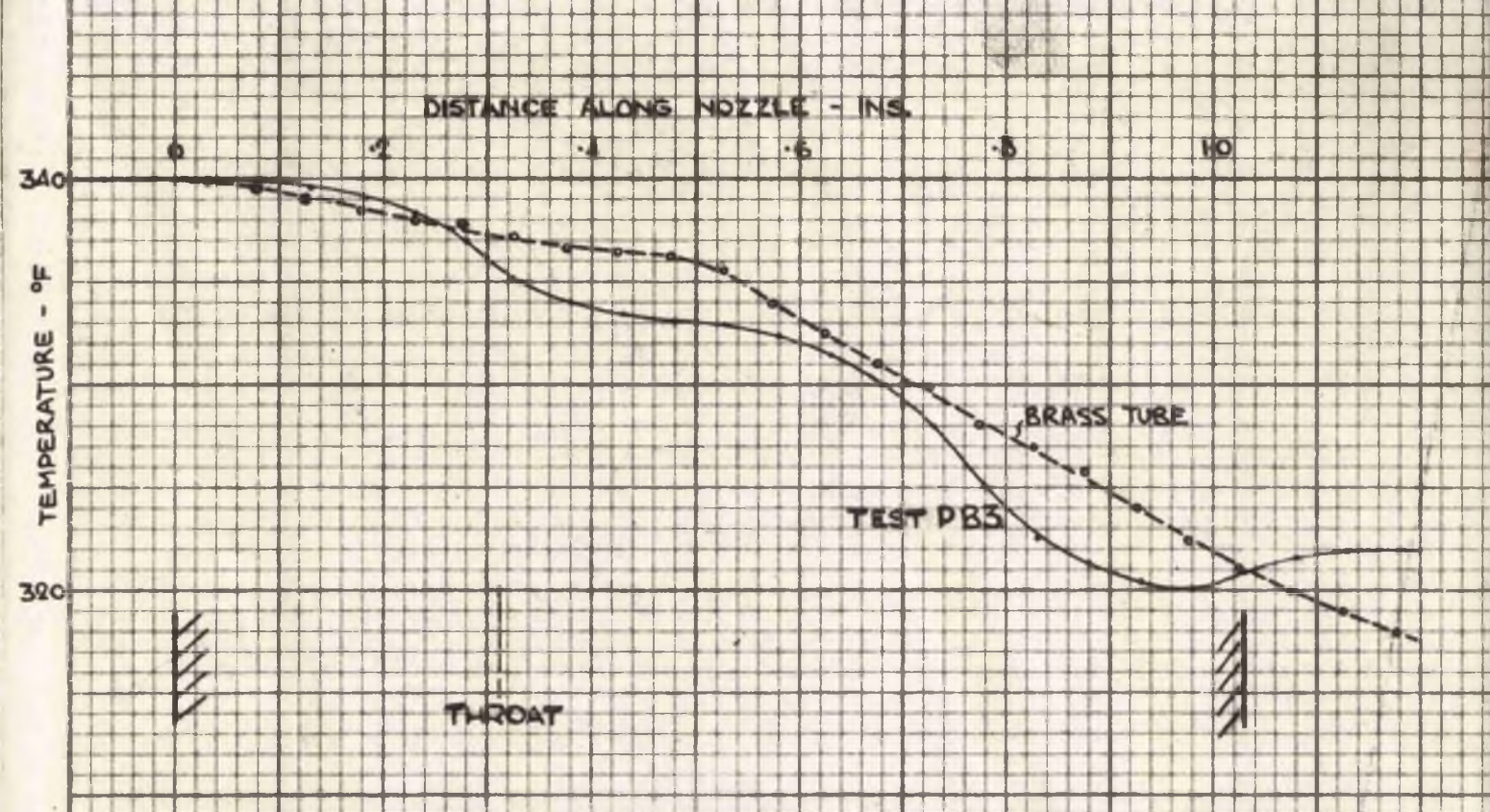
FIG 23   TEMP READINGS (t₃ᵤ)
FROM BRASS SEARCH TUBE.

divergent part of the nozzle the temperatures recorded were generally higher than the saturation values, only falling to them at isolated parts until after the nozzle exit. Unstable temperature readings were found to be a feature of this two phase type of flow, and often average readings had to be taken from the potentiometer.

When the readings below the saturation values in the inlet portion of the nozzle were obtained, the pressure gauges were checked while still hot, but no differences from the previous calibrations were found. The valves C and J were then closed simultaneously, bringing the steam within the system to rest at a pressure of 20 lb./sq.in. When the flow had stopped, the search tube thermocouple recorded the saturation temperature corresponding to this pressure. Again, the stagnation thermocouple gave readings below the saturation temperature under the same conditions of flow. It was therefore concluded that these readings were a feature of the flow in the system.

Readings from the Brass Search Tube.

In Fig. 23 it is seen that the readings from the brass search tube compare closely with those made with the Sindanyo tube, though there is evident a reduction in the temperature gradients at all points throughout the length. Owing to the erratic results obtained for the wet steam tests, this comparison was not considered satisfactory, and therefore a test was made with pressure conditions PB and a supply temperature of 340°F. The broken line in Fig. 23 shows the readings obtained in this test, while for comparison is shown test PB3 which was made with the usual Sindanyo tube at the same conditions of temperature and pressure. In this case the net temperature difference across the

nozzle is greater (70°F.) than in the wet steam test (46°F.) and conduction from the tube ends might be considered to have more effect. It will be seen that the resulting variation bears no resemblance to that obtained by the Sindanyo tube, none of the now familiar effects being reproduced. It would be difficult to estimate the precise effect of tube conduction at any point. As well as the obvious amount of heat transmitted between two points on the tube, there would be heat transmitted to or from the steam as a result of the higher or lower wall temperature which in turn would affect the temperatures of succeeding portions of the wall. The use of this tube was discontinued in view of the difference in results from the Sindanyo type of tube. It is probable that the conduction effects could be neglected if the expansion was such that smaller temperature gradients were encountered. The advantage of such a search tube would be that high pressures could be used and there would be no erosion effects as in the Sindanyo type of tube.

Flow Quantity Measurements.

The flow quantities obtained by weighing the condensate are tabulated below, both for initially superheated and initially wet steam tests. The theoretical values of mass flow, calculated on the assumption of isentropic expansion, are shown for initially superheated and dry steam. These calculations are based on the cross-sectional area at the throat. Since this is near the entrance the boundary layer is thin and has only a small effect on the calculated flow quantities. In tests employing initially wet steam, such evaluation is not possible as the fraction of moisture in the mixture is unknown. In such cases the flow quantities

serve as a qualitative indication only of the steam condition.

Table 4.

Test.	m (actual) lb./min.	m (theor.) lb./min.
A1	1.295	1.316
A2	1.317	1.325
A3	1.332	1.351
A4	1.386	1.393
A5	1.428	1.430
A6	1.410	1.428
B1	1.309	1.316
B2	1.294	1.338
B3	1.322	1.360
B4	1.377	1.392
C1	1.290	1.314
D1	1.658	1.663
D2	1.732	1.722
D3	1.729	1.750
D4	1.778	1.802
D5	1.832	1.840
D6	1.820	1.840

Wet steam tests

Fig. 21a	1.707
Fig. 21b	1.493
Fig. 21c	2.046

The experimental results for superheated steam are seen to be of normal order with the coefficient of discharge varying from 0.967 to 1.005.

ANALYSIS AND DISCUSSION.

Stream Conditions.

The first stage was to calculate the variation of the steam condition along the nozzle during the expansion. To do so, the stream temperature was evaluated at ten points throughout the length, the positions of these, a, b etc., being shown in Fig. 15. In the evaluation of the stream conditions for any point, the specific volume was first obtained from the solution of the quadratic equation 69, (p. 61) presented in Part I.

The nozzle diameters at the specified sections were obtained from the geometry of the profile and the required areas calculated therefrom, subtracting that occupied by the 1/4" diameter search tube.

During each test, the barometric pressure was recorded and so the absolute supply pressure evaluated. From this and the pressure ratio curves, the absolute pressures at the sections noted were calculated.

The constant temperature recorded by the search tube for the region explored before the nozzle was taken as the temperature of the steam at rest i.e. the total or stagnation temperature t_t. Calculation shows a typical pipe velocity at this part to be 6.5 ft./sec. which is low enough to be neglected. The kinetic energy can be considered negligible in comparison with the enthalpy for the region before the nozzle. From the supply pressure and temperature, the enthalpy H was obtained by interpolation in the superheated steam tables of reference 59. The flow quantity m, measured during the tests, completes the data necessary for the solution of the equation.
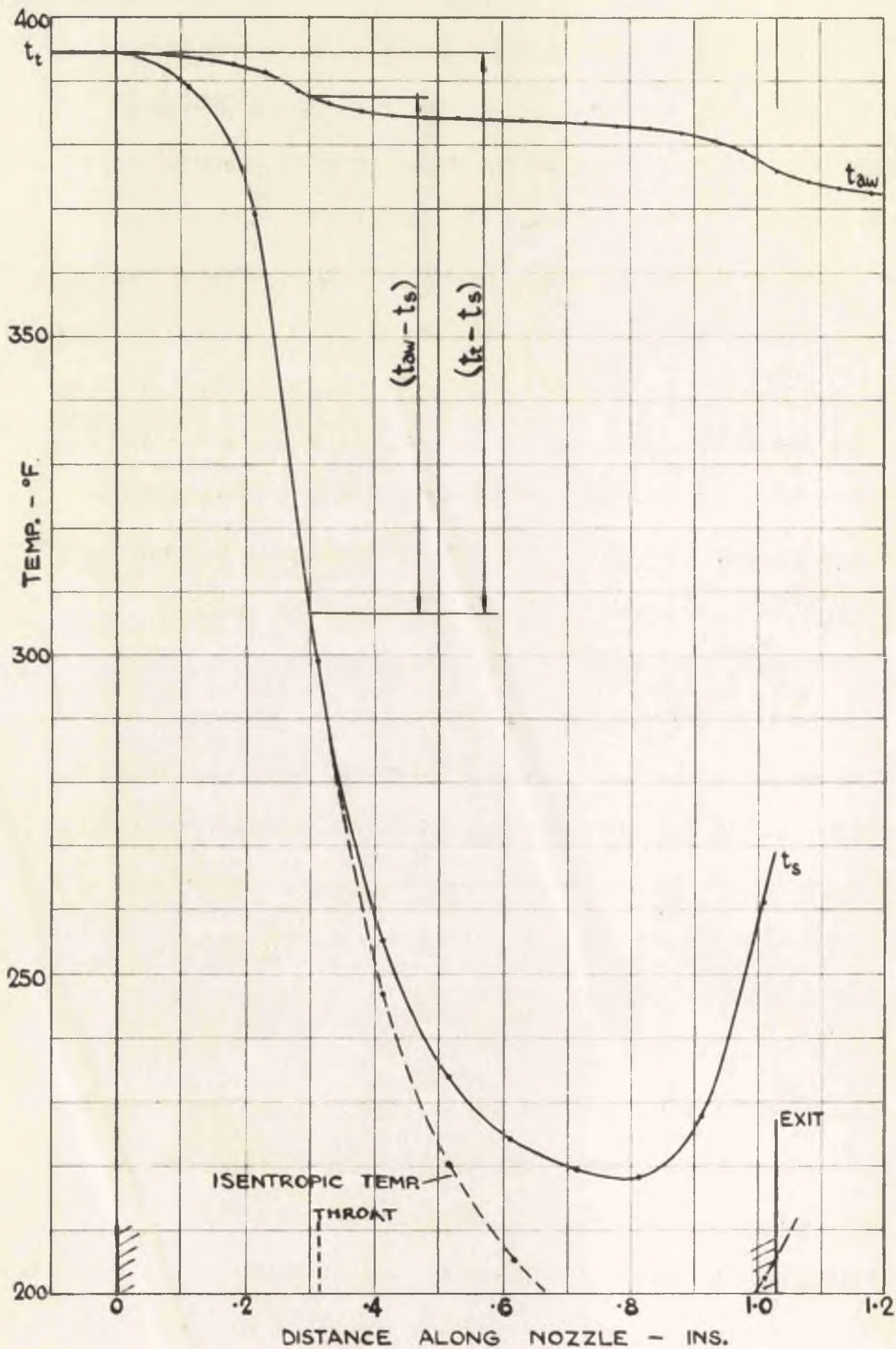
FIG 24 TEMP. DISTRIBUTION, TEST PA1.

When the specific volumes had been obtained by solution of
this equation, the temperatures were evaluated by interpolation at
the calculated pressure in the steam tables. The temperatures were
then plotted against the nozzle length to ensure that they gave a
consistent form for the expansion. Such forms may be seen in Figs.
24 and 25. It was found that the stream temperature obtained by this
method was almost the same as that for isentropic expansion up to the
throat, after which the actual stream temperature rose above that
corresponding to frictionless adiabatic conditions. Accordingly the
procedure was slightly modified in that the temperatures for sections
a, b and the throat were obtained by interpolation for constant
entropy in the steam tables, and the others as before.

The methods available for the estimation of the steam
temperatures when the expansion produced supersaturated conditions were
also outlined in Part I. After trial, and comparison with results for
superheated steam, the Goudie charts were discarded. The temperatures
were then estimated from both the Stodola chart and the equation $PV = 85.8T$. By plotting all results against the nozzle length the best
estimate was obtained.

The temperatures thus obtained are mean temperatures over the
cross-section as can be seen from the method of derivation from
equations 66 - 68, and are designated "mean, free stream".

The Calculated Values of Recovery Factor.

The local value of the recovery factor was evaluated at the
ten points along the nozzle length previously referred to, using the
equation
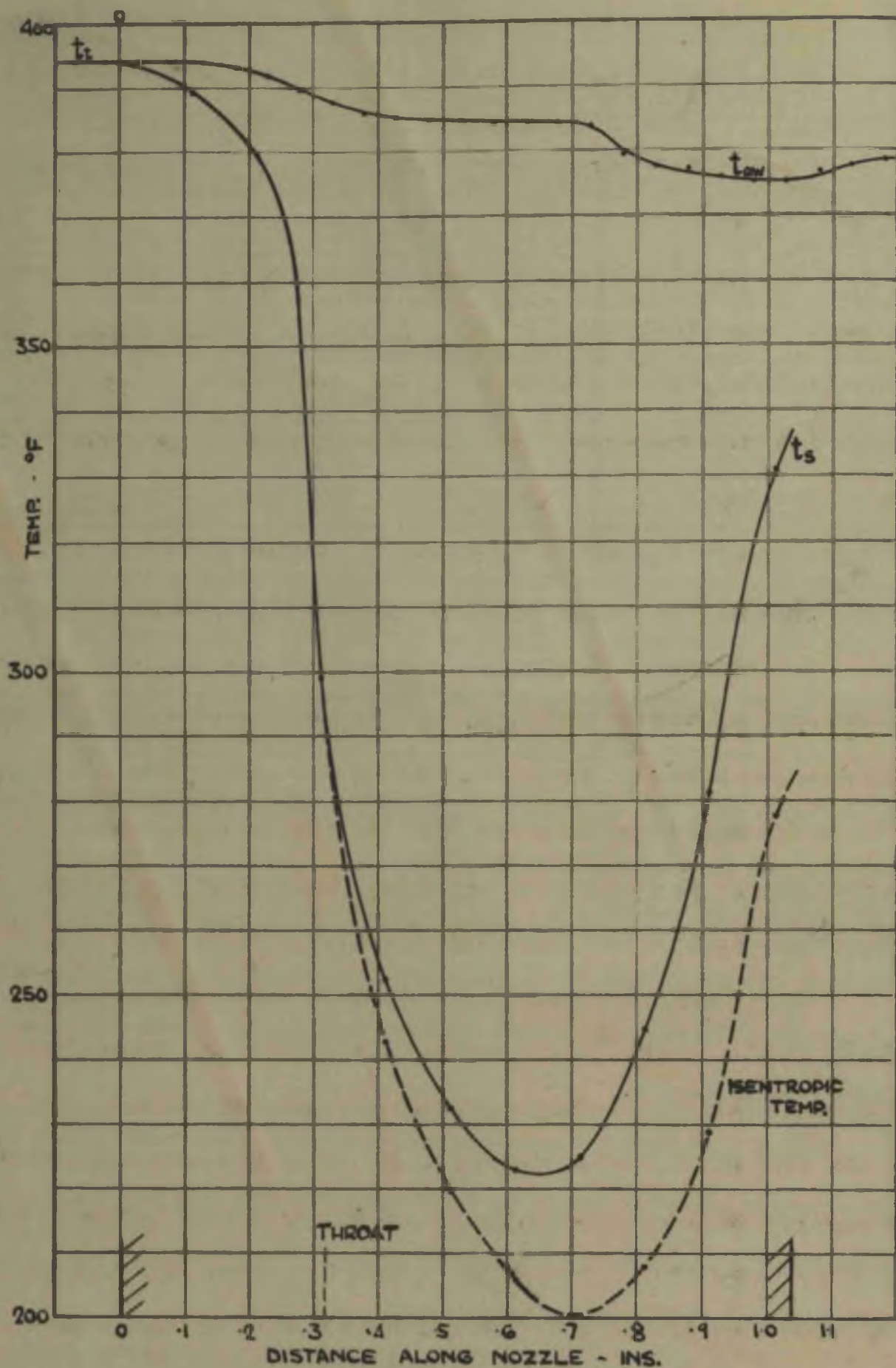
FIG. 25. TEMP. DISTRIBUTION, TEST PBI

$$\frac{t_{aw} - t_s}{t_t - t_s} = r$$

The values of the adiabatic wall temperature taw were taken from smoothed curves of the experimental data as shown in Figs. 18 - 21. The total temperature t_t used was the stagnation value measured during each test. The stream temperature t_s was the mean value obtained for the free stream calculated as shown above. The recovery factor thus obtained has been designated the "local-free stream recovery factor" by Rubesin and Johnson (47) to distinguish it from others obtained on different bases of temperature evaluation. The method relies on identical pressure variation in the pressure and temperature searches.

The temperature differences which constitute the ratio above are shown diagrammatically in Fig. 24. It can be seen that small errors in t_s have not nearly so great an effect on the recovery factor as have errors of the same order in taw or t_t. In the usual range of calculations 0.1°F. change in taw produces an effect on the recovery factor which would require about 1.5°F. change in t_s to cancel it.

The calculated values of the recovery factor are listed in Table 1a in the Appendix, and are shown plotted against the nozzle length for eleven of the tests in Fig. 26. The tests in series PA show the recovery factor curves rising in the convergent portion of the nozzle, flattening out between the throat and section d; gradually falling from d to g; and falling off sharply thence to section j, which is almost at the nozzle exit. In series PB the variation is similar, with the curves falling away very rapidly after section f and reaching the low value of 0.71 at the nozzle outlet. In curve PC the ascent is hardly

TEST PD1

PD2

PD3

PD4

TEST PB1

PB2

PB3

PB4

TEST PA1

PA2

PA3

PA4
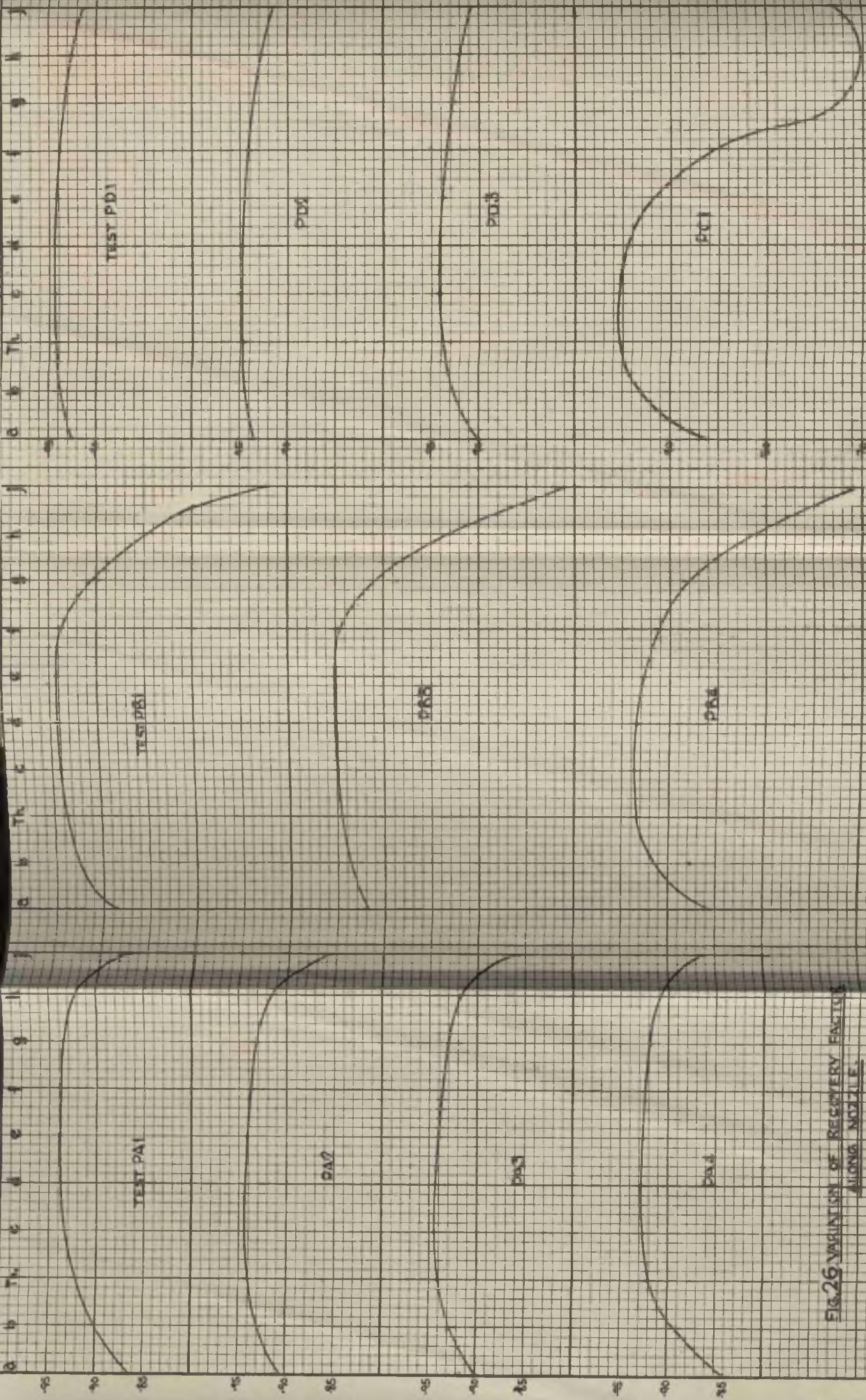
FIG.26 VARIATION OF RECOVERY FACTOR ALONG NOZZLE.

completed before the curve falls steeply to a similar low value, recovering slightly thereafter. These curves reproduce for the recovery factor the effect of earlier recompression previously noted for the adiabatic wall temperature curves. Series PD has a much flatter type of curve, with the large drop at the exit entirely absent, which again reflects the variation of the adiabatic wall temperature.

The lowered values of recovery factor at recompression is doubtless owing to a partial destruction of the boundary layer caused by the normal shock wave occurring under such conditions.

The more gradual fall of the recovery factor in the latter part of the nozzle is probably owing to the one dimensional method of obtaining the stream temperature. The recovery factor would doubtless remain constant if the stream temperature was the maximum temperature t_s and not the bulk temperature t_B. The difference between t_s and t_B will increase as the boundary layer thickens along the nozzle length.

The rise in the convergent portion of the nozzle is almost certainly owing to the build up of the boundary layer at this part.

A more complete examination must wait on the analysis of boundary layer conditions, and on the evaluation of the physical qualities and dynamical conditions which may affect the magnitude of the recovery factor. It is proposed to investigate these factors in the subsequent section of the discussion.

Evaluation of Pr. M and Re and Analysis of Boundary Layer Conditions.

A discussion on the Prandtl number for steam is given in Part I, where it was seen that this could be taken as 1.06 for the range of conditions encountered in the tests.

The local value of Mach number M was calculated at the sections of the nozzle previously used. The steam velocity was evaluated from the flow equation 67

$V = mv/a$ and the speed of sound from:

$$Va = (\gamma . gpv)^{\frac{1}{2}} \dots\dots\dots\dots\dots\dots\dots(76)$$

where γ, the mean isentropic index, was taken as 1.3 for superheated and supersaturated steam. The other quantities have been obtained previously.

In the calculation of Reynolds numbers, the values for viscosity were those given by Keenan and Keyes (59). The values listed in Table 6 were plotted on lines of constant pressure to a temperature base, and the resulting diagram extrapolated to the region of temperature and pressure required.

For the diameter Reynolds number, Re_D, it is necessary to substitute the equivalent diameter De for D in the equation $Re_D = \rho DV/u$. This is taken as four times the hydraulic mean depth of the annulus. The evaluation was made from the total wetted surface, as is customary in the calculation of fluid friction -

$D_e = D - D_t$, where D is the diameter of the nozzle and D_t that of the search tube.

As the growth and condition of the boundary layer are a function of the length of the body immersed in the fluid, the Reynolds number based on this length must be evaluated.

For the case of a flat plate, the Reynolds number Re_1 for any section is equivalent to $\rho Vx/u$, where x is the distance from the leading edge to the section considered. The thickness of the boundary layer, that

is the region which is affected by viscosity, is a function of Re so calculated, while the type of flow in this region, i.e. laminar or turbulent, is dependent on whether Re exceeds a certain critical value. In the apparatus used in these tests we are interested in the development of the boundary layer along the surface of the search tube, on which surface the adiabatic wall temperature was measured. The search tube has no true leading edge as the front portion lies in the inlet pipe where flow is very slow, and the real flow may be considered to commence only at the nozzle inlet, at which point it rapidly assumes very high velocities. The arrangement possesses the advantage that disturbances caused in the region of a leading edge are entirely absent in the boundary layer along the search tube. The nozzle inlet has been substituted for the leading edge in the calculation of Re_1 and x becomes the distance from the inlet to the section under consideration.

Some development of the boundary layer will occur before the inlet, but, on the other hand, a favourable negative pressure gradient has the effect of retarding the growth of the boundary layer. Such will be the case in the entrance region of the nozzle, where there is a sudden drop in pressure. It is therefore reasonable to take the nozzle inlet as equivalent to the leading edge of a flat plate.

Again, a favourable pressure gradient has a stabilising effect on the flow in the boundary layer. Thus, though a large degree of turbulence may be expected in the approach pipe, owing to the right angle turn in the receiver, the thermometer pocket, the coiled tube containing the thermocouple and the search tube guide, this turbulence will be damped by the sudden pressure drop at the entrance. The boundary layer

DISTANCE ALONG NOZZLE - INS.
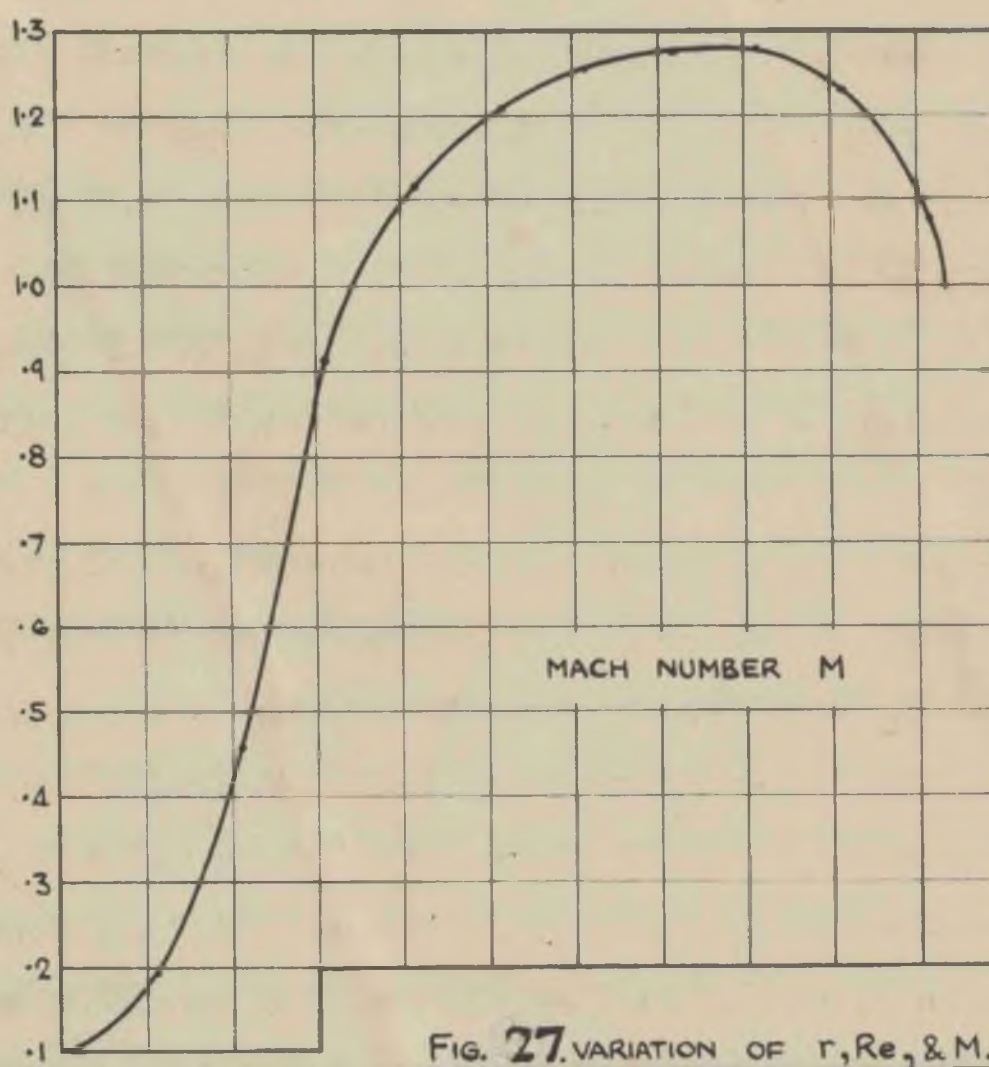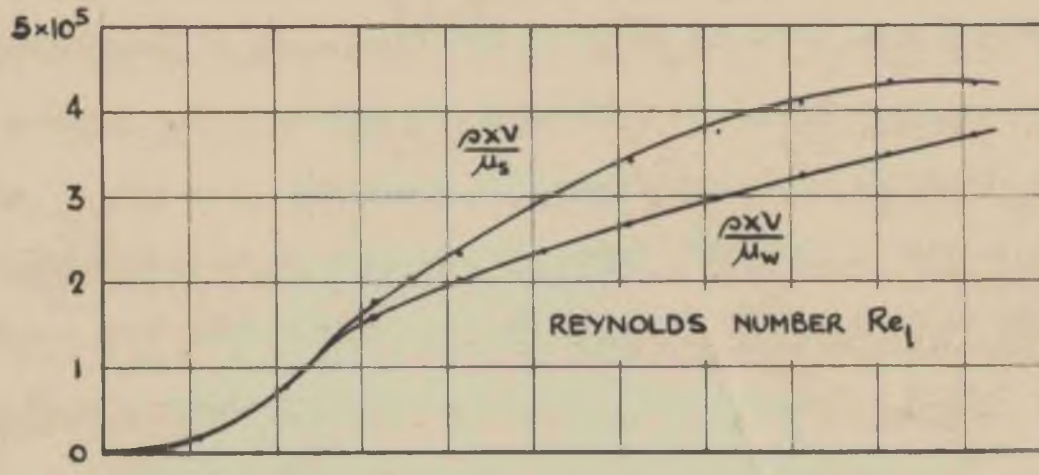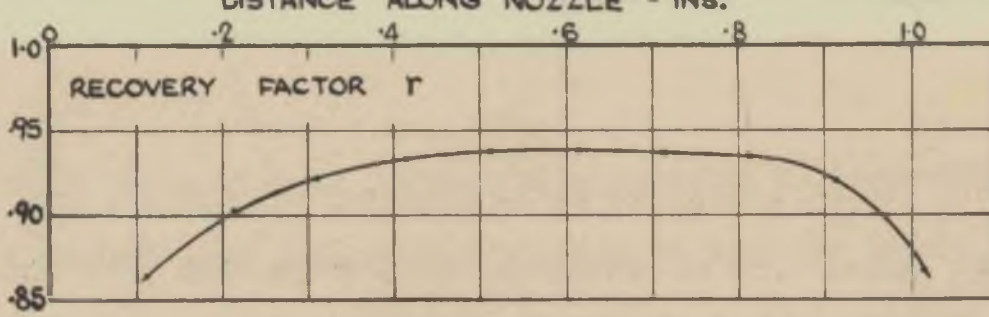
FIG. 27. VARIATION OF r, Re, & M.

TEST PA1.

will therefore start as laminar as is usual for flow over a flat plate. The critical length Reynolds number at which transition from laminar to turbulent flow takes place is also increased by a negative pressure gradient.   For flat plates the transition to turbulence in the boundary layer occurs between Re_1 = 9×10^4 and 1.1×10^6, the most usual value being 3×10^5 (33).   Flow within a nozzle or pipe will have the same order of critical value as for a flat plate, for the entrance region. In the present case, with the static pressure falling throughout the length, the critical Re_1 may be expected to have a value somewhat greater than this.

In previous heat transfer calculations the viscosity term in the dimensionless groups Pr and Re has been variously evaluated at the temperature of the stream, of the boundary film, or the boundary surface. In these calculations the free stream value of viscosity was used in evaluating Re, since all other factors in the groups are based on the free stream, and Re_1 as a criterion of dynamical similarity is always thus evaluated.

Fig. 27 shows a typical variation of recovery factor, length Reynolds number, and Mach number along the nozzle (for test PA1).   The variation of Re_1 based on stream viscosity is shown $\rho Vx/\mu_s$, as well as that obtained from viscosity evaluated at the surface temperature $\rho Vx/\mu_w$, to show the order of change effected by such a substitution. The film temperature is usually taken as $t_s + 0.5 (t_w - t_s)$, where t_w is the wall temperature.   As viscosity variation with temperature may be taken as linear within the range t_w to t_s the value of Re resulting from viscosity evaluated at such a frictional layer temperature would be midway
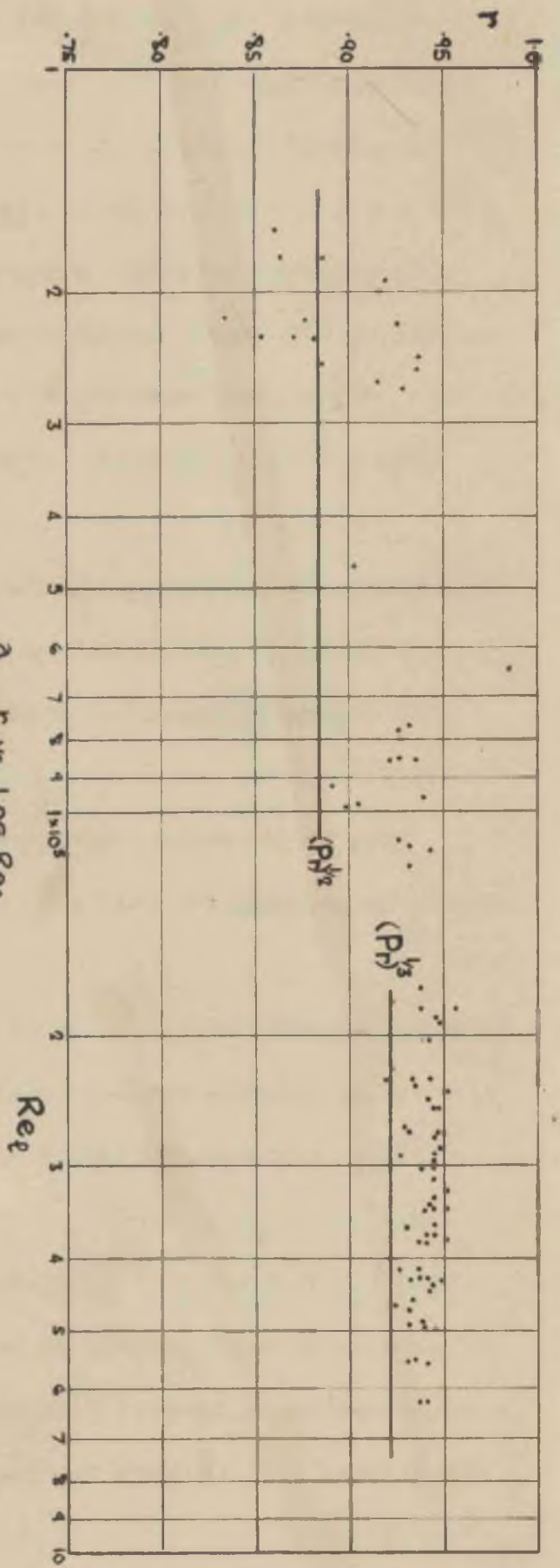
a. r vs. Log. Reℓ
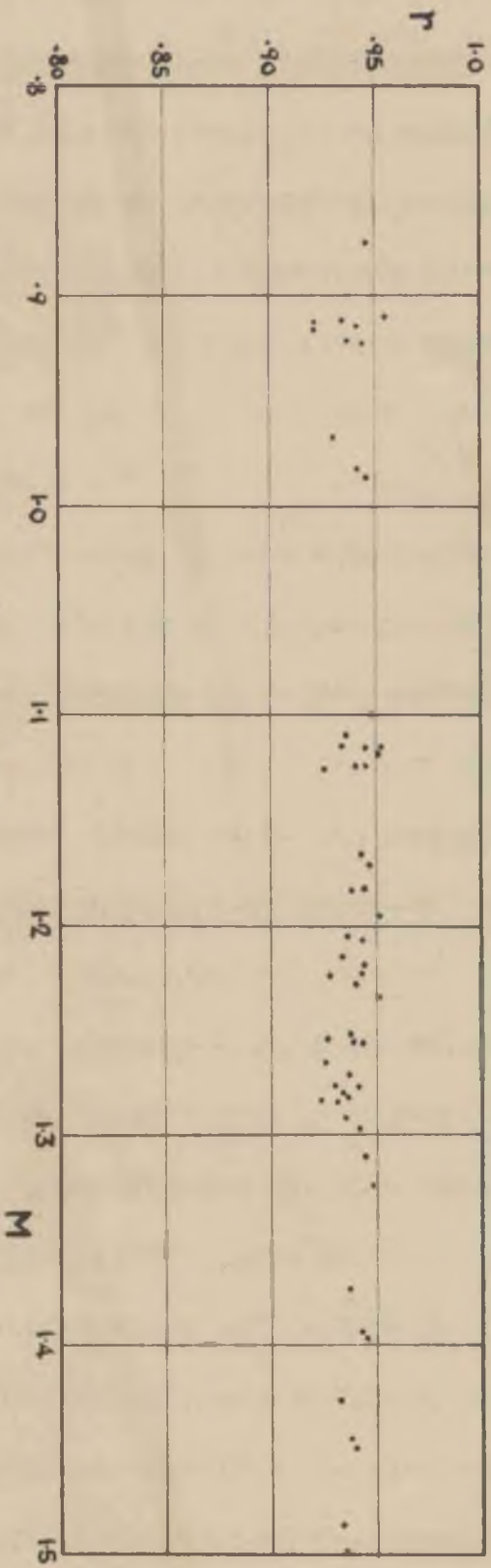
b. r vs. M

FIG. 28.

between the two values shown here.

The Reynolds numbers calculated on the basis of the equivalent diameter of the annulus D_e do not indicate the boundary layer conditions. The evaluation for test PA_1 showed Re_D varying from 38,500 at section a, through a maximum of 62,200 at e to 55,800 at j.

The Recovery Factor for Steam.

It is apparent from the behaviour of the adiabatic wall temperature and the value of recovery factor presented that recovery factors for steam flow are what may be expected from any normal gas i.e. the value is approximately unity.

The main variations of the value of r may be accounted for as far as they are influenced by physical considerations of an obvious nature.

In Fig. 28a are shown recovery factors plotted against Re . Values from sections near the nozzle exit which were judged to be affected by the shock wave occurring at recompression have been omitted. Up to a value of $Re_1 = 1.7 \times 10^5$ the results in Fig. 28a show a considerable amount of scatter. The results in this region all come from the convergent portion of the nozzle. The small temperature differences between the wall and the stream in this region lower the accuracy in the calculation of r considerably. Also, it is difficult to estimate the cross-sectional area in this portion.

For higher Re_1, the results are seen to be grouped about the line of r = 0.94. It has been seen that no transition from laminar to turbulent flow can be expected for Re_1 below 3×10^5 but rather that transition would occur at some higher value. There is no apparent

discontinuity in the value of r over the range of Re_1 shown in Fig 28a. It appears therefore that the value of 0.94 would represent the value of r for laminar flow in the boundary layer.

As soon as recompression occurs in the divergent portion of the nozzle, the values of recovery factor were found to drop sharply.   Since this occurs in all cases at a value of Re_1 which is above the critical for flow over a flat plate with zero pressure gradient, it is apparent that the large adverse pressure gradient will cause an immediate transition to turbulence.   In the case of the nozzle, therefore, the transition to turbulence does not depend on the value of the length Reynolds number, but rather on the conditions which cause recompression to occur.   Lower values of r are therefore found to hold for the turbulent boundary layer.   The values obtained do not assume a constant value but evidently correspond to a transition region.   They cannot be considered reliable as the normal shock wave occurring at recompression is liable to cause separation of the flow.   This would probably have the effect of further decreasing the value of r.   It can only be stated that the value of r for turbulent flow is lower than that for laminar flow.

The values of recovery factor were obtained from too restricted a range of conditions to make further analysis of the results conclusive. A more extensive range of expansions would have to be used in order to produce more variation of Mach and Reynolds numbers.

In attempting further evaluation of the relationship

$$r = K(Pr)^a \ (M)^b \ (Re)^c$$

the term $(Pr)^a$ was assumed constant which is the case for the conditions encountered in the tests.   A value of Mach number was then chosen at
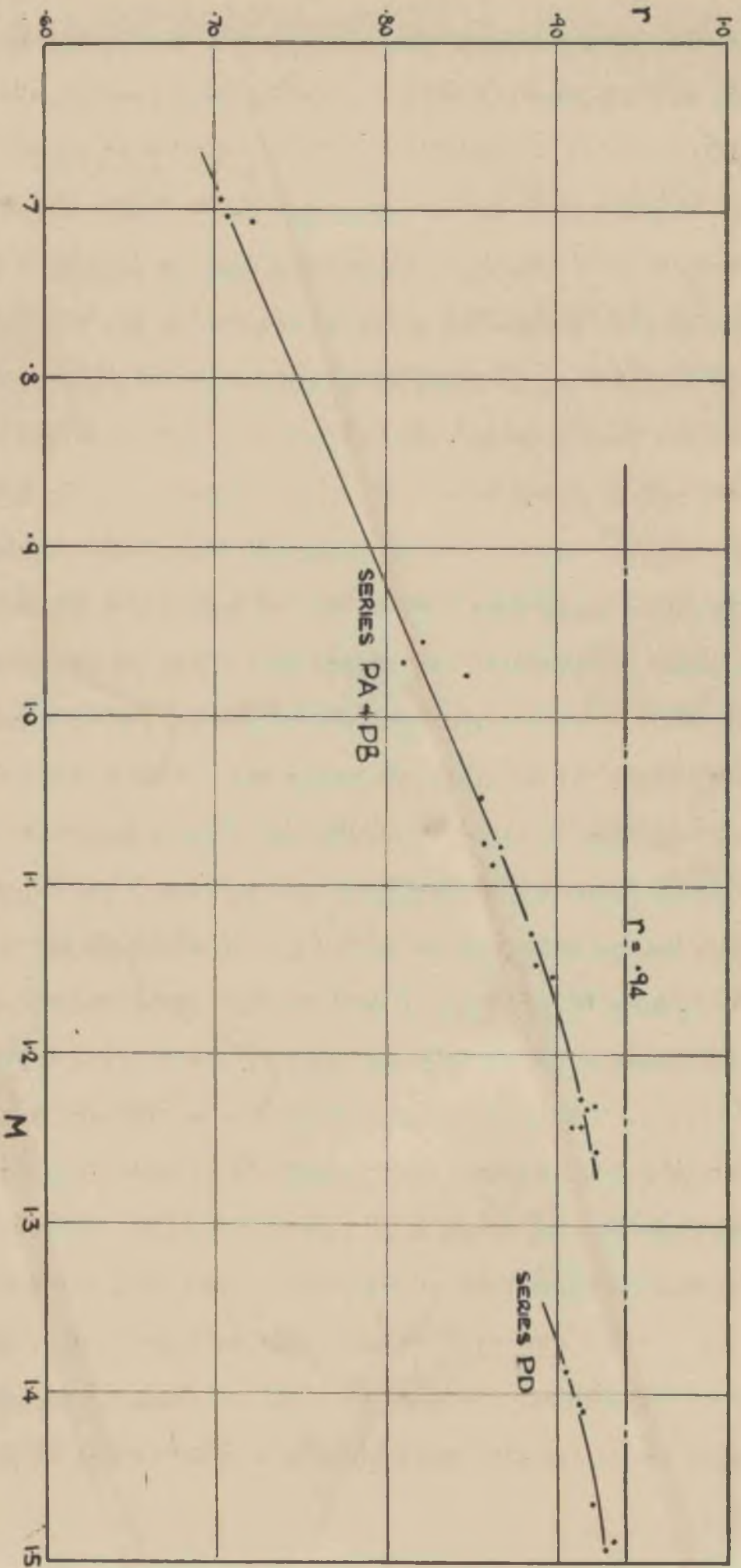
Fig. 29. VARIATION OF RECOVERY FACTOR
AFTER RECOMPRESSION.

which reliable values of r were obtained in all cases viz. M = 1·2.
The value of recovery factor and Reynolds number corresponding to M = 1·2
was then obtained for each test (from graphs as in Fig. 27). The results
were so scattered and from such a constricted range of Re that further
analysis was obviously futile. In the absence of such definite results
as would thereby be obtained the influence of Mach and Reynolds numbers
can only be estimated qualitatively.

Fig. 28b shows the values of recovery factor obtained for laminar
boundary layer conditions plotted against the corresponding Mach numbers.
The variation of Re is ignored, Pr being assumed constant. The values
can be seen to lie about the line of r = .94 with a maximum variation of
2.0%. As far as can be seen, Mach number has no influence at all in the
laminar range. The constant value for all Mach numbers is in agreement
with the results obtained by Eckert and Weise (26) and Ackermann (1).
It differs from those of Kraus (65) who found higher values which varied
with M and also from those of Kaye, Keenan and McAdams (54) who found
lower values which varied with M.

In the case of turbulent flow for the sections after recompression,
a variation of recovery factors with Mach number was found. A decreasing
Mach number produces a rapidly falling recovery factor which assumes very
low values. If the values obtained after recompression for series PA and
PB are plotted to a base of Mach number they give the same characteristic
as that obtained in reference (54) for flow in a pipe. This is shown in
Fig. 29. The curve is not of universal application, however, and is only a
phenomenon of the change in Mach number taking place under these conditions.
The comparable values for series PD where the reversal takes place at a

different value, follow a separate curve.

The constant value of 0.94 obtained for the recovery factor in the laminar boundary layer region cannot readily be made to substantiate the theroetical value of $(Pr)^{\frac{1}{2}}$. If Pr is taken as 0.78 as given by McAdams (72) for steam, then $(Pr)^{\frac{1}{2}}$ is 0.883 and the experimental values are far higher than this. However, latest measurements of the properties of steam lead to a value of Pr nearly equal to 1. Then values of recovery factor should also be unity, while both Shirokow's (90) equation;
$r = 1 - 4.55 (1 - Pr)Re^{-0.2}$, and Ackermann's (1) equation of $r = (Pr)^{\frac{1}{3}}$ would also result in a value of unity for the recovery factor for the turbulent boundary layer. The observed values of recovery factor are thus seen to be lower than the theoretical values by about 6% for laminar conditions and even more so for turbulent conditions. Reliable values for the latter have not however been obtained.
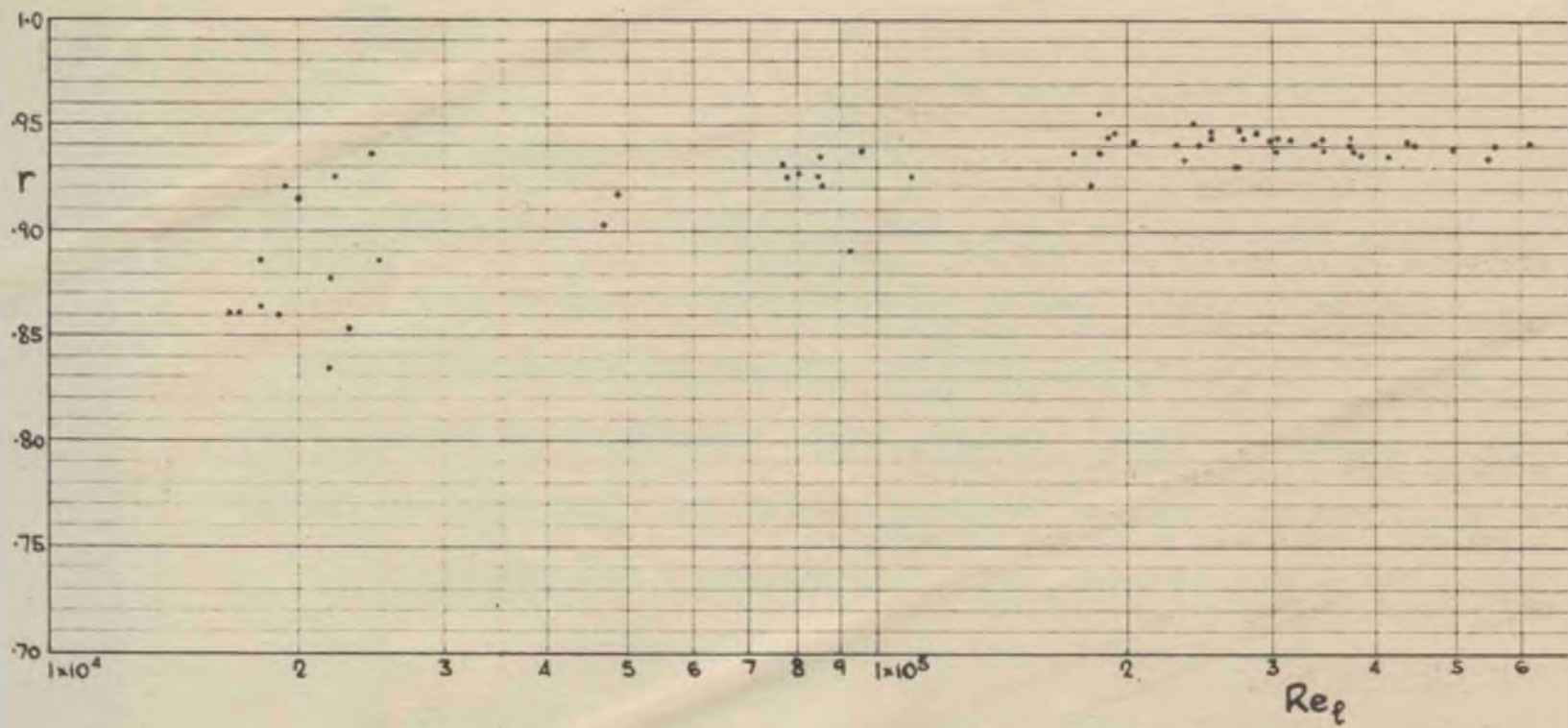
a. SUPERHEATED STEAM.
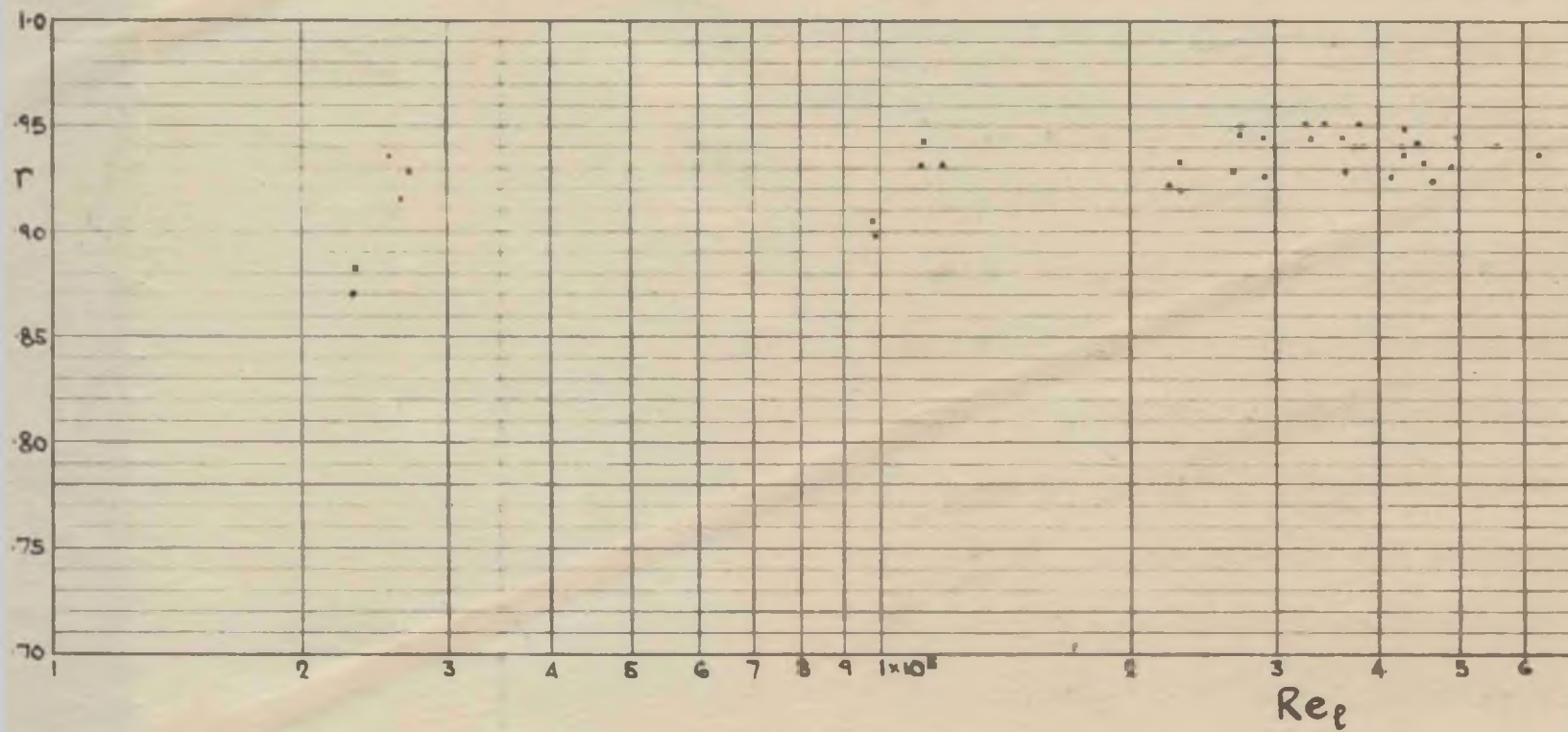
b. SUPERSATURATED STEAM.

FIG. 30 RECOVERY FACTOR VARIATION.

SUPERSATURATED STEAM.

In several cases the values of recovery factor which have been referred to in the above discussion have been obtained for expansions which proceded beyond the saturation point into the supersaturated region. For instance, in tests PA3, PA4, PB3, PB4, PD2 and PD3 the steam condition changes from superheated to supersaturated at points between the sections b and c. There are no changes apparent in the behaviour of the adiabatic wall temperature, or the recovery factor when the expansion proceeds into the supersaturated region. Also for tests which start with initially dry or slightly superheated steam it has been shown that no change from normal conditions of adiabatic wall temperature occurs until the points in the expansion which are indicated in Figs. 18 and 21 by the start of the broken lines. Further, they also exhibit normal recovery factors up to these points (Appendix, Table 1a, tests PA5, PA6, PD4, PD5, PD6).

The lack of any difference between these states is illustrated by Figs. 30a and b. Fig. 30a shows the recovery factors calculated for superheated steam where the amount of superheat varied from zero to 150°F. plotted against Re and Fig. 30b shows the recovery factor for super-saturated steam, where the undercooling ranged from zero to about 80°F., plotted to a similar base. In both these cases values of recovery factor from sections near the nozzle exit which were judged to be affected by recompression have been omitted.

In both Figs. 30a and 30b the results are seen to be grouped round the line of $r = 0.94$. The only difference is in the distribution around the line. For the supersaturated steam results the values are scattered in a broader area around this value. This is no doubt owing to
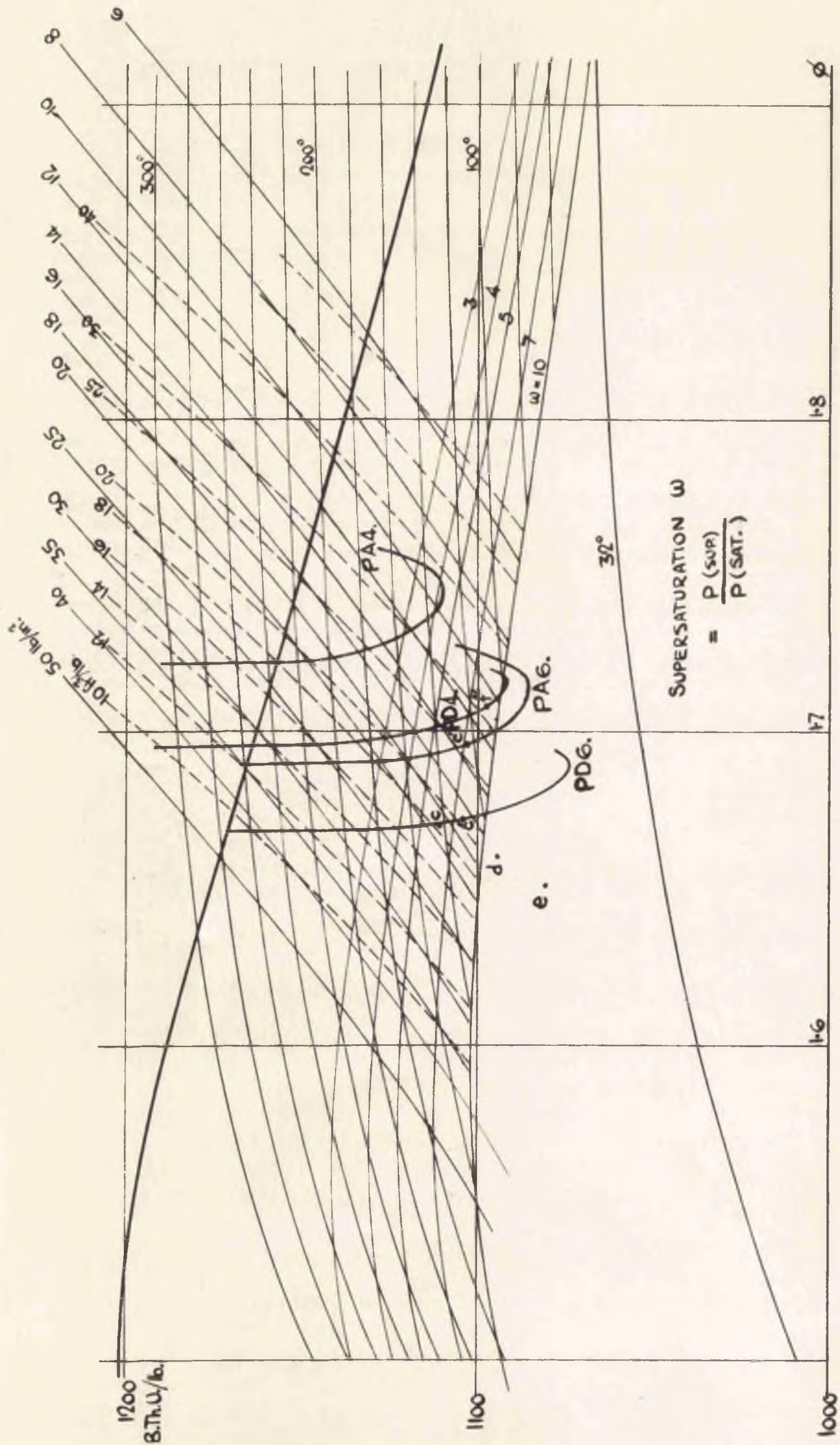
FIG. 31. H-φ CHART FOR SUPERSATURATION.

the relative lack in accuracy in determining stream conditions for supersaturated conditions.

It is thus seen that the recovery factor conception is valid for steam, superheated, dry and for supersaturated conditions up to certain limits.

This limit, to which supersaturation may extend in the expansion of steam through nozzles has been the subject of much theoretical and experimental investigation. Nearly all these investigations have been concerned with the establishment of a limiting supersaturation ratio. The degree of supersaturation ω is defined as the ratio of the actual pressure of the supersaturated steam to the saturation pressure corresponding to the undercooled steam temperature and the amount of supersaturation is commonly referred to as ω fold.

The evaluation of stream conditions makes a closer inspection of the tests with initially dry or slightly superheated steam possible. It has already been mentioned that the stream temperatures were obtained by the use of the H - $\emptyset$ chart for supersaturated steam prepared by Stodola. Fig. 31 shows a reproduction of this chart, with lines of constant pressure, volume and temperature. The expansion for test PA4 is shown plotted. This yielded a perfectly normal adiabatic wall temperature curve and the expansion is of the same shape as one lying entirely in the superheat field. For tests PA6, PD4 and PD6 curves are plotted assuming the expansion occurs normally. On each of these curves are marked the points at which the adiabatic wall temperature diverged from the normal shape i.e. points c, f and c respectively. These divergences are seen to occur at points where the expanding steam has attained the supersaturation ratios of 7.5, 8.5 and

8 respectively according to this estimate. When the actual values for these tests were calculated, however, they were found to coincide with the assumed curves up to the region of $\omega = 5$ to 6 and then to differ by rapidly increasing amounts. This is illustrated for test D6 where the intersections of the pressure and volume values are indicated for the points c, d and e. The difference between the actual point c and the estimated point shows that the character of the expansion changes at $\omega = 5$. Beyond this ratio, the points d and c lie progressively further to the left. This does not mean that a decrease in entropy has taken place, which is, of course, impossible, but that the equations for supersaturated steam are no longer valid for these points. The only reason for this invalidity is the condensation of part of the steam i.e. reversion to conditions of thermal equilibrium. The equation $H = A + Bpv$ which is used in the calculation of specific volume only holds for super-heated and supersaturated steam. It will not apply for steam containing water droplets and therefore specific volumes evaluated on a basis of it are meaningless.

Reduction of the adiabatic wall temperature below normal values is thus shown to coincide with the breakdown of supersaturated conditions. The reversion occurs at various extents of supersaturation beyond $\omega = 6$ from plotting of the volume values on this chart. The Wilson limit corresponds to eight-fold supersaturation, while Stodola found reversion at $\omega = 3.3$ in steam liberally supplied with nuclei. As these tests were made with precautions against the presence of water droplets in the original supply, the limiting values are seen to be reasonable.

As expansion proceeds beyond the supersaturation limit, small

DISTANCE ALONG NOZZLE - INS.

THROAT

TEST PA.6

AFFECTED TEST

Ltd
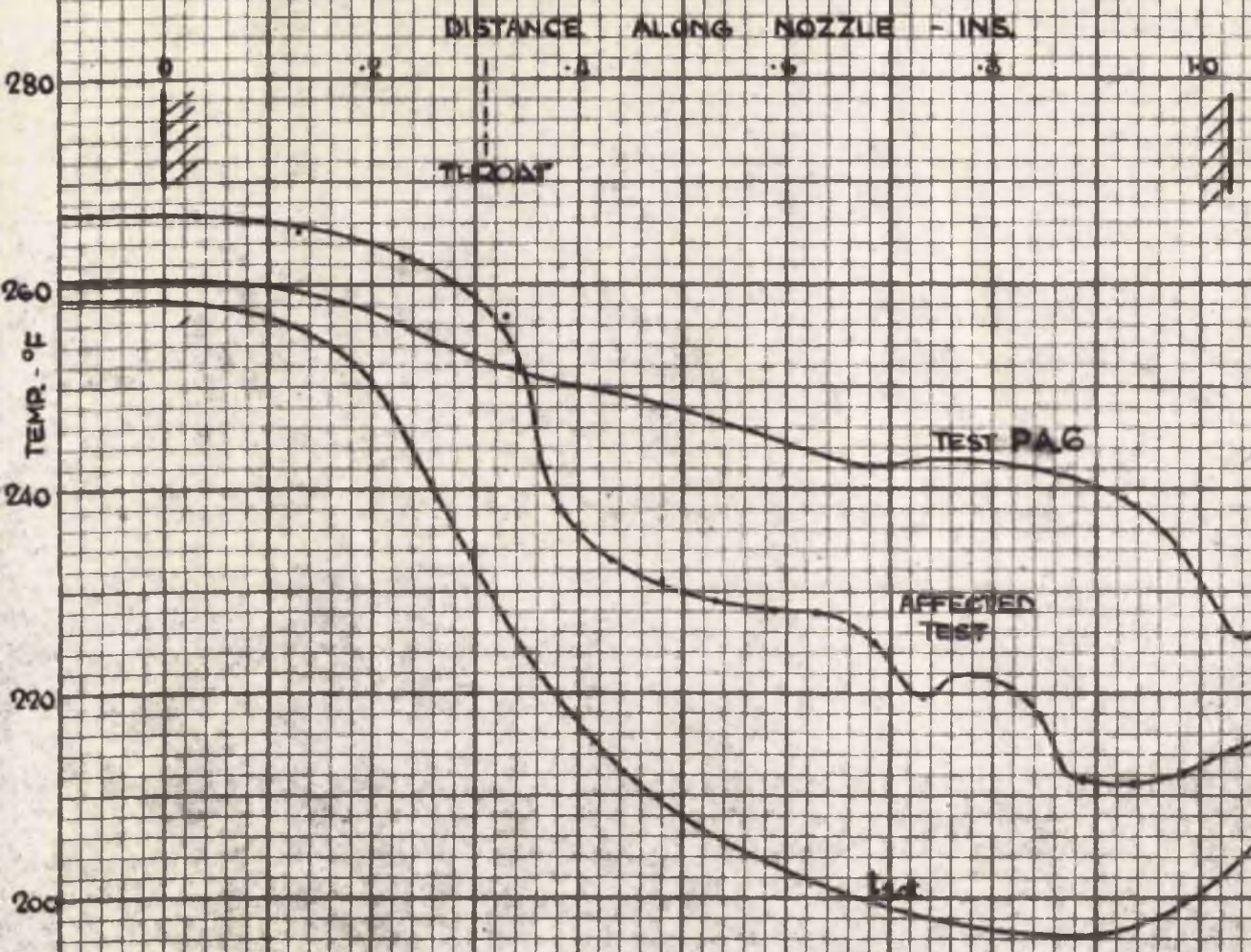
FIG.32 WALL TEMP. AFFECTED BY WATER IN SUSPENSION.

droplets of water are formed in the steam. It is because of these that
a reduction in adiabatic wall temperature is recorded, whereas the
temperature of the stream actually rises with reversion. This has been
demonstrated by tests in which the limit of supersaturation was reached
during expansion, and by those in which initially wet steam was expanded
through the nozzle.

An illustration of the effect produced by water in the system
was obtained early in the investigations, before the procedure had been
perfected for tests with initially dry or only slightly superheated steam.
In the course of making the first such test attempted, using a normal
Sindanyo tube, the system was drained in the normal manner for high
superheat tests before starting. As the test proceeded the temperatures
recorded became very unsteady. For positions of the thermocouple after
the throat the potentiometer needle oscillated slowly over a small range,
occasionally dipping violently to a much lower value. In noting the
results these large dips were at all times ignored and the mean of the
prevailing range taken as the best reading. The results obtained are
shown in Fig. 32.

When it was later attempted to measure t_{aw} for dry saturated
inlet conditions, these fluctuations had increased to such an extent as to
make accurate readings impossible. On opening the drain valve afterwards,
a large amount of water was discharged from the receiver. The drain was
then adjusted to discharge steam continuously from the receiver during
tests, and the results already shown were obtained without further trouble.
In Fig. 32 the results of test PA6 are plotted for comparison, along with

the saturation temperature variation. This shows that the wall temperature in the original test, although starting 7°F. above that in A6, rapidly fell to 18°F. below it and eventually to nearly 30°F. below it.

The only conclusion possible is that these low temperatures were caused by the presence of water particles carried over from the receiver despite the small initial superheat. This deduction is substantiated by the improvement gained in stability and continuity of temperature readings with continuous draining, while the presence of water in suspension was proved conclusively by the mass flow readings, the average value being 1.452 lb./min. which is higher than for dry inlet conditions. This average value was obtained from four tests, each about thirty minutes duration, spread over the test period of three hours. The results were consecutively 1.425, 1.451, 1.454 and 1.478 lb./min. showing a marked increase as the test proceeded and water accumulated in the receiver.

For tests with initially wet steam it has been seen that values near the saturation temperatures are recorded by the search tube. It would seem therefore that the discrepancy between wall temperature readings and the normal curve is dependent on the amount of water present in the stream.

For tests starting with slightly superheated steam the divergence of the adiabatic wall temperature from the normal distribution is only gradual at first and temperatures are still far above the saturation values. This would seem to indicate that only a partial reversion takes place within the nozzle. Presumably the steam carries small drops of water in suspension but is still mainly undercooled vapour.

This type of mixture has been referred to by Keenan (57) and has been deduced to be present after the supersaturation limit. In it the steam is in thermal equilibrium with very small drops of condensate and under-cooled. This "second type" of supersaturated steam is undercooled despite the presence of water because normal steam table values are evaluated for an equilibrium mixture of steam with infinitely large drops of water. Equilibrium can exist between the steam and the droplets if the vapour pressure of the droplets is equal to the pressure of the steam. This condition has been considered by Kelvin (61) and Von-Helmholtz (40) and leads to the well known equation

$$\log_e \frac{p}{p_s} = \frac{2\sigma v}{RT \rho r} \quad \dots\dots\dots\dots\dots\dots\dots\dots\dots\dots(77)$$

where p_s is the saturation vapour pressure corresponding to the temperature T, while σ is the surface tension of water of density ρ and R is the usual gas constant. This relationship gives the supersaturation ratio if a droplet of radius r is to be in equilibrium with the vapour about it. It is probable, however, that the growth in size of the droplet will rather depend on the time of expansion than on the above relationship.

As expansion proceeded beyond the supersaturation limit the adiabatic wall temperature fell rapidly below normal values corresponding to the increase in the amount of condensate present in the steam. It is likely that both the number of the water droplets and the size will increase. With this water in suspension the steam temperature must have risen above the normal fully undercooled values, but its value cannot be estimated. Recovery factors must therefore be of a very low order; so low, in fact, as to be meaningless. The reason for the lowering of the wall temperature has been attributed by Kerr, Scott and Sorour (64) to the re-evaporation of

water droplets in the boundary layer, which is still at a much higher temperature than the main stream. The provision of latent heat entailed would lower the film temperature and probably also cause a reduction in its thermal resistance, through the disruptive effect of such an action. It could also be due, in these cases considered, to changes wrought in the physical properties of the fluid by the presence of water particles.

In the tests made with wet steam this second type of super-saturation seems to have occurred also, despite the initial presence of moisture in the inlet section of the nozzle, since temperatures recorded were definitely below the saturation values. These low temperatures did not persist long, however, except in case C. Towards the exit of the nozzle the recorded temperatures on the average were slightly above saturation values. Very little is known about the behaviour of a mixture of vapour and water drop flowing in a duct. During the expansion the temperature of the vapour will fall with falling pressure but the temperature of the liquid will be reduced mainly by transfer of heat to the vapour. Temperature equilibrium will not be attained, because the drops will always be hotter than the vapour (reference 56 p. 447). Solution of the states of such non-equilibrium mixtures will depend largely on the time rate at which transfers of heat and mass occur. In these cases it is doubtful if a true boundary layer exists at all. Probably most of it is water at a slightly higher temperature than the stream.

In the expansion of steam through a nozzle, therefore, if a supersaturation ratio of approximately seven is attained, there will take place a reversion from the first type of supersaturation to the second type. This will be a partial reversion but the number and size of the water droplets

will rapidly increase. With further expansion there will be a final reversion with the condensation of the remaining amount of steam necessary to restore thermal equilibrium.

In the present investigation the expansion did not proceed far enough for the final reversion to take place. In the report by Sorour (92), however, tests are described where expansion with the second type of supersaturation conditions occurred. Adiabatic wall temperatures were recorded which were nearly 20°F. below the saturation temperature. Towards the exit a sudden jump in the wall temperature readings to the saturation value was observed, indicating that reversion had occurred. This reversion was found to coincide with recompression, the shock wave at this point evidently being the determining factor in causing the reversion. The shock wave in these circumstances was, however, observed to be much more severe than when total reversion did not take place.

CONCLUSIONS OF THE PRELIMINARY INVESTIGATION.

The investigation demonstrates that steam is a suitable medium for experiments on heat transfer at high velocities, and is more convenient than dry air which is normally used. Doubts as to the suitability of the use of steam, raised by the results obtained by previous investigators who attempted to measure steam temperatures, are removed.

Temperature recovery takes place within the boundary layer in the same manner as for air, and the value of the recovery factor is of the same order as that expected for gases. Experimental results, however, were lower than the value of unity indicated by theory. For a laminar boundary layer r was observed equal to 0.94 and lower values were obtained for a turbulent boundary layer. As indicated by theory the value was found to be independent of Reynolds and Mach numbers.

These values are limited to steam which is superheated or dry and also to supersaturated steam which is purely gaseous.

The presence of water in either equilibrium or non-equilibrium mixtures with any of the above states renders the concept invalid. The recovery factor is reduced to very low values, the reduction being proportional to the amount of water present, and for wet steam the recovery factor is approximately zero.

PART III

THE MEASUREMENT OF RECOVERY FACTORS FOR STEAM

FLOWING IN A SIX INCH LONG ANNULAR DUCT.

SEARCH TUBE

TO CONDENSER

SCALE ~ HALF SIZE

TEST LENGTH

SINDANYO
BUSHES

STIRRUP
GUIDE

THERMOCOUPLE
TUBE
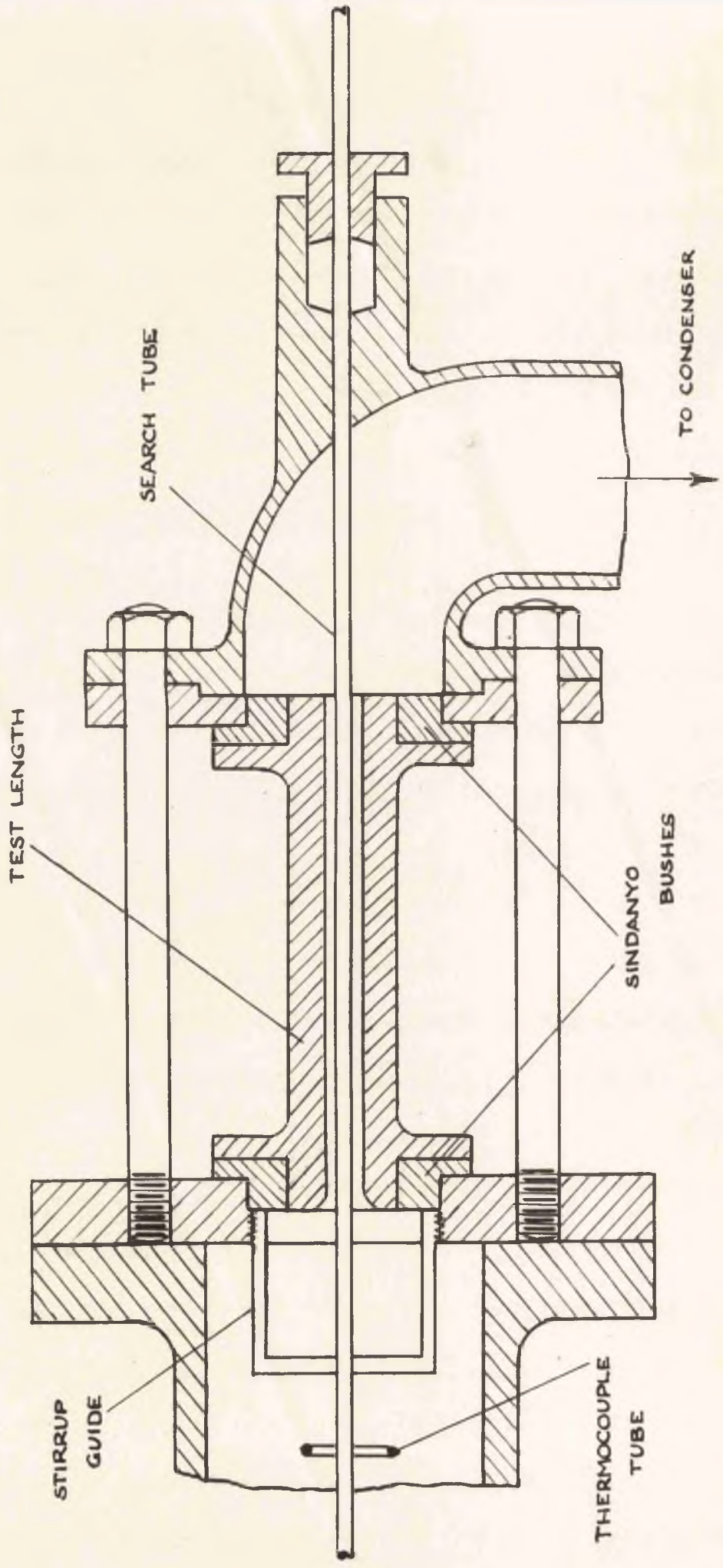
Fig. 33. DETAIL OF APPARATUS

THE MEASUREMENT OF RECOVERY FACTORS.

The tests described in this part of the thesis were carried out in order to obtain values for the recovery factor for steam flowing under the same conditions as tests for which heat transfer coefficients would be obtained. The apparatus for this purpose was designed to prevent heat loss from the steam and so enable the expansion to be taken as adiabatic.

APPARATUS.

The general arrangement is the same as that used in the preliminary investigation and which is shown in Fig. 11. After the receiver, however, the steam passes through a six inch long annular duct formed by a brass nozzle and a central tube or probe. The arrangement is shown in Fig. 33. It is seen that the brass nozzle is supported by tie-bolts between two steel flanges but separated from these by Sindanyo bushes.

After expanding through the nozzle, the steam passes into the exhaust chamber and through the exhaust pipe to the condenser. The pressure in the exhaust chamber is again recorded on a calibrated Bourdon gauge. The search tube passes through a stuffing box at the rear of the exhaust chamber. Attached to this stuffing box is a rigid scale which supports the end of the search tube and pressure gauge if used, the search tube being attached to a steel block. This block has a square hole which fits and slides along the square-sectioned rule, and a vernier inscribed on the block enables the position of the search tube to be observed.

The whole assembly from the flange of the receiver to the exhaust pipe is attached to a cast iron bracket. This is mounted on the horizontal slides attached to the wall at the back of the apparatus. Thus the nozzle can be moved horizontally to enable the zero reading for the search tube to
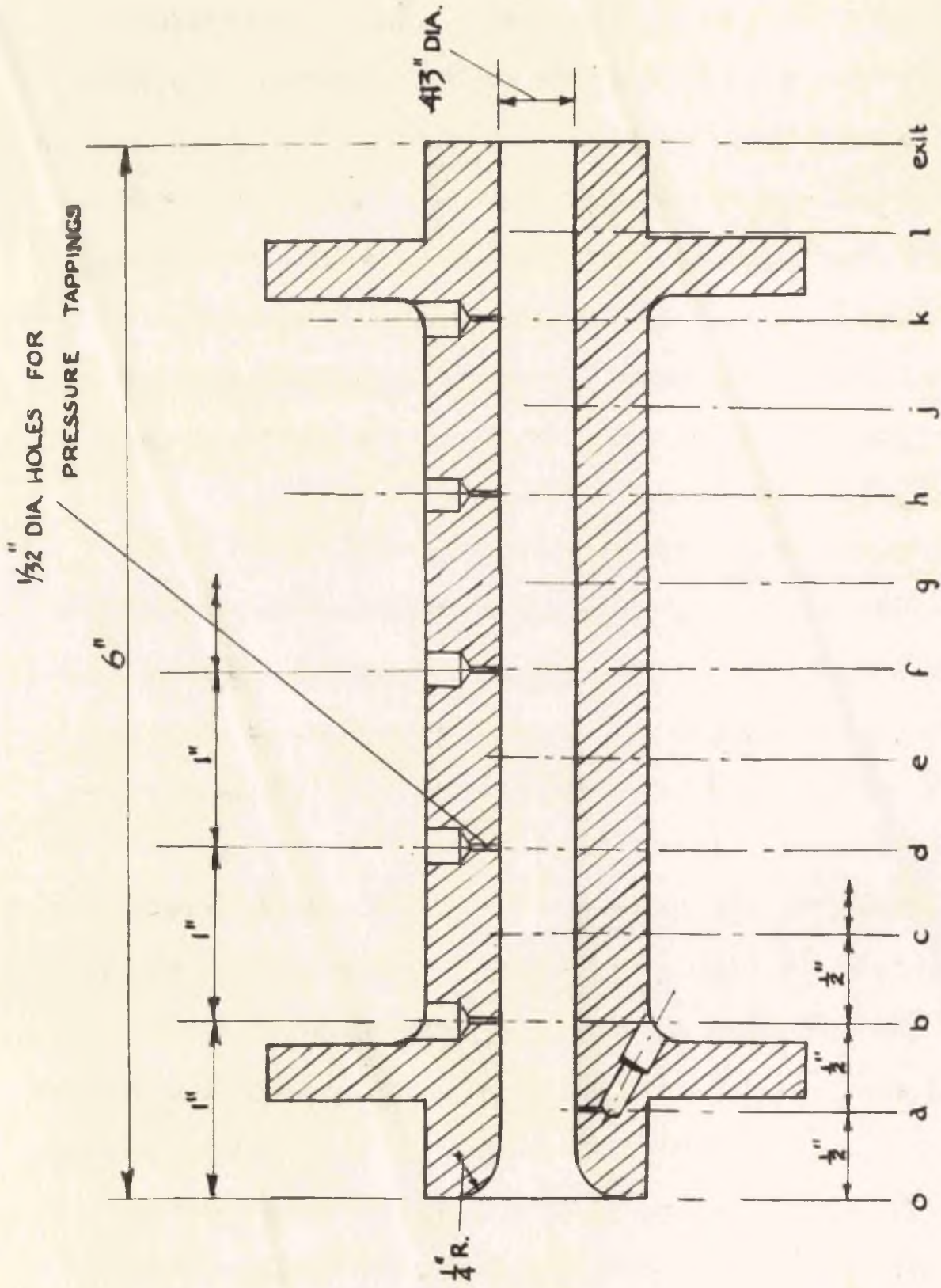
Fig. 34. DETAIL OF TEST LENGTH

SCALE - FULL SIZE.

be determined easily.

Fig. 34 shows details of the test length. The entrance is bell-mouthed to give a smooth entry for the flow of steam. The diameter of the bore is 0.413 ins. Provision is made for static pressure tappings in the wall at intervals of 1 in., an additional tapping being situated at 1/2 in. from the entrance. These tappings were made by drilling 1/32 in. diameter holes from the outside. Copper tubes of 1/8 in. outer diameter transmitted the pressure to a manifold and thence to a pressure gauge. By opening the appropriate cock on the manifold the pressure at any of the tappings could be read on the gauge.

The bore of the nozzle was obtained by first drilling to a diameter of 13/32 in. The pressure tapping holes were then drilled. The final diameter was obtained by lapping, using an aluminium lap and fine carborundum grinding powder. In this way a smooth parallel bore was produced, and any burs left by drilling of the 1/32" tapping holes removed.

The brass pressure search tube is 3/16 in. outside diameter. A 1/32 in. diameter hole drilled diametrically through the walls transmits the static pressure through the tube to the pressure gauge.

The temperature search tube was of similar construction to that used beforehand in the searches with the short nozzle. Tufnol was used, however, as the material for the insulating length, instead of the Sindanyo. The smaller diameter of 3/16 in. caused the manufacture of this length from Sindanyo to be difficult. The Tufnol is less brittle and has better machinability properties being less friable. The Asp brand of this material was found to be able to withstand the highest

BRASS PLUG , SCWD.10B.A.

3/16" DIA.

4"

SCREWED 3B.A.

1/16" DIA. HOLE

FIG. 35   TUFNOL SEARCH TUBE

SUPPLY
TEMP.

REFERENCE
JUNCTION
IN ICE

SEARCH
TUBE

Cu   fe

fe   Cu

fe   Cu

POTENTIOMETER

SELECTOR
SWITCH
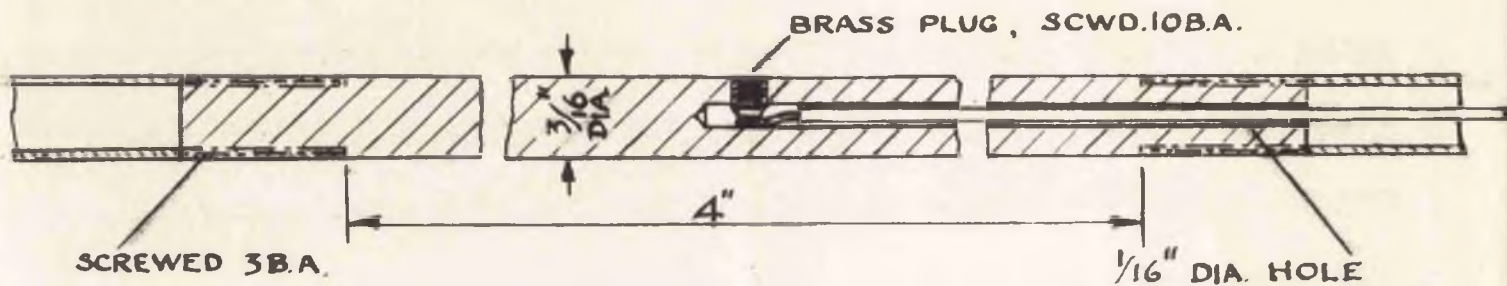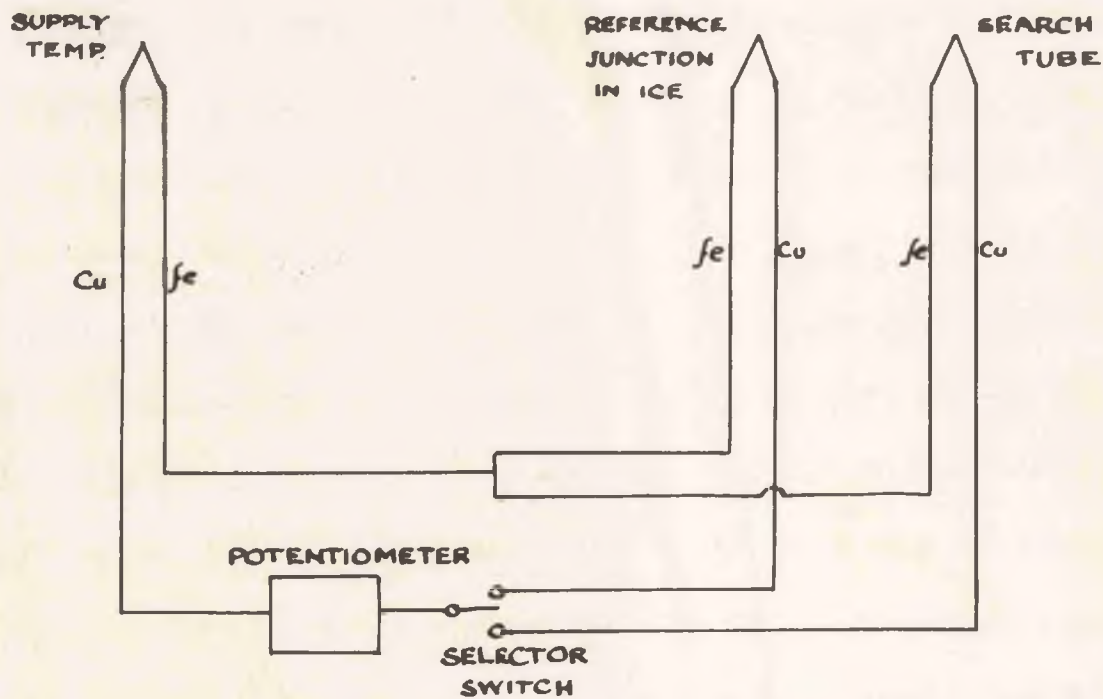
FIG. 36 DIAGRAM OF THERMOCOUPLE CIRCUIT

temperatures encountered. The length of the insulating portion was again 4-5 in. Fig. 35 shows the dimensions. The thermojunction was again formed by welding the ends of the copper and constantan wires and a brass plug screwed down on to the junction. "Stag" brand jointing paste was again used for sealing the screwed joints. The whole surface was made flush and polished with fine emery paper.

Though the Tufnol search tubes stood up to conditions better than the Sindanyo ones, through time the erosion of the steam caused a roughening of the surface. Since further polishing would have resulted in a diameter smaller than 3/16 in. it was necessary to renew the insulating portion. Four such search tubes were used in the tests.

The thermocouples were arranged so that the difference of the e.m.f. between the stagnation couple and the search tube couple was indicated. A switch also enabled the e.m.f. of the stagnation thermocouple to be observed for a circuit in which the reference junction was immersed in oil surrounded by melting ice. A portable pontiometer was used for measuring the e.m.f. A diagram of the circuit is shown in Fig. 36. The arrangement simplified the reading of the wall temperatures. Though readings were never taken unless the stagnation thermocouple indicated that the supply temperature was steady, there was a slight delay in changing the position of the switch and in reading the search tube temperature. In this time there was the possibility of a slight change in the supply temperature, and so causing an erroneous reading, since it was observed that a change in supply temperature caused an instantaneous change of the same magnitude along the length of the test section. The advantage of the above arrangement is that the two temperatures could be

measured simultaneously. If any change occurred in the supply temperature, the difference which is recorded is still the same. Naturally, however, the same care was taken to maintain the supply temperature at a constant value. There was also a gain in accuracy by this arrangement, in that the difference between the total and the adiabatic wall temperatures was measured directly. It is in this value that the greatest accuracy is necessary when computing recovery factors.

The Sindanyo bushes separating the brass test length from the steel flanges prevent heat loss by conduction from the test portion to the surroundings. To prevent further heat loss the nozzle was surrounded by an immediate layer of insulation consisting of a pad of magnesia. The whole apparatus was then surrounded by a blanket of insulation. Photographs (Figs. 48a and b) taken while heat transfer runs were in progress give an indication of the arrangement of the apparatus and show the test length with and without the insulation.

EXPERIMENTAL PROCEDURE AND RESULTS.

The Pressure Searches.

The procedure was similar to that for the searches described in Part II. About two hours were required to heat the system and for steady conditions to be attained. The valve at the foot of the receiver was adjusted to drain continuously. This ensured that completely dry steam was supplied to the test section.

Pressure readings were started when the search hole was set at 1 in. before the entrance and completed after traversing the whole length. The intervals between the positions at which the pressure was observed varied according to the rate of pressure change. For the first inch of the length readings were taken at 0.1 in. intervals and at 1/4 in. intervals for the remainder. Time was allowed at each setting for a stable pressure to be attained. It was observed that this time was much less than that necessary in the previous investigation. This was doubtless owing to the smaller diameter of the tube (3/16 in. against 1/2 in. diameter) passing through the exhaust chamber and which is exposed to temperature variations.

The results of the tests are plotted in the form of pressure ratios along the nozzle length. Table 5 lists the tests and pressure conditions.

In all cases with atmospheric exhaust pressure, the pressure at the exit was below the critical for isentropic expansion. Not until the exhaust pressure was raised to the critical of 0.545 p_0, was there a variation in the pressure distribution.
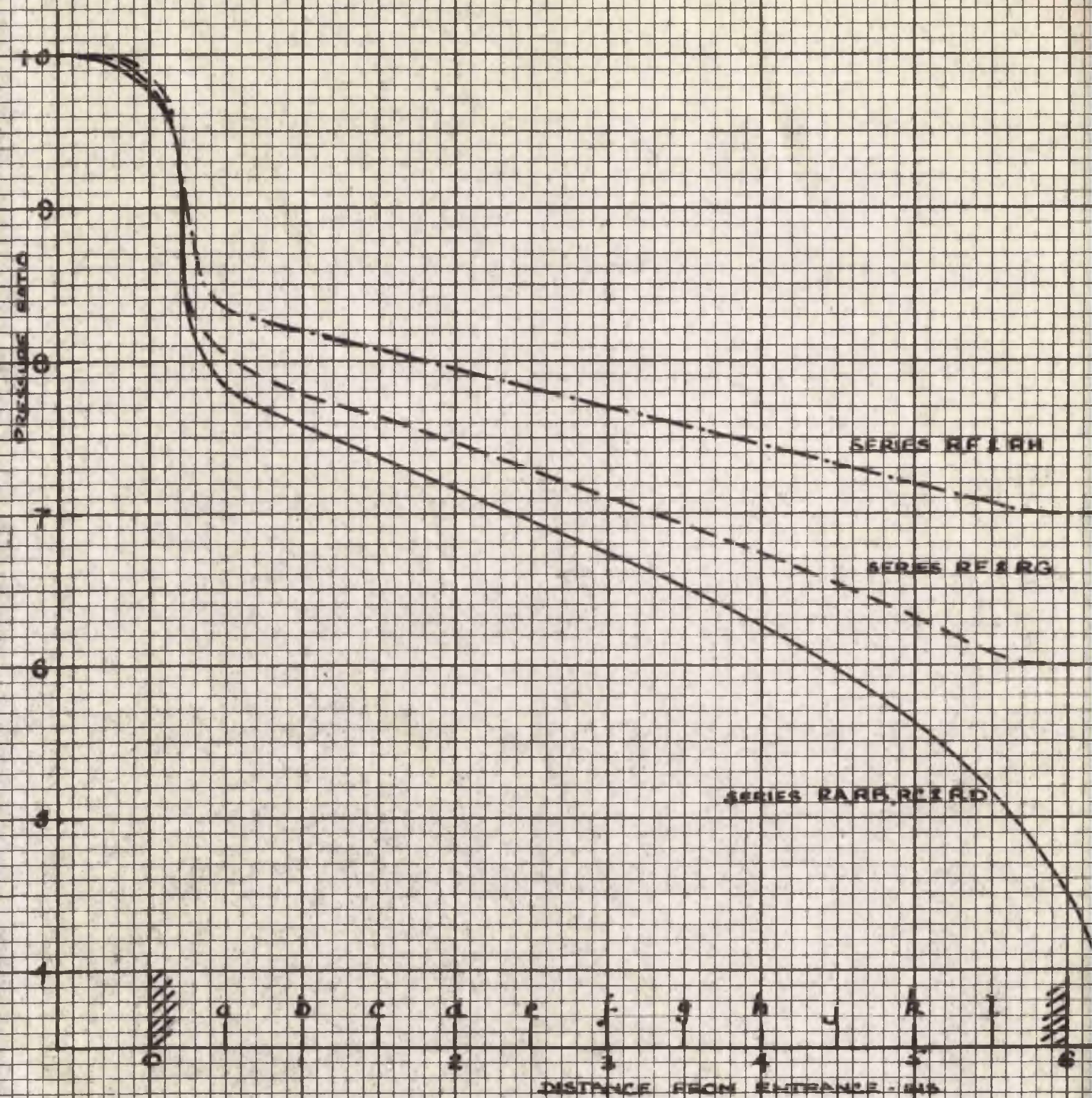
Fig 37   PRESSURE   RATIO   P/P₀

<u>Table 5.</u> - Pressure Searches.

Letter	Supply Pressure Lb./Sq.In.Gauge.	Back Pressure	Overall Pressure Ratio
RA	20	Atmospheric	-
RB	30	"	-
RC	40	"	-
RD	50	"	-
RE	20	-	0.6
RF	20	-	0.7
RG	30	-	0.6
RH	30	-	0.7

Plots of the pressure ratios are shown in Fig. 37. In all cases there is a sudden drop in pressure in the first 1/2 in. corresponding to the decrease in area in the bell-mouth entrance. Thereafter there is a more gradual fall in pressure, the gradient being almost constant. In the cases where the exhaust pressure is atmospheric, towards the exit the pressure falls increasingly rapidly, and the gradient beyond the exit is very steep. With the increased back pressure the curve flattens out to the final value just at the exit.

For each initial pressure, several tests were carried out with varying superheats of from 100°F. to 250°F. As in the case of the previous tests it was found that the curves of pressure ratio along the length were independent of both initial pressure and initial superheat. For a short nozzle this may be expected, as it may be demonstrated that the pressure ratio is simply a function of the area as follows:

From Bernoulli's equation $\dfrac{W}{a} = \sqrt{2g\,\dfrac{P_0}{V_0}\cdot\dfrac{\gamma}{\gamma-1}\left(\dfrac{p}{P_0}\right)^{2/\gamma}\left[1-\left(\dfrac{p}{P_0}\right)^{\frac{\gamma-1}{\gamma}}\right]}$ ...(78)

The maximum flow obtained when the sonic velocity is attained at the throat is given by:

$$\frac{W}{a_m} = \sqrt{2g\,\frac{P_0}{V_0}\cdot\frac{\gamma}{\gamma+1}\cdot\left(\frac{2}{\gamma+1}\right)^{\frac{2}{\gamma-1}}}$$ ....(79)

From these two equations, there is obtained the relation:

$$\frac{a}{a_m} = \sqrt{\frac{\gamma-1}{\gamma+1}\left(\frac{2}{\gamma+1}\right)^{\frac{2}{\gamma-1}}\cdot\frac{1}{\left(\frac{p}{P_0}\right)^{2/\gamma}\left[1-\left(\frac{p}{P_0}\right)^{\frac{\gamma-1}{\gamma}}\right]}}$$ ....(80)

a_m is the minimum or throat area.

So long then as the critical pressure is attained at the throat, the pressure ratio is a function of the area at that section only and is independent of initial conditions.

Obviously the above relationship does not apply to the present case, since the area remains constant while the pressure decreases. The reason is that the analysis leading to the above result, being based on isentropic expansion, does not apply to flow which is largely affected by friction. For the short nozzle the thickness of the boundary layer, that is the region affected by friction, is very small and may be neglected. The above formula cannot, however, be applied in the present case, even for the core of fluid unaffected by viscosity. Though here the expansion is isentropic, the continuity equation, on which the analysis is also based, does not hold since the mass of fluid in the core becomes progressively less.

Values of friction coefficients, calculated from the data obtained in the pressure searches, are given later in Part IV.

During the pressure searches, measurements were taken of the
static pressures obtained by the tappings on the outer wall of the
annulus. At first trouble was encountered in gaining accurate readings.
Any slight leakage at the manifold was found to cause a considerable
pressure drop along the copper tubing, since the bore is only 1/16 in.
diameter, and friction is therefore high. Also there was interference
between the different tappings if any leakage past the cocks occurred.
These were therefore ground into a proper seating, and care taken to
prevent leakage. With these precautions it was found that the pressure
readings then obtained corresponded exactly with those obtained from the
central search tube. This is as expected and is in agreement with the
assumption that the static pressure is constant over any cross-section.
This assumption has also theoretical support. It can be proved from the
basic differential equations for the flow of fluids that the static
pressure throughout the boundary layer is constant perpendicular to the
surface (Goldstein pp 117-118 ref. 33). When the flow in a parallel duct
is fully developed, therefore, the static pressure will be constant across
any section. Where this is not the case, a core will remain in the flow.
Since this region is unaffected by viscosity, the velocity is constant,
and the flow being parallel, the static pressure will also be constant.
Under all circumstances the static pressure is therefore constant over any
cross-section.

The advantage of obtaining static pressure readings from the wall
tappings was observed when temperature searches were carried out. At the
same time as the adiabatic wall temperature was recorded, the pressure
distribution could be noted. Thus it could be ensured that the flow
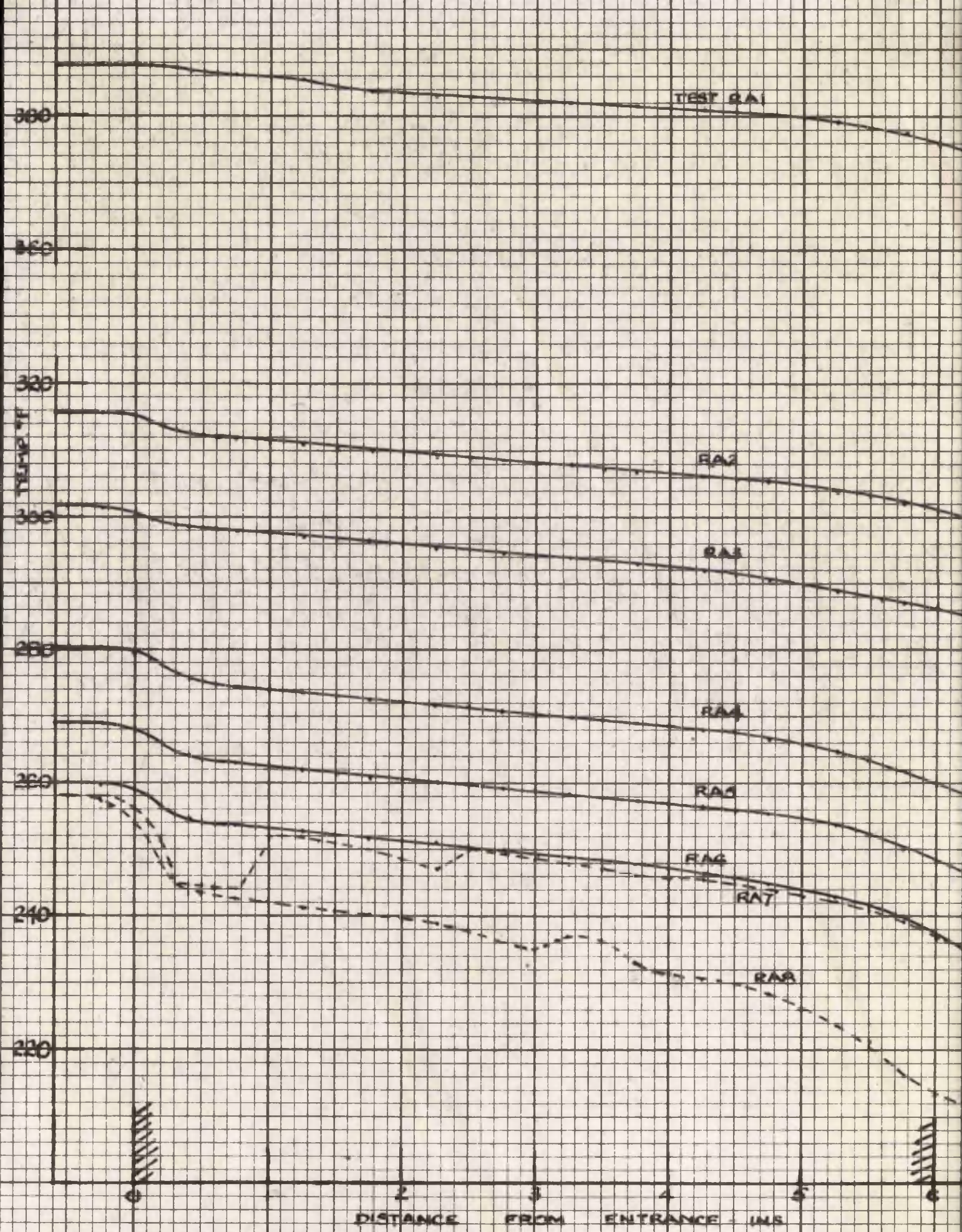
FIG.28   READINGS OF THE ADIABATIC WALL TEMPERATURE (t_a)
SERIES RA

conditions were identical for both the pressure and temperature searches. Any irregularity in the pressure distribution indicated a change in the stream conditions, most likely caused by an unevenness on the surface of the insulating portion of the search tube.

In using the pressure gauges every precaution was taken to ensure that they gave correct readings. They were calibrated by a portable gauge tester, over the range of pressure encountered in the tests, at frequent intervals, usually every three of four days. The calibration was also carried out while the gauges were warm as different temperature conditions can cause slight differences in the readings. As the pressure gauges could be read to within 0.2 lb./sq.in. and carrying out the above measures, the pressure measurements could be relied on to have an accuracy of about 1%.

The Temperature Searches.

The usual care was taken to establish steady conditions before starting each search. A period of three hours was normally sufficient for this purpose.

Temperature readings were taken over the same range as for the pressure readings, and again at intervals of 0.1 in. for the first inch and at intervals of 0.25 in. thereafter.

A complete search occupied from three to four hours. Superheater 2 was found to be able to maintain the steam at the required temperature.

A series of 21 tests was carried out, which are listed in Table 6. During each test at least three separate measurements of the flow quantity were made. The static pressure was also noted at each of the wall tappings. As stated above, from these readings it could be observed

FIG. 38 ctd. READINGS OF THE ADIABATIC WALL TEMPERATURE (t_a)

SERIES RB

TEST RB1

RB2

RB3

RB4

RB5

TEMP - °F

480

460

400

380

360

340

320

300

280

DISTANCE FROM ENTRANCE - INS.

0   2   4   6
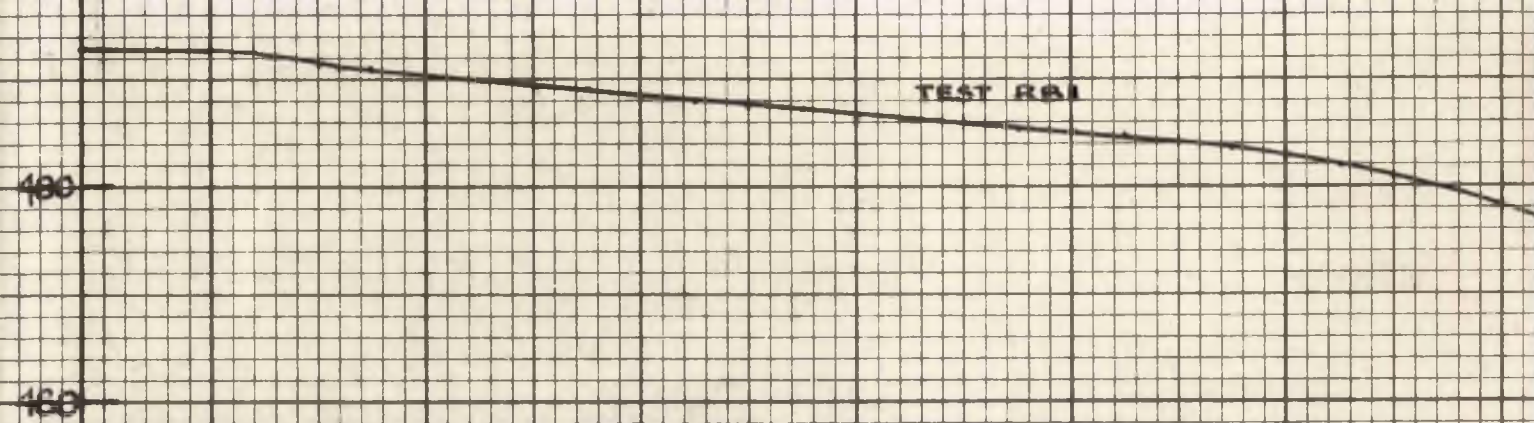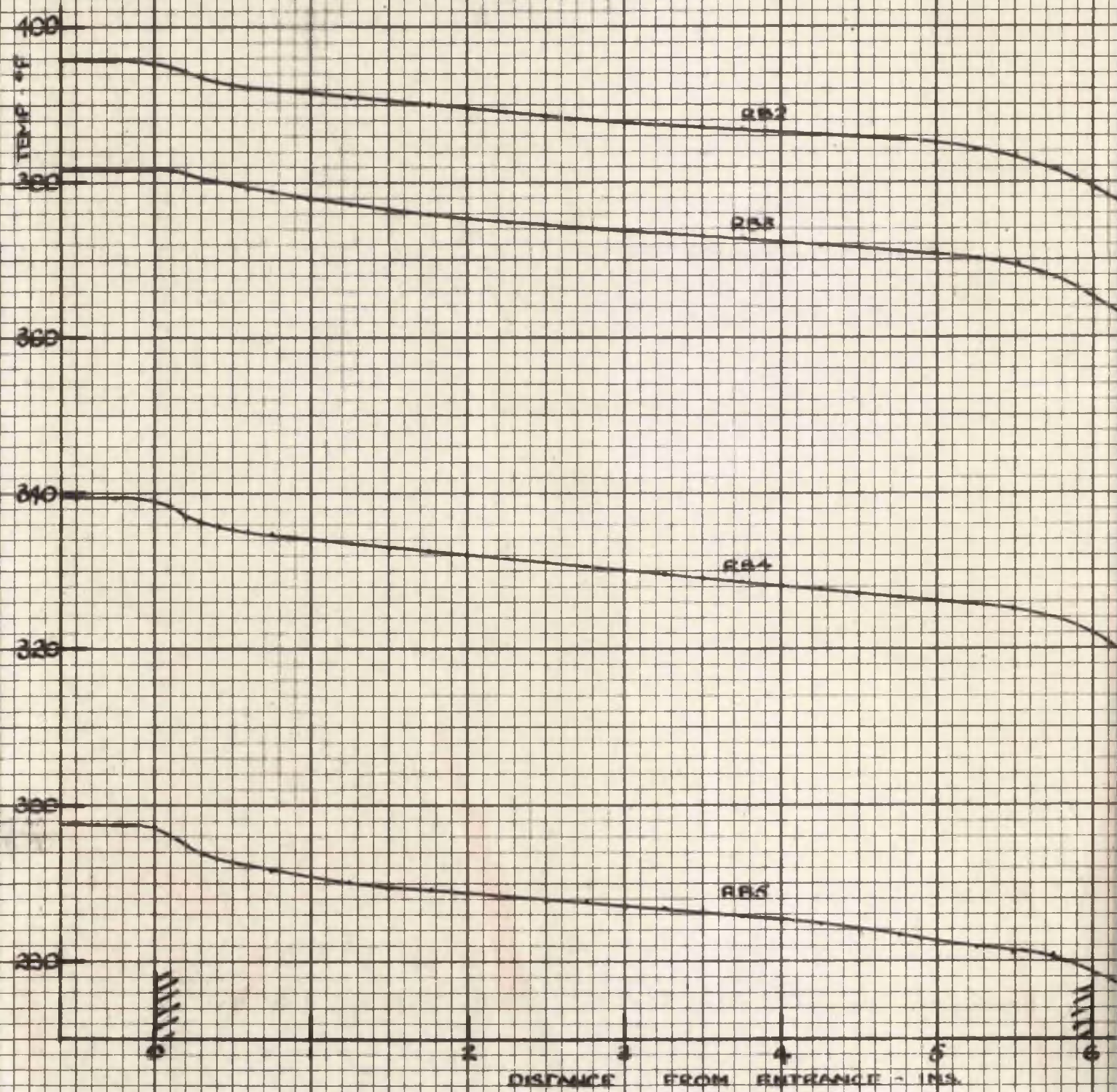
whether or not the flow was normal.

<u>Table 6.</u>

Pressure Conditions.	Test.	Supply Temp. °F.
RA	1 2 3 4 5 6 7 8	388 316 302 280 269 260 258 258
RB	1 2 3 4 5	493 396 382 339 298
RC	1	369
RD	1	355
RE	1 2	399 393
RF	1 2	417 398
RG	1	375
RH	1	358

The variations of the adiabatic temperature are shown for all the tests in Fig. 38, plotted against the distance from the nozzle inlet. All the plots show similar characteristics. There is a steep drop from the
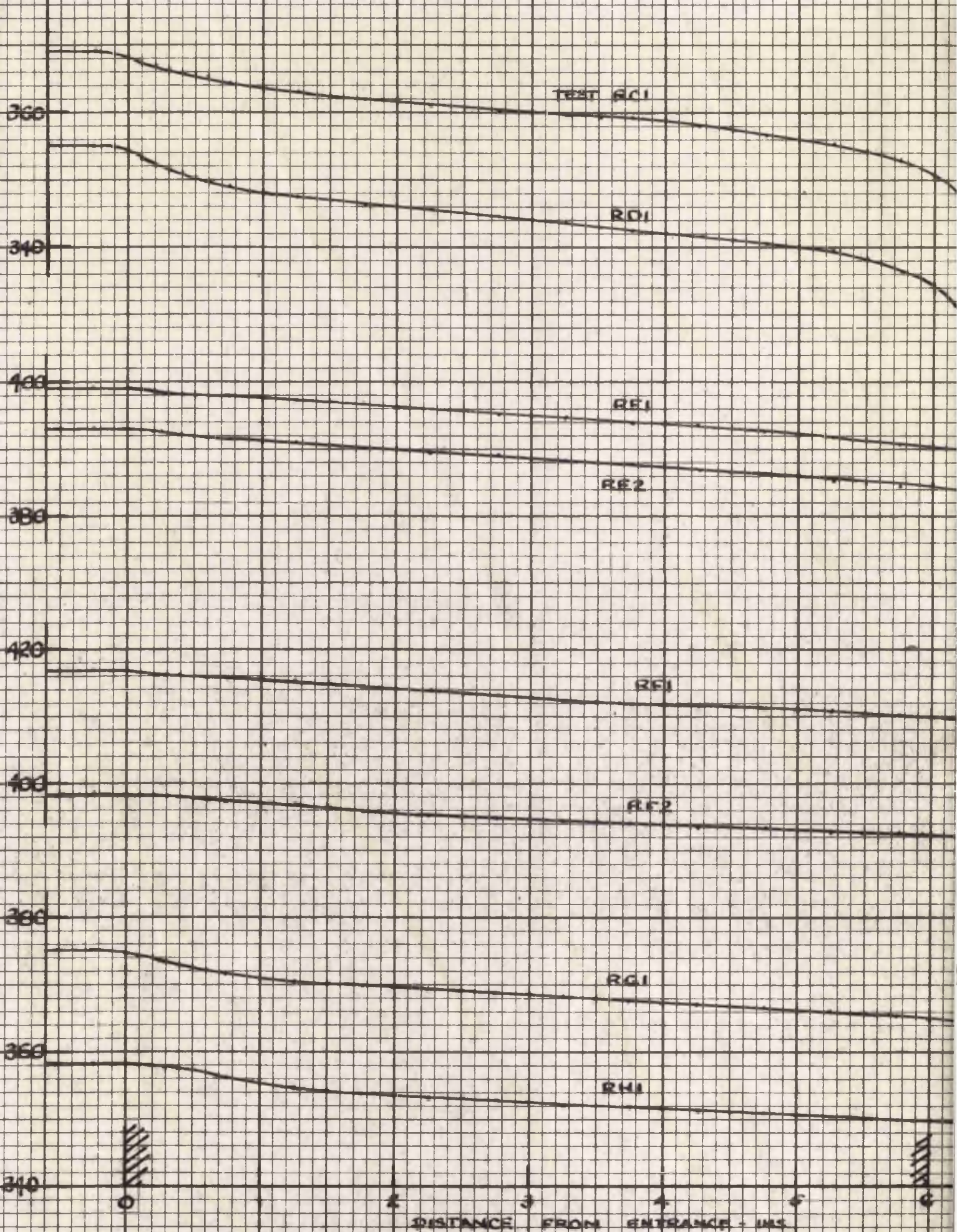
FIG.38. ctd. READINGS OF THE ADIABATIC WALL TEMPERATURE (i

constant value before the inlet in the first 1/2 in. of the length.
Thereafter there is a more gradual and uniform decrease until about 1 in.
before the exit, where the temperature begins to fall more rapidly. This
distribution can be seen to correspond to the variation in stream
temperature. The initial drop occurs when the pressure falls with the
decrease of cross-sectional area at the entrance. Thereafter expansion
of the steam occurs more gradually until near the exit.

It can be observed that as the temperature of the supply steam
is reduced, the magnitude of the initial drop increases, and also the
average gradient is somewhat greater. Tests RA7 and RA8 were carried
out with initially wet steam. In test RA7 the superheater was lit, but
the gas taps were not opened sufficiently for the steam to be completely
dried, while in test RA8 no heat was supplied at all at the superheater.
In both these tests the readings were unsteady, the variations being
greater in the latter test. It is thus seen again that the presence of
water particles cause lower temperatures than normal to be recorded. In
some positions near the inlet, temperatures were observed which were below
the corresponding saturation temperature indicating supersaturated
conditions.

FIG. 39   VARIATION OF STREAM TEMPERATURE AND ADIABATIC WALL TEMPERATURE WITH LENGTH   TEST RB2
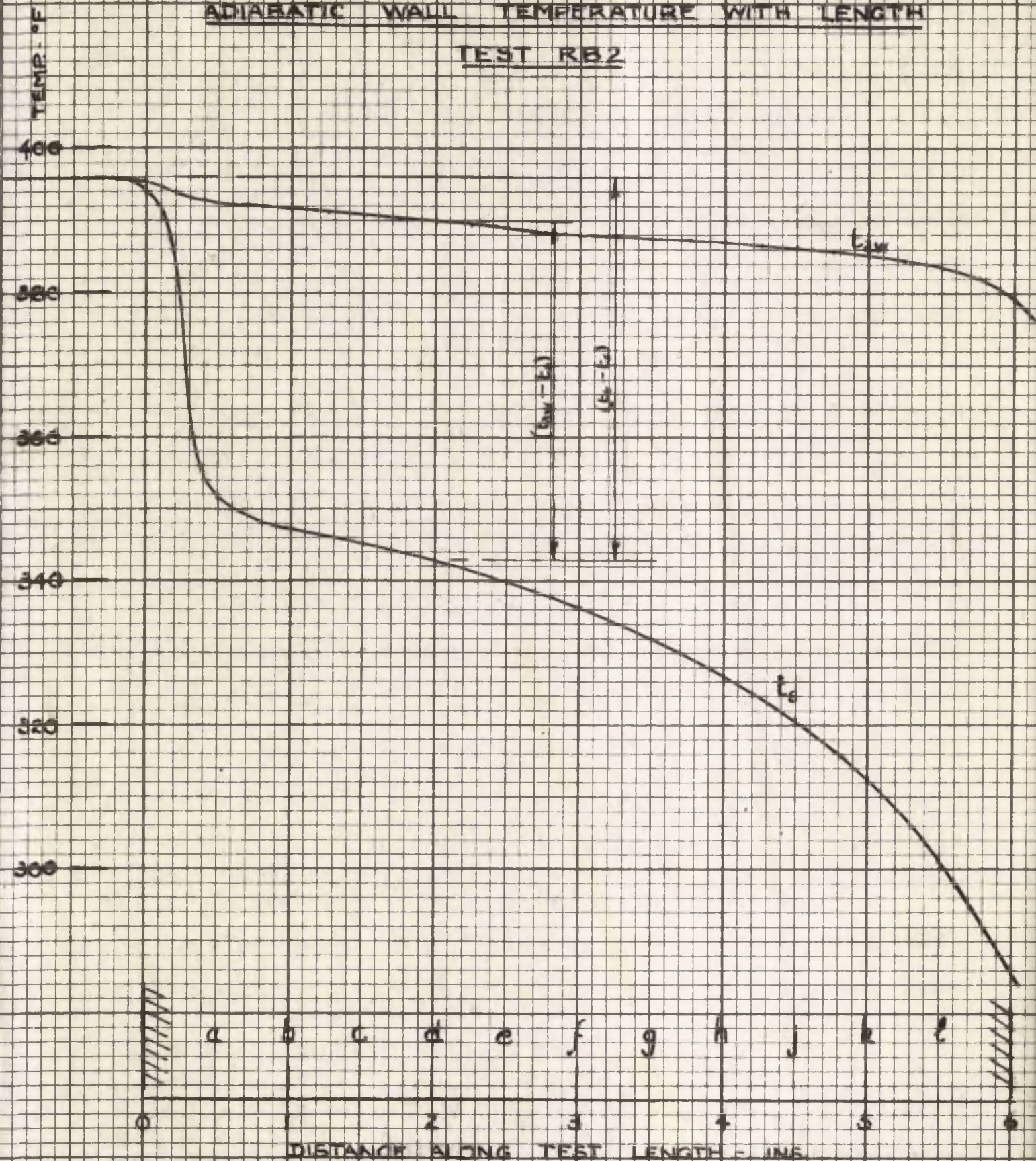
ANALYSIS AND DISCUSSION.

Stream Conditions.

The first stage in the calculations was again the lengthy evaluation of the steam temperatures throughout the expansion. This was carried out for eleven positions along the length. These points are at 1/2 in. intervals and are numbered a to l, the position being shown in Fig. 34.

The specific volume was first calculated from equation 69. The calculations were somewhat simpler than those for the investigation described in Part II, in that at all sections where the specific volume is evaluated the cross-sectional area is the same. For each test, then, the only variable is the value of p.

Knowing the specific volume and pressure at each section, the temperatures were then evaluated by interpolation in reference 59. The temperature so obtained was then plotted against the length to ensure that a consistent form of variation was obtained. Such a curve is shown in Fig. 39 for a typical test (RB2), together with the variation of the adiabatic wall temperature along the length.

Where the expansion proceeded beyond the saturation line and the value of the temperature could no longer be found by interpolation in the steam tables, use was made in this case of Van der Waals equation of state:

$$p = \frac{RT}{v - b} - \frac{a}{v} \qquad \dots\dots\dots\dots\dots\dots\dots\dots\dots\dots\dots\dots\dots(74)$$

The constants a and b were evaluated from known values of p, v and T for two state points in the superheated field. The expansion was found to proceed into the supersaturated field in the tests RA4-6 and RB5. From

FIG. 40 VARIATION OF RECOVERY FACTOR WITH LENGTH

the curves of adiabatic wall temperatures in Fig. 38 it can be seen that there is no fundamental change of form when supersaturation conditions are encountered, apart from the fact that the temperature diverges to a greater extent from the stagnation value. It was seen, however, that where the expansion is completely in the superheated field the wall temperature falls more rapidly with decreasing supply temperature. Only in the case where initially wet steam was expanded, was there any appreciable difference noticed in the form of the temperature distribution.

Having calculated the stream temperature, the values of the recovery factor were easily obtained using the equation:

$$r = \frac{t_{aw} - t_s}{t_t - t_s} \quad \dots\dots\dots\dots\dots\dots\dots\dots\dots\dots\dots(81)$$

t_{aw} was obtained from the plots in Fig. 38 and t_t was the stagnation temperature for each test. Since t_s is the mean stream temperature for each section, the recovery factor evaluated thus is the "local free stream recovery factor". The value of r was calculated for each of the eleven points a to l. These are listed in the Appendix, Table 2a, and are shown plotted against length for a few typical tests in Fig. 40. All the tests show the recovery factor decreasing rapidly immediately after the inlet, the rate of decrease becoming more gradual throughout the length. In most cases a constant value is assumed towards the outlet, while in a few tests the recovery factor is still falling slightly at the exit. The curves for the tests with the greater mass flows showed the flattening out occurring earlier, while the tests which showed no such flattening out were generally those where the exhaust pressure was above atmospheric.
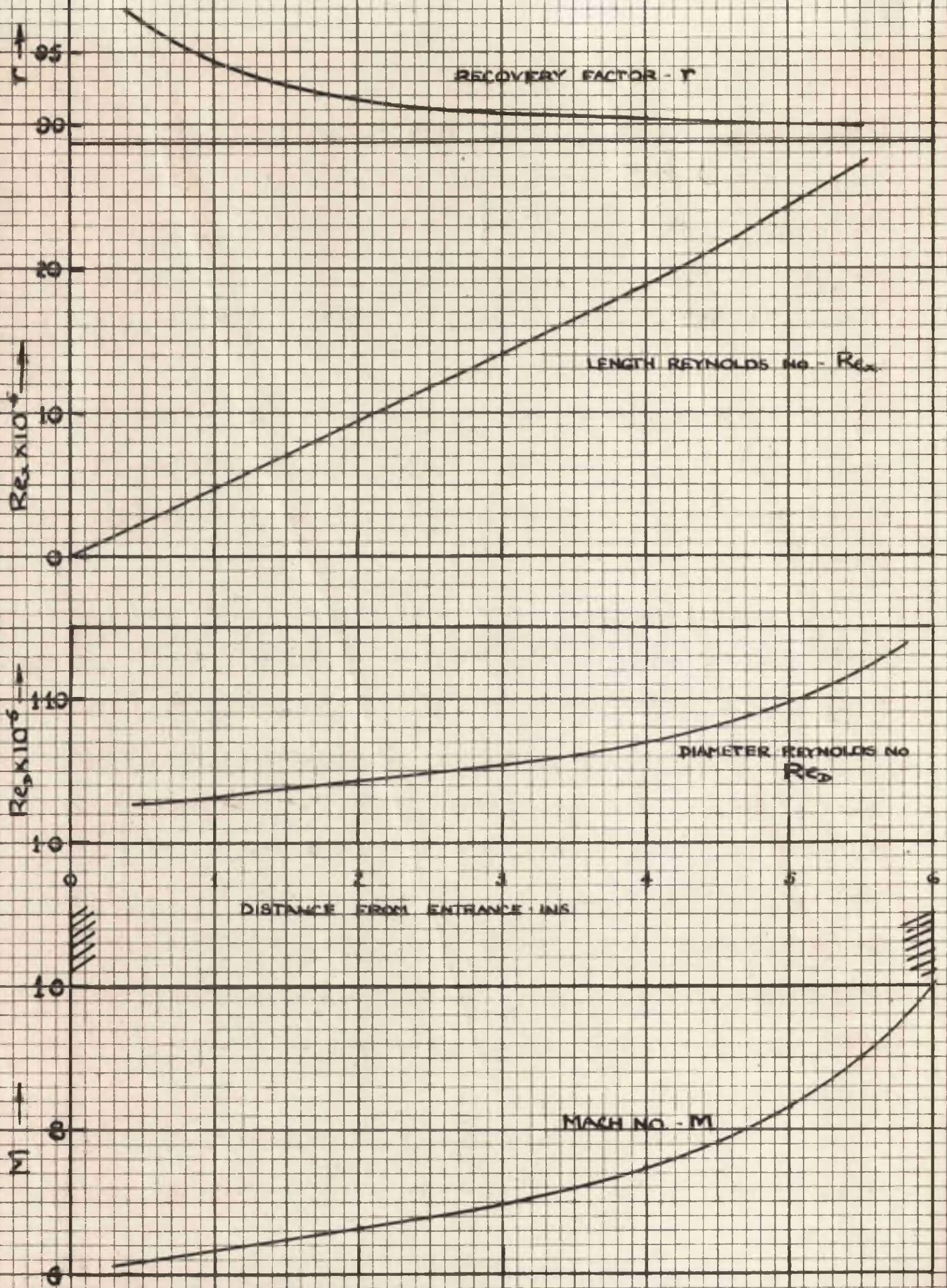
FIG. 41   VARIATION OF r, Re, Re₀ & M WITH LENGTH
TEST RAI

Evaluation of Pr, M and Re and the Characteristics of the Flow.

In order to investigate the variation of the recovery factor the physical quantities of the flow were analysed and the boundary layer conditions examined.

The Prandtl number can again be taken as 1.06 for all conditions of the steam encountered in the tests.

The Mach number was obtained by dividing the actual velocity found from equation 67 by the sonic velocity found from equation 76. The local value of M was calculated thus for the eleven positions along the length.

In the calculation of the diameter Reynolds number, the length dimension is the equivalent diameter $De = D_2 - D_1$, while for the length Reynolds number the length was taken as the distance from the extrance to the section considered. Values of Re_d and Re_l were obtained also for each section. As De is the same for all these positions, the value of Re_d is very nearly constant for each test, since $Re_d = \rho VDe/\mu = GDe/\mu$, and G is a constant where the cross-sectional area is constant. The only variation in Re_d is caused by a slight change in viscosity with the steam conditions. Since the viscosity decreases both with fall in pressure and fall in temperature, the value of GDe/μ increases slightly as expansion proceeds.

Fig. 41 shows a typical variation of recovery factor, length Reynolds number, diameter Reynolds number and Mach number along the length (Test RA1).

In all cases where the state of maximum entropy was attained at the exit, sonic velocity is also reached. Whether such a state exists

can be determined from the pressure at the exit.

The pressure of maximum entropy can be determined as follows:

For this condition, $ds = 0$ for small changes of pressure.

Now $ds = (du + pdv)/T = 0$

But $dh = du + pdv + vdp$

$\therefore (dh - vdp)/T = 0$ or $dh = vdp$ ....(82)

Since $h = A + Bpv$

at maximum entropy

$dh = B(pdv + vdp) = vdp$

$\therefore \dfrac{dp}{p} = -\dfrac{B}{B-1} \dfrac{dv}{v}$ ....(83)

From the energy equation and continuity

$h + \dfrac{G^2 v^2}{2g} = ho$

$\therefore dh \pm \dfrac{G^2}{g} vdv = 0$ ....(84)

For maximum entropy (82) and (84) give:

$vdp + \dfrac{G^2}{g} vdv = 0$ ....(85)

and with (74) $- \dfrac{v}{p} \dfrac{dp}{dv} = \dfrac{G^2}{g} \dfrac{v}{p} = \dfrac{B}{B-1}$

Solving for v and substituting this and the h, p, v relation into the Fanno equation (93):

$A - P_s^2 \dfrac{B^2}{1-B} \cdot \dfrac{g}{G^2} + \dfrac{G^2}{2g} \cdot \left(\dfrac{B}{1-B}\right)^2 \cdot \left(\dfrac{g}{G^2}\right)^2 = ho$

where ps = pressure at maximum entropy.

$\therefore P_s = \dfrac{(B-1)G}{B} \cdot \sqrt{\dfrac{2(ho - A)}{g(2B-1)}}$ ....(86)

It can further be seen from equation 85 and since $G = V/v$ that $V = \sqrt{g \gamma pv}$

i.e. the velocity of sound.

Therefore at the state of maximum entropy, the Mach number is 1. This pressure is seen to be no longer the critical for isentropic flow when $p_s/p_0 = (2/\gamma - 1)^{\frac{\gamma}{\delta - 1}}$ = 0.545 for superheated steam. In most cases for the present tests it was found to give a pressure ratio of 0.45. This pressure ratio was calculated by equation 86 for each test and compared with the actual pressure ratio obtained from the pressure searches. In all cases except tests carried out under pressure conditions RE, F, G and H, it was found that the state of maximum entropy was attained at the exit. There is, however, some difficulty in estimating the pressure ratio at the exit, since the pressure falls very rapidly at this point.

By differentiating the equation of conservation of energy, the continuity equation and the equation of state, and considering the equilibrium with frictional forces acting, the following expression is obtained:

$$(M^2 - 1) \cdot \frac{dV}{V} = \frac{da}{a} - \frac{\tau \gamma \, dA}{\rho \, a v_a^2} \quad \dots\dots\dots\dots\dots\dots(87)$$

This equation shows that convergence of the stream tube and friction cause acceleration of a subsonic flow and deceleration of a supersonic flow. Also, in the presence of friction, sonic flow is reached in a slightly divergent channel rather than at a throat. This indicates that a Mach number of 1 would not be reached in the test section, but this would be obtained immediately afterwards, where the jet is free to expand. In plotting the variation of Mach number along the length for the above tests, it is sufficiently accurate to assume the value is equal to unity at the exit.

The above reasoning is again based on a one-dimensional flow model. Such a postulation is to a certain extent anomalous, since in the actual flow friction acts at the boundaries and destroys the one-dimensional character. As, however, the flow in the downstream sections is turbulent, the velocity over the greater part of the cross-sectional area will be nearly uniform and the above expression will give a good indication of the characteristics of the flow.

In the calculation of Reynolds number, the viscosity was evaluated at the average of the wall and the bulk temperatures. This is the reference temperature normally employed in the calculation of the dimensionless parameters for heat transfer.

It is interesting to note here that Brainerd and Emmons (7) studied the effect of variable viscosity on the boundary layer. They showed analytically that the variation of viscosity with temperature does not alter the equlibrium temperature of the plate and hence the value of the recovery factor.

The length Reynolds number was based on the length taken as the distance from the entrance to the section considered. There is some difficulty in fixing the actual zero for this calculation. The very rapid pressure decrease in the converging entrance will inhibit the growth of the boundary layer and a truer value for the Reynolds number might have been obtained by basing the length as that from the end of the converging portion. The error involved will be small, however, and within the accuracy of the data relating to the boundary layer based on the Reynolds number. The zero was retained as being at the entrance as the calculation was somewhat simplified by doing so.

Fig 42   RECOVERY FACTOR   vs. LENGTH REYNOLDS NUMBER
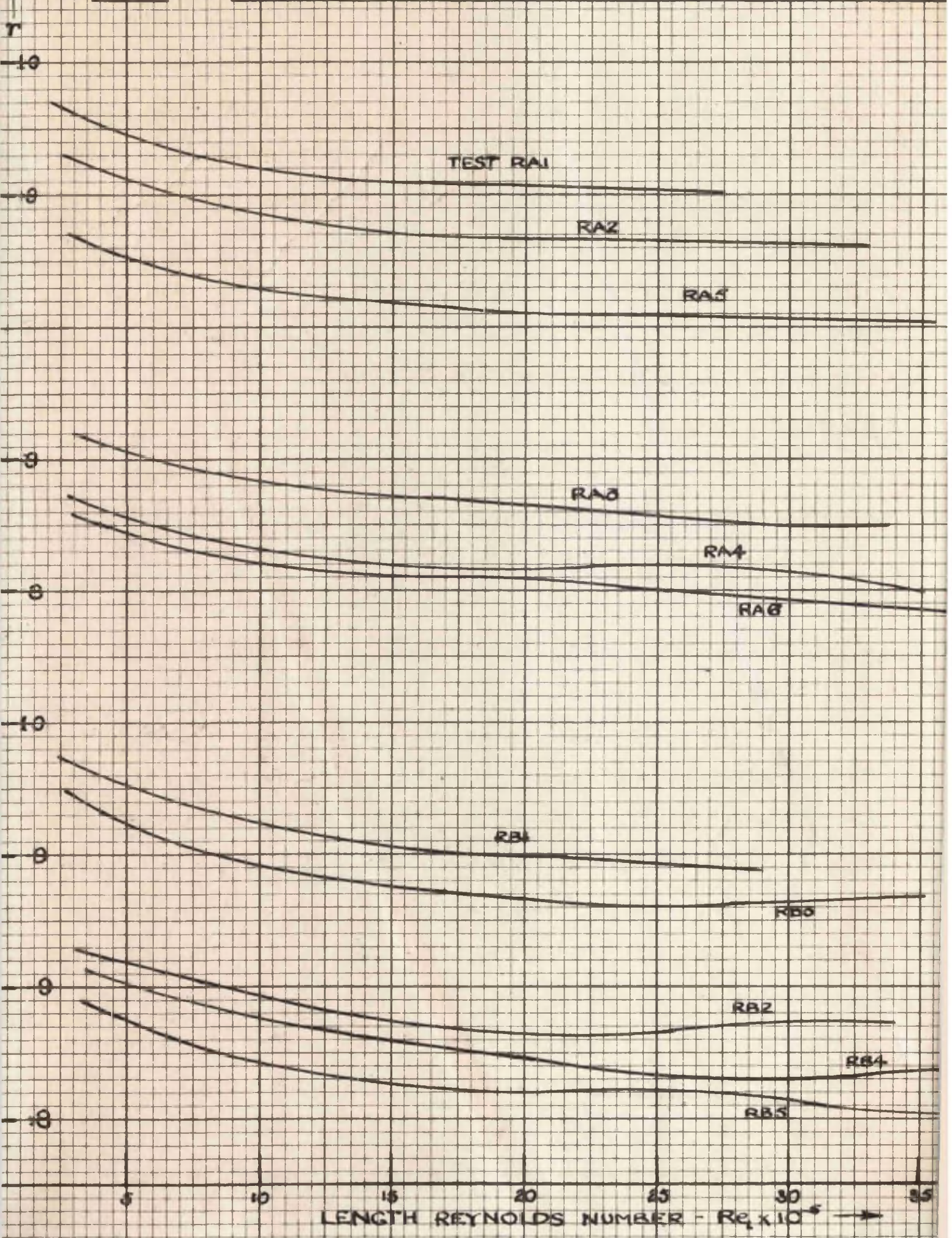
The favourable pressure gradient continues along the whole test length. The effect of this will be to stabilise the boundary layer and to delay the point of transition. The critical Reynolds number is likely to be much above the value of 3×10^5 taken for flow over a flat plate with zero pressure gradient. There are no disturbances in the duct liable to favour transition since both the outer and inner walls of the annulus are straight and smooth. Any turbulence in the free stream will also be damped out in the sudden convergence at the entrance.

The Recovery Factor.

The recovery factor is mainly influenced by the condition of the boundary layer. Now the type of flow in the boundary layer is dependent on the value of the length Reynolds number, since transition occurs before the flow becomes fully developed. The recovery factor was therefore plotted against length Reynolds number for all the tests carried out. These plots are shown in Fig. 42.

Whereas before the curves for the recovery factor versus length from the entrance showed much variation, the curves of r plotted against length Reynolds number are all of one pattern. The initial decrease is found to extend over the same range and the shape of curve for this decrease is similar in each case. For all values of Re_1 of 20×10^5 and over the value of r is substantially constant.

It is evident that the steady value of the recovery factor corresponds to that for a turbulent boundary layer. The value of $Re_1 = 20 \times 10^5$ is that at which it would be expected turbulence would be attained, under the flow conditions.

The initial decrease of r may be owing to the build up of the

FIG. 42 CTD RECOVERY FACTOR vs LENGTH REYNOLDS NUMBER
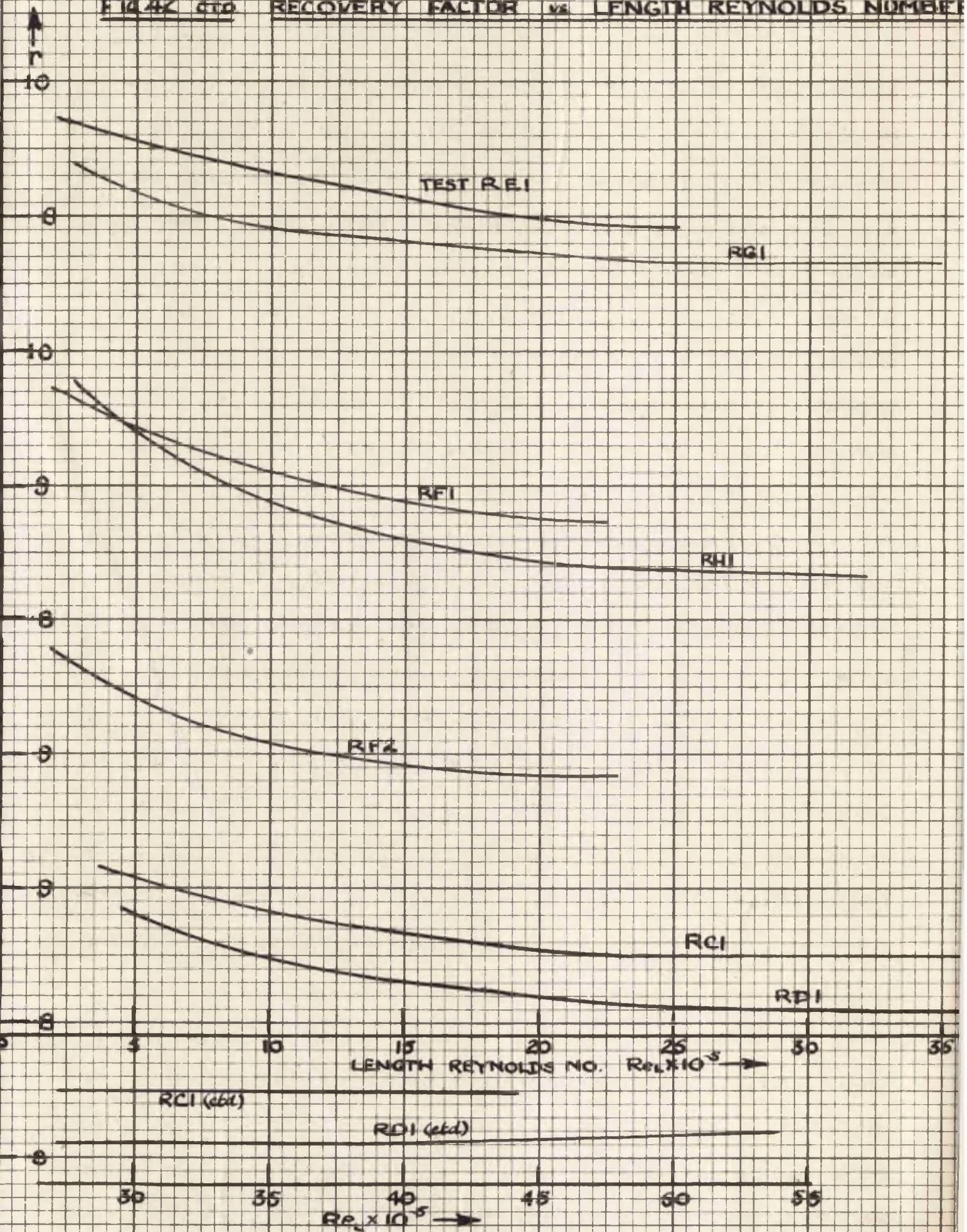
laminar boundary layer, but is probably caused by a gradual transition to turbulent flow. It has been observed before in the previous investigation that the recovery factor for a turbulent boundary layer is lower than that for laminar flow. This is confirmed by the present tests. There will always exist a short section at the entrance where flow is laminar, and it is seen that the higher values of r occur at this region. There is, however, no indication of a constant value for the recovery factor for any position near the entrance as was obtained for the short nozzle. This is probably owing to the fact that stream conditions and recovery factors were only calculated at 1/2" intervals, whereas previously these were calculated for every 0.1 in. of length. A true laminar boundary layer probably exists only for a short distance. There will then take place a transition to turbulence, indicated by the recovery factor gradually assuming a constant value. Since there are no disturbing influences in the stream, the transition will be gradual, taking a considerable length of the test section to be completed. So long as the laminar layer exists only a small area of the cross-section will be affected by viscosity. Even after the transition to turbulence, the boundary layer will not completely fill the cross-section, fully developed flow probably being attained only near the exit, if at all. The thickening of the turbulent boundary layer therefore does not appear to have an effect on the value of the recovery factor.

In this manner the variation in the value of the recovery factor can be explained in the light of the nature of the boundary layer. There still remain, however, variations in the value of r which are not explained by the above. It can be observed that values of r for tests with higher initial superheats are higher than those for tests with lower steam supply
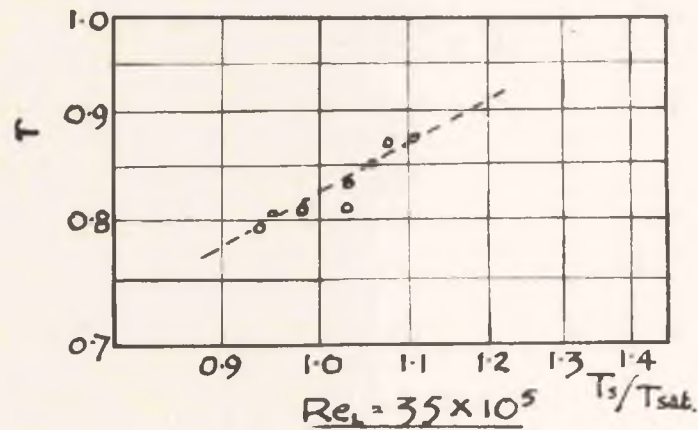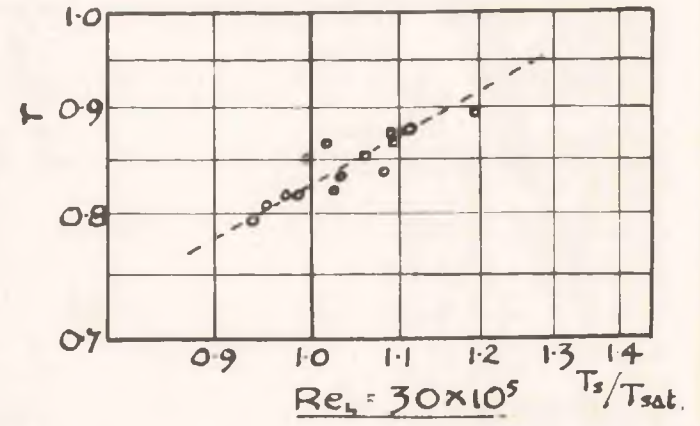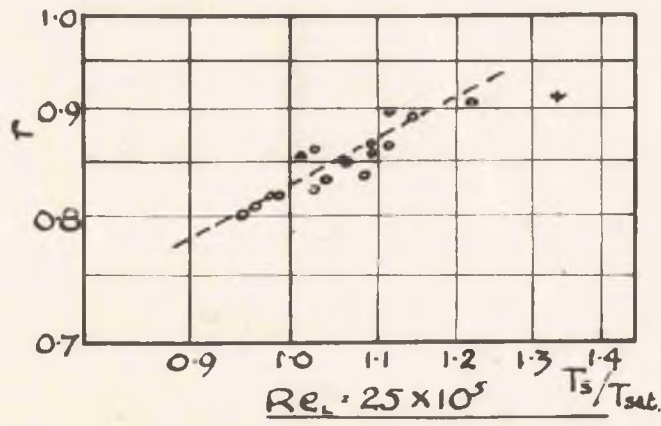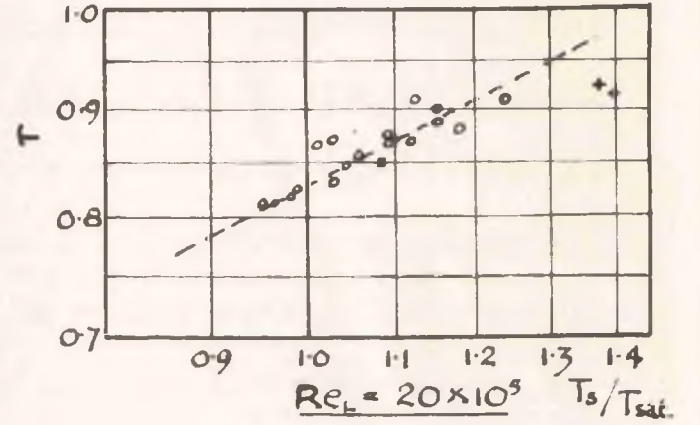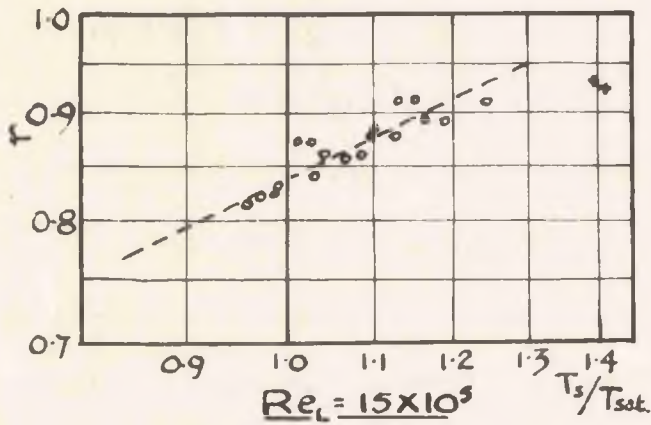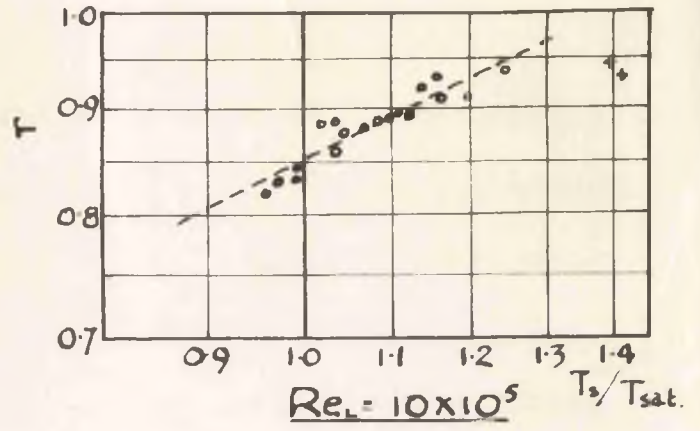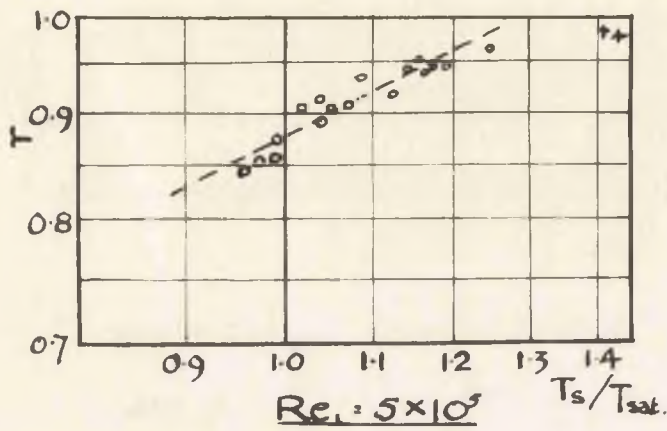
FIG. 43   RECOVERY FACTOR   vs.   RATIO – $T_s/T_{sat.}$

temperatures. In order to be able to predict recovery factors for future tests with heat transfer it is necessary to obtain a law governing this temperature effect.

Plotting r against the stream temperature for any one value of length Reynolds number gave an almost linear variation for each set of tests under the same pressure conditions, but there was no correspondence for all the tests. The controlling feature was evidently the degree of superheat. The ratio of the absolute steam temperature to the absolute saturation temperature corresponding to the pressure was therefore calculated and plotted against Re_1 for each test. The recovery factor was then plotted against $Ts/Tsat.$ on a logarithmic scale. This was carried out for values of length Reynolds numbers of multiples of 5×10^5 from 5 to 40×10^5, values of r and $Ts/Tsat.$ being picked off from the plots vs. Re_1. The plots are shown in Fig. 43. In each case the variation of r with $Ts/Tsat.$ can be represented by a straight line of the form

$$r = K \left(\frac{Ts}{Tsat.} \right)^{\eta} \qquad \dots\dots\dots\dots\dots\dots\dots\dots(88)$$

The value of η was found to be 1/2 for all values of Re_1. For positions where Re_1 is equal to or greater than 20×10^5 the value of K is 0.827 while for Re_1 equal to 5, 10 and 15×10^5, the values of K are 0.879, 0.85 and 0.834 respectively. Values of r and $Ts/Tsat.$ are tabulated in the Appendix (Table 3a).

It is also seen that the relationship between r and $Ts/Tsat.$ holds for values of $Ts/Tsat.$ both greater and less than unity i.e. in both the superheated and the supersaturated fields. This is in agreement with the findings of the investigation with the short nozzle, in that there is no

fundamental difference between the superheated and supersaturated states
of steam in the temperature recovery in the boundary layer.   In the
present case, the problem of the limit of supersaturation does not arise.
Owing to the reheating effect of friction, the degree of supersaturation
in the most extreme case was not greater than 2.5.   This is much less
than the limiting value as observed in any previous investigation.   To
obtain a greater degree of supersaturation, a much more rapid expansion
of the steam would be necessary.

A relationship is therefore obtained from which values for the
recovery factor can be predicted once the stream conditions are known.
These conditions can be calculated from a knowledge of the initial steam
condition, the pressure variation along the length and the mass flow, which
all can be readily measured.

The formulae for the recovery factor thus derived are strictly
emperical and are in no way derived from or in support of theory which
demonstrates that r is only dependent on the Prandtl number and will have
a value very nearly equal to 1.   The use of the equations must therefore
be limited to the same range of conditions as those of the tests i.e. to
the flow of steam in the entrance region of an annular duct.   The supply
pressure varied from 20 to 50 lb./sq.in. gauge, while the supply
temperature ranged from saturation values to 500°F., or rather the upper
limit is given by $T_s/T_{sat.}$ equal to 1.25 for any point in the test length.
The equations for recovery factor cannot be extrapolated beyond these
limits with assurance.

With increasing stream temperatures the formulae for r indicate
that the value would also increase indefinitely.   As this seems rather
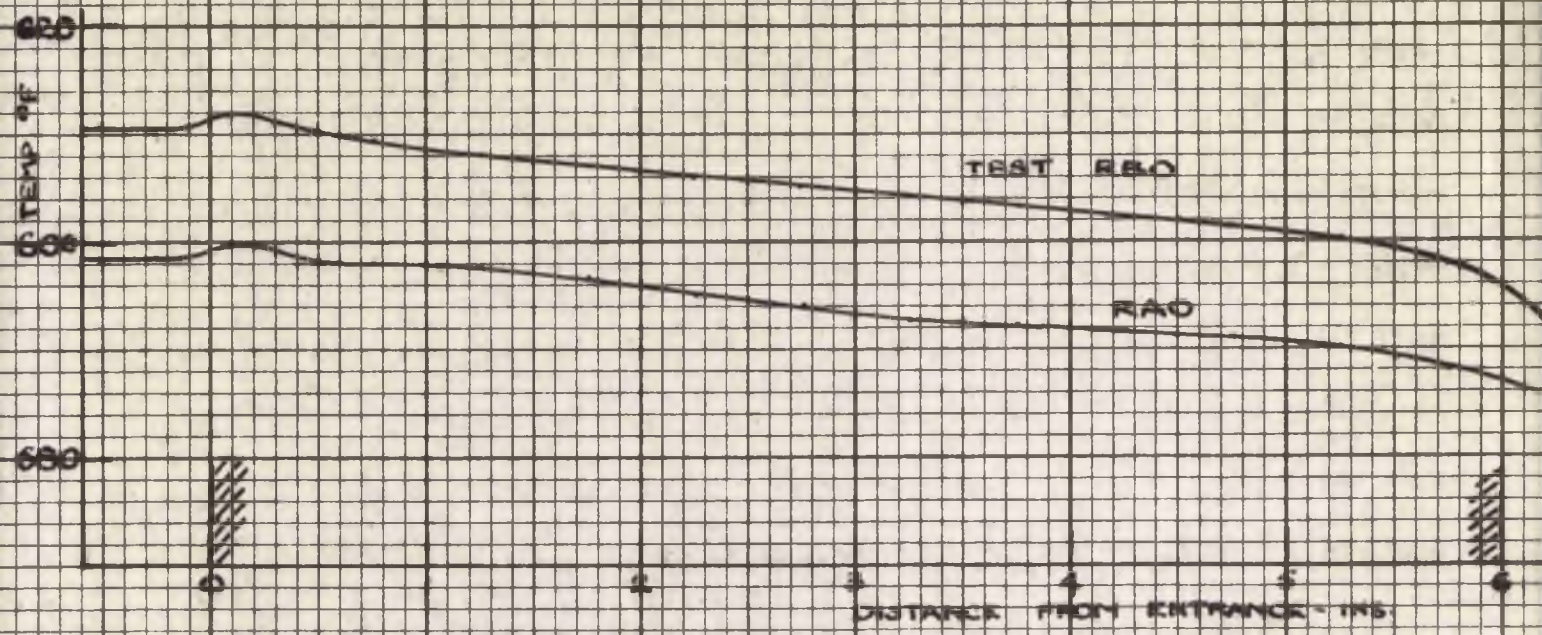
a. ADIABATIC WALL TEMPERATURE t_{aw}
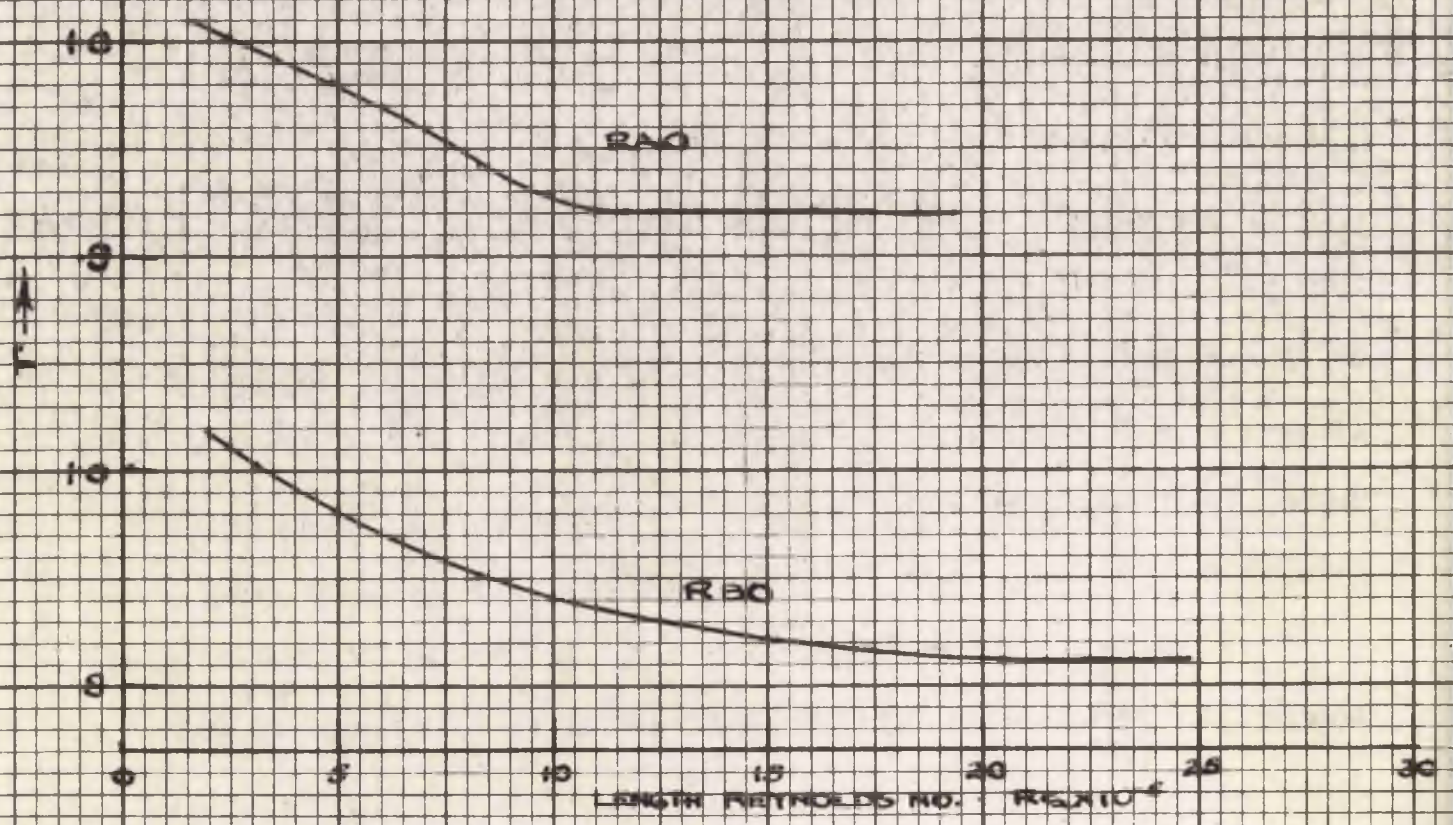
b. RECOVERY FACTOR vs LENGTH REYNOLDS NO.

FIG 44   RESULTS OF HIGH TEMPERATURE TESTS

unlikely it was later decided to undertake tests with as high an initial superheat as could be maintained. Two tests were carried out, one with a supply pressure of 20 lb./sq.in. gauge and the other 30 lb./sq.in. The supply temperature was approximately 600°F. in each case. The apparatus was the same as in previous tests. Additional lagging was however applied to the supply pipe between the superheater and the receiver, while larger gas jets were fitted to the superheater burners. This enabled the higher temperatures to be obtained, together with the required uniformity.

In Fig. 44a, are shown plots of the adiabatic wall temperature against length along the duct. It is seen that in the entrance region, for a length of about 1/2 in., the wall temperature is slightly above the total temperature. Thereafter there is a gradual decrease throughout the length, the distribution being the same as for the tests with lower temperatures. The fall in temperature is, however, more gradual than in the previous tests.

Recovery factors were calculated in the usual manner. These are shown plotted versus length Reynolds number in Fig. 44b. The curves are of similar shape to the previous ones, with an initial decrease and flattening out at a value of Re_1 between 15 and 20 x 10^5. At first the value of r is greater than unity corresponding to the region in which the adiabatic wall temperature is above the total or stagnation temperature.

The ratio of steam temperature to the corresponding saturation pressure was then calculated and the recovery factor plotted against this ratio for the selected values of length Reynolds number. These points are shown in Fig. 43 where they are indicated by crosses. It is seen that for all values of Re_1 they lie considerably below the straight line $r = K(T_s/T_{sat.})^n$ which represents the values obtained from tests with lower

temperatures.

It would indeed be unreasonable to expect this equation to hold for all values of temperature, since by increasing the ratio $T_s/T_{sat.}$ the value of r obtained by this formula could be also increased indefinitely. Such behaviour of the recovery factor is improbable. It is possible that the value of r for the turbulent region will approach the theoretical value of unity asymptotically as the temperature increases. This would be supported by the values obtained in the tests with higher supply temperatures.

DISCUSSION ON THE RESULTS OF THE RECOVERY FACTOR MEASUREMENTS.

Values of recovery factor measured in the investigations described in Parts II and III of the thesis are of the same order as those for air. They are, however, considerably lower than those predicted by theory. For both laminar and turbulent boundary layers, the theoretical value is unity, since Pr is very nearly equal to 1 for the range of steam conditions encountered in the tests. Only in a few instances were recovery factors as high as this obtained.

For the laminar boundary layer a value of 0.94 was recorded for r, and no temperature variations was observed for the range of temperatures employed. This is 6% below the theoretical, which is generally agreed to be equal to $(Pr)^{\frac{1}{2}}$.

Results for the turbulent boundary layer showed values of recovery factor lower than for laminar flow, and further, that the value varied with the difference between the stream temperature and the saturation temperature. There is less agreement as to what the correct value should be for the turbulent boundary layer. It is more difficult therefore to compare the values obtained in the present investigations for steam with those which may be expected for turbulent flow.

For both laminar and turbulent flow, however, it appears that the value of the recovery factor for steam is lower than that which is based on the theoretical expressions and on the measurements for air.

Three reasons may be put forward to account for these low values: (i) Radiation (ii) Steam near the saturation level does not behave as a pure gas and (iii) The theory is not complete but predicts values which happen to be approximately true in the case of air.

(i) Radiation. Water vapour is one of the gases which absorb and radiate heat, unlike elementary gases, such as hydrogen, oxygen and nitrogen which radiate no heat and are perfectly transparent to heat radiation. Now in the present adiabatic test runs, the wall assumes with frictional heating a higher temperature than the free stream. There will therefore be a certain exchange of heat by radiation between the walls and the steam which does not occur with a transparent gas such as air. There is, of course, no net exchange of heat between the outer and inner walls of the annulus since they are both at the same temperature.

To calculate the temperature assumed by the wall when radiation takes place, the boundary conditions for the convective equations (22 - 24 for laminar flow) must be modified. $\frac{\partial t}{\partial y}$ will no longer be zero for $y = 0$, but such that heat transferred at the boundary equals heat transmitted by radiation. A general equation for q_r, the heat transferred by radiation, cannot be given, as this depends on the shape of the gaseous volume, and the pressure, besides being dependent on the final temperature assumed by the wall, which is not known. The solution of the partial differential equations under these circumstances would be difficult if not impossible.

The amount of heat transferred by radiation is, however, very small. Later in the method of calculation for heat transfer results in Part IV, it is shown how the correction for heat transferred by radiation is calculated. It is seen there that this quantity is negligible compared with the amount of heat transferred by other means.

A correction can be calculated and applied to the measured wall temperature, to enable the temperature to be found which the wall would assume if there were no heat transfer by radiation. It is assumed that

the modified law, $q = hA (t_w - t_{aw})$ holds. Here t_{aw} is the temperature which is to be found, t_w is that measured, and q is the heat transferred by radiation.

q May be calculated from the formula given in Part IV. In this case, since both walls of the annulus are at the same temperature, the formula simplifies to

$$\left(\frac{q}{A}\right)_r = 0.173 \, \epsilon'_w \left\{\left(\frac{T_w}{100}\right)^4 \propto \, L_1 \, -\left(\frac{T_g}{100}\right)^4 \cdot \, \epsilon_g \, L \right\} \quad \ldots\ldots(89)$$

For a typical test, say RB2, $T_w = 849^\circ R$ and $T_g = 800^\circ R$. Since the temperature measured is that of the brass pin inserted in the insulating portion, the value of ϵ'_w is taken as that for brass at T_w, and in this case $\epsilon'_w = 0.525$.

Taking $\epsilon_g = 0.094$ and $\propto L_1 = 0.0928$, then:

$$\left(\frac{q}{A}\right)_r = 0.173 \times .525 \left\{\left(\frac{849}{100}\right)^4 \times .0925 - \left(\frac{800}{100}\right)^4 \times .094\right\}$$

$$= 8.67 \; B.T.U./hr.ft.^2$$

Then $\delta t = \frac{q}{A} \cdot \frac{1}{h} = \frac{8.67}{261} = 0.033^\circ F.$

It can therefore be seen that the effect of radiation will not appreciably affect the temperature measured at the insulated wall of the annulus.

(ii) It is well known that vapours near the saturation conditions in many respects do not behave as true gases. Thus the perfect gas law, $pv = RT$, no longer holds true even approximately, and the deviation from this law increases as the saturation line is approached. The theoretical relationships for heat trasnfer and more especially the recovery factor are derived assuming that the perfect gas law holds true or rather that the variation of

the internal energy with respect to temperature is a pure temperature function - a property of the ideal gas. When there is a departure from the ideal state it may be expected therefore that the normal equations, such as that giving the value of the recovery factor, will no longer hold exactly.

It has already been observed that the presence of water particles in the steam results in lower adiabatic wall temperatures being recorded. Though it is not to be expected that any water droplets can exist in steam which is dry or superheated, yet similar effects may be caused by water droplets on a molecular scale and become apparent as the saturation line is approached. It also has already been noted that steam in the first type of the supersaturated state proceeds into the second type as expansion takes place, without the occurrence of any sudden discontinuity of the characteristics. Thus the growth of water droplets in the second type of supersaturated state results in only a gradual divergence of the adiabatic wall readings from the normal. It is probable that there is a similar merging from the state of the perfect gas reached at high temperatures and low pressures, to conditions near the saturation values, and so on to the supersaturated conditions and the gradual reversion to the second type of supersaturation.

That the above considerations may account for the low values of recovery factor is supported by the temperature dependency observed. For conditions near the saturation line, and for the supersaturated states, low values of recovery factor were obtained, while with increasing temperature the recovery factor also increased and appeared to approach asymptotically the theoretical value of unity. It would be interesting to carry out tests

at high temperatures in order to discover whether the theoretical value is attained. Such tests, however, would not be easy to accomplish as, many of the insulating materials suitable for the construction of the search probe are not capable of withstanding high temperatures, and also the obtaining, and maintaining at a steady value, of the steam temperature is difficult.

(iii) The theoretical relationships for the recovery factor in general show that the value is a function only of the Prandtl number. In order to verify this experimentally it would be necessary to carry out experiments with gases having a range of Prandtl numbers. So far the only investigations have used air as the working fluid, and thus the range of Prandtl number for which values of r have been obtained is strictly limited. To confirm beyond doubt that the theoretical relationships are correct it will be necessary to investigate over a much wider range of Prandtl number. In view of the discrepancies between theory and experiment so far observed, the theoretical relationships can in no way be taken as verified. It appears that a good deal of experimental work has yet to be undertaken. In the meantime the measured values will be accepted and these will be used in the measurement of heat transfer coefficients.

It is a point of interest that while the heat transfer coefficient is dependent on the thickness of the boundary layer, the recovery factor is independent of this thickness. In the entrance region of a pipe and near the leading edge of a flat plate, where the boundary layer has only started to grow, the heat transfer coefficient has a higher value than in the down-stream regions. The dependence of the coefficient on the thickness of the boundary layer is allowed for in the equations for heat transfer by the

inclusion of the Reynolds number, since the growth of the boundary layer
is dependent on the value of this parameter.

The generally accepted equations for the recovery factor do not
contain the Reynolds number, showing that r is independent of the thickness
of the boundary layer.   In the experiments with flow along the 6 in. long
annular duct, it was observed that once the turbulent flow was fully
established in the boundary layer, the value of the recovery factor
remained unchanged.   Yet after the transition to turbulence the boundary
layer still continues to increase in thickness since the evidence indicates
that fully developed flow is only attained at a point very near the exit
if at all.   In the case of laminar flow through the short nozzle it was
also noted that the values of r obtained were independent of the length
Reynolds number and the growth of the boundary layer (Fig. 28a).   The
results of the present investigations therefore support the theoretical
relationships in that the Reynolds number should not appear in the
expression for the recovery factor.

THE MEASUREMENT OF HEAT TRANSFER COEFFICIENTS
AND FRICTION COEFFICIENTS.

In this part of the thesis are described the experiments undertaken to obtain values of heat transfer coefficients for the high velocity flow of steam and to compare them with values for low velocities. For these tests, values of recovery factor obtained previously for flow under similar conditions were employed in estimating the adiabatic wall temperature required in the calculation of heat transfer coefficients. Friction coefficients were also evaluated from previous measurements of the pressure distribution, and the results are examined in relation to the analogy between momentum and heat transfer.

APPARATUS.

The arrangement of the apparatus in so far as the flow of steam is concerned is identical with that described in Part III. Steam from the boiler passes through the superheater and so to the receiver. From there it passes through the annular test section of exactly similar dimensions. The outer wall of the annulus is formed by the same brass nozzle as before, but the inner surface is the outside wall of a 3/16 in. diameter brass tube. The steam thence passes through the exhaust pipe to the condenser.

It was the intention in these experiments to study heat transfer from the steam to the inner surface of the annulus. To do so, heat is abstracted from the steam by passing a cooling fluid through the inner tube. Since the fluid must have a continuous path, the 3/16 in. diameter brass tube is passed right through the receiver and out the opposite side through a stuffing box. This stuffing box is fitted to a flange on this side of

the receiver. On the exhaust side the tube passes through the same stuffing box as was used for the temperature and pressure search tubes.

The Air Circuit.

The choice for the cooling medium lay between the most commonly used fluids; water and air. As it was intended to investigate the coefficient of heat transfer when the wall temperature was near to the adiabatic or natural wall temperature, only small amounts of heat could be abstracted. For this reason air is most suitable.

A further advantage in the use of air is that the direction of heat transfer could be reversed by heating the air to a sufficiently high temperature before passing it through the test section.

The air not only served as a coolant, but by measuring the temperature rise and the flow, the quantity of heat transferred could be calculated. A means of metering the air was therefore included in the air circuit.

Air is supplied by a two-stage compressor driven by a double acting steam engine. The compressor discharges to a large storage tank, the pressure in which can be maintained at any desired value by altering the compressor speed. This pressure was kept at 10 lb./sq.in. gauge throughout the tests. Pressure variations owing to the reciprocating nature of the compressor are damped out in this tank and also a certain proportion of the moisture contained in the air is condensed and can be drained from the foot of the tank. A stop valve placed conveniently near was used for fine adjustment of the pressure.

Some difficulty was encountered in obtaining a suitable means of measuring the flow of air. The most convenient method of measuring air

flow is to record the pressure drop across an orifice plate or nozzle placed in the air stream. In the present case the air flows along a tube which is approximately 1/8 in. inner diameter and about 4 ft. long. In this length the pressure drop is only a few inches of water. To obtain a reasonable pressure drop across a nozzle plate for such a flow, the orifice must be of such small dimensions that it is doubtful if the published discharge coefficients would apply. Furthermore, it would be very difficult to manufacture a standard orifice or nozzle of such small size. If, on the other hand, a non-standard orifice were used, calibration would be difficult. The standard method of calibration such as described in reference 81 involves the use of a calibrating pipe traversed by a total head tube. It can be realised how difficult this would be on the scale of these tests.

For the quantities of air used in the experiments the most suitable method of measurement is the use of a gas meter. Gas meters are of two types - the dry meter and the wet meter. The latter is much more accurate than the former, having an accuracy of the order of 0.1% when carefully calibrated. However, a wet meter of sufficient capacity was not easily obtainable, while several of the dry type were. The maximum capacity of the wet meter in the laboratory was 6 cu.ft. per hour, whereas the flow of air to be measured was approximately 30 cu.ft. per hour. A wet meter for such flows would be inconveniently large. The procedure adopted therefore was to calibrate the dry meter against the wet meter by passing air in series through both at an hourly rate of somewhat less than 6 cu.ft. The percentage error in the readings of volume obtained was then assumed to be the same for the higher rates of flow. The accuracy of the wet meter was in turn checked by passing a known volume, obtained by
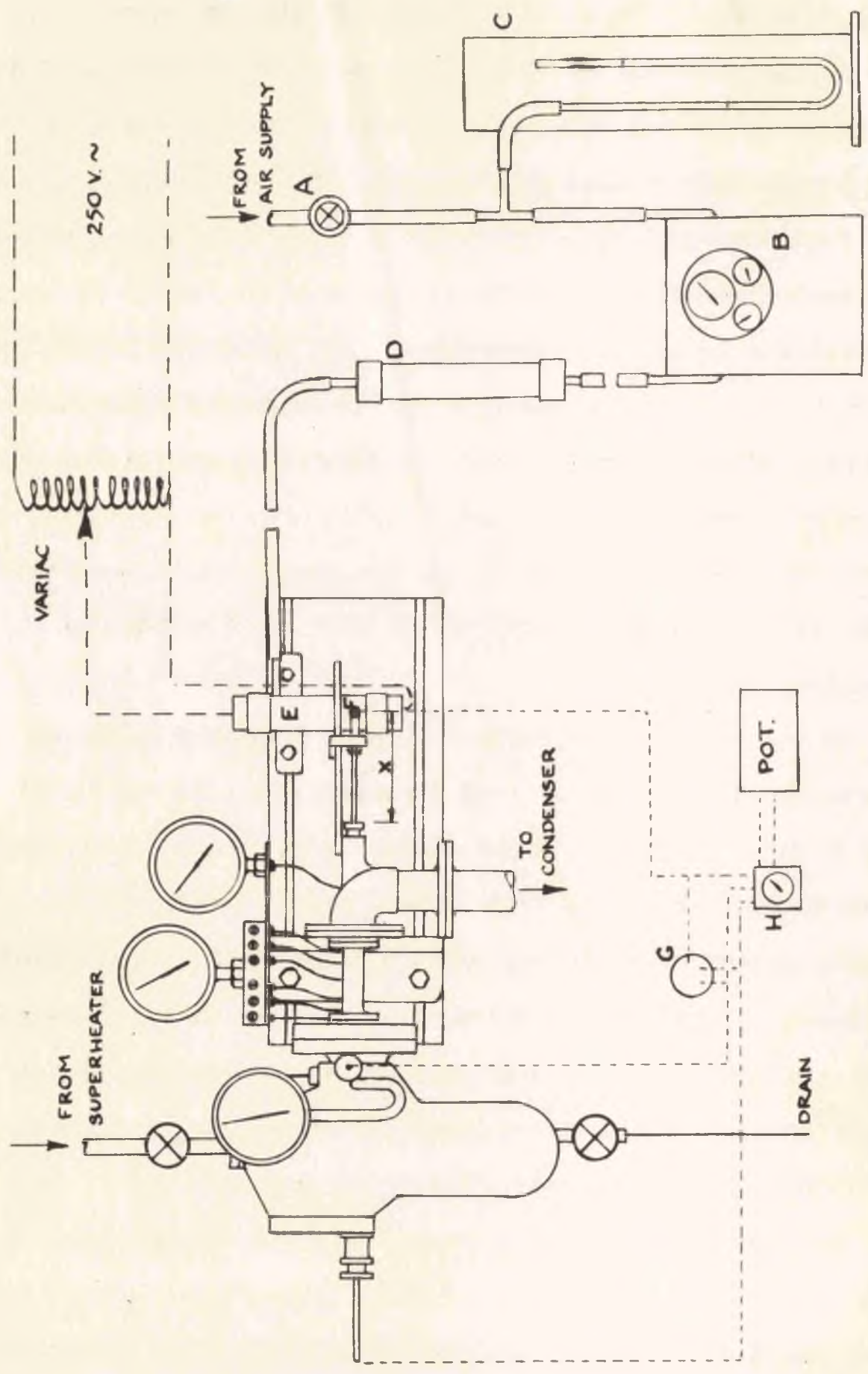
Fig. 45 GENERAL ARRANGEMENT OF APPARATUS FOR HEAT TRANSFER TESTS

displacing a standard volume of air by water, through the meter. By opening and closing the appropriate cocks, repetition of this operation enabled an accumulative reading to be obtained. No error could be observed for the meter reading when this check was carried out.

The dry meter is not a precision instrument, the usual guaranteed accuracy being about 3%. A certain proportion of the inaccuracy is owing to the stretching of the flexible bellows. For this reason, after a period of service a calibrated meter can no longer be considered reliable. As two meters were available, this difficulty was overcome by calibrating one against the wet meter while the other was being used for the tests. The two meters were then interchanged frequently, usually after each day's testing. In this way the accuracy of the meter could be taken as considerably increased.

In Fig. 45 the air circuit is shown in diagrammatic form in relation to the steam circuit. From the stop valve A the air is led directly to the gas meter B. A tee piece tapping is inserted in the rubber tubing immediately before the meter. This is connected to a water manometer C enabling the inlet air pressure to be noted. By maintaining this pressure constant (usually somewhat below 30 in. water) by manipulation of valve A, a steady flow of air is ensured. A knowledge of the pressure is also necessary, together with the temperature, to calculate the mass rate of flow of air from the volume recorded by the meter.

From the meter the air is led to the silica gel air drier D. This consists simply of a length of 2 in. conduit tubing of sufficient length to contain 1 lb. of silica gel. Suitable end connections for attachment of the rubber tubing are screwed onto the ends. A fine mesh brass gauge

retains the silica gel. The amount of silica gel contained in the drier was based on the following considerations.

Air under atmospheric pressure and at room temperature and at 80% relative humidity contains 64 grains of water per pound. This moisture is carried with the air in its passage through the compressor to the storage tank. Here the temperature will revert to that of the room. Under the conditions here - absolute pressure 25 lb./sq.in. and temperature 65°F., say - the air will become saturated. The moisture content calculated from $S = 0.622 \, ps/(p - ps)$, is then 53 grains per lb. The excess water vapour is condensed and can be drained off at the foot of the tank.

The rate of flow of air is approximately 3 lb. per hour. In a test lasting 8 hours, therefore, 24 lbs. will be passed and this will contain $24 \times 53/7000 = 0.18$ lb. of water. For 100% efficiency of removal of water vapour, the silica gel should not absorb more than 20% of its weight of moisture. Therefore 1 lb. of gel will completely dry sufficient air for one day's testing.

Two such air driers were therefore constructed. While one was in use, the other was reactivated by passing air through at approximately 300°F. This removes all moisture from the silica gel and the operation is completed within a few hours. Between each test the driers were then interchanged.

The air drier is included in the circuit after the gas meter because very dry air should not be passed through this type of meter. The bellows are coated with a thin layer of grease, and this will be removed unless the air or gas contains a certain amount of moisture. The moisture carried in the air before drying is sufficient to ensure that the

½" COPPER TUBING

2" CONDUIT TUBING

GAUZE RETAINER

15"

SILICA-GEL

(b) THE AIR DRIER

2" CONDUIT TUBING

10½"

1 K.W. SPIRAL HEATER

2 B.A. TERMINAL

AIR INLET

AIR OUTLET

SINDANYO END PIECE
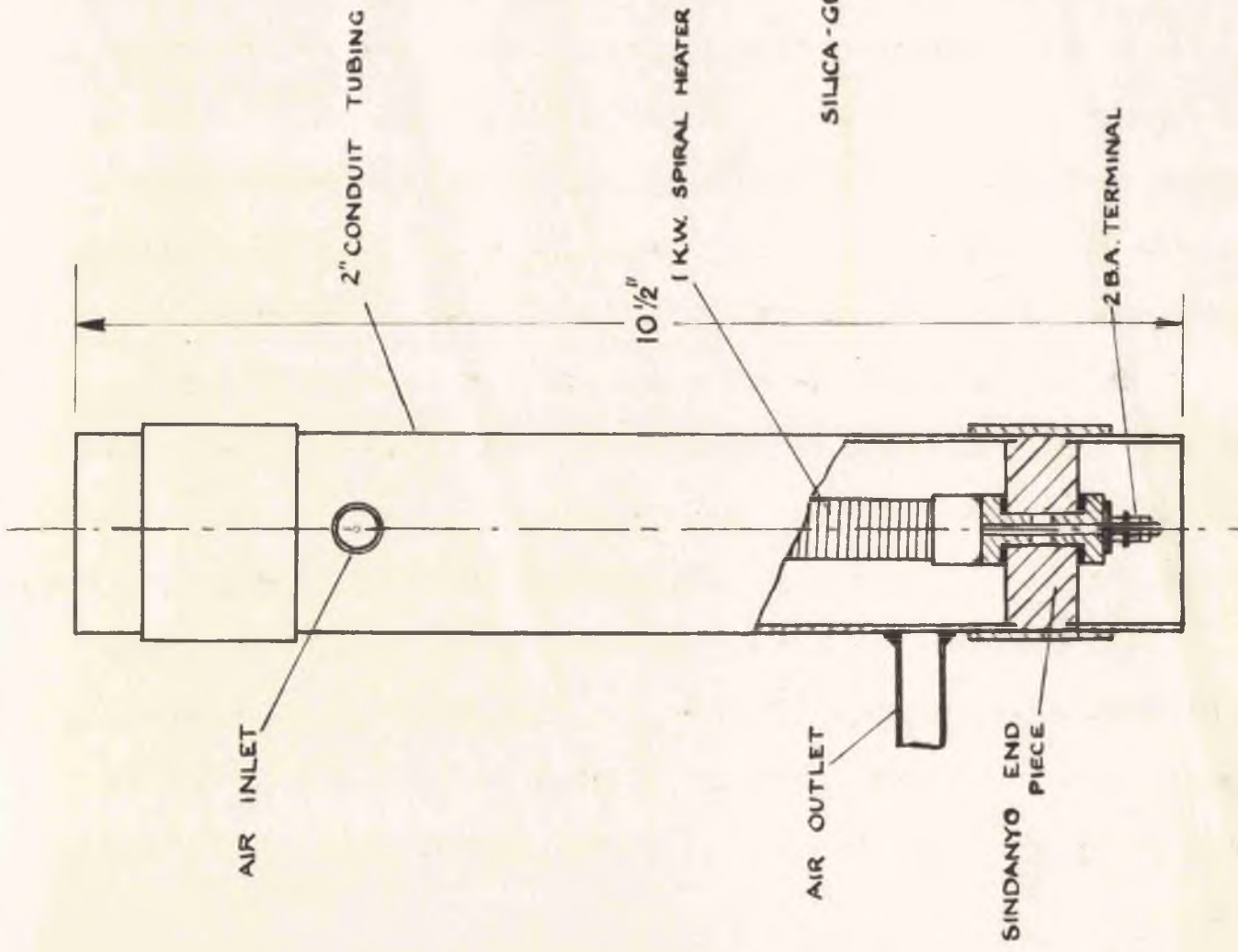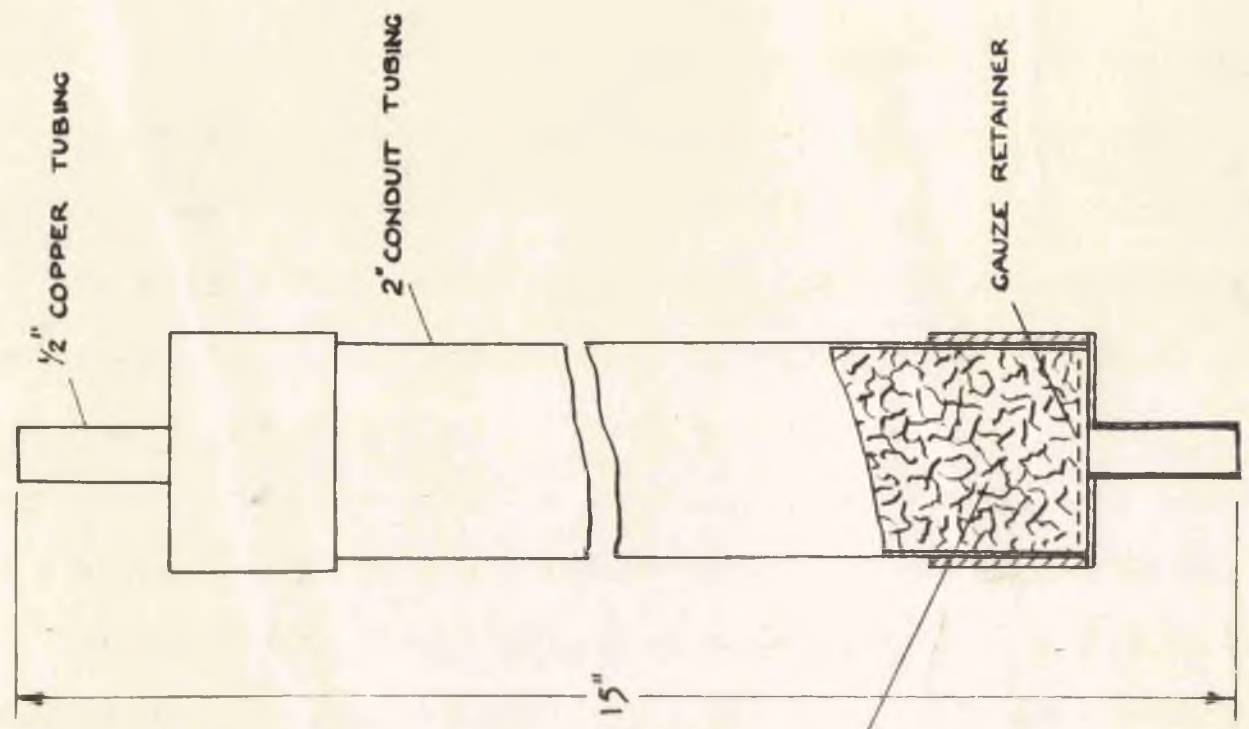
(a) THE AIR HEATER

Fig. 46.

efficiency of the meter will not be impaired.

From the drier the air passes to the air heater E. This again
is constructed from 2 in. conduit tubing. A 1 KW commercial spiral heater
is supported axially in the centre of the tube by means of Sindanyo end
pieces, the terminals passing through these Sindanyo discs. The heater is
mounted vertically, air being passed in at the top and led out at the bottom.
A suitable arrangement of baffle plates in the heater and also in the outlet
tube prevents convection currents in the heater and ensures a steady outlet
air temperature. This temperature is measured by a copper-constantan
thermocouple F placed in the outlet tube. The thermocouple wires, together
with the insulation are passed through 1/8 in. o.d. copper tubing and the
junction brazed to the closed end. A considerable length of the tubing is
then exposed to the air stream to avoid conduction effects. Current is
supplied to the heater from the 250 volt A.C. mains, the voltage being
regulated by a "Variac" auto-transformer. In this way the temperature of
the air entering the test section can be varied over a wide range.

The air drier and the air heater are shown in Figs. 46a and b.
Both were checked for leaks by immersing in water and applying air pressure
to the inside. Any leaks then became apparent immediately. No difficulty
was encountered on account of air escaping from the rubber tubing connections.

The air heater is directly connected to the search tube through
the steel block which slides on the scale. The weight of the heater was,
however, taken by a bracket which was attached to the slides on the wall
behind the apparatus and which could be moved horizontally with the search
tube.

After passing through the search tube, the air is allowed to
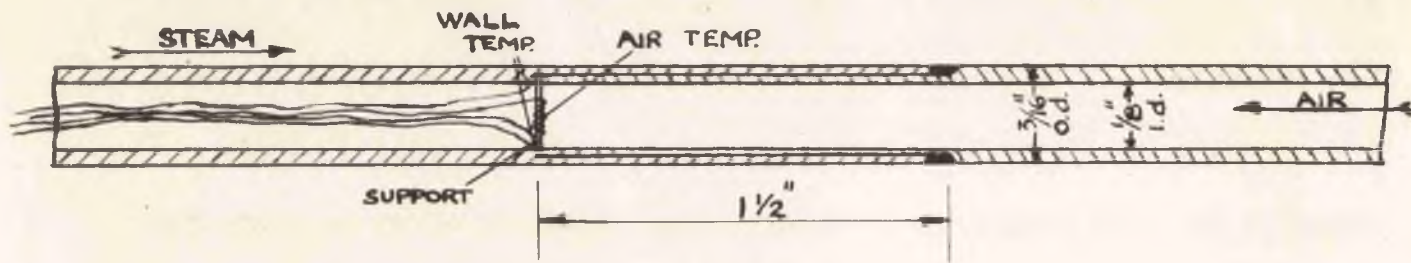
(a) ORIGINAL ARRANGEMENT
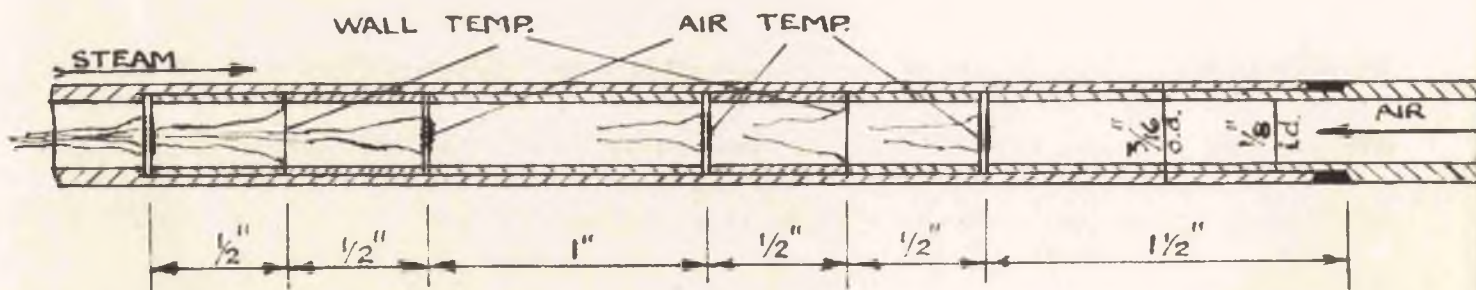
(b) FINAL ARRANGEMENT

FIG. 47 SEARCH TUBE FOR HEAT TRANSFER TESTS

escape to atmosphere. It is seen that, with this arrangement, the air flows in counterflow to the steam. Counterflow normally results in a more uniform distribution of temperature difference. In the present case it is the adiabatic wall temperature for the steam side which decreases as the steam passes through the test section, while the temperature of the air passing in the opposite direction rises in passing through. This results in a much more even distribution of difference between the adiabatic wall temperature and the actual wall temperature. With parallel flow this difference would be very large at the entrance and would diminish rapidly towards the exit. This would make the measurement of local heat transfer coefficients more difficult.

The Search Tube.

In calculating the heat transfer coefficients from the steam to the inner wall of the annulus, the formula

$$h = \frac{q}{A} \quad \frac{1}{(t_{aw} - t_w)} \quad \dots\dots\dots\dots\dots\dots\dots\dots\dots\dots(90)$$

is employed. The value of A is obtained from the geometry of the system and is the area of the surface of the inner tube through which the amount of heat q is transferred. The heat transferred over a certain length of tube can be calculated from a knowledge of the rise in air temperature over this length and the rate of air flow. The temperature t_{aw} can be found from the results of the previous experiments but t_w must be measured. It is therefore necessary to measure the distribution of air temperature throughout the length and the wall temperature. These measurements, made by thermocouple, are achieved by constructing the search tube as shown in Fig. 47. Brass tubing 3/16 in. o.d. was used, the wall thickness being

24 S.W.G. and the inner diameter 0.144 in.

In the first such tube constructed, shown in Fig. 47a, two such pieces of tubing were joined together by drilling the end of one section until half the thickness of the tube wall was removed for a length of 1.1/2 ins., and reducing the outer diameter of the other piece to an appropriate push fit diameter. The thermocouple wires were brought along the inside of the tube from the air flow outlet. The thermocouple for measurement of the air temperature was wrapped round a small wooden pillar supported by the inside shoulder and held in place by the mating of the other portion of tube. The few turns round the support provide protection against breakage of the thermocouple joint and minimise the effects of heat conduction along the wires, since a length of insulated wire is maintained at constant temperature. The wall temperature is measured by the ends of the two wires being jammed at diametrically opposite points between the two walls of the mating tubes.

On assembly of the search tube, the external joint was brazed, the excess brazing being filed off and the whole polished to 3/16 in. diameter. The overlapping of the two tubes was such that this external junction was downstream on the steam side from the point of measurement of wall and air temperatures. However, every care was taken to obtain a smooth finish to the tube, since with interference of the boundary layer by any roughness, the heat transferred to the air before the point of measurement would be influenced.

By this arrangement the air and tube wall temperature can be recorded at the same point. By moving the tube longitudinally throughout the length, a complete distribution of both wall and air temperature could

be obtained.   The position of the thermocouples are indicated by the
reading of the vernier attached to the steel block at the end of the search
tube on the scale attached to the stuffing box at the exhaust side of the
apparatus.   From the measurements of wall temperature and the rise in air
temperature which can be obtained for any length from the measured air
temperature distribution, the heat transfer coefficient can be calculated.
The coefficients so calculated are true local heat transfer coefficients,
since the heat transferred per unit area is not taken as a mean over a
certain length but is found from the actual gradient at the position
concerned.

Using this set-up, a series of 21 tests was carried out.   The
results from these tests, however, proved to be unsatisfactory.   When the
coefficients were plotted against Reynolds numbers a wide scatter of points
was obtained.   The values were also somewhat lower than expected.   It was
observed, too, that tests in which the inlet air was heated to a higher
temperature yielded values of heat transfer coefficients which were higher
than those with lower inlet air temperatures.

The failure of these tests was evidently due to the assumption
made that the temperature of the air entering the test section was constant
during any one test for all positions of the search tube.   It can be seen,
however, that the exposed length of search tube between the heater and the
entrance into the exhaust section of the apparatus varies throughout an
axial traverse.   The length marked X in Fig. 45 is a source of heat loss
from the air flow inside when high temperatures are employed, or heat gain
when the air is at a lower temperature than the surrounding atmosphere.
This would result in a lower temperature being recorded for the air in the

latter part of the nozzle when a greater length of tube is exposed for tests with high air temperatures. Thus the gradient of the temperature distribution curve would appear to be greater than in reality. This apparently larger gradient explains why higher heat transfer coefficients were obtained for such tests, since the coefficients as calculated are directly proportional to this gradient. In order to reduce the heat losses or gains for the length X of the tube, an attempt was made to insulate this section. Several cylindrical blocks of magnesia insulation were made up, each 1" diameter and 1" long, with a 3/16 in. diameter hole for the search tube. These were split axially and could be clipped onto the search tube as the exposed length increased during a traverse. Though this step was taken early on in this series of tests, the results were as indicated above.

A second type of search tube was therefore constructed as shown in Fig. 47b, whereby the rise of air temperature over a certain distance could be measured. Two thermocouples are supported in the airstream, spaced 1 in. apart, while the wall temperature is measured by thermocouple midway between these positions. The construction is somewhat similar to the previous type, again being of 3/16 in. o.d. brass tubing and 24 S.W.G. wall thickness. The inner diameter of the first portion of tubing was, however, drilled out for a length of 4.1/2 in. Care was taken to ensure that the inner hole was drilled concentric with the outer surface since any variation in thickness of the wall would affect the heat transfer. The outer diameter of the other portion was reduced to the corresponding push fit diameter for a length of 1.1/2 in. Sections of this same reduced diameter were also produced; 4 of 1/2 in. length and 1 of 1 in. length. These sections were

inserted into the enlarged diameter of the first portion of tube and between the ends of these, the thermocouples were supported, as shown in Fig. 47b. Suitable grooves were made in the ends of these sections, so that they could be pushed together to form a flush inner surface while leaving room for the wooden pillars and thermocouple wires. When the two portions of tubing were finally assembled together, the outer joint was brazed and finished to form a smooth surface as before. Again it was arranged that this joint was downstream from the points where wall and air temperatures were measured. With this method of construction the wall temperature can be measured at two points 2 in. apart while the air temperature is measured at positions 1/2 in. on either side of these points. It is then no longer necessary to assume that the air temperature at the point of entry to the test section is constant, as the quantity of heat transferred can be measured for whatever conditions exist at each setting of the search tube. It was with this type of search tube that the experiments described subsequently were carried out.

The thermocouples used for measurement of air and wall temperatures are copper constantan, the wires being 40 S.W.G. As for the 30 S.W.G. braided thermocouples used in the previous investigations and for other purposes in the present tests, these wires were calibrated against standardised 38 S.W.G. copper constantan wires.

This arrangement of thermocouples results in twelve separate wires being brought up the search tube from the air outlet. The wires were all separately insulated with woven cotton. Being of such small diameter they did not interfere with the flow of air.

In measuring the quantity of heat transferred through the walls of
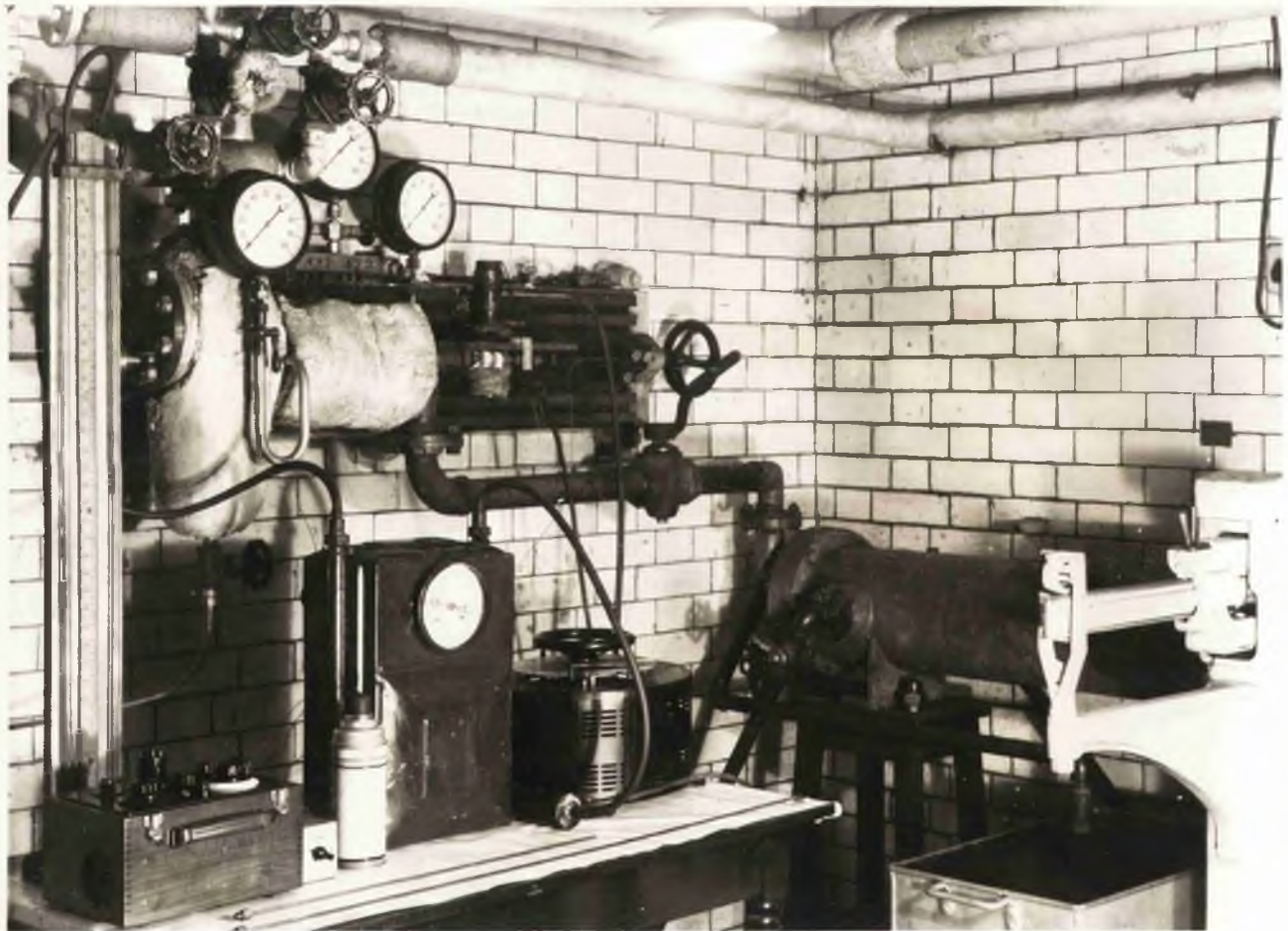
Fig. 48a PHOTOGRAPH OF APPARATUS

DURING TEST

the tube by observing the rise of air temperature over the corresponding
length, it is assumed that the heat added to the air results in a rise in
temperature throughout the cross section. This one-dimensional simplifica-
tion will apply more accurately when the air flow is turbulent than when
laminar flow prevails. The turbulent mixing process results in a more
uniform temperature distribution. Calculation of the Reynolds number
based on the measured air flow showed that this was above the critical
value for transition from laminar to turbulent flow, usually being about
6,000, while the critical value is taken as 3,000. In order, however, to
ensure that the flow was fully turbulent, certain obstructions were
inserted as turbulence promoters upstream from the points of temperature
measurement. The obstructions and wires of the thermocouples would, of
course, ensure that the stream remained turbulent. With these precautions
it may be assumed that the temperatures of the air measured near the
centre of the tube at two points will give a true indication of the amount
of heat transferred to the stream in this length.

The cold junctions of the 40 S.W.G. thermocouples as well as those
of the 30 S.W.G. couples used for measurement of the supply temperatures of
steam and air were maintained at 32°F. by immersing them in oil contained in
a glass test tube. This test tube is surrounded with melting ice contained
in a thermos flask (G fig. 43). The copper wires of each circuit are led
to an eight position two pole selector switch H which connects each thermo-
couple in turn to a Cambridge portable potentiometer.

The photograph in Fig. 48a was taken while tests were in progress,
while Fig. 48b shows a close up of the test section with the insulation
removed.
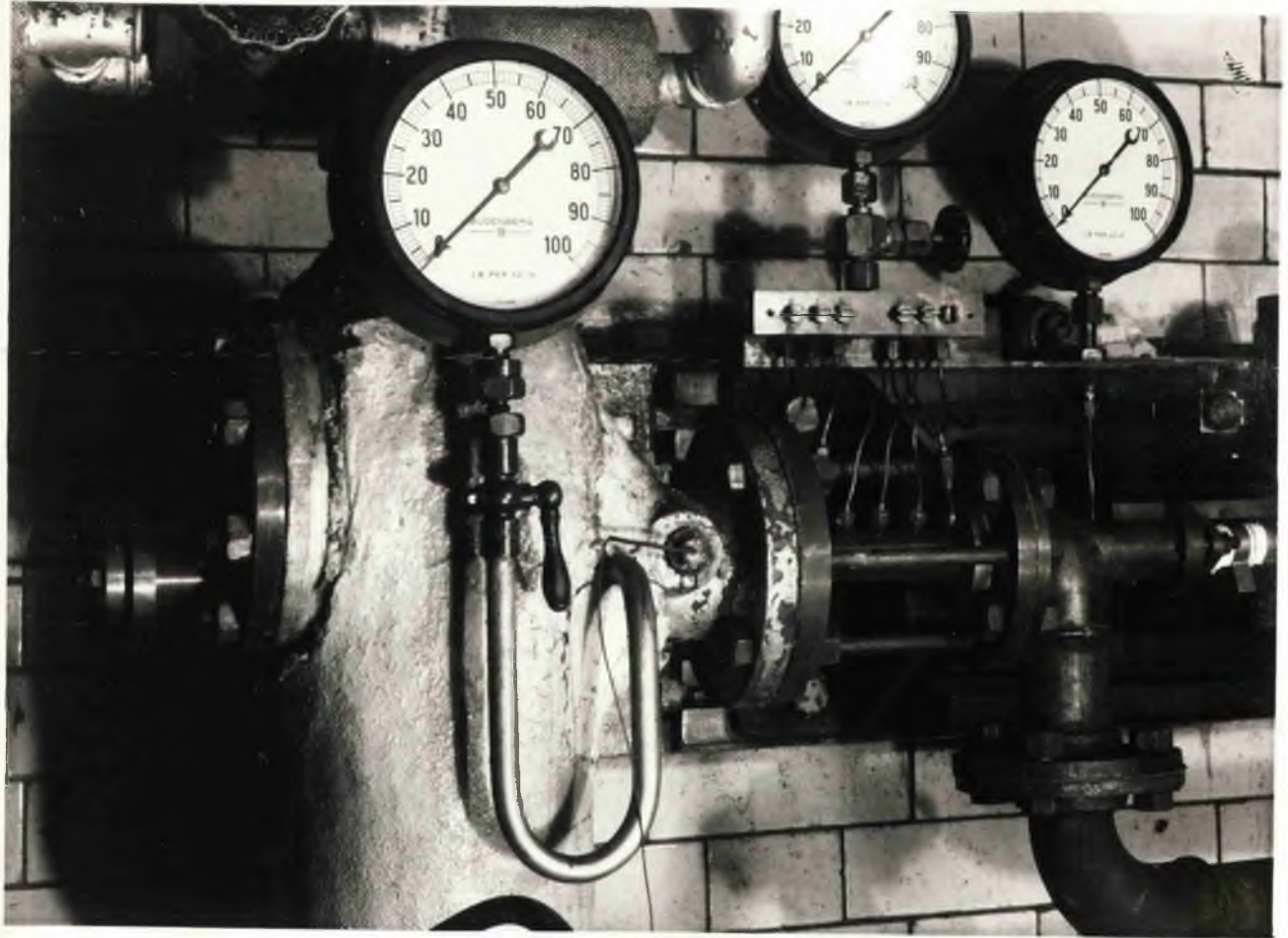
Fig. 48b PHOTOGRAPH OF TEST SECTION WITH INSULATION REMOVED

EXPERIMENTAL PROCEDURE.

The procedure for the heat transfer tests was similar to that for the previous investigations in the establishing and maintaining a flow of steam with constant supply pressure and temperature. A period of two to three hours was usually allowed for steady conditions to be assumed. In this time the air compressor was run up and the storage tank charged to the normal working pressure of 10 lb./sq.in. By opening valve A (Fig. 45) air was admitted to the system. By adjustment of this valve suitable throttling was obtained to maintain a pressure high enough to ensure that the flow of air in the search tube was turbulent but not too high for the efficient working of the gas meter. Though the meter was actually calibrated under the same pressure as that in the tests, the bellows of the meter are not able to withstand any great pressure.

The amount of heat abstracted from the steam was controlled by varying the temperature of the air at inlet. With the highest inlet air temperatures a suitable choice of voltage on the "Variac" resulted in the temperature required being attained within thirty minutes. Lower temperatures could be obtained in less time. Once the required value was reached, the temperature was found to remain nearly constant. Good control could, however, be obtained by use of the "Variac" which was capable of fine adjustment. The air supply pressure was also found to remain very steady throughout a test. Fine adjustment could again be made by means of valve A.

The test was started when the search tube was in such a position that the thermocouple for measuring the wall temperature was opposite the nozzle inlet. Readings of wall and air temperatures were then noted by

the appropriate settings of the potentiometer. The search tube was then moved 1/2 in. and the temperatures again noted. This was repeated until a complete distribution for wall and air temperatures throughout the test length was obtained.

After each setting of the search tube sufficient time was allowed for the temperatures to attain steady values. After about fifteen minutes no further change in either wall or air temperatures could be observed in any case. This interval was always allowed therefore before noting the readings. The usual care was taken to ensure that the supply temperatures of the air and the steam were remaining steady before readings were taken. If any variation did occur it was often necessary to wait for longer periods than the above fifteen minutes until the supply temperatures returned to the correct value and had remained long enough at that value for conditions to settle. A complete test with the measurement of wall and air temperatures for thirteen different positions of the search tube usually occupied from four to five hours.

As the test proceeded, a greater length of search tube was exposed to the surrounding atmosphere between the heater and the stuffing box. This section was insulated by clipping on the blocks of insulating material mentioned above, as the length increased. It was not necessary, of course, to maintain a constant temperature at the inlet to the test section, but in the tests with higher air temperature it was important to reduce the heat loss to as small a value as possible. Especially was this the case when the air was at a higher temperature than the steam and heat loss could not be prevented from the section of the tube passing through the stuffing box and the exhaust chamber.

As the dimensions of the annular duct were exactly the same as for the previous investigation, the pressure distribution throughout the length was also similar for tests with corresponding initial conditions. As a check that flow conditions were the same for the heat transfer runs, the pressure was noted at each of the six wall tappings during testing. These observations confirmed that the pressure distribution was identical to that found previously, and also showed that the surface of the search tube had the desired degree of finish. Any irregularities would result in a variation of pressure from the normal.

During each run the mass flow of steam was measured by observing the time taken for a known weight of condensate to collect in the tank placed on the platform balance. The air flow was measured by noting the reading indicated on the gas meter at half-hourly intervals.

The pressure gauges were calibrated at frequent intervals during the investigation.

A total of 22 tests was carried out under the same pressure conditions as had been used in the pressure searches and tests for measuring adiabatic wall temperatures, except in the last case, HJ1, when a supply pressure of 60 lb./sq.in. gauge was used. Since the adiabatic wall temperature had not been measured for any tests with such a high pressure, the values for recovery factor had to be extrapolated in the calculation of heat transfer coefficients. The results for this test therefore cannot be considered reliable. In all the tests the exhaust pressure was atmospheric, the valve J (Fig. 11) being fully opened.

Table 7 shows a list of the tests carried out. The letters A, B etc. indicate the pressure conditions, which are listed in Table 5, while
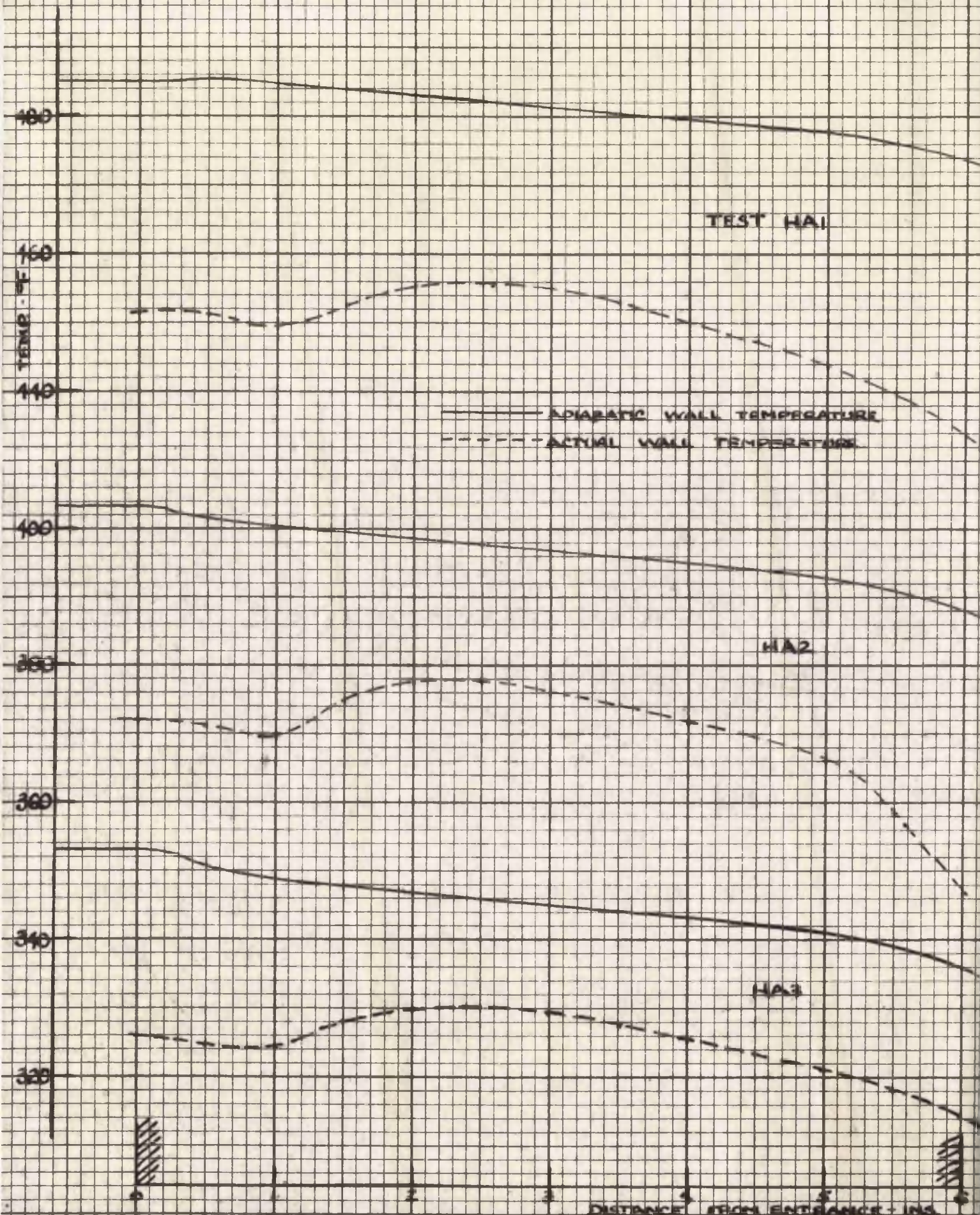
Fig 49 RECORDED WALL TEMPERATURE AND ADIABATIC WALL TEMPERATURE t_w & t_{aw}

the initial letter H indicates heat transfer runs. The air temperatures indicated in the table are those measured by the thermocouple F (Fig. 45) placed in the air stream immediately after the heater. The temperature of the air entering the test section in general has a different value from that indicated here.

It can be seen that to obtain larger quantities of heat transfer from the steam to air, tests were carried out with the steam supplied at a high temperature while the air was supplied at a little above room temperature. In all cases a small voltage was supplied to the air heater by means of the "Variac" in order to have a measure of control should the air temperature rise.

Table 7.

Pressure Conditions.	Test.	Supply Temp. °F.	Air Temp. °F.
HA	1	485	89
	2	403	89
	3	353	89
	4	318	89
	5	318	407
	6	318	586
HB	1	601	89
	2	462.5	89
	3	462	89
	4	390	89
	5	332	89
	6	332	420
	7	332	586
HC	1	446	89
	2	397	89
	3	346	89
	4	346	407
	5	346	586
HD	1	353	89
	2	353	420
	3	353	631
HJ	1	360	89

FIG 49 CTD RECORDED WALL TEMPERATURE AND ADIABATIC WALL TEMPERATURE t_w & t_{aw}
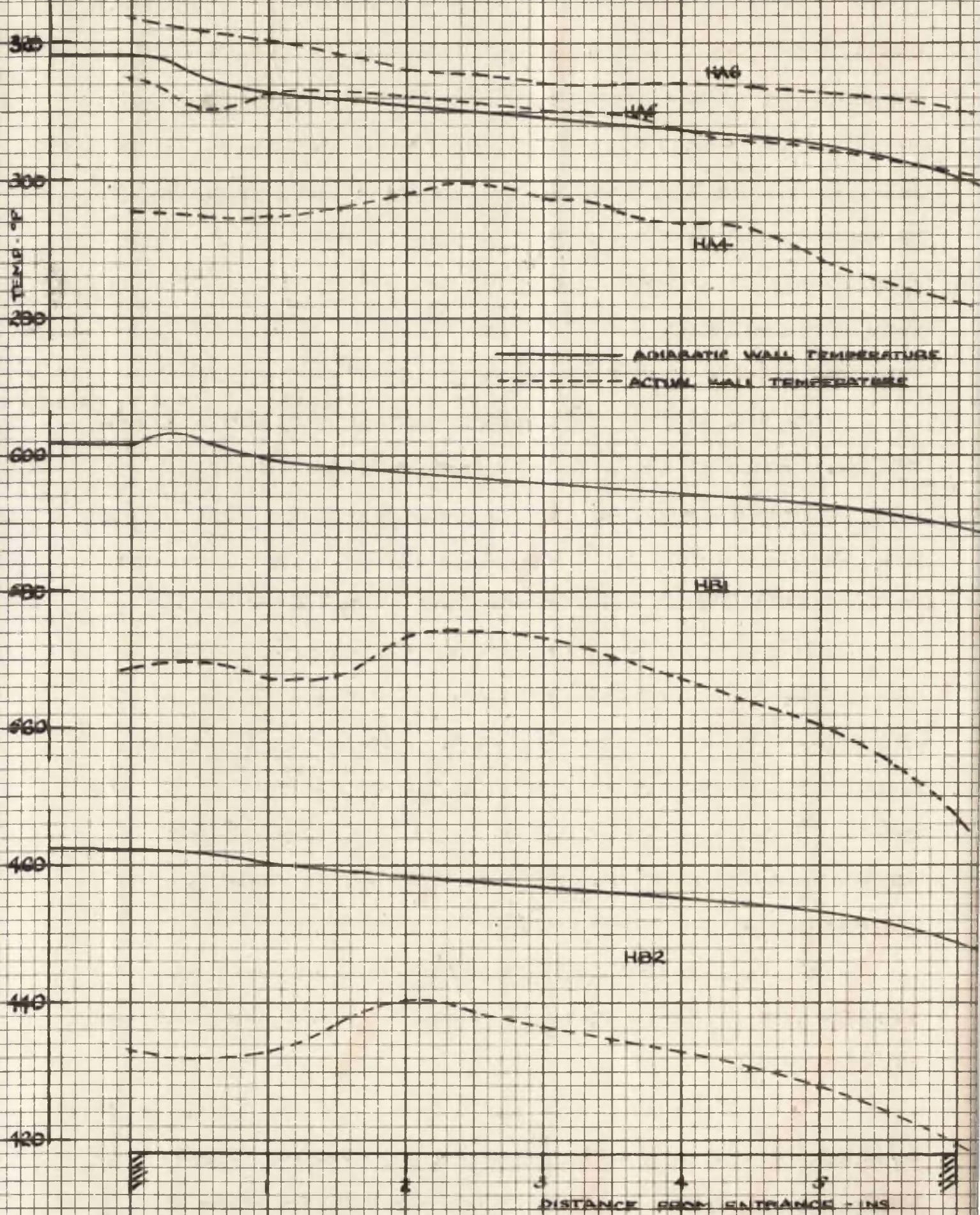
Smaller amounts of heat transfer were obtained by decreasing the initial superheat until further decrease would result in the expansion proceeding into the supersaturated field. With this lowest steam supply pressure for each pressure condition tests were then carried out with the air heated. In the tests with the air heated to the higher temperatures it was observed from readings of air temperature in the test section that the air stream was being cooled on the way through the search tube and heat was therefore being transferred from the air to the steam.

The runs in which higher temperatures were encountered (HD3 and HB1) were carried out last. After completion of the tests, the search tube was carefully taken apart and the thermocouples examined. It was found that the supports for the air temperature thermocouples had begun to char slightly, but all thermocouples were in the correct positions.

In Fig. 49 are shown the recorded wall temperatures t_w plotted against length throughout the test section. Also shown are the adiabatic wall temperatures taw for the corresponding conditions. The method of obtaining t_{aw} is given later under the method of calculation. For tests where the steam supply conditions are the same, the adiabatic wall temperature distribution is also identical and the corresponding tests are grouped together e.g. HA4, 5 and 6.

The readings of the air temperature thermocouples are not tabulated since it is the difference between the readings which is used in the calculation.

The rise or fall in air temperature for the 1 in. length was found to change only gradually as the search tube was traversed throughout the length. For a typical test HB5, the difference for the search tube
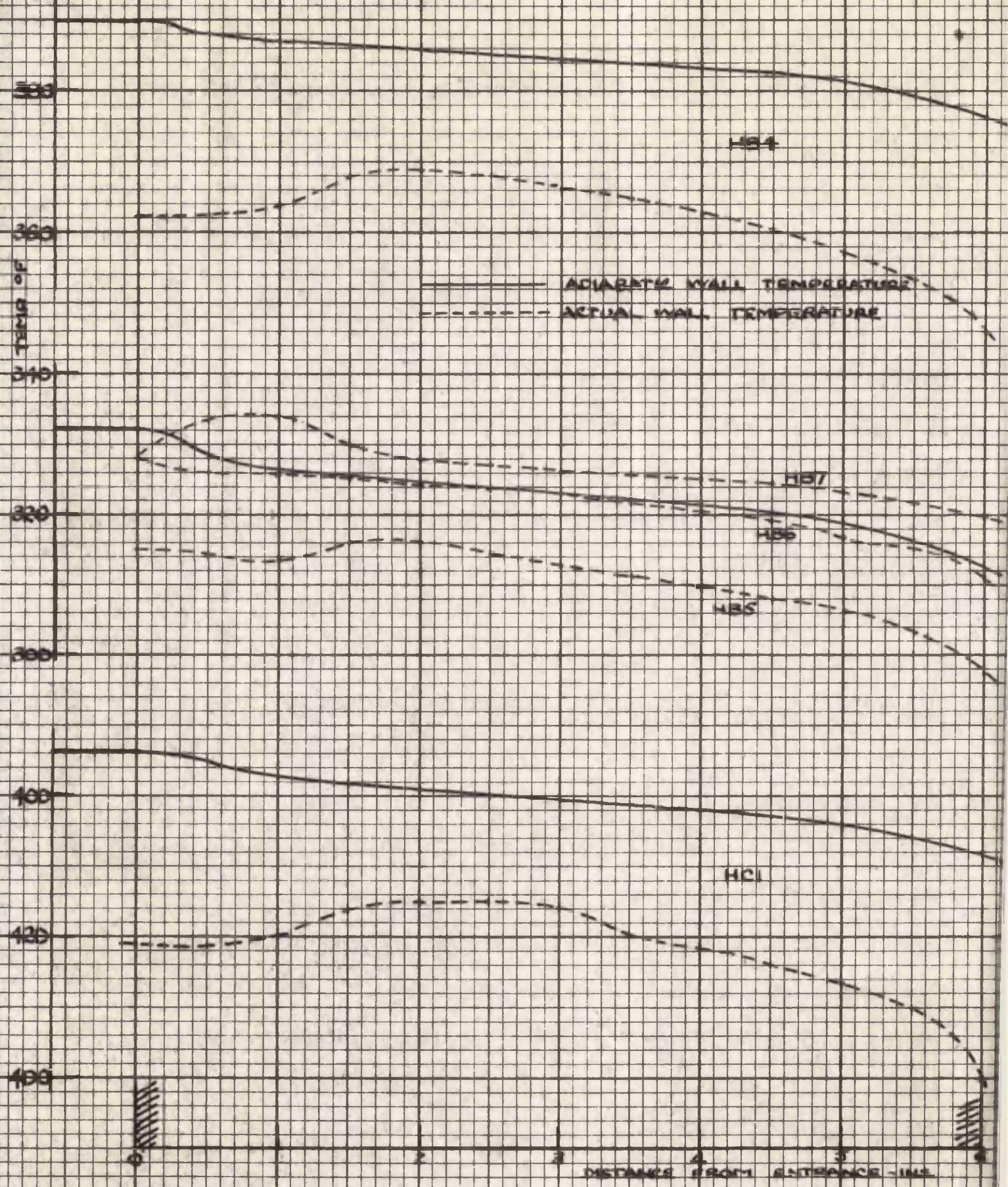
FIG 49 CTD. RECORDED WALL TEMPERATURE AND
ADIABATIC WALL TEMPERATURE t_w & $t_{a.w}$

positioned at the start of the run was 12°F. and for the final position
was 20°F.   Since this value remains nearly constant, it is the difference
between the wall temperature and the adiabatic wall temperature which is
significant.   Curves of these temperatures (Fig. 49) are seen to approach
most closely at a point 2 to 3 ins. from the entrance and from then on the
distance between gradually increases towards the exit.   The wall
temperatures have been shown in Fig. 49 as a fair curve.   This is not
necessarily so, since the readings represent separate conditions, the air
temperature at the entrance to the test section not being constant.   In
the calculations the actual readings of wall temperature and the corresponding
rise in air temperature were employed to obtain the heat transfer
coefficient for each point.

In tests HA5, HB6, HC4 and HD2 it is seen that the measured wall
temperature is very near to the adiabatic wall temperature.   The
differences in air temperature correspondingly approach zero.   For tests
HA6, HB7, HC5 and HD3 the wall temperature is above the adiabatic wall
temperature.   Here the air temperature difference is reversed, that is the
air was cooled in the passage through the test length.

The tests therefore confirm in a qualitative way that the
temperature gradient in the heat transfer equation $q = hA.\Delta t$, should be
based on the adiabatic wall temperature.   Any other temperature would
result in negative coefficients, or coefficients dependent on the
temperature.

Fig. 49 ctd   RECORDED WALL TEMPERATURE AND
ADIABATIC WALL TEMPERATURE   tw & taw

METHOD OF CALCULATION.

It has already been seen that the heat transfer coefficients are to be calculated from the equation:

$$h = \frac{q}{A} \cdot \frac{1}{t_w - t_{aw}} \quad \ldots\ldots\ldots\ldots\ldots\ldots(90)$$

All the quantities in this equation can be readily obtained from the results of the heat transfer tests except the value of t_{aw}, the adiabatic wall temperature. This could probably be obtained with a fair degree of accuracy from measurements of the adiabatic wall temperature carried out previously for runs having approximately the same supply conditions. A greater degree of accuracy can be obtained, however, by use of the generalised relationships previously found for the recovery factor for flow under similar conditions. This involves the lengthy calculation of the stream temperature, but this would have to be carried out in any case in order to obtain values for the Reynolds number and other physical properties of the flow. Also conditions are not exactly the same as in the adiabatic runs, since a certain amount of heat is abstracted from the stream.

The stream temperature can be calculated directly on a one-dimensional basis since the heat transferred up to any section is known from the rise in air temperature. The adiabatic wall temperature can then be found for the condition of flow at each section. It can be seen that this method of obtaining t_{aw} is also only approximate owing to the definition of the recovery factor as the "local free stream value" and to the one-dimensional basis of the calculations. Since the thermal and hydrodynamic boundary layers may be taken as having the same thickness, heat abstracted

at the walls will not alter the stream temperature in the core until the flow becomes fully developed hydrodynamically. Heat transfer calculations are based on considerations of temperature distribution across the boundary layer. If the stream temperature outside the boundary layer is unaltered by the amount of heat transferred, then the adiabatic wall temperature to be used in calculating the coefficient will also remain the same. The difficulty arises, however, in determining when the boundary layer completely fills the cross-section. In fact the amount of heat transferred is very small compared with the other quantities of heat involved in the calculations and the difference in the final value obtained for the wall temperature is negligible.

The method of calculating the stream temperature is similar to that used previously, the specific volume being first found and the temperature interpolated from steam tables. The quadratic equation, which is to be solved for the volume has an extra term, however, as the energy equation now has the form

$$Ho = H + \frac{v^2}{2gJ} + Qx \quad \dots\dots\dots\dots\dots\dots\dots(71)$$

where Qx is the amount of heat transferred up to the section considered.

In a typical test, say HB5, the rise in air temperature over the 6 in. length of the test section was 60° F. The flow of air was 3.2 lb./hr. The heat transferred per hour is then $3.2 \times .241 \times 60$ B.T.U. As the steam mass flow was 3.595×60 lb./hr., the quantity Qx which is the heat transferred per pound of steam is $3.2 \times .241/3.595 = 0.215$ B.T.U./lb. As the value of Ho - 851.1 is 351.3 B.T.U./lb. it can be seen how small an effect the amount of heat transferred has on the result of the calculations.

The stream temperature was found for the eleven points a to l
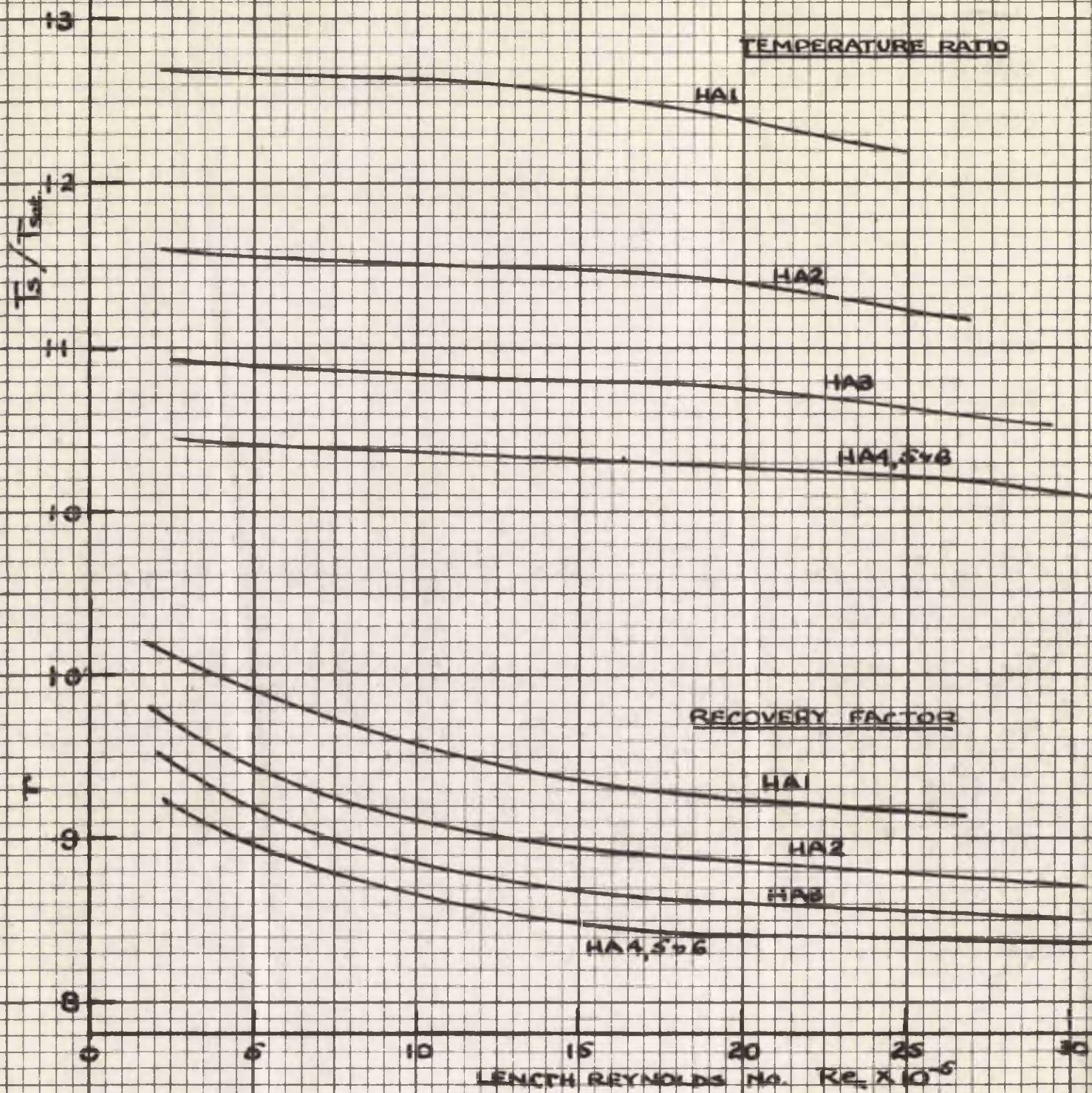
FIG. 50   CURVES USED IN THE CALCULATION OF THE ADIABATIC WALL TEMPERATURE

throughout the length, so that the complete distribution could be obtained from the calculated points. The adiabatic wall temperature could then be calculated from the equation $t_{aw} = t_s + r(t_t - t_s)$, since the stream temperature t_s and the total temperature t_t are both known.

The value of r was obtained by employing the relationship $r = K(T_s/T_{sat.})^{\frac{1}{2}}$ found as described in Part III. T_s and $T_{sat.}$ were obtained from the calculations of the stream conditions and K was taken for the appropriate value of Re_1.

In Fig. 50 are shown a set of typical curves used in the calculation of adiabatic wall temperature. The shape of the graph of r versus Re_1 is the same as those plotted from experimental results. From this curve the values can be read off for the points a, b, c etc.

In this way the curves for t_{aw} shown in Fig. 49 were obtained. The adiabatic wall temperature is shown as one curve for tests HA4, 5 and 6; HB5, 6 and 7; HC3, 4 and 5; and HD1, 2 and 3, since the heat transferred has no appreciable effect on the stream conditions.

Once the adiabatic wall temperature had been found, the values of the terms in equation 90 could be inserted and the coefficient so obtained.

Consider an inch length of the inner tube.

Let $\Delta T = T_2 - T_1$, the rise in air temperature over the length. Then the amount of heat, q, transferred to the air is $C_p m_a . \Delta T$, where m_a is the flow of air in lb./hr.

Therefore $h = \dfrac{q}{A} \dfrac{1}{t_{aw} - t_w} = \dfrac{C_p m_a . \Delta T}{A} \dfrac{1}{t_{aw} - t_w}$

$$= \frac{C_p}{A} . m_a . \frac{\Delta T}{t_{aw} - t_w} \quad \ldots\ldots\ldots\ldots(91)$$

The value of C_p/A is constant for all the tests, since the specific heat

of air can be taken as constant over the range of temperatures encountered in the tests. Moreover the value of m_a is constant for any one test. Therefore to calculate the heat transfer coefficient for any point in a test it is only necessary to multiply the ratio of rise in air temperature to difference between wall and adiabatic wall temperatures by a constant.

The values of A and ΔT refer to a length of 1 in. of tube while the value $t_{aw} - t_w$ is that for a point in the centre of this length. The ratio $\Delta T/A$, which occurs in the equation, is equal to $\Delta T/\pi D_1 . \Delta L$, where D_1 is the diameter and ΔL is 1 in. It has already been seen that the air temperature rise ΔT as observed during the tests changes only very gradually throughout the test length. Because of this

$$\frac{1}{\pi D_1} \cdot \frac{\Delta T}{\Delta L} = \frac{1}{\pi D_1} \cdot \frac{dT}{dL}$$

and $h = \dfrac{C_p}{A} . m \cdot \dfrac{\Delta T}{t_{aw} - t_w} = \dfrac{C_p m}{\pi D_1} \cdot \dfrac{dT}{dL} \cdot \dfrac{1}{t_{aw} - t_w}$

As dL approaches zero, the value of h becomes the heat transfer coefficient for a point. On account, therefore, of the fact that the rise of air temperature is nearly constant for all positions of the search tube, the heat transfer coefficient evaluated in the above manner can be taken as the local coefficient for the point where $t_{aw} - t_w$ is measured.

There remains two effects for which it may be necessary to apply corrections; the temperature gradient through the wall of the tube and the effect of radiation.

The Temperature Gradient through Tube Wall.

It can be seen from the method of constructing the search tube that the temperature recorded by thermocouple during the tests is that of the inner surface. The wall temperature t_w to be used in the calculation

of the heat transfer coefficients is that of the outer surface, since it
is the transfer of heat between steam and metal which is of interest.
The temperature gradient across the wall is easily calculated since the
amount of heat conducted through the metal is known.

For a tube of length l, of metal whose thermal conductivity is k,
the amount of heat q conducted when the temperature gradient is Δt_w is
given by:

$$q = k \frac{2 \pi l}{\log r_2/r_1} \cdot \Delta t_w \dots\dots\dots\dots\dots\dots\dots\dots\dots(92)$$

where r_2 and r_1 are the inner and outer radii.

For a brass tube of the dimensions used in the tests and for a
length of 1 in., the relation between temperature gradient and heat
transmitted is then:

$$\Delta t_w = .006907 \, q.$$

The heat transmitted can be observed from the rise in temperature
of the air passing inside the tube: $q = m_a C_p (T_2 - T_1)$

$$\therefore \quad t_w = .001664 \, m_a (T_2 - T_1) \text{ since } C_p = 0.241.$$

In the runs carried out, the largest differences between the two
air measurement thermocouples were observed for test HCl, while the flow of
air, m_a, was nearly constant for all the tests. In test HCl, for a section
near the exit, a rise in air temperature of 32° F. was recorded, while the
value of m_a was 3.4 lb./hr. Substituting these values in the above
relationship, it is seen that the temperature gradient $\Delta t_w = 0.181^\circ$ F.
This is within the degree of accuracy of the temperature measurement by
thermocouple. The gradient across the walls for the other tests will in
most cases be much less than this, since the rise in air temperature for

the 1 in. length is considerably less. The effect on the temperature
readings caused by the conduction of heat through the walls of the tube
may therefore be neglected, and the wall temperatures which were observed
were taken as that desired in the calculations.

Radiation.

The present investigation is concerned with the transfer of heat
by the combined mechanism of conduction and convection and the heat
transfer coefficient to be determined is for such a case. A certain
amount of heat, however, will be transmitted by radiation from the steam
to the metal or vice versa, since steam is one of the gases which absorb
and emit radiant heat. An estimate must therefore be made for the
radiation and a correction applied. In heat transfer between a gas and
a wall exchanging heat by radiation and convection, some interference
between both methods of heat exchange occurs and it is very difficult to
calculate this effect. Therefore usually both parts of the total heat
flow are calculated separately and summed up. Since the heat flow by
convection is expressed by a film heat transfer coefficient, it is usual
to build a heat transfer coefficient h_r for the radiated heat in the same
way, by dividing the heat flow per unit area by the temperature difference.
Such a coefficient, of course, depends very much on the temperature. In
the present case the heat transferred by radiation (q_r/A) from the steam to
the metal is to be subtracted from the total flux (q_t/A). The heat
transfer coefficient is then

$$h = \frac{\frac{q_t}{A} - \frac{q_r}{A}}{t_w - t_{aw}} = \frac{\frac{q_c}{A}}{t_w - t_{aw}} \qquad \dots\dots\dots\dots(93)$$

An equation, suitable for calculating (q_r/A) in the present case is given in the Appendix of reference 73. This equation was derived from an exact solution by the method of Hottel and Egbert for calculating the heat transfer by radiation in tests of similar conditions to the present. In these experiments radiation took place from the central heating element to steam flowing in the annulus and to the outer walls. In the present tests the surface of the inner tube is also at a higher temperature than the steam, though in this case the outer wall is at the highest temperature. The equation will, however, give the net heat exchanged by radiation. The simplified form is:

$$\left(\frac{q}{A}\right)_r = 0.173 \; \epsilon_i' \left\{ \left(\frac{T_i}{100}\right)^4 \left[\alpha_{L_1} + (1-\alpha_{L_1})\epsilon_o\right] - \left(\frac{T_o}{100}\right)^4 \epsilon_o(1-\alpha_{L_2}) \right.$$
$$\left. - \left(\frac{T_g}{100}\right)^4 \cdot \epsilon_{gL_2} \right\} \qquad \dots\dots(94)$$

where

α = gas absorptivity for specified beam length and pressure

ϵ_g = emissivity of steam for specified beam length and pressure

ϵ_o = emissivity of outer wall

ϵ_i = emissivity of inner wall at Ti

ϵ_i' = effective emissivity of inner wall equal to $(1 + \epsilon_i)/2$

T_i, T_o, T_g = absolute temperatures of heating element, jacket and steam respectively in deg. Rankine.

L_1 = effective beam length for gas radiation from inner wall to gas

L_2 = effective beam length for gas radiation from gas to inner wall

Beam lengths L_1 and L_2 are assumed equal to 1.4 times the clearance between inner and outer walls.

In the application of the equation, values of emissivity ϵ_o and ϵ_i for

the brass walls of the annulus were taken from Table XIII in the Appendix of reference 72. Emissivities and absorptivities for gas radiation reduced to zero pressure were taken from Fig. 29 of the same reference and were multiplied by the correction factor C_1 entrapolated from Fig. 30.

A calculation is given below, taking test HB4 and section e as representative. From the calculation of stream conditions the temperatures can be obtained as

$T_i = 828^{\circ}R$; $T_0 = 845^{\circ}R$; and $T_g = 808^{\circ}R$.

T_0 is taken as the adiabatic wall temperature at the corresponding section.

$\epsilon_i = \epsilon_0 = 0.05$ and $\epsilon_i' = (1 + .05)/2 = .525$.

The product $P_wL = \dfrac{31}{14.48}$ x 1.4 x $\dfrac{.11275}{12}$ = .02815 ft. atm.

$\epsilon_g = 0.0475$ x C_1

$= 0.0475$ x $2 = 0.095$ and $\alpha = 0.0935$.

Then $\left(\dfrac{q}{A}\right)_r = .173$ x $.525 \left\{ \left(\dfrac{828}{100}\right)^4 \left[.0935 + (1 - .0935) \text{ x } .05 \right] \right.$

$\left. -\left(\dfrac{845}{100}\right)^4 0.05 (1 - .0935) - \left(\dfrac{808}{100}\right)^4 \text{ x } .095 \right\}$

$= .173$ x $.525$ x 16.4 B.T.U./hr. ft.^{2}

For 1 in. length of tube the heat radiated is then

$q_r = .173$ x $.525$ x 16.4 x $.00409 = .00609$ B.T.U./hr.

The total heat transferred over this section can be calculated from

$q_t = m_a C_p . \Delta T$ for the air flow

$\therefore q_t = 3.54$ x $.241$ x $22 = 18.8$ B.T.U./hr.

The amount of heat transferred by radiation is therefore 0.032% of the

total heat transferred.   Calculation for other sections and different
conditions showed the amounts of heat radiated to be of the same order
as above.

Since the heat transmitted by radiation was such a small
percentage of the total, it could be neglected and no correction was
necessary.   The heat transfer coefficients could therefore be calculated
directly by use of equation 91.

FIG 51   TYPICAL VARIATIONS OF HEAT TRANSFER
COEFFICIENTS WITH LENGTH
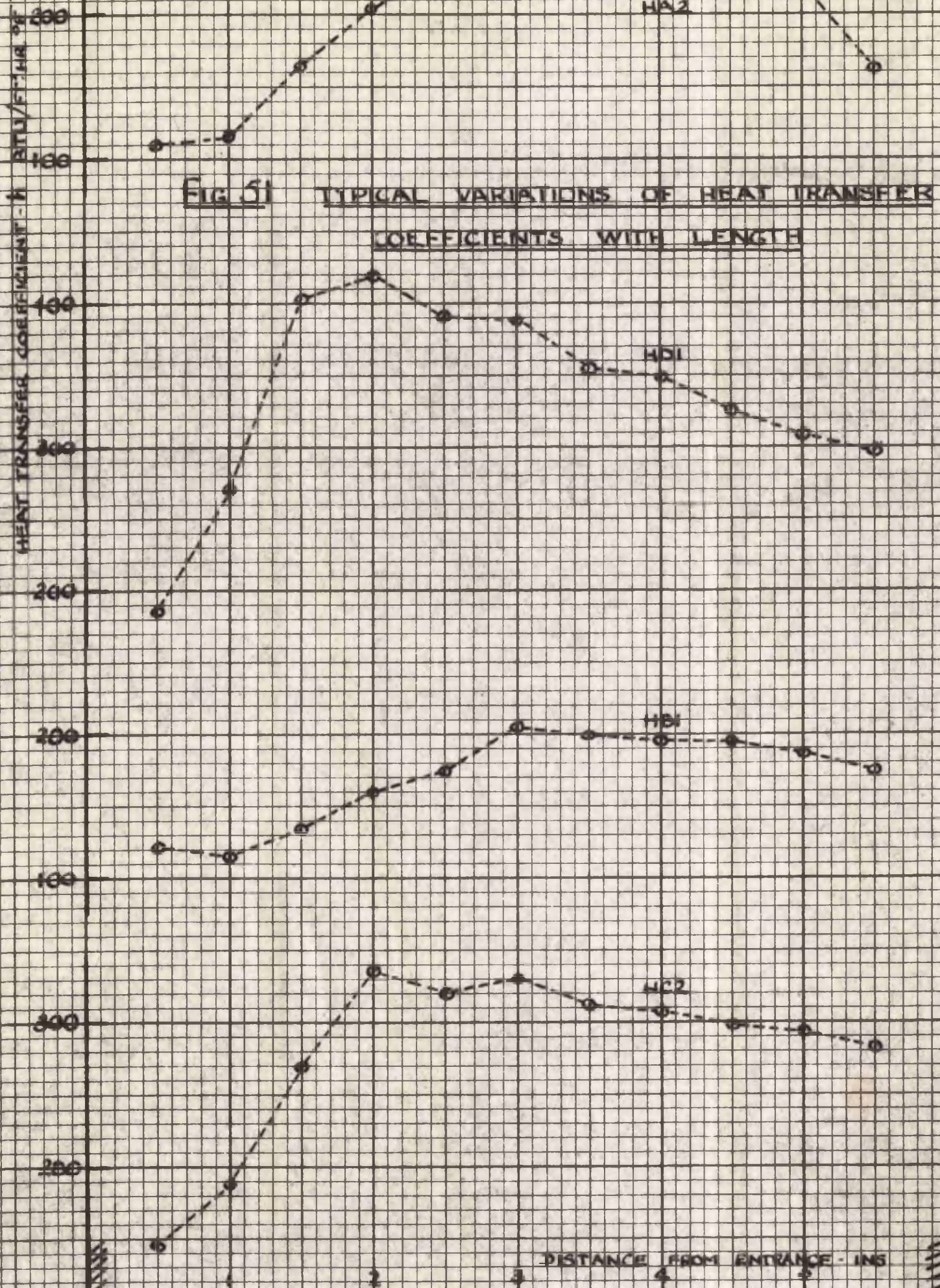
ANALYSIS AND DISCUSSION.

Heat transfer coefficients were calculated by the method outlined in the previous section for the eleven points throughout the length of the test section and for all the tests carried out. The values obtained are listed in Table 4a in the Appendix. Plots of h versus length are shown for a few tests in Fig. 51.

In order to compare the coefficients with those for low velocity flow, it is necessary to find a correlation in terms of the factors influencing the value. It is usual to present such correlations in dimensionless form, the heat transfer coefficient being included in one dimensionless group, another dimensionless group representing the flow conditions and another the fluid properties etc. Therefore for each point considered, the diameter Reynolds number $\rho VDe/\mu$, the length Reynolds number $\rho Vx/\mu$ and the Stanton number h/C_pG were calculated. The Prandtl number $C_p \mu /k$ could be taken as constant and nearly equal to 1 for the steam under the range of conditions encountered in the tests. The Reynolds numbers were calculated in exactly the same manner as indicated in Part III.

In Part I a discussion was given on the temperature at which property values should be evaluated. It was seen there that most investigations pointed to a reference temperature taken as the average of the wall and the bulk temperature. In computing the Stanton and Reynolds numbers for the present investigation, the properties were therefore evaluated at such a temperature. Since the temperature differences were small, the effect of inserting values at the bulk temperature or at the wall temperature does not greatly affect the final correlation, especially
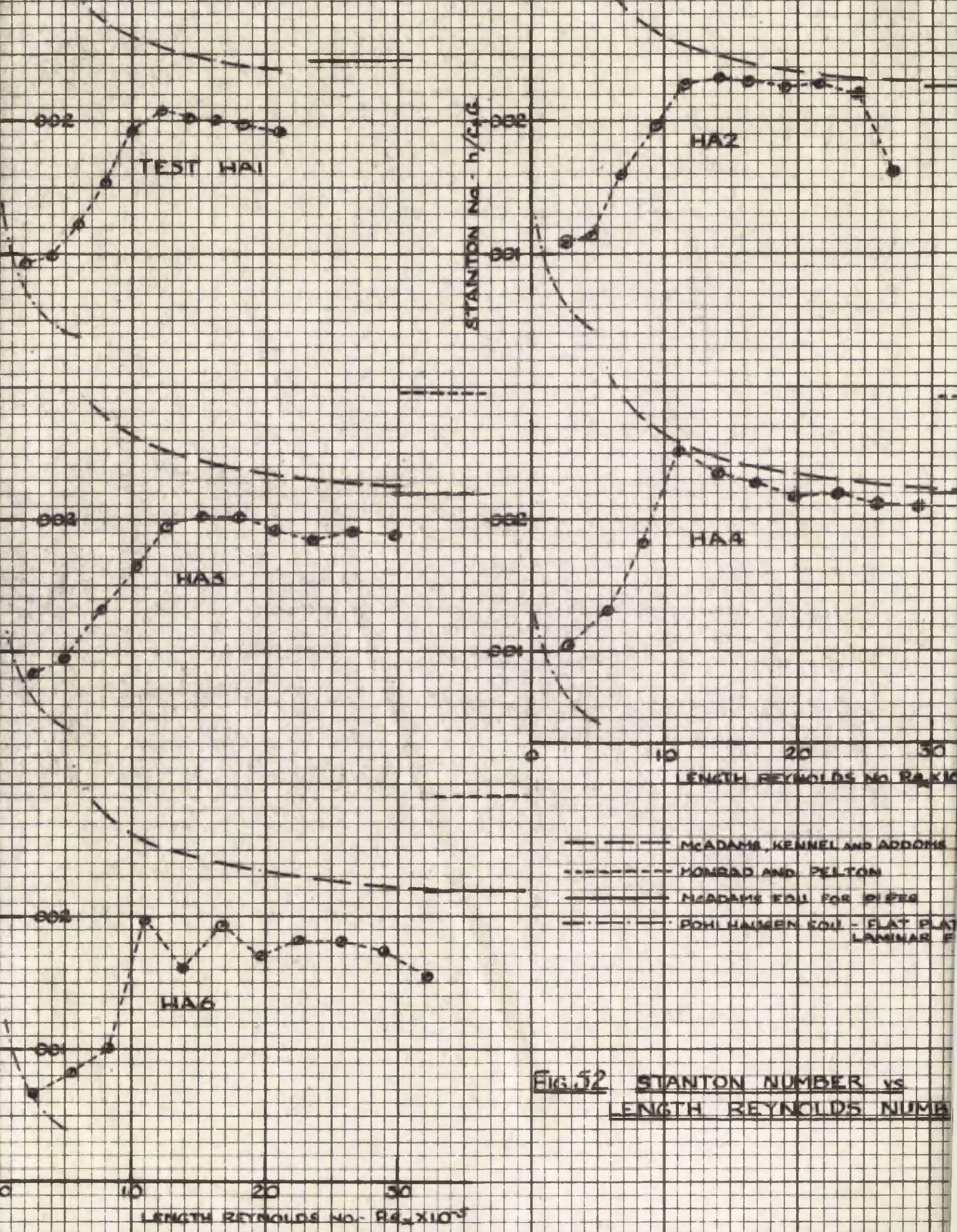
Fig. 52 STANTON NUMBER vs LENGTH REYNOLDS NUMBER

as the Reynolds number appears with the power 0.2.

The equivalent diameter $De = D_2 - D_1$ was used in the calculation of the diameter Reynolds number, while the length dimension, x, was taken as the distance from the entrance of the test section to the point considered for the case of the length Reynolds number.

In calculating the Stanton number, the value of the specific heat at constant pressure, C_p, was taken from Fig. 6 of reference 59. The value of G, the mass flow, is constant for any one test since the cross-sectional area is the same for all the points throughout the length for which calculations were made. Values of St, Re and Re_1 are also listed in Table 4a in the Appendix.

The Stanton number is employed in the presentation of the heat transfer results rather than the more popular Nusselt number, $Nu = hL/k$. This is the method of representing heat convection data recommended by Colburn (13). The usual method is to plot $Nu(Pr)^{-1/3}$ against Re. It can be easily shown that $Nu(Pr)^{-1/3}$ is equal to $[St(Pr)^{2/3}]$. $Re = jRe$. Thus plotting $Nu(Pr)^{-1/3}$ versus Re almost means plotting a function against itself, whereas plotting the factor j versus Re shows the characteristic variation in a clearer form.

Further, the Stanton number allows a comparison with the friction factor. It has been seen in Part I that for a fluid for which $Pr = 1$, $St = f/2$. In the case where $Pr = 1$, a relationship can be found between the Stanton number and the friction factor.

An important consideration in the present tests is that the Stanton number can be used in the comparison of the heat transfer results with either flow over a flat plate, or fully developed flow in a pipe.
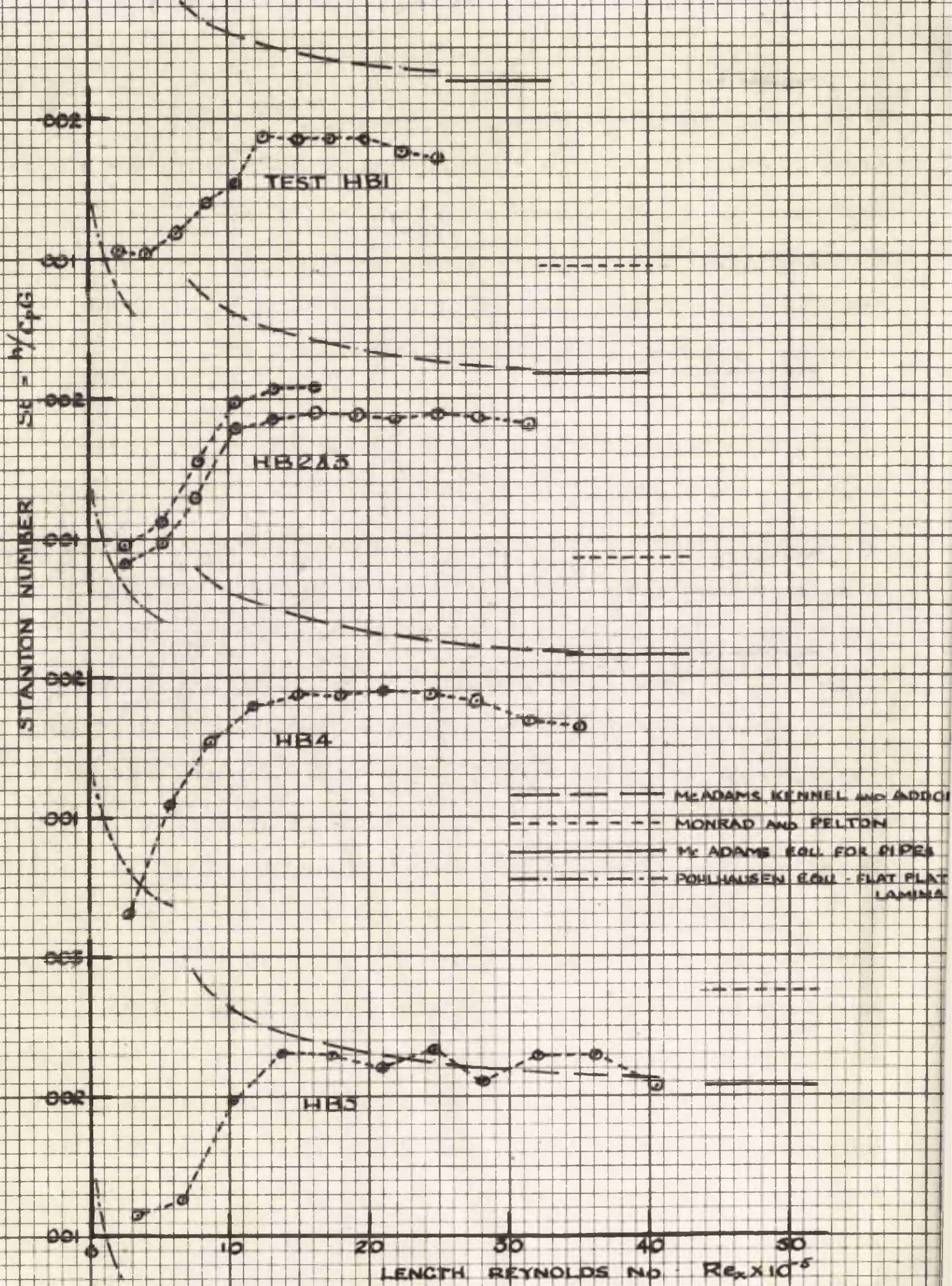
Fig 52 ctd. STANTON NUMBER vs LENGTH REYNOLDS NUMBER

If the Nusselt number were used, this would have to be built up with the length dimension x equal to the distance from the start of the test length when comparison is made with heat transfer for a flat plate, while the diameter would be employed in building up this group when comparison is made with fully developed flow in a duct. Thus it would be necessary to calculate two numbers hx/k and hD/k for many of the points.

From the method of calculating the Stanton number, it can be seen that the variation for any one test will correspond to the variation of the heat transfer coefficient throughout the length. The only difference is caused by the value of the specific heat, and this only alters slightly over the length. Plots of Stanton number against length throughout the test section therefore would show the same characteristics as plots of the heat transfer coefficients shown in Fig. 51.

In order to examine the heat transfer results in relation to the boundary layer development, the Stanton numbers were plotted against the length Reynolds numbers for each test separately, as in the case of recovery factors. These plots are shown in Fig. 52.

All these curves show the Stanton number rising quite steeply at first to a maximum and then falling more gradually towards the exit. The maximum, which in most cases is a definite peak, occurs at a length Reynolds number of between 15 and 20 x 10^5. The variation of the Stanton number can only be accounted for by the transition of the type of flow in the boundary layer at this point. The heat transfer coefficient always has a higher value for turbulent flow, and turbulence would be expected at a corresponding value of length Reynolds number. Such was observed to be the case in the investigation on recovery factors described in Part III
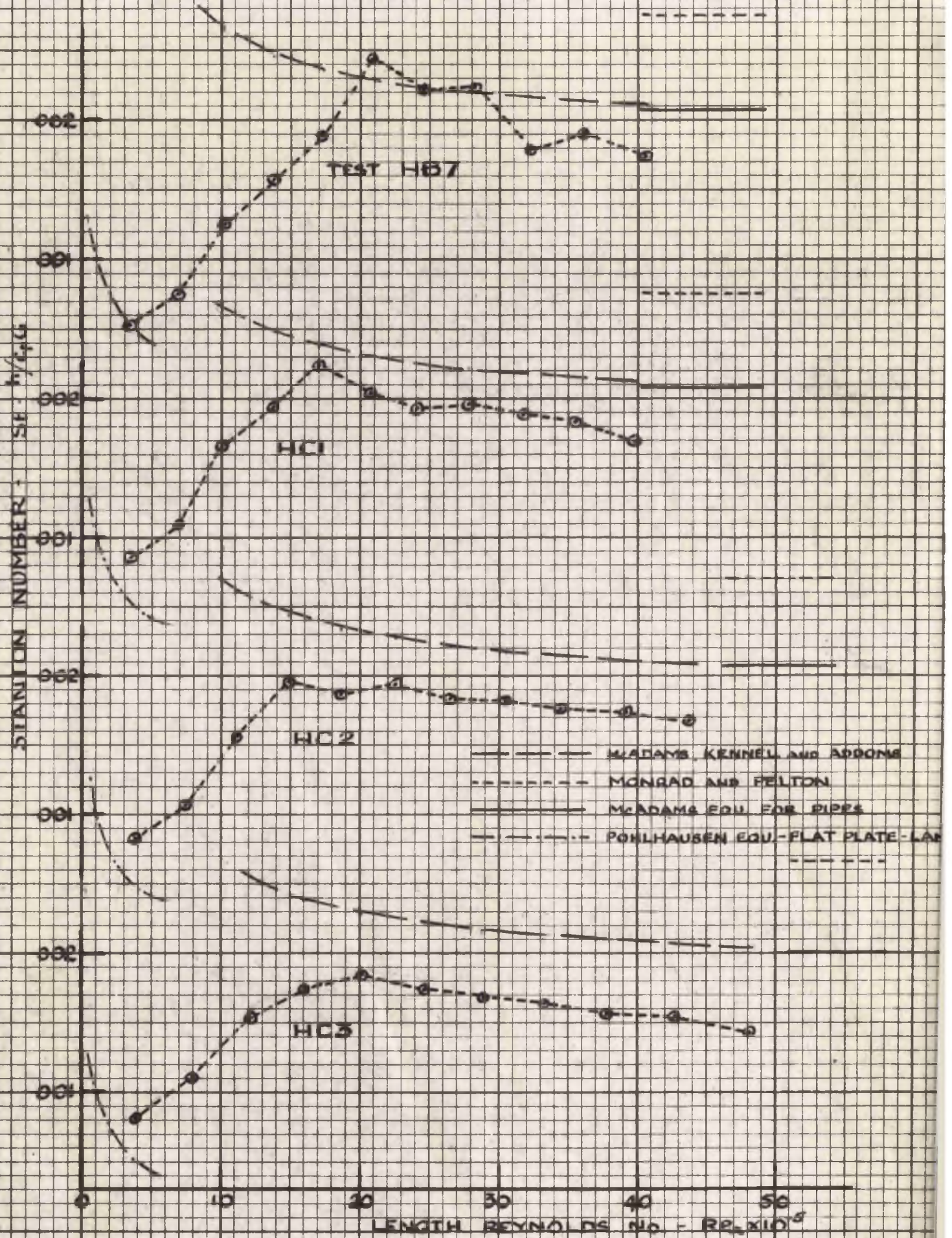
FIG. 52 ctd. STANTON NUMBER vs LENGTH REYNOLDS NUMBER

of the thesis.   The rising value of Stanton number up to this point
would indicate a gradual transition from laminar to turbulent flow and
correspond to the falling value of recovery factor in this region and
finally flattening out to a constant value of Re_1 above 20×10^5.
The gradual fall of Stanton number after the maximum is owing to the
increase in thickness of the turbulent boundary layer and indicates that
the flow is not fully developed.   An initial fall would also be expected
at the entrance to the test length owing to the build up of the laminar
boundary layer, and corresponding to the case for flow over a flat plate.
As in the case of the recovery factor, however, there is no evidence of
laminar flow at the entrance, except for a few tests with the smaller
mass flows.   The length Reynolds number at the first few stations in
these tests is small enough for the flow to be purely laminar.

Since the thickness of the laminar boundary layer at the entrance
is very small compared with the radius of curvature, the heat transfer
coefficients may be compared with those for flow over a flat plate.   The
Pohlhausen equation which gives the local heat transfer coefficient is

$$St \ = \ 0.332 \ (Pr)^{-2/3}. \ (Re_x)^{-1/2} \ \dots\dots\dots\dots(29)$$

The curve for this equation is shown by a broken line in Fig. 52.   It is
seen that this drops very steeply from the entrance, and in only a few
tests do the Stanton numbers calculated from the observed data for the
first stations fall on this curve.

Since only a few points correspond to laminar flow, and no
satisfactory correlations exist for heat transfer for the transition
region, attention was concentrated on the results for the turbulent

TEST HD1

HD2

HD1

McADAMS, KENNEL AND ADAMS
MONRAD AND PELTON
McADAMS EQU. FOR PIPES
POHLHAUSEN EQU. - FLAT PLATE
LAMINAR F

STANTON NUMBER + $S_E = h/c_p G$

$Re_x \times 10^{-4}$

LENGTH REYNOLDS NO - $R_{4x} \times 10^{-4}$
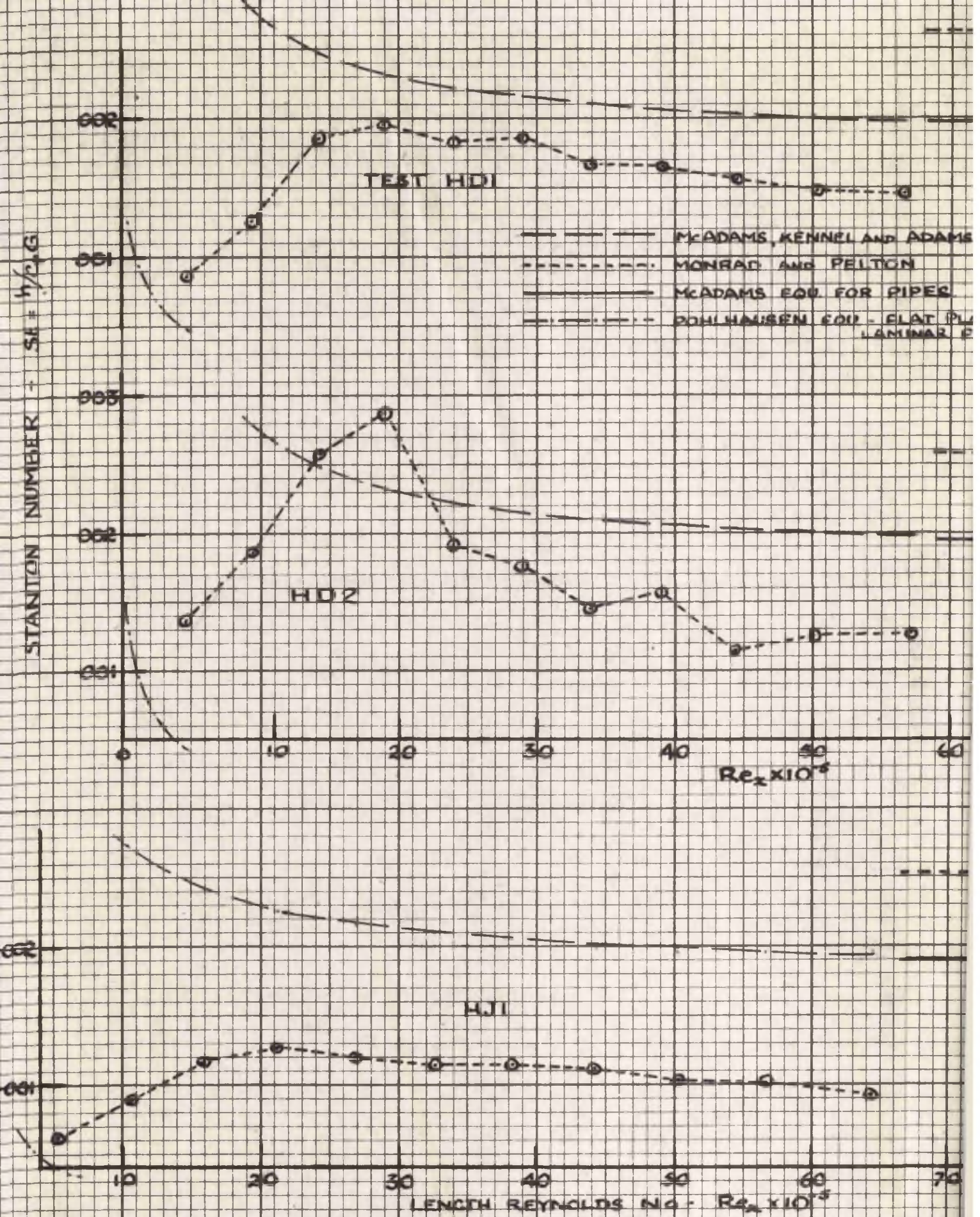
FIG. 52 ctd. STANTON NUMBER vs. LENGTH REYNOLDS NUMBER.

boundary layer. Heat transfer coefficients considered as those for fully turbulent flow were those taken from points where the curve had reached the maximum and thereafter. An attempt was therefore made to correlate the results in the same form as for low velocity flow. Also the results were compared with those predicted by suitable formulae for low velocity flow in annuli.

It is evident that the heat transfer law which holds in this region is no longer that for flow over a flat plate. In that case the Stanton number would be dependent only on the length Reynolds number, while it can be observed that for one value of Re_1, the Stanton number is no longer constant. The reason is that the boundary layer no longer increases in thickness in the same way as for a flat plate but the growth is impeded both by the falling pressure and interference owing to the boundary layer growing on the opposite wall of the duct. The heat transfer is then more similar to that for fully developed flow in a pipe or duct. However, the falling values for the heat transfer coefficient indicate that the boundary layer is still increasing in thickness, though more slowly than in natural growth. In similar cases, such as are encountered in the starting lengths of ducts, it is usually considered that the length to diameter ratio (x/D) is the controlling factor in the boundary layer growth and the term (D/x) raised to a suitable power is included in the equations for heat transfer. As x increases, the flow becomes fully developed and the influence of the (D/x) term diminishes, the Stanton number then being only dependent on the diameter Reynolds number.

In the present case the value of D was taken as that of the
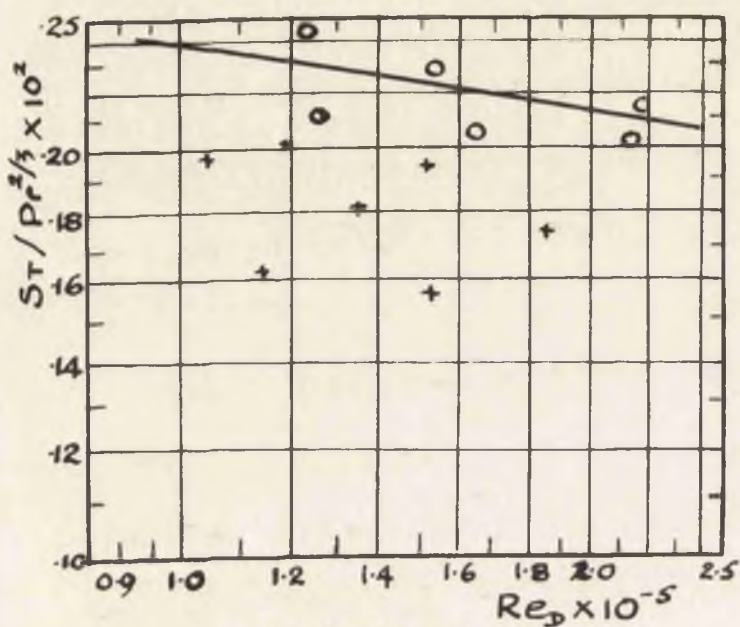
STATION - d
$L/D_e = 8.868$
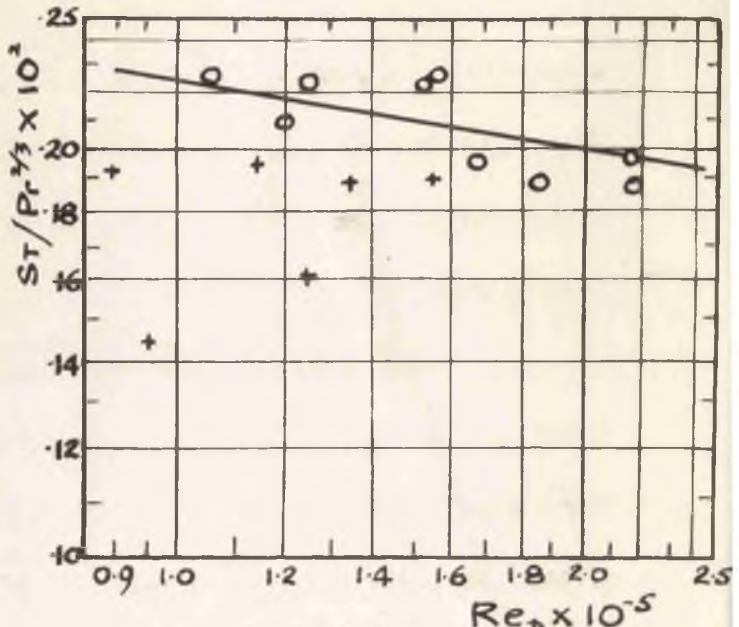
STATION - e
$L/D_e = 11.085$

+ TURBULENCE NOT ESTABLISHED
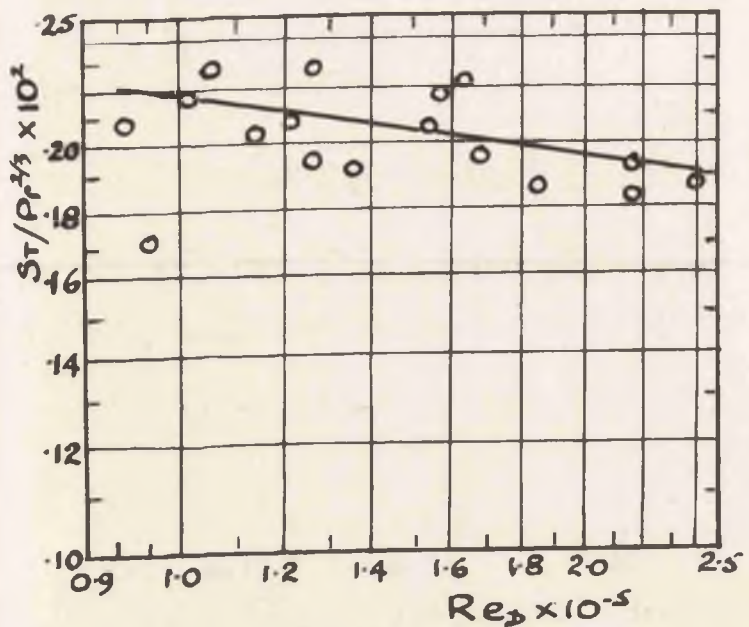
STATION - f
$L/D_e = 13.302$
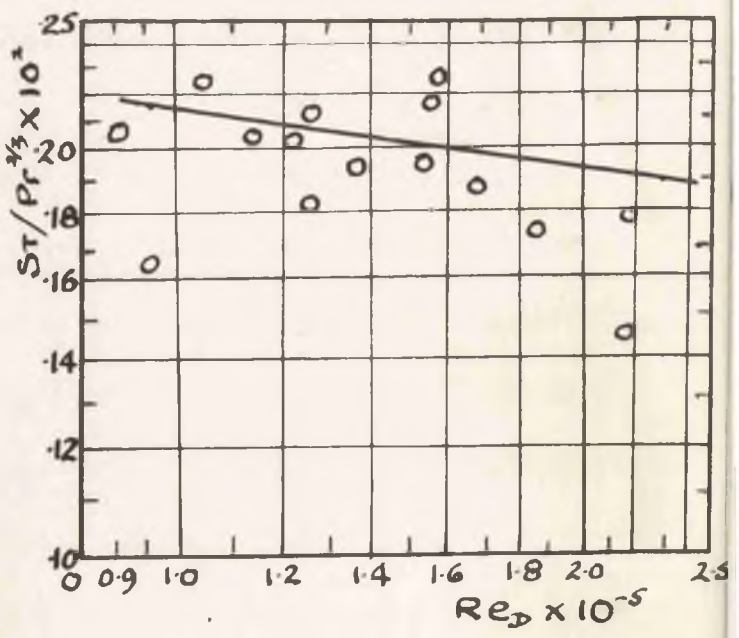
STATION - g
$L/D_e = 15.519$

FIG 53   STANTON NO. vs. DIAMETER REYNOLDS No.

$S_T/Pr^{2/3}$ vs. Re_D

equivalent diameter, $De = D_2 - D_1$.   The value of x/De was then taken as the distance to each section considered from the entrance divided by the equivalent diameter.   The maximum value of x/De was 26.6 at the exit of the nozzle.

The formulae for heat transfer for flow in annuli have already been given in Part I.   It was also seen that the equation which seemed most applicable to the present circumstances was that developed by McAdams, Kennel and Addams (73) for flow of superheated steam in an annulus.   The Nusselt number built up from the local coefficient of heat transfer is given by

$$Nu = 0.0214 \, Re^{0.8} . \, Pr^{1/3} . \, (1 + \frac{2.3}{x/De}) \ldots\ldots\ldots\ldots(18)$$

Converting into the relationship for the Stanton number and taking $Pr = 1$, this equation is then

$$St = 0.0214 \, Re^{-0.2} . \left(1 + \frac{2.3}{x/De}\right) \ldots\ldots\ldots\ldots(95)$$

Stanton numbers were calculated from this equation for all the points throughout the length for each test.   The resulting curves are shown in Fig. 52 for comparison with the points obtained from the experimental results.

Also indicated at the right hand side of this figure are the values for fully developed flow derived from the formulae of Monrad and Pelton and of Davis for annuli and from the McAdams equation for pipe flow with the substitution of the equivalent diameter in the Reynolds number.

It can be seen from this figure that the values of Stanton numbers obtained from the results of the present investigation are somewhat lower than those obtained from formulae derived in previous investigations for low velocity flow.   This point will be discussed later and an explanation
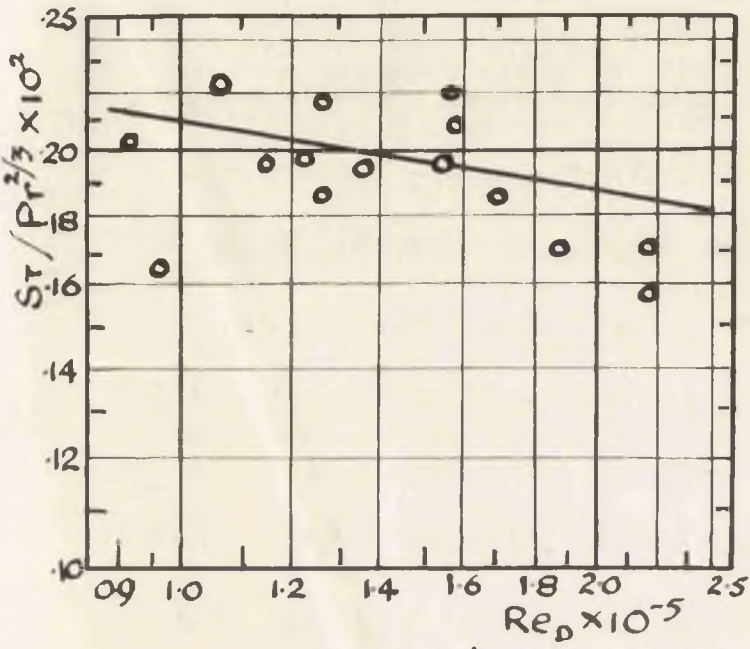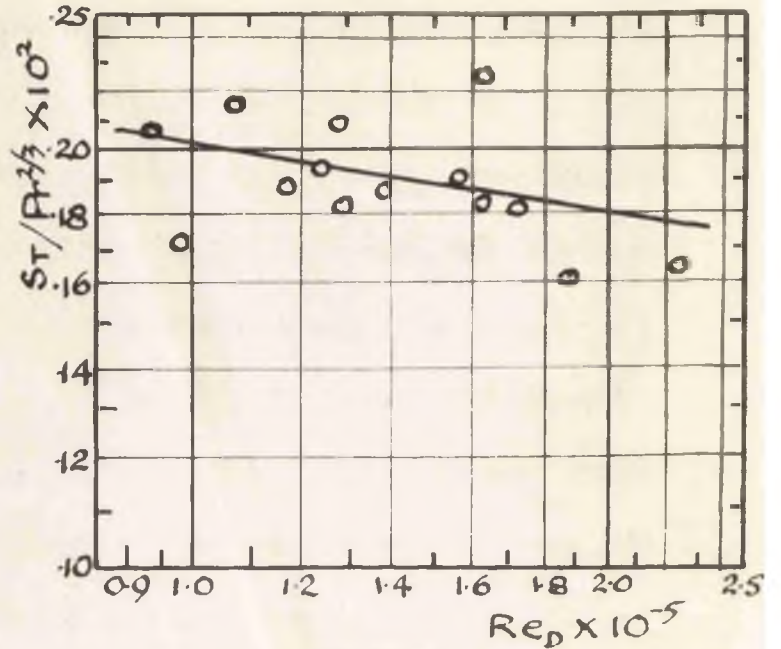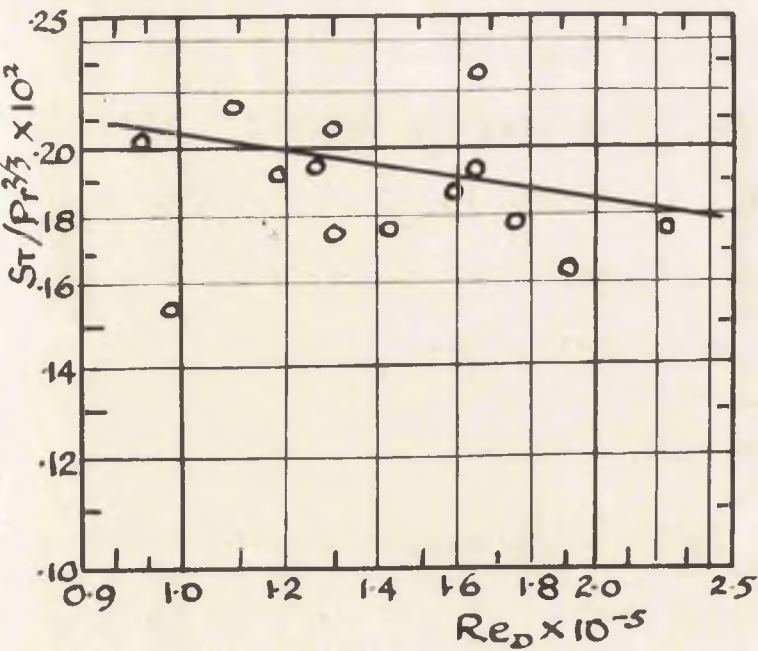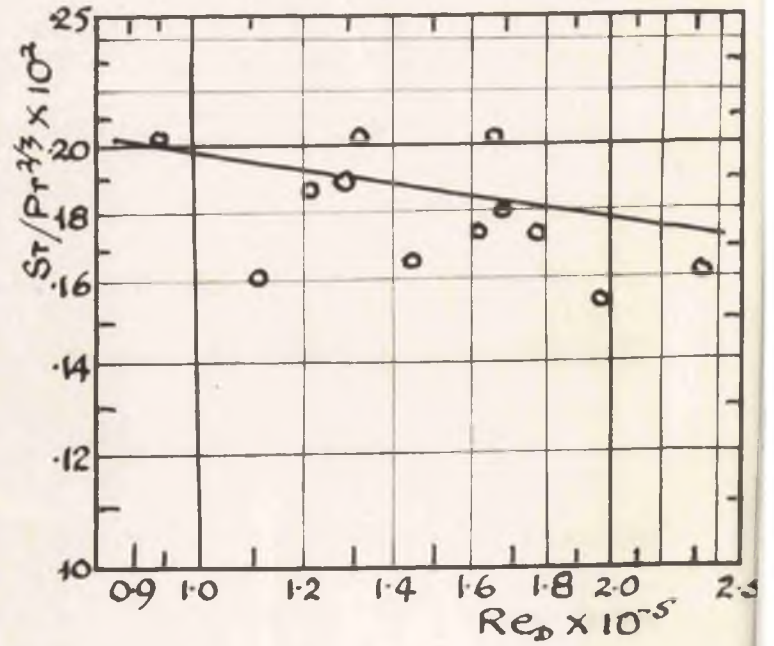
FIG. 53 CTD. STANTON No. vs. DIAMETER REYNOLDS No.

$S_T / Pr^{2/3}$ vs. Re_D

given for this apparent discrepancy,

To obtain a correlation of the results in dimensionless form the following procedure was adopted. Local Stanton numbers were plotted against the diameter Reynolds number for x/De equal to 8.868, 11.085, 13.302, -24.387 corresponding to points d, e, f etc. These plots on a logarithmic scale are shown in Fig. 53. The best straight line was drawn through each set of points, to represent the equation $Y = K (X)^m$. The co-ordinate Y actually is equivalent to the value of $\left(\dfrac{h}{c_pG}\right) \left(\dfrac{Cp\,\mu}{k}\right)^{-2/3}$ but since $Pr = 1$, the term $(Cp\,\mu/k)$ can be omitted. This fact thus eliminates any uncertainty as to the correct power to which this term should be raised. The diameter Reynolds number Re_d is the X co-ordinate.

From the gradient of the straight line on the logarithmic scale of Fig. 53 it was found that the value of m was -0.2. This agrees with the conventional power on the Reynolds number. To obtain a fadeaway function for x/De similar to that in the revised correlation given in the Addendum of reference 73 the values obtained for K were plotted against x/De on a linear scale as shown in Fig. 54(a). This yielded the equation:

$$K = 0.0183 \left(1 + \frac{2.5}{x/De}\right) \quad \dotfill (96)$$

To obtain a correlation including the conventional term $(D/x)^1$, the value of K was plotted against (De/x) on a logarithmic scale (Fig. 54b). This led to the equation:

$$K = 0.0269 \, (De/x)^{1/13} \quad \dotfill (97)$$

The final correlation involving the local coefficients of heat transfer are given in Figs. 55(a) and (b). These correspond to the equations:

$$\left(\frac{h}{CpG}\right)\left(\frac{Cp\mu}{k}\right)^{2/3} \cdot \frac{1}{1 + \dfrac{2.5}{x/De}} = 0.0183 \left(\frac{DG}{\mu}\right)^{-0.2} \dotfill (98)$$

$S_T / Pr^{-2/3}. Re_D^{-0.2} = .0183 (1 + 2.5 \, D/L)$

(a)   LINEAR   SCALE

$S_T / Pr^{-2/3}. Re_D^{-0.2} = 0.269 (D/L)^{1/13}$
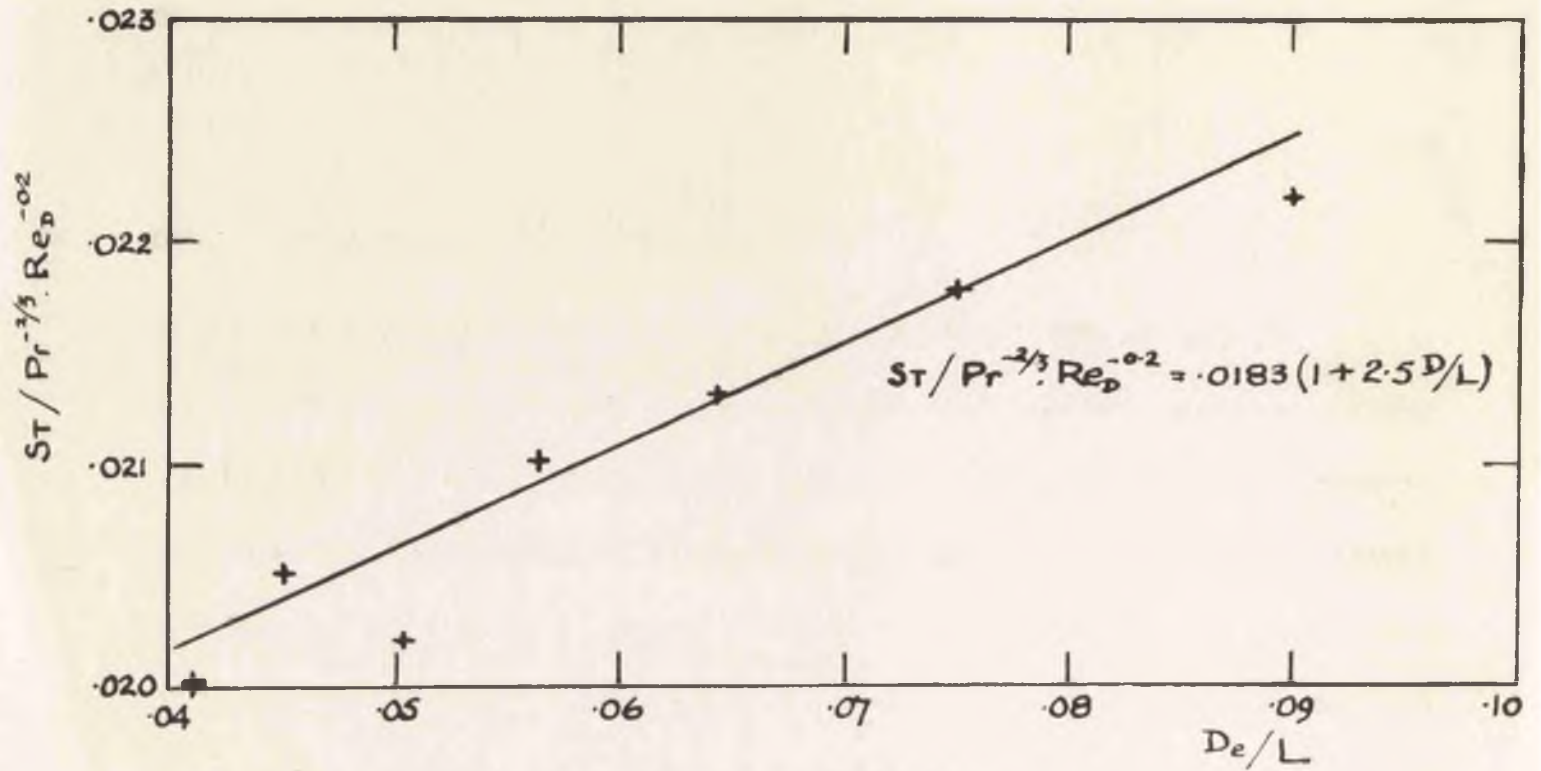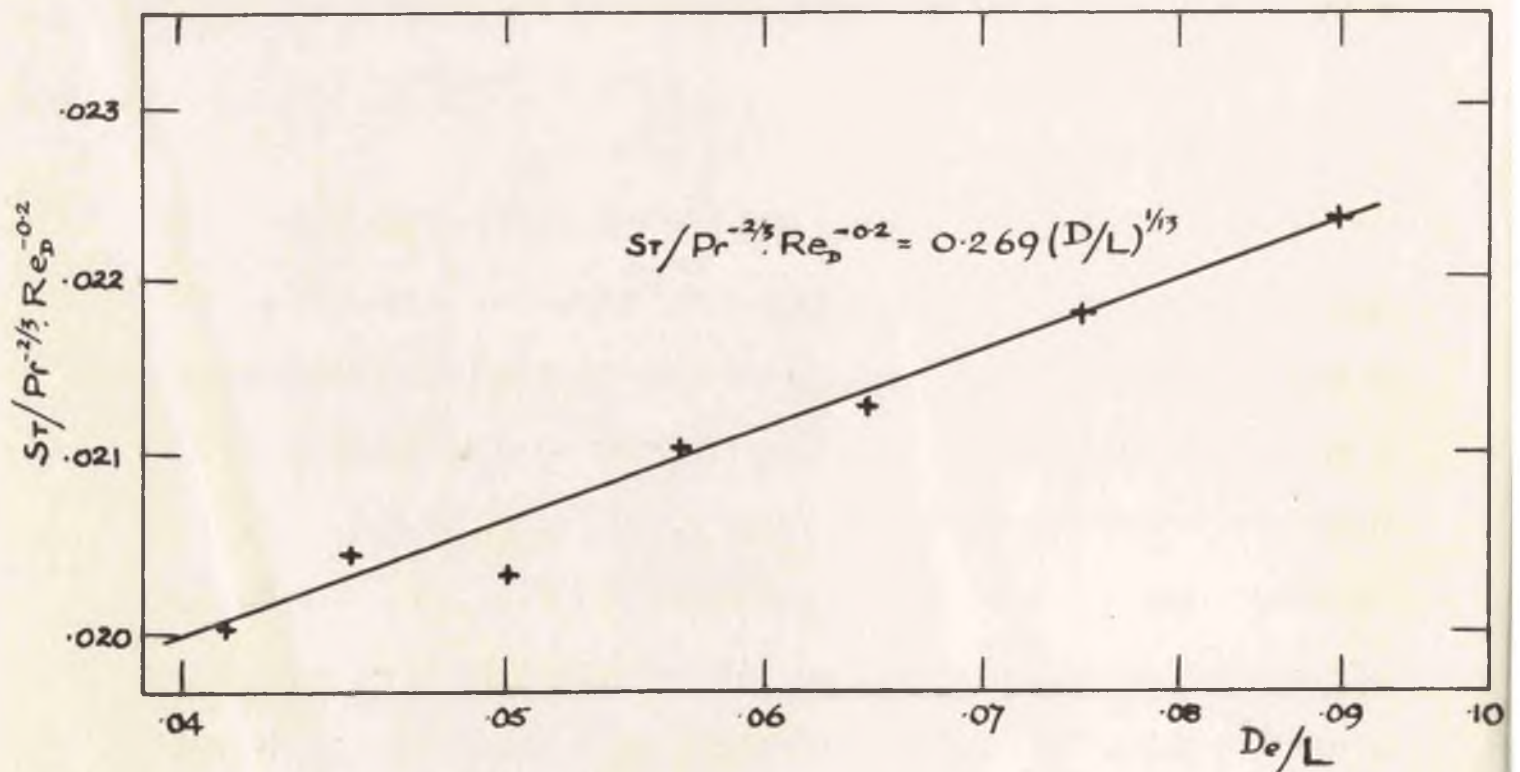
(b)   LOGARITHMIC   SCALE

FIG.54   VALUES OF $K = S_T . Pr^{2/3} Re_D^{0.2}$ AT   VARIOUS L/D.

and

$$\left(\frac{h}{CpG}\right)\left(\frac{Cp\mu}{k}\right)^{2/3}\left(\frac{x}{De}\right)^{1/13} = 0.0269\left(\frac{DG}{\mu}\right)^{-0.2}\ldots\ldots\ldots(99)$$

It can be seen that equation 99 represents the experimental results somewhat better than equation 98. The scatter of points obtained in both cases and which is rather greater than in some other investigations on heat transfer is owing to the fact that measurements were taken with small temperature differences between wall and adiabatic wall. Because of this, the results are of more value in that they throw light on the mechanism of heat transfer when skin friction plays a considerable part. By the use of large temperature differences more accurate results could be obtained and the scatter would be expected to be less, but the temperature distribution across a section of the annulus would be little different from that existing in low velocity flow, not being greatly influenced by frictional heating.

A justification is necessary for taking the distance x as that from the entrance of the test section to the point considered. It might be thought that a better correlation would be obtained by measuring this distance from the start of turbulent flow or that at least it would be dependent in some way on the position of the point at which turbulence started. The x/D term, however, is introduced to allow for the variable thickness of the boundary layer. The turbulent layer already has a certain thickness as it originates from the laminar layer. However, according to Prandtl (82), calculations from formulae giving the thickness of the turbulent layer in terms of the length Reynolds number agree satisfactorily with measurements if the thickness of the boundary layer is
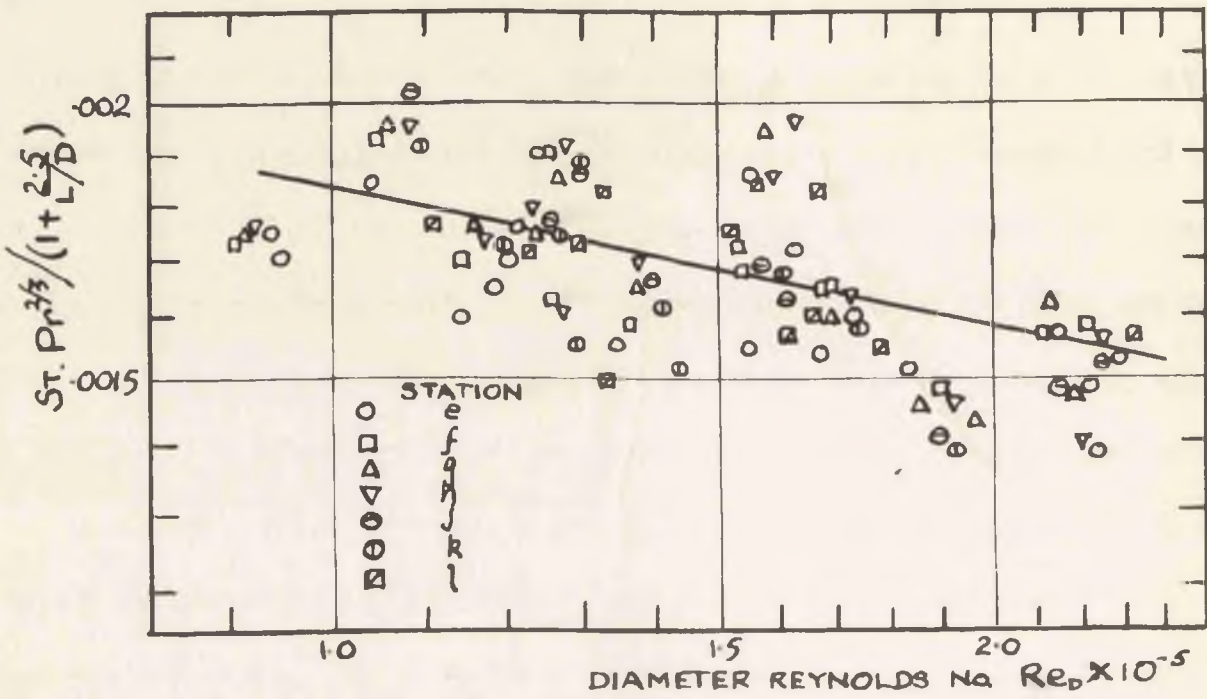
(a) COMPARISON WITH EQU - $St. Pr^{2/3}/(1 + \frac{2.5}{L/D}) = 0.0183 \, Re_D^{-0.2}$
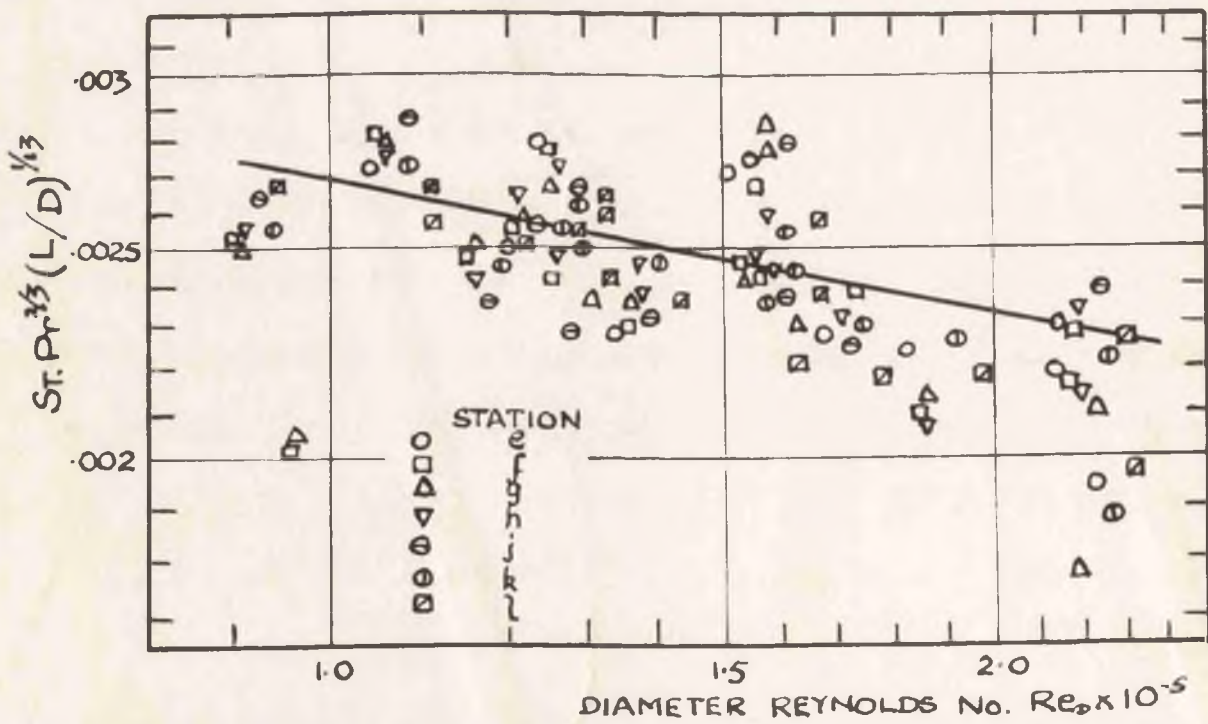
(b) COMPARISON WITH EQU - $St. Pr^{2/3} (L/D)^{1/3} = 0.0269 \, Re_D^{-0.2}$

FIG. 55   CORRELATION   OF   HEAT   TRANSFER   DATA.

determined as if it began directly from the start as fully turbulent and zero thickness. Newer measurements indicate that this is not quite correct but this simple assumption is sufficiently exact for the present purpose. It can be seen then, that the thickness of the boundary layer in the present case will be a function of the distance from the entrance of the test section, and so the value of the heat transfer coefficient will be dependent on this distance, other factors being equal.

Before finally comparing the experimental results with those obtained from the well known relationships for low speed flow, one point remains to be discussed.

Comparison of Heat Transfer for High and Low Velocity Flows in Ducts.

The theoretical analyses for heat transfer with high velocity flow have all been concerned with the flow over a flat plate. The results of the theory indicate that the temperature difference in the heat transfer law should be redefined as that between the adiabatic wall and the actual wall temperatures. The heat transfer coefficient is then equal to that for low velocity flow under similar conditions, when the temperature difference is that between the surface and the stream temperature at an infinite distance from the wall. This latter temperature t_s is, of course, constant outside the thermal and hydrodynamic boundary layers.

In fully developed flow in a tube, the boundary layers have met at the axis. The temperature at the tube axis then corresponds to the temperature t_s of the stream outside the boundary layer for the flat plate flow. It is usual, however, to establish the heat transfer with the bulk

temperature t instead of the temperature t_s at the axis. Such a procedure is not quite correct, but the resultant error is small. The heat transfer coefficient will, however, have a value appreciably different from that based on the temperature of the fluid at the axis.

When velocities become high for flow in a tube and frictional heating becomes appreciable, then it is to be expected that the heat transfer coefficient based on the difference between adiabatic wall and actual wall temperatures will have the same value as for low velocities. But the temperature difference on which heat transfer coefficients are based in the latter case must be that between the actual wall and the fluid at the axis of the tube to correspond with the fluid temperature at an infinite distance from the surface for flow over a flat plate - the case considered by theory. The coefficients that are obtained for high speed flow are therefore not the same as those given in the literature for fully developed pipe flow. This point has been overlooked by investigations of heat transfer at high velocities in pipes and the experimental values of coefficients obtained appeared to be lower than expected.

A relationship between the two types of coefficient of heat transfer may, however, be obtained. Denoting the coefficient based on the bulk temperature of the fluid as h_B and that based on the temperature at the axis as h_s, then:

$$q = h_B \cdot A(t_w - t_B) = h_s A(t_w - t_s)$$

Then $h_s = \dfrac{t_w - t_B}{t_w - t_s} \ h_B$ ....(100)

The temperature ratio $\dfrac{t_w - t_B}{t_w - t_s}$ is denoted by θ

For laminar flow $\theta = 0.583$, while for turbulent flow the value is considerably higher and is a function of both the Reynolds numbers. Boelter, Martinelli and Jonassen obtained values for θ in this range and these are presented in graphical form in reference 5.

Investigations concerned with heat transfer for high velocity flow in pipes have been carried out by McAdams, Nicolai and Keenan (74), Lelchuck (69) and Guchman, Iljuchin, Taassowa and Warschawski (36) for subsonic flows and Kaye, Keenan and McAdams (54) for supersonic flow. The data for all the subsonic flows are presented in reference 74, the heat transfer coefficients being recalculated where they had not previously been based on the difference between the actual and the adiabatic wall temperatures. These values, which are all shown in Fig. 2, were found to vary from 4% to 14% below the equation:

$$\frac{h}{c_p G} = 0.025 \left(\frac{DG}{\mu} \right)^{-0.2} \dots\dots\dots\dots\dots\dots\dots\dots (1)$$

The generally accepted equation for fully developed turbulent flow of air in a tube is, however,

$$\frac{h}{c_p G} = 0.0275 \left(\frac{DG}{\mu} \right)^{-0.2} \dots\dots\dots\dots\dots\dots\dots\dots (101)$$

which is represented by the topmost line in Fig. 2. This would yield values higher by 9% than equation 1. The experimental values therefore average 18% below those derived from the normal equations for heat transfer in pipe flow. The latter, being based on the bulk temperature of the fluid, should, however, be multiplied by the temperature ratio θ for comparison with the experimental values. For $Re_d = 100,000$ and $Pr = 0.74$, the values holding for these investigations, θ according to reference 5 is 0.83. It is seen therefore that the experimental values will agree well
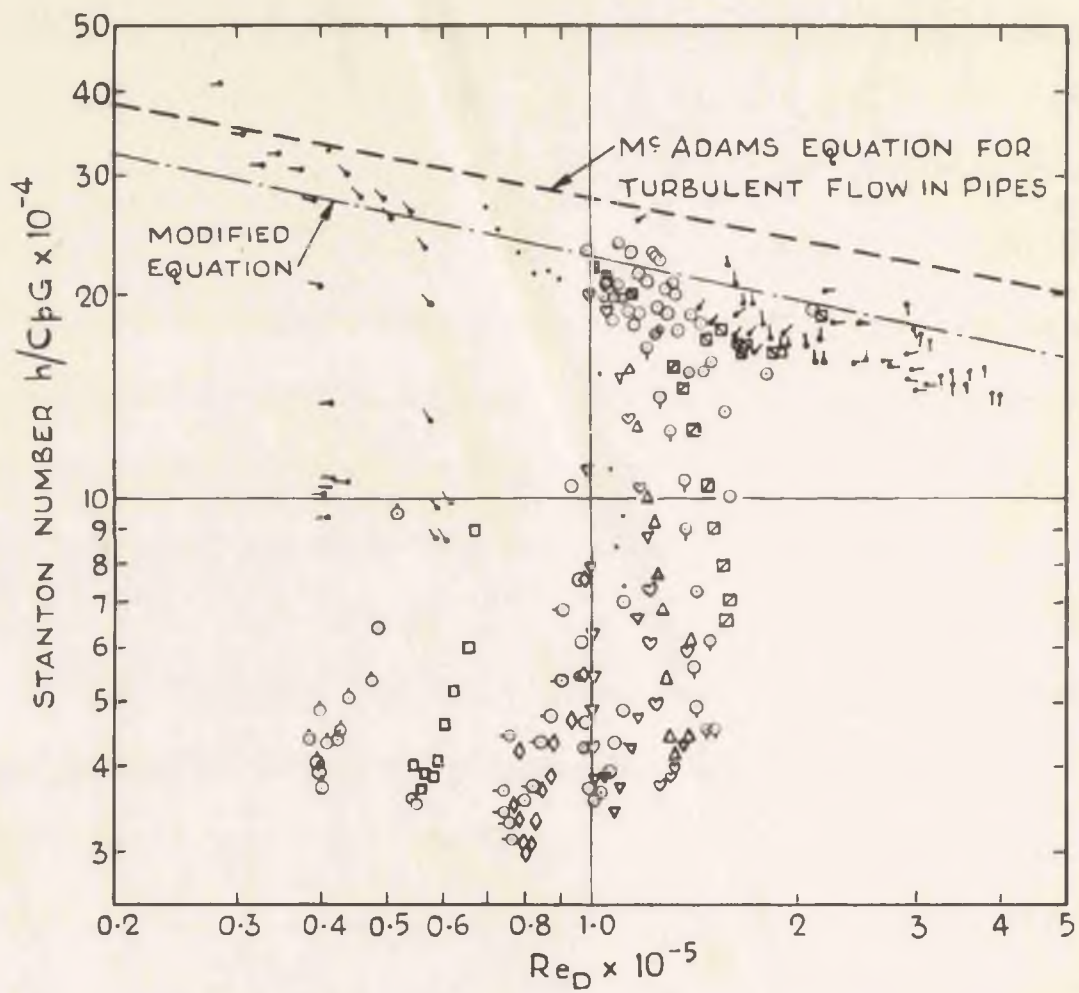
FIG. 56.   HEAT TRANSFER DATA OF KAYE, KEENAN
AND McADAMS

STANTON No. vs. DIAMETER REYNOLDS No.

with those usually taken for low speed flow when corrected for the
different basis of evaluating the temperature gradient.

The experimental results for heat transfer coefficients for
supersonic flows are presented in Figs. 12 and 13 of reference 54. The
coefficients in the form of Stanton numbers are plotted against the length
Reynolds number in the one figure and against the diameter Reynolds number
in the other. Since at the entrance of the pipe, coefficients correspond
to those for flat plate laminar flow neither method of representation is
satisfactory for all the points. A wide scatter is therefore obtained in
these figures. For the tests at higher Reynolds numbers, however, the
coefficients rise slowly towards the downstream end and seem to approach
a limiting curve when plotted against diameter Reynolds number, which is
presumed to be the curve for fully developed flow. The curve for the
empirical equation of McAdams for fully developed turbulent incompressible
flow is shown in Fig. 13, a reproduction of which is shown (Fig. 56). It
is stated in the paper that this seems to lie a little above where the
limiting line of the data would be. Once again, however, the usual pipe
flow equations result in higher values since they are based on bulk fluid
temperatures. The value of θ , the temperature ratio for the correspond-
ing values of Prandtl and Reynolds number is again 0.83. The Stanton
number should therefore be correspondingly reduced by multiplying by this
ratio. The resulting line is shown in Fig. 56 and it can be observed
that this represents the limiting value of the Stanton numbers more closely.

The Experimental values of Heat Transfer Coefficient.

We are now in a position to discuss the experimental values for
heat transfer obtained in the present investigation and to compare the

results for the high velocity flow with those generally accepted for low velocities.

For a short length after the entrance the coefficients correspond to those for laminar flow over a flat plate, the boundary layer being thin compared with the tube radius. Laminar flow persists for such a short length, however, that only a few values were observed for this region.

With increasing distance from the entrance, a gradual transition to turbulence occurs. Comparison with other values is therefore not possible for this region. Available data for the transition zone as given by Seider and Tate (91) and Colburn (14) refer to the transition from laminar to turbulent flow when the flow is fully developed and which is dependent on the diameter Reynolds number and is therefore not applicable to the present case where turbulence occurs before the boundary layer completely fills the cross-section and is dependent on the length Reynolds number.

After turbulence has been attained, it has been seen that coefficients correspond to those for fully developed flow in an annulus, allowance being made for the starting effects by the inclusion of a (D/x) term. It appears that the best equations for heat transfer in an annulus are obtained by the substituting of the equivalent diameter D_e in the normal equations for pipe flow. It would indeed be difficult to apply the formulae for annuli to the present case, since they would need to be corrected to give a coefficient based on the difference between the wall temperature and the temperature at some position in the cross-section of the annulus where it remains constant and corresponds to the temperature at an infinite distance from a flat plate. No data are available,

however, for θ , the ratio of difference between wall and bulk temperatures to the difference between wall and maximum temperature for flow in an annulus.

From equation 98, it can be seen that, by taking x as infinite, the equation for fully developed flow in the annular section will be obtained as:

$$\frac{h}{C_p G} = 0.0183 \left(\frac{C_p \mu}{k} \right)^{-2/3} \cdot \left(\frac{DG}{\mu} \right)^{-0.2} \quad \dots\dots\dots\dots\dots (102)$$

This may be compared with the well known McAdams equation (equation 4c p. 168 reference 72) for fully developed turbulent flow in a pipe:

$$\frac{h}{C_p G} = .023 \left(\frac{C_p \mu}{k} \right)^{-2/3} \left(\frac{DG}{\mu} \right)^{-0.2} \quad \dots\dots\dots\dots\dots (103)$$

Coefficients in this equation, being based on bulk temperature of the stream, should be multiplied by θ to obtain the more logical coefficient. For Pr = 1 and the Reynolds numbers encountered in the experiments, θ = 0.85 from the graph of reference 5. The equation containing this coefficient will then be:

$$\frac{h}{C_p G} = 0.0195 \left(\frac{C_p \mu}{k} \right)^{-2/3} \cdot \left(\frac{DG}{\mu} \right)^{-0.2} \quad \dots\dots\dots (104)$$

The percentage difference between the coefficients obtained from equations 102 and 104 is therefore 7%, which is within the accuracy of most experimental investigations on heat transfer.

In order to compare equations 98 and 99 with existing equations for heat transfer in starting regions, an attempt was made to put them in the form containing the average value of heat transfer coefficient over

the length x from the entrance. It was seen in Part I that this can be carried out by integrating the equation

$$\delta q = h_1 . \delta A . \Delta t \quad \dots\dots\dots\dots\dots\dots\dots\dots\dots(56)$$

where h_1 is the local coefficient.

It can be observed from Fig. 49 that Δt, which in this case is the difference between the wall temperature and the adiabatic wall temperature, remains substantially constant for the region of turbulent flow.

Equation 99 is of the same form as equation 62 which was considered previously. Here i is 1/13 and Δt can be taken as constant. Equation 64 may then be integrated directly giving:

$$q = \frac{1}{1 - i} h_1 . A . \Delta t = h_m . A . \Delta t \quad \dots\dots\dots\dots\dots(105)$$

and so $h_m = 13/12 \, h_1$.

Thus equation 99 put into the form containing the average value of heat transfer coefficient is:

$$St = 0.0291 \, (Pr)^{-2/3} . \, (Re_d)^{-0.2} . \, (De/L)^{1/13} \quad \dots\dots(106)$$

For equation 98, where the equation for the local heat transfer coefficient includes the term $(1 + 2.5/\frac{x}{D})$, the integration may be carried out in two parts. For the second part, i = 1. This will result in an infinite value for the average coefficient. It is doubtful therefore if the variation of the local heat transfer coefficient can be represented by such a term, and it would appear that the inclusion of a (D/x) term will be more satisfactory for allowing for the variation in the starting region. The advantage of the inclusion of the term $(1 + \frac{k}{x/D})$ is that the coefficient assumes a definite value with increasing x.
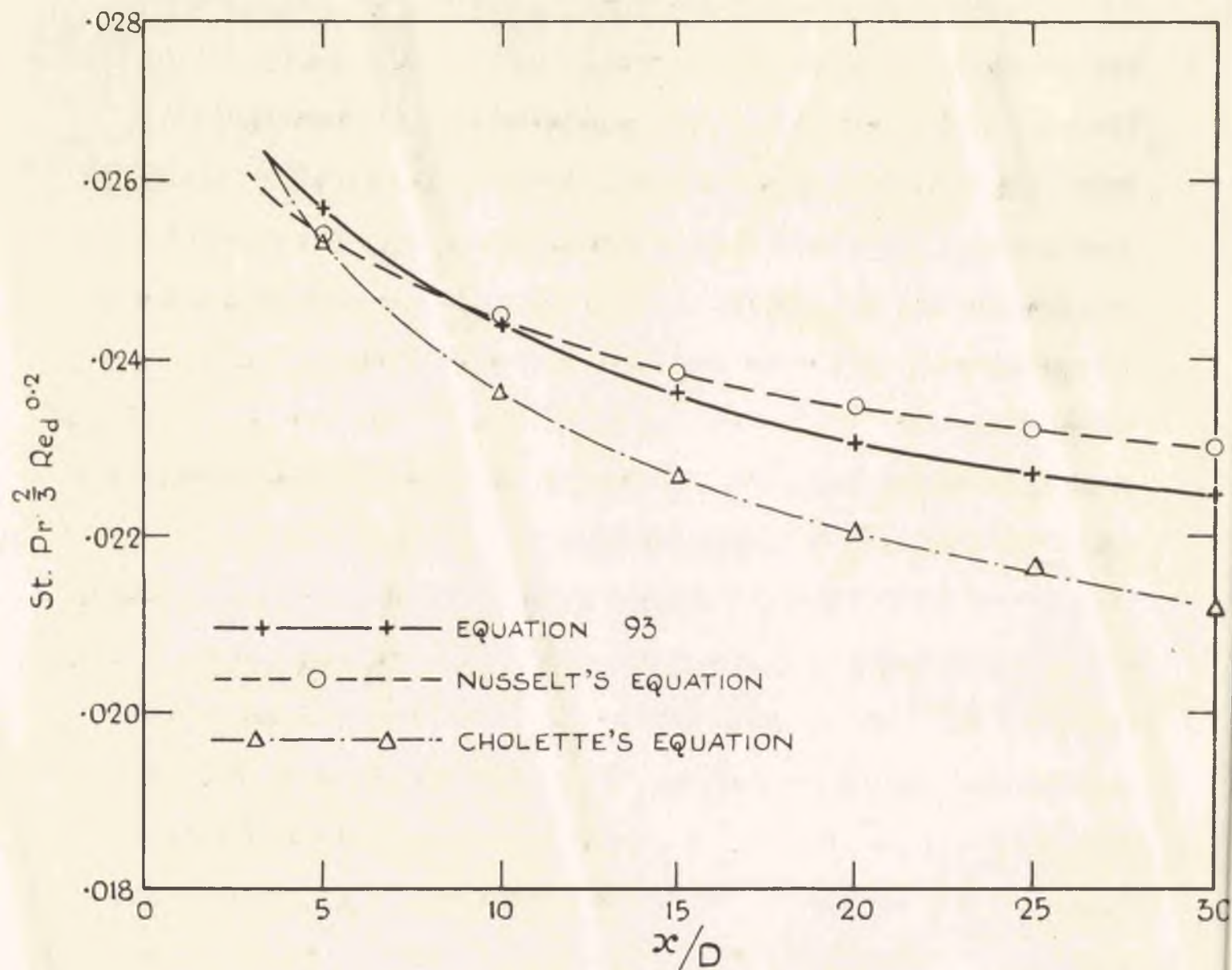
FIG. 57. VARIATION OF $St.Pr^{\frac{2}{3}}Re_d^{0.2}$ WITH x/D. RESULTS

OF TESTS COMPARED WITH DATA OF NUSSELT & CHOLETTE

It can be seen that equation 95, derived by McAdams, Kennel and Addoms and which is of this form, predicts the variation of the heat transfer coefficient with length reasonably well for turbulent flow. This is seen in Fig. 52 where the equation is represented by the upper broken line. This curve is, of course, higher than the measured coefficients for the reasons mentioned above. The average difference is approximately 10% which could probably be accounted for by assuming a value of 0.9 for θ for flow in an annulus. The value of θ will, of course, be higher for an annular than for a circular cross-section since since the distribution is more uniform.

It is difficult to compare an equation of the form of equation 106 with existing ones for heat transfer in the starting region. Unless the power to which the (D/x) term is raised is the same, the value of the constant may vary considerably. Yet a large variation in this power may mean quite a small variation in the actual curve of the coefficient versus length. The equation was therefore represented in graphical form by plotting $Y \equiv (St)(Pr)^{2/3}(Re_d)^{0.2}$ against x/D as shown in Fig. 57. Shown for comparison are the variations of Y with length obtained from other equations for the starting region. The constants in these equations were multiplied by 0.85, the value of θ for the conditions in the present tests.

The measurements of heat transfer coefficients made in the present investigation are therefore in line with other previous investigations on heat transfer at high velocities. The fundamental theory is confirmed, that, to allow for frictional heating, the temperature potential in the heat transfer equation should be redefined as the difference

between the actual wall and the adiabatic wall temperatures and the value of the coefficient will then be the same as for low velocity flow.

Previous investigations confirming this theory have been carried out with large temperature differences, where the effect of frictional heating is small compared with the total heat transferred. In the present investigation the actual wall temperature was not greatly different from the adiabatic wall temperature, and therefore the frictional heating would have a considerable influence on the temperature distribution throughout the boundary layer. The results are therefore of greater value in confirming that the redefined temperature potential results in a heat transfer coefficient independent of temperature difference.

It is interesting to note that most readings were obtained when the wall temperature was less than the adiabatic wall temperature but greater than the bulk stream temperature. From the normal heat transfer equations it would be expected that heat would be transferred from the metal to the steam, whereas heat transfer actually took place in the opposite direction. To have based the calculation of the coefficient on the normal temperature difference would have resulted in negative values. It was also shown that coefficients obtained from runs where heat was transferred from metal to steam had the same values as for heat transfer in the other direction. The coefficient based on this definition of temperature potential is therefore independent of the temperature difference.

Since true local coefficients of heat transfer were measured, these showed a variation with length seldom observed in previous investigations for starting regions in pipes. In the case of supersonic

flow, Kaye, Keenan and McAdams (54) attributed the initial fall in values of the heat transfer coefficient to a thickening laminar boundary layer. Afterwards the coefficients increased as transition to turbulence took place. There was little evidence of a second decrease with thickening of the turbulent boundary layer.

The similar variation observed by Cholette (12) for low speed flow has already been noted in Part I, though here the dependence of the coefficient on the boundary layer was not realised. The smaller length Reynolds numbers (approx. 2×10^5) at which transition occurred, compared with those observed for the present tests, was doubtless due to the sharp-edged entrance to the tubes in the heat exchanger.

FRICTION.

Method of Computation.

The friction coefficients were obtained from observations of the pressure distribution throughout the length of the duct for the adiabatic runs. The method is similar to that employed by Keenan (58) in order to evaluate friction factors for the compressible flow of steam. The theory, adapted for flow in an annulus, is outlined below.

By consideration of the pressure and frictional forces acting on a section of the duct of length d_x, the equation is obtained:

$$- adp - dF = \frac{W}{g} \, dV \quad \dots\dots\dots\dots\dots\dots\dots\dots\dots\dots(107)$$

where dF = frictional force at the wall.

The friction coefficient is defined as:

$$f = \frac{\tau}{\frac{1}{2}\rho V^2} \quad \dots\dots\dots\dots\dots\dots\dots\dots\dots(108)$$

where τ = frictional force per unit area of wall surface

$$\therefore \quad dF = \tau \, \pi(D_2 + D_1) \, dx = f V^2 \cdot \frac{\pi(D_2 + D_1)dx}{V g}$$

Then substituting in (107)

$$\frac{dp}{V} + \frac{G}{g V} \, dV + \frac{f}{2} \cdot \left(\frac{V}{V}\right)^2 \cdot \frac{\pi(D_2 + D_1)}{a \cdot g \cdot} \cdot dx = 0$$

where $\quad G = \frac{W}{a} = \frac{V}{V}$

$$\therefore \quad \frac{dp}{V} + \frac{G^2}{g} \cdot \frac{dv}{V} + \frac{f}{2} \cdot G^2 \cdot \frac{\pi(D_2 + D_1)}{\pi/4(D_2^2 - D_1^2)g} \cdot dx = 0$$

$$\therefore \quad \frac{dp}{V} + \frac{G^2}{g} \cdot \frac{dv}{V} + \frac{2 f G^2}{D_e g} \cdot dx = 0 \quad \dots\dots\dots\dots\dots(109)$$

This is the dynamic equation of flow through an annulus and it

can be seen that the equivalent diameter to be used is $D_e = D_2 - D_1$.

Assuming f constant between stations 1 and 2, then (109) becomes:

$$\int_1^2 \frac{dp}{v} + \frac{G^2}{g} \log_e \frac{-v_2}{v_1} + \frac{2 f G^2}{De\ g} (x_2 - x_1) = 0 \ldots\ldots\ldots(110)$$

In order to obtain the value of the first term, the relationship between pressure and specific volume along the path must be known.   Such a relationship can be obtained from the three equations employed in the evaluation of stream conditions:

$$H + \frac{v^2}{2g} = H_0 \ldots\ldots\ldots\ldots\ldots\ldots\ldots\ldots\ldots\ldots\ldots(66)$$

$$V = Gv \qquad \ldots\ldots\ldots\ldots\ldots\ldots\ldots\ldots\ldots\ldots(67)$$

$$H = A + Bpv \ldots\ldots\ldots\ldots\ldots\ldots\ldots\ldots\ldots\ldots(68)$$

These three equations give

$$A + Bpv + \frac{G^2 v^2}{2g} = H_0 \ldots\ldots\ldots\ldots\ldots\ldots\ldots\ldots\ldots(111)$$

$$\therefore \quad \frac{dp}{v} = - \frac{G^2}{2gB} \cdot \frac{dv}{v} - \frac{H_0 - A}{B} \cdot \frac{dv}{v^3} \ldots\ldots\ldots\ldots\ldots(112)$$

Integrating and substituting in equation 110

$$\frac{G^2}{g} \left(1 - \frac{1}{2B} \right) \log \frac{v_2}{v_1} + \frac{H_0 - A}{2B} \left(\frac{1}{v_2^2} - \frac{1}{v_1^2} \right) + \frac{2 f G^2 (x_2 - x_1)}{g De} = 0$$

or $$f = \frac{g De}{2G^2 (x_2 - x_1)} \left[\frac{H_0 - A}{2B} \frac{1}{v_1^2} - \frac{1}{v_2^2} - \frac{G^2}{g} (1 - \frac{1}{2B}) \log \frac{v_2}{v_1} \right] \ldots(113)$$

If measurements are therefore made of the initial state, rate of flow and pressure at different points along the length, the specific volume can be calculated and the coefficient of friction then found from (113).

For the conditions for which friction coefficients were computed, the specific volume had already been obtained for each station while
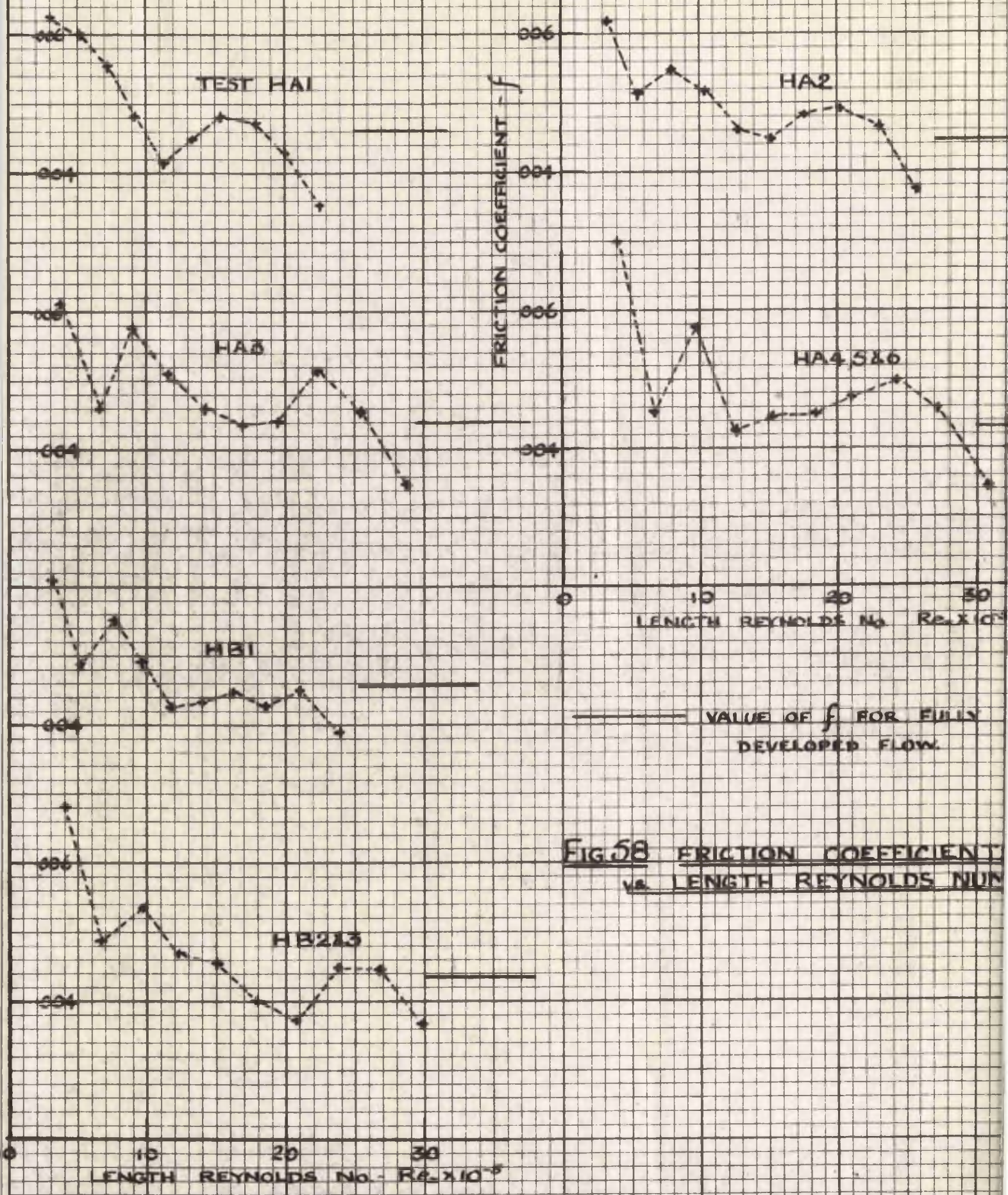
FIG.58 FRICTION COEFFICIENT vs. LENGTH REYNOLDS NUMBER

evaluating the stream conditions. There only remained to substitute these values of specific volume in equation 113 in order to obtain the value of f. The value of friction coefficient obtained in this way is then the average for the length between any two stations, a, b etc.

The coefficients thus found correspond to adiabatic flow. For runs with heat transfer, no change in pressure distribution could be observed. The amount of heat transferred could be allowed for in the calculations by the inclusion of a term Qx in equation 66. It has already been seen, however, that this term is negligible compared with the values of the other terms since only small quantities of heat were abstracted. The same values of coefficient could therefore be taken as holding for all tests having the same initial conditions.

The calculated values are listed in Table 5a in the Appendix and are shown in Fig. 58 plotted against the length Reynolds number. Some of these curves show the coefficients for several tests where the initial conditions were the same. The values of f are then identical since the exhaust pressure was in all cases below the pressure of maximum entropy and therefore the pressure distribution was always the same.

The coefficients found in the manner indicated above are termed apparent friction coefficients. The true friction coefficient at any cross-section of the stream is $2\tau/\rho V^2$, where τ is the shear stress at the duct wall, ρ the mean density and V the mean velocity. The true and the apparent coefficients are identical only if the velocity across each section is so nearly uniform that the mean velocity found from the flux of kinetic energy is identical with that found from the flux of momentum, or if the flux of momentum and the flux of kinetic energy do not

FIG.58 CTD ERICTION COEFFICIENT VS LENGTH REYNOLDS No

change from section to section (60). Since the velocity distribution changes considerably from section to section, particularly in the region of transition from laminar to turbulent flow, the apparent coefficients will differ from the true friction coefficients. The flow of a compressible fluid actually satisfies neither condition, though it is probable that the first is nearly satisfied at a great distance downstream from the entrance.

The measurement of true friction coefficients is, however, very difficult. To do so by observing the actual shear stress at the wall would involve great experimental difficulties while analytical difficulties would be involved in deducting values from pressure measurements.

The above considerations must be borne in mind while discussing the measured friction coefficients and comparing them with theoretical values. It is as apparent coefficients, however, that the results of previous experimental investigations have been presented, such as those of Frossel (32), Keenan (58), Keenan and Neumann (60) and Kaye, Keenan and McAdams (54).

All the curves of friction coefficients shown in Fig. 58 are of similar shape. The coefficient falls rapidly at first and then more gradually towards the exit of the test length. It would be expected that, for a short length at the entrance where a thin laminar boundary layer exists, the friction coefficients would correspond to those for flow over a flat plate. Such values were calculated from the formula.

$$f = 0.664/(Re_1)^{\frac{1}{2}} \qquad \dots\dots\dots\dots\dots\dots\dots\dots\dots(114)$$

and these are indicated in Fig. 58. It is seen that the experimental
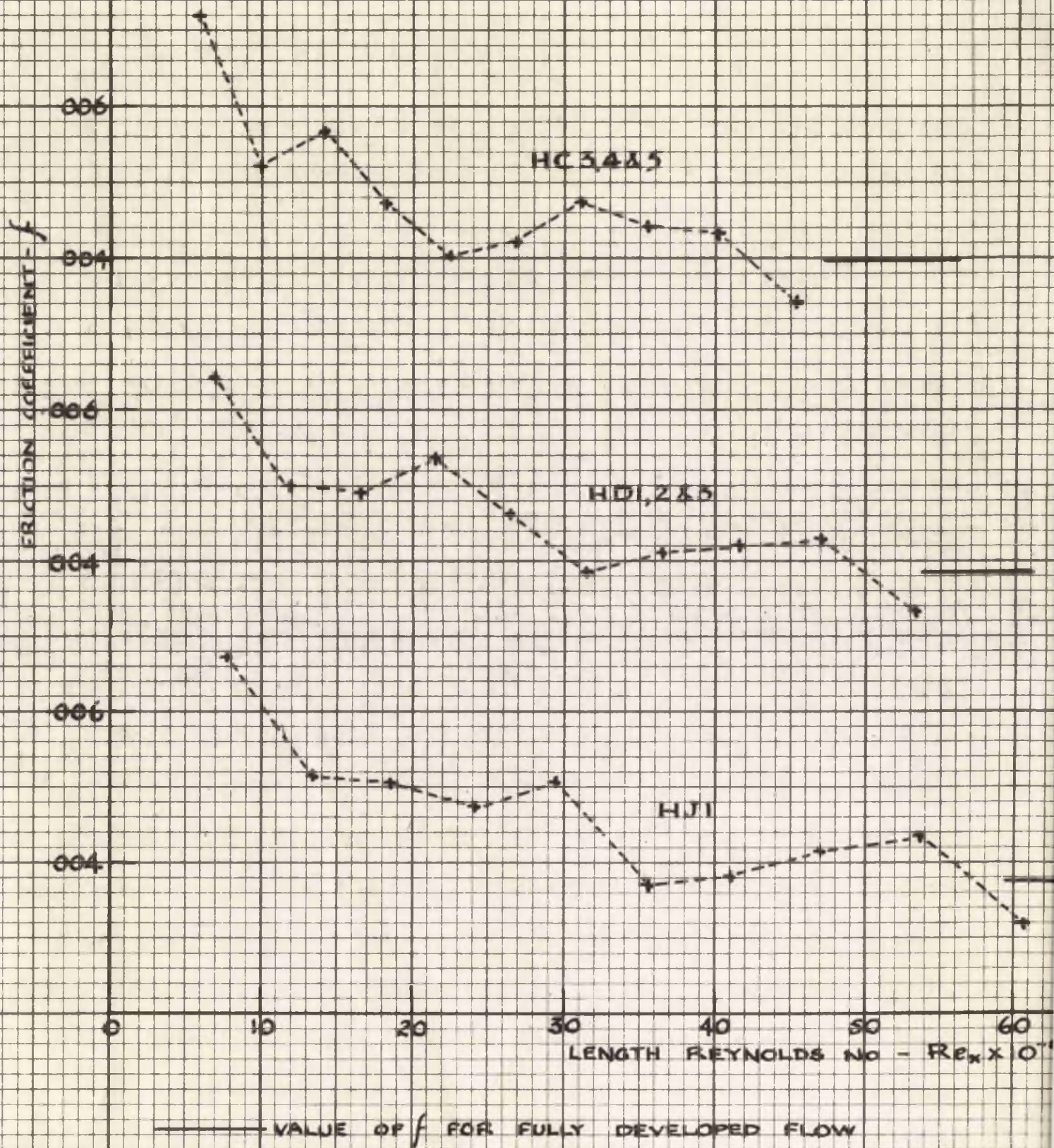
Fig.58 ctd. FRICTION COEFFICIENT vs. LENGTH REYNOLDS NUMBER

values are well above the theoretical curve. This is, of course, owing to the rapid growth of the boundary layer in the entrance region, the changing velocity resulting in a high apparent friction coefficient.

Langhaar (66) subjected the laminar flow in the entrance region of a straight pipe to a complete analysis. Starting from the Navier-Stokes equations, he obtained a relationship for the pressure drop, and from this the apparent friction coefficient may be obtained. Unfortunately it would be very difficult to adapt Langhaar's analysis to flow in the entrance region of an annulus.

As the boundary layer continues to increase in thickness more gradually the effect of the changing velocity profile will become less pronounced and the apparent friction coefficient will approach the value of the true coefficient. This results in a more rapid fall of the apparent coefficient than would result only from the effect of increasing boundary layer thickness on the wall shearing stress. However, it has been seen that a gradual transition to turbulence takes place only a short distance from the entrance and this would result in higher values for the friction coefficient. It is doubtful whether maximums which occur in the curves of friction coefficients for values of Re_1 about 15×10^5 correspond to the start of the fully turbulent boundary layer. The calculated value for f was found to be very sensitive to small variations of static pressure. Small variations in the friction coefficient may not therefore be of much significance. It is probable that more accurate pressure measurements than can be obtained by the use of the standard pressure gauge would result in curves of friction coefficients which would throw more light on the type of flow.
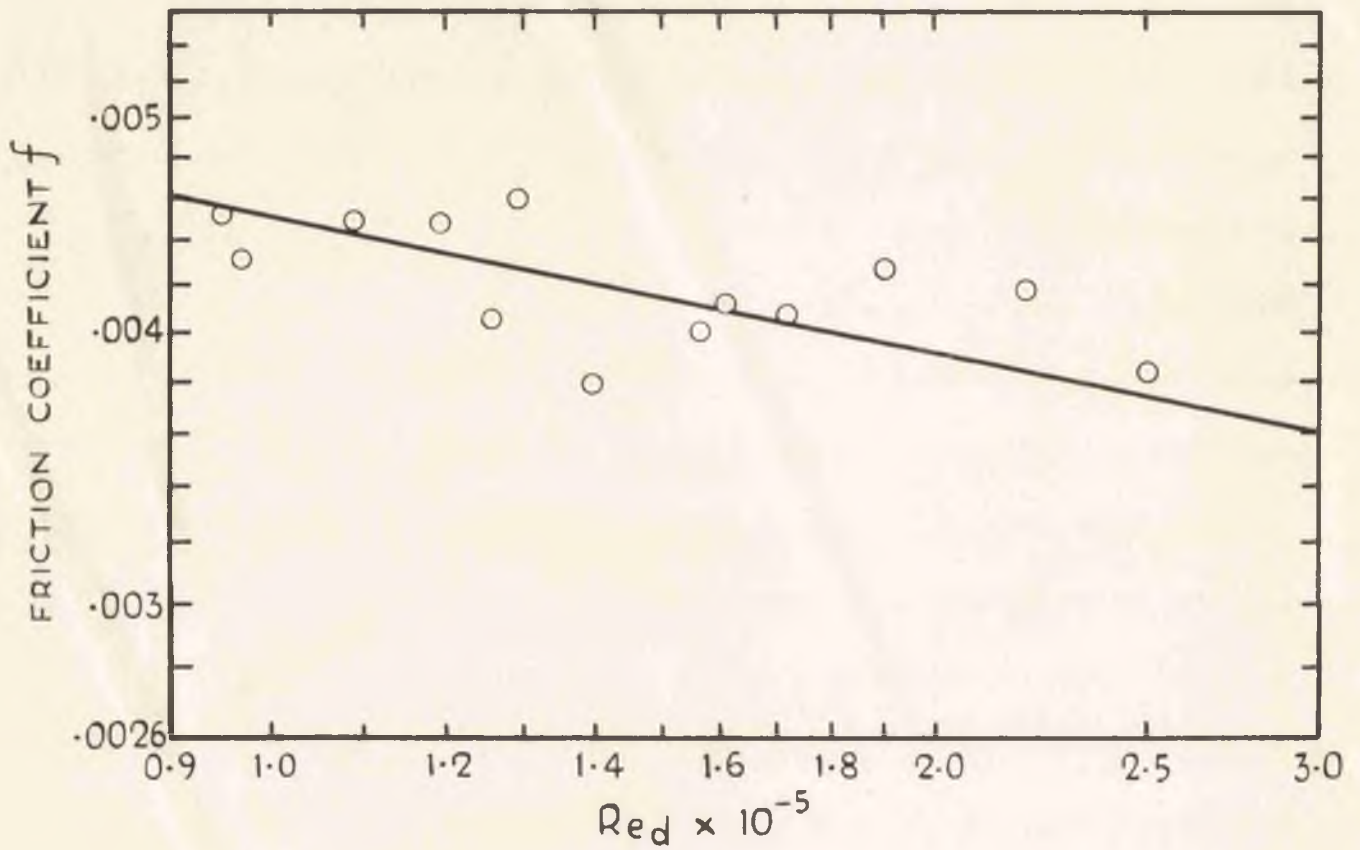
FIG. 59. THE VARIATION OF THE COEFFICIENT OF FRICTION WITH REYNOLDS NUMBERS. THE SOLID LINE REPRESENTS VON K'ARM'AN'S EQUATION FOR INCOMPRESSIBLE FLUIDS

Once the boundary layer becomes turbulent, the flow resembles fully developed pipe flow more closely than that over a flat plate. The variation with length is then dependent on the L/D ratio. No information is available, however, on the effect of L/D on either the apparent or the true coefficient of friction for either the incompressible or compressible flow of fluids. The fact that in this region the coefficient decreases only gradually indicates that the velocity distribution only changes slowly and this in turn means that the apparent coefficient will not be very far from the true coefficient.

The value of f will continue to decrease until the boundary layer completely fills the cross-section and the flow is fully developed. The coefficients for such conditions may then be compared with those obtained from the well established formulae. The usual equation is the Karman-Nikuradse which holds for high values of Re_d :

$$\frac{1}{\sqrt{4f}} = -0.8 + 2 \log (Re . \sqrt{4f}) \quad \ldots\ldots\ldots\ldots\ldots\ldots(115)$$

The value of f obtained from this equation for the value of Reynolds number at the exit is indicated at the right-hand side of Fig. 58. In calculating Re_d , the equivalent diameter $De = D_2 - D_1$ was used. The formulae for pipe flow then apply to the annular cross-section. It can be seen that in most cases the curves appear to approach this value of f asymptotically.

In Fig. 59 values of f which each curve appears to approach for fully developed flow are plotted against Reynolds number. The line representing the Karman-Nikuradse equation is shown for comparison.

The results of the calculations for friction are therefore, in so

far as they go, in line with previous investigations on friction in compressible fluids. Values of the coefficient are the same as those for incompressible flow under similar conditions. For fully developed flow the coefficients are in line with the Karman-Nikuradse equation. No conclusion can be drawn from the data for other regions owing to the difference between apparent and true values.

COMPARISON OF HEAT TRANSFER WITH FRICTION.

It is well known that an analogy exists between heat transfer and friction. When the Prandtl number of the fluid is unity, which is the case for steam under the range of conditions for which the experiments were carried out, the relationship between the coefficients of heat transfer and friction become greatly simplified and is that first derived by Reynolds (85). This is owing to the fact that, for Pr = 1, the heat transfer in laminar and turbulent flow are connected in the same way with the shearing stress. The ratio of the temperature difference in the laminar sublayer to that in the turbulent zone equals the ratio of the corresponding velocity differences, and the profiles of both temperature and velocity are similar. The question arises, therefore, whether this relationship will hold for high velocity flow.

Some care is necessary, however, in applying these relationships to the present circumstances. Starting with the general equation derived by Von Karman, giving the relationship between the heat transferred and the wall shearing stress, the relationship between the coefficient of heat transfer and the coefficient of friction may be obtained easily. Von Karman's equation is:

$$\frac{q}{\gamma c_p \, u_s \, (t_w - t_s)} = \frac{w/\rho u_s^2}{1 + \sqrt{\dfrac{\tau_w}{\rho u_s^2}}\left[5(Pr - 1) + 5 \log_e \dfrac{5Pr + 1}{6}\right]} \quad ...(116)$$

The subscript s refers to conditions outside the thermal and hydrodynamic boundary layers.

For a flat plate $\tau_w/\rho u_s^2 = f/2$ and $q/\gamma c_p u_s \, (t_w - t_s) = St.$

In adapting the equation to a tube, it must be kept in mind that the heat transfer coefficient is usually built with the bulk temperature

t_B , and the relationship between friction coefficient and the shearing stress at the tube wall also contains the average velocity u_m. Then $f/2 = \tau_W/\rho \, u_m^2$ and $St = q/\gamma C_p u_m \, (t_w - t_B)$. If the velocity ratio $u_m/u_s = \phi_m$ and the temperature ratio $t_w - t_B /t_w - t_s = \theta$, then

$$St = \frac{(\phi_m/\theta) \cdot f/2}{1 + \phi_m \sqrt{\frac{f}{2}} \left[5(Pr - 1) + 5 \log_e \frac{5 Pr + 1}{6} \right]} \quad \ldots (117)$$

If $Pr = 1$ approximately, then there is no great inaccuracy involved in neglecting the terms ϕ_m and θ in this relationship, since ϕ and θ are usually very nearly equal and so the ratio ϕ_m/θ very nearly equals 1. This, in fact, is often done in presenting the results of comparison between heat transfer and friction measurements.

In the present investigation, for flow in an annular duct, the subscripts refers to the conditions at some position of the cross-section where the rate of change of velocity and temperature with distance from the wall is zero. This, of course, will be the case for a circle concentric with the walls, probably not far from the mid-way point between them. The friction coefficient, as calculated in the manner shown in the previous section, is again given by $f/2 = \tau_W/\rho \, u_m^2$, where u_m is the average velocity. As for the Stanton number, $St = h/C_p G$, G was taken in the calculations as based on the mean values of velocity and specific volume i.e. $G = \delta.u_m$. It has been shown that the heat transfer coefficient is based on a temperature difference which corresponds to $t_w - t_s$ in low speed flow, and so $St = q/\delta C_p u_m \, (t_w - t_s)$. The relationship that would be expected between the Stanton number evaluated from the tests and the friction coefficient is then:
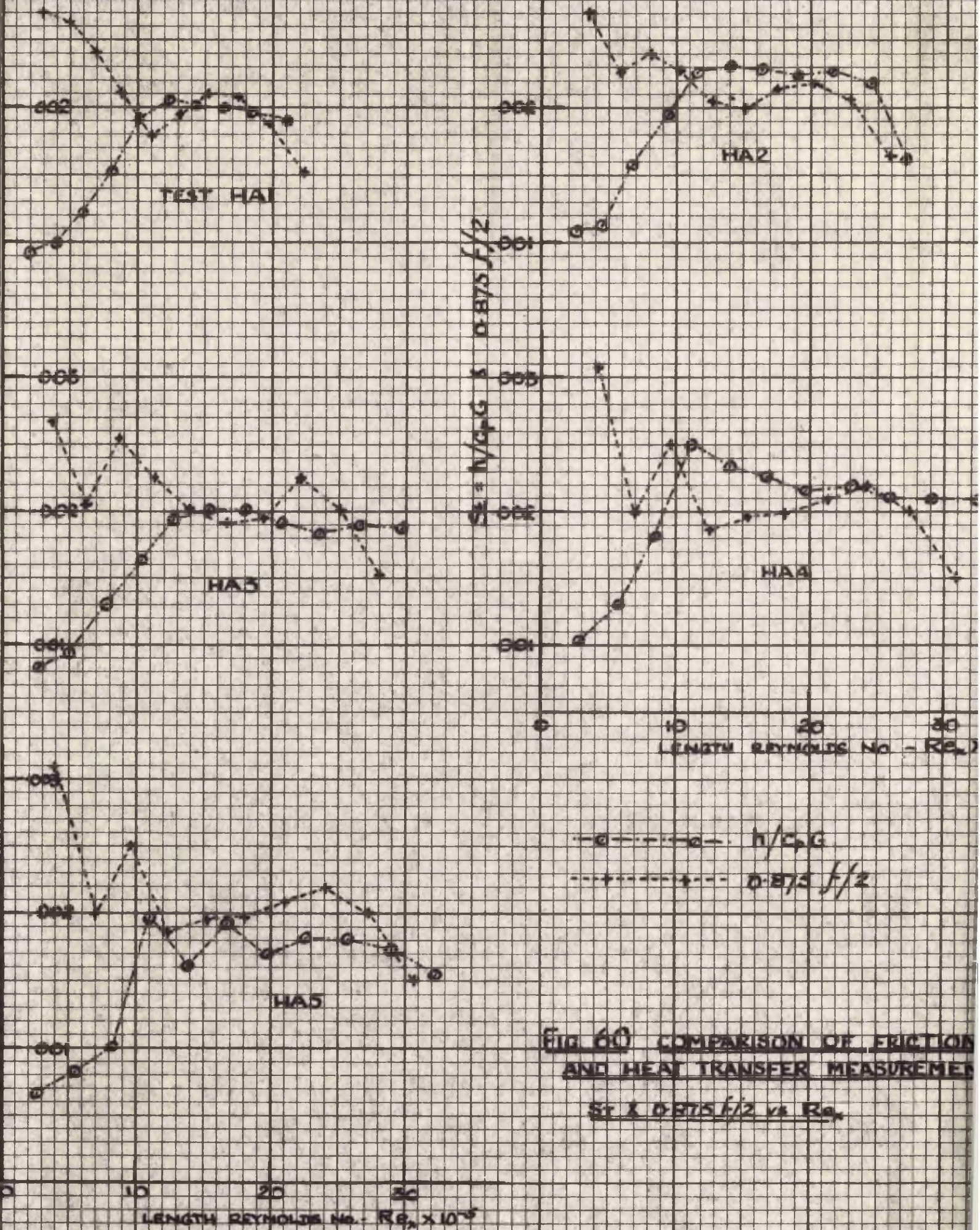
FIG. 60 COMPARISON OF FRICTION
AND HEAT TRANSFER MEASUREMENT
$St \times 0.875 \, f/2$ vs Re_x

$$St = \frac{\phi \cdot f/2}{1 + \phi \sqrt{\frac{f}{2}} \left[5(Pr - 1) + 5 \log_e \frac{5Pr + 1}{6} \right]} \quad \ldots\ldots(118)$$

And since $Pr = 1$

$$St = \phi \cdot f/2 \quad \ldots\ldots\ldots\ldots\ldots\ldots\ldots\ldots\ldots(119)$$

The value of $\phi = U_m/U_s$ for flow in an annulus can be obtained by assuming that the turbulent velocity distribution follows the usual seventh-root law and also that the maximum velocity occurs midway between the walls. Integrating over such a velocity profile in order to obtain the average velocity, it was found that the ratio ϕ was independent of the relative diameter and was equal to 0.875.

However, Rothfus, Monrad and Senecal (86) discussed the velocity distribution in annuli in detail and obtained the radius of maximum velocity for fully developed turbulent flow as:

$$r_m = \left\{ (r_i^2 - r_0^2) / 2 \log_e r/r_0 \right\}^{\frac{1}{2}} \quad \ldots\ldots\ldots\ldots(120)$$

From this, and the Karman-Prandtl seventh root law, the ratio U_m/U_s was calculated by Mizushina (76) who found:

$$\phi = \frac{60}{7} \cdot \frac{r_i + r_0}{7r_i + 7r_0 + r_m} \quad \ldots\ldots\ldots\ldots\ldots\ldots(121)$$

Substituting into this equation the values of the inner and outer radii r_i and r_0, and the radius of maximum velocity r_m from equation 131, the value of ϕ for the dimensions of the annulus for which flow was investigated was found to be 0.874.

The friction coefficients, computed from the pressure distribution, were therefore divided by 2 and multiplied by 0.874 and plotted against length Reynolds numbers for each heat transfer test. Superimposed in the same ordinates were plotted the values of the measured
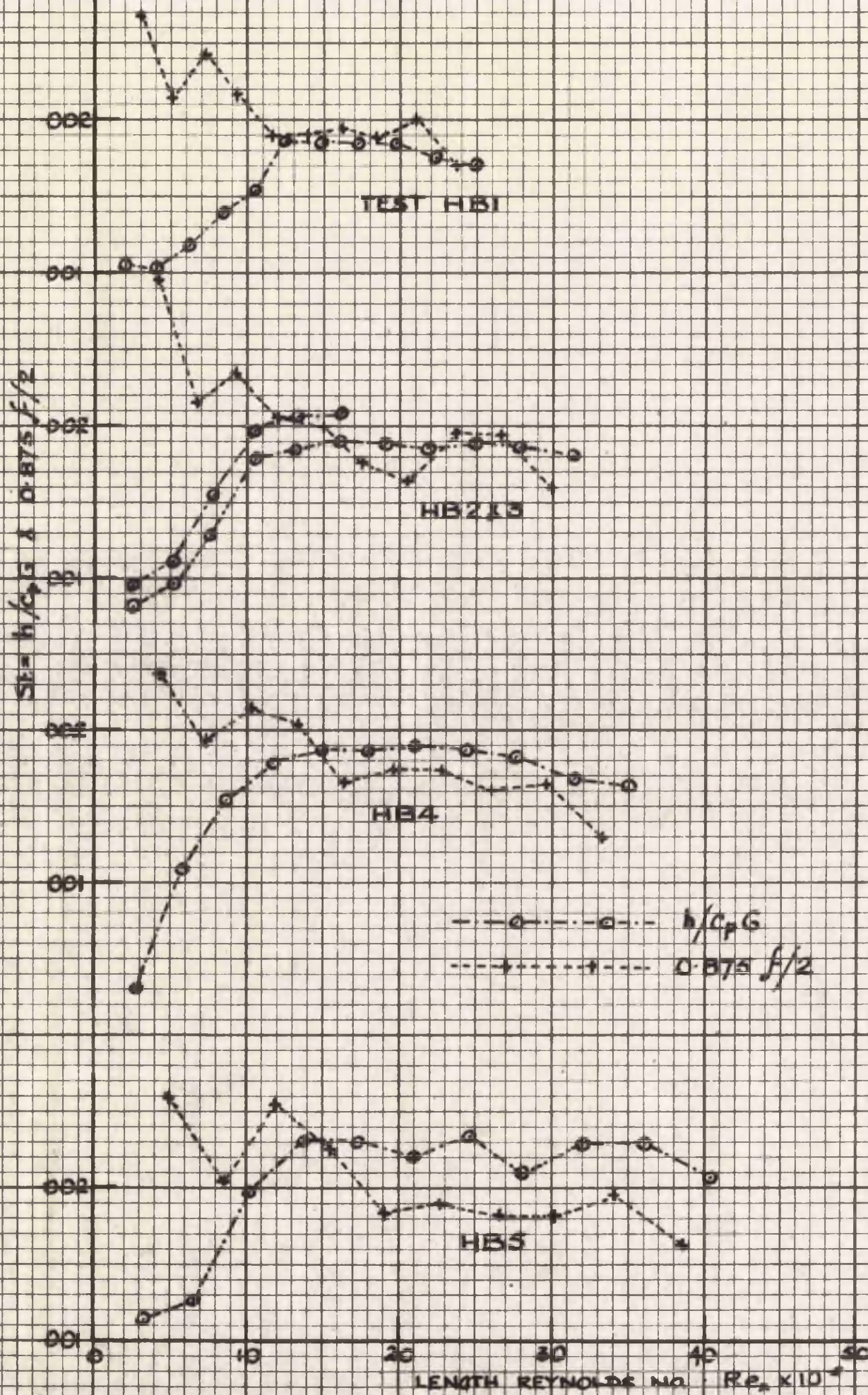
FIG 60 ctd. COMPARISON OF FRICTION AND HEAT TRANSFER MEASUREMENTS
St & 0·875 f/2 vs Re
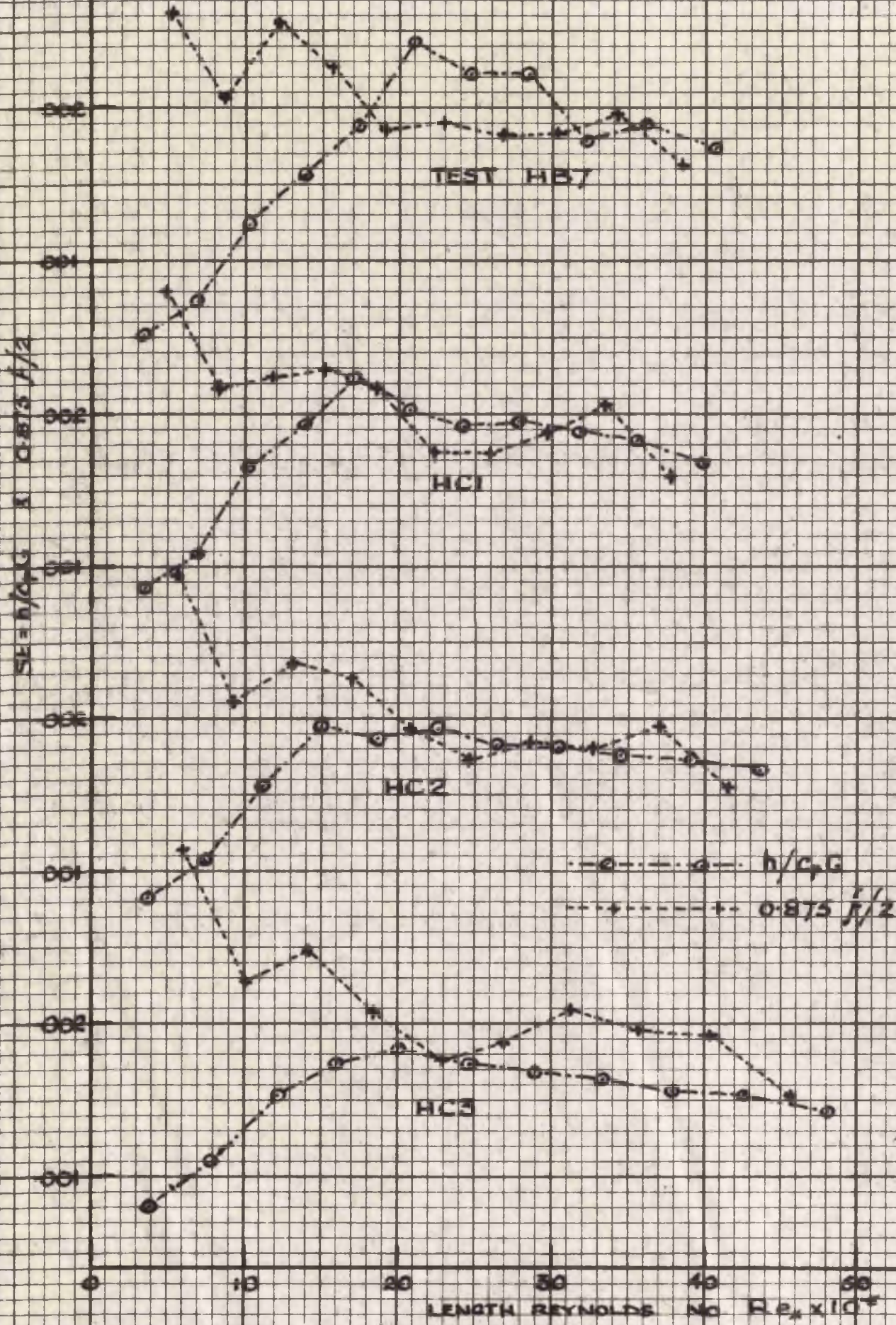
FIG. 60 CTD COMPARISON OF FRICTION AND HEAT TRANSFER MEASUREMENTS

St δ 0.875 $f/2$ vs Re_x

Stanton numbers.   The curves so obtained are shown in Fig. 60.

It can be seen that, while there is a wide divergence between the values in the entrance region, the agreement between the two curves is very good once turbulence is established.   The reason for the divergence at the start is, of course, owing to the fact that the apparent friction coefficients which are measured are much higher than the true coefficients in the starting region where the velocity distribution is changing rapidly.   Also, the value of f was based on fully developed turbulent flow and will not hold for regions where a laminar boundary layer is building up.   The fact that there is good agreement between friction and heat transfer measurements in the turbulent zone indicates that, while the boundary layer is evidently still gradually increasing in thickness, the change in the velocity distribution from section to section is so slight that there is no substantial difference between the apparent and true values of friction coefficient.

These measurements indicate therefore that the same relationship holds between heat transfer and friction for high velocity flow when the heat transfer coefficient is based on the temperature difference between the wall and adiabatic wall temperatures as exists between these values at low velocity, the normal definition for temperature potential being used for obtaining the heat transfer coefficient.   This is, of course, to be expected since all investigations on friction at high velocities indicate the friction coefficients have the same value as for low velocity flow, and values of heat transfer coefficients are also the same as for low velocities, so long as the appropriate temperature difference is employed. Such is also indicated by the theoretical analysis of Eckert and Drewitz (25).

TEST HD1

$- \cdot \ominus - \cdot - \ominus - \cdot -$ $h/c_p \, G$

$- + - - - + - - -$ $0.875 \, f/2$

$S_t = h/c_p G$ & $0.875 \, f/2$

HD2

$Re_x \times 10^{-6}$

HJ1

LENGTH REYNOLDS NO - $Re_x \times 10^{-6}$
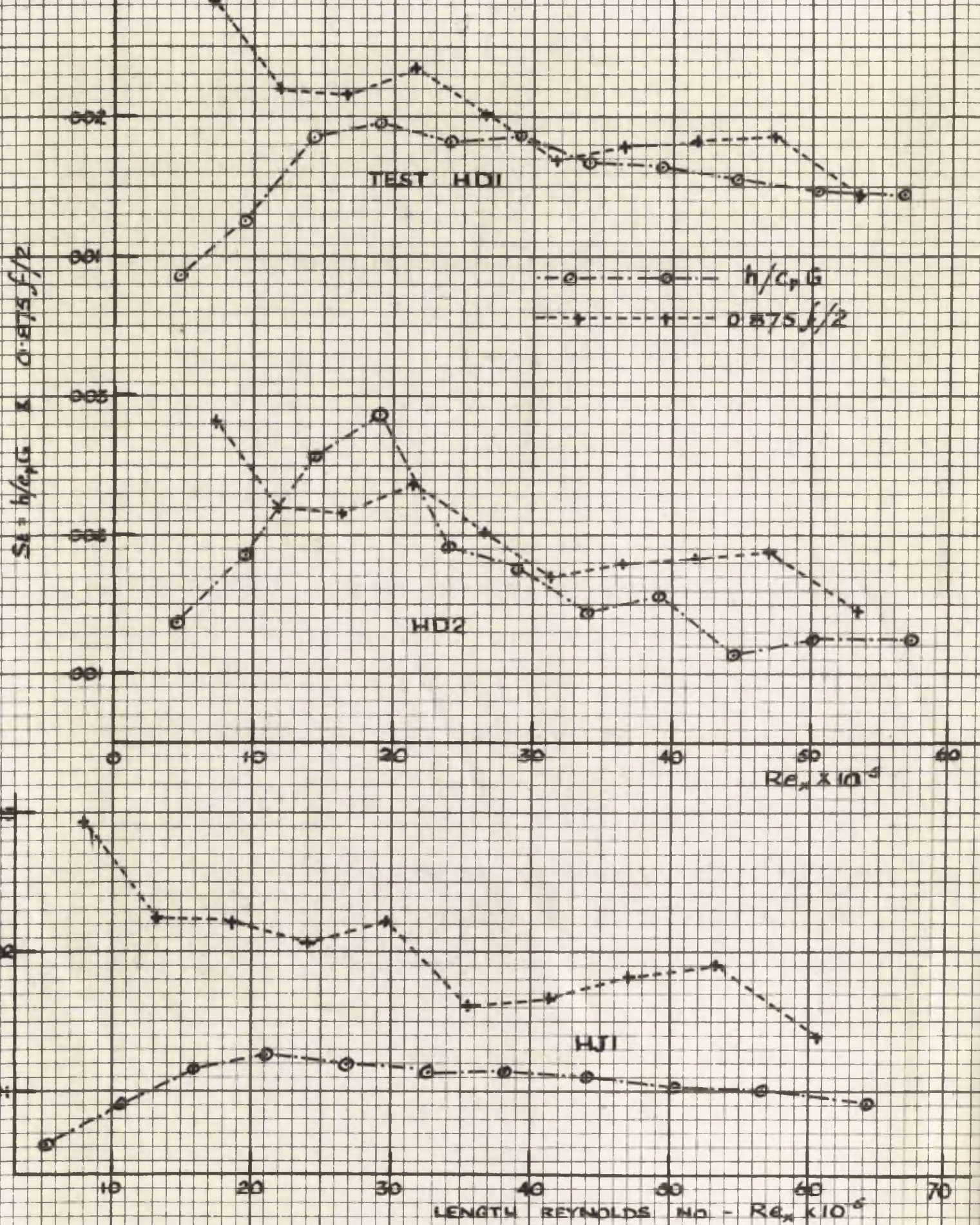
FIG 60 CTD COMPARISON OF HEAT TRANSFER AND FRICTION MEASUREMENTS

S_t & $0.875 \, f/2$ vs. Re_x

FURTHER ANALYSIS OF FLOW CONDITIONS.

It is now possible to examine further the nature of the flow in the parallel annular duct in the light of measurements of friction and heat transfer. It has been demonstrated that a Mach number of 1 is attained at the position of maximum entropy. This pressure was observed at the exit of the duct in tests where the exhaust pressure was atmospheric which was the case for all the heat transfer runs.

The reasoning which leads to this conclusion is based on a one dimensional flow model and the Mach number is that obtained from the mean value of velocity and of sonic velocity at the section. It is known, however, that owing to viscous effects the stream velocity is greatest at mid-stream and decreases to zero at the boundaries of the flow. The variation of Mach number across each section will be similar to that of velocity and in most cases the profile will be slightly more exaggerated since the higher temperature at the boundaries results in a higher sonic velocity in these regions than in mid-stream. Since then the average Mach number is unity and there are regions where this number is less than 1, there must therefore be regions where it is greater than 1. It would then appear that supersonic flow occurs over a part of the cross-section at the exit of the duct.

This fact may be demonstrated from a different viewpoint and in a more quantitative way. It has been seen that values of both the heat transfer coefficient and the friction coefficient decrease from maximum values at first rapidly but always continue to fall up to the exit. This decrease can only be explained by the growth of the boundary layer, since all other factors influencing heat transfer and friction are constant along
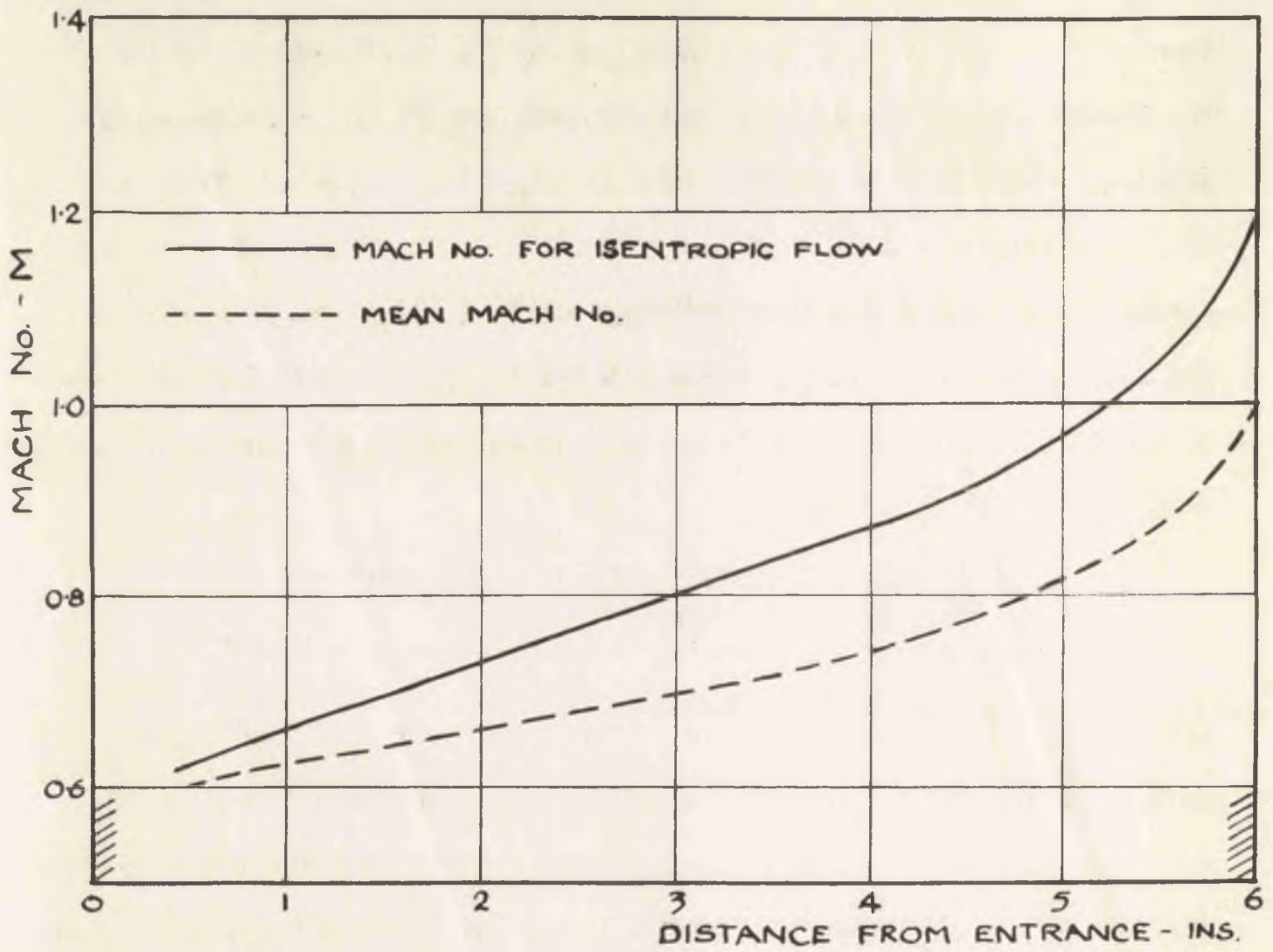
FIG. 61   VARIATION OF MACH No. WITH LENGTH

the length.   This continuing growth in turn means that there is a core
outwith the boundary layer unaffected by viscosity.   To the isentropic
flow in this core Bernoullis theorem may therefore be applied and a
relationship found between the velocity and the static pressure at any
section.   It may be noted that this relationship is derived from the
laws of motion and assumes the absence of fluid shear and adiabatic flow
(there is, of course, no heat exchange to the core).   The continuity
equation is not required and could not readily be applied since the area
of the core is not known and also fluid is exchanged between the isentropic
core and the boundary layers.

The Mach number was calculated from the equation:

$$M = \sqrt{\frac{2}{\gamma-1} \cdot \left\{\left(\frac{p_0}{p}\right)^{\frac{\gamma-1}{\gamma}} - 1\right\}} \quad \dots\dots\dots\dots\dots(122)$$

assuming γ , the ratio of specific heats to be constant and equal to
1.31.   In Fig. 61 is shown the distribution of the Mach number in the
core along the length, for test HB3.   The distribution for other tests
will be very nearly the same since the pressure ratio was observed to vary
but slightly for different supply conditions.

It can be seen therefore that over a length of nearly 1 in. before
the exit supersonic flow occurs in the central regions of the duct.   As
may be expected, there is no discontinuity in the values of heat transfer
or friction coefficients as the Mach number reaches and exceeds unity.
Discontinuities normally only occur at supersonic velocities with
decelerating flow when shock waves are liable to occur.   The effect of
compressibility cannot, of course, be examined with velocities only slightly
exceeding the acoustic value, but previous investigations lead to the
conclusion that such an effect is small for Mach numbers around 1.

CONCLUSIONS.

The results obtained in these investigations indicate that superheated steam is a suitable fluid for studying heat transfer at high velocities. It was found to be convenient in use and the apparatus was much simpler than that used in experimental investigations with air.

Measurements of heat transfer coefficients and recovery factors showed that these values were in line with data relating to air and indicate the advantage of undertaking a programme of research using superheated steam as a gas having different property values.

The one-dimensional method employed in the solution of the stream conditions was found satisfactory in analysing the characteristics of the flow.

In the flow through the short convergent-divergent nozzle a Mach number of unity is attained at the throat. Thereafter the flow proceeds into the supersonic region until recompression.

A laminar boundary layer is established at the walls and persists until recompression, when the sudden adverse pressure gradient causes a transition to turbulence and probably separation of the flow.

For the laminar region, the recovery factor, obtained by recording the surface temperature of the central insulated probe, was 0.94 and was independent of Reynolds and Mach numbers.

Lower values were observed for the turbulent region, though the results cannot be considered accurate as the probable separation of flow would render the calculation of stream conditions erroneous.

In the flow through the 6 in. long parallel annular duct, there is little evidence of a laminar boundary layer at the entrance. A fully

developed turbulent boundary layer is attained at a length Reynolds
number of between 15 and 20 x 10^5. The gradual transition in the type
of flow up to this point usually occupies nearly half the test length.

Considering mean values, the Mach number is unity at the exit.
Since the boundary layers do not completely fill the cross-section,
however, isentropic flow persists within a central core; here sonic
velocity is attained about 1 in. from the exit.

The value of the recovery factor was observed to fall throughout
the transition zone but becomes constant for fully turbulent flow. This
value can be represented by the equation:

$$r = 0.827 \left(T_s / T_{sat.} \right)^{\frac{1}{2}}$$

where T_s is the absolute steam temperature and T_{sat} the absolute
saturation temperature for the corresponding pressure. For fully
turbulent flow r is again independent of Reynolds and Mach numbers.

The heat transfer coefficient was observed to rise in the
transition zone, a maximum being reached at the point where the boundary
layer becomes fully turbulent. Thereafter the coefficient gradually
decreases as the turbulent layer continues to increase in thickness. For
this region h can best be represented by the equation:

$$\frac{h}{C_p G} = .0269 \left(\frac{DG}{\mu} \right)^{-0.2} \left(\frac{C_p \mu}{k} \right)^{-2/3} \left(\frac{De}{x} \right)^{1/13}$$

Values obtained for the recovery factor are below the value of
unity indicated by theory for both the laminar and turbulent boundary
layers. Whether the discrepancy is due to the inadequacy of the theory
or a peculiarity of steam as not being a true gas is not determined. The
dependency of the recovery factor on temperature points to the latter
conclusion.

The values of heat transfer coefficient correspond to those for laminar flow over a flat plate for positions near the entrance when length Reynolds number is sufficiently small. In the turbulent region coefficients agree with those obtained from formulae for flow in the entry region of pipes. In these formulae the equivalent diameter, $D_e = D_2 - D_1$, is to be substituted for the pipe diameter, and a correction must be applied to allow for the fact that the heat transfer coefficients for pipes is built up with the bulk fluid temperature.

In order to overcome the effect of frictional heating, the temperature difference which is to be employed in the heat transfer equation must be taken as that between the actual wall temperature and the adiabatic wall temperature. The experimental results show that the heat transfer coefficient is then independent of temperature difference and is the same as that for low velocity flow under similar conditions, the temperature difference being that between the wall and the stream in the region uninfluenced by heat transfer.

Friction coefficients, calculated from pressure observations, approach, for downstream sections of the test length, those for fully developed turbulent low velocity flow.

Since the Prandtl number can be taken as 1, the Reynolds equation connecting Stanton number and friction coefficient holds, the Stanton number being calculated from the heat transfer coefficient based on the redefined temperature gradient.

Steam, initially near the saturation temperature, when expanding through a nozzle, first passes into the first type of supersaturation in which the steam is dry and obeys exactly the same laws as for superheated

steam, and then into the second state of supersaturation in which small water droplets exist though the steam is still undercooled. With continuous expansion there is a gradual transition from the first to the second type.

For the first type of supersaturation, observation of the adiabatic wall temperature yields the same values of recovery factor as for superheated steam. The presence of water droplets, however, causes lower wall temperatures to be recorded and the recovery factor for very wet steam is nearly zero.

ACKNOWLEDGMENTS.

BIBLIOGRAPHY.

1. G. ACKERMANN; "Plate Thermometer in High Velocity Flow with Turbulent Boundary Layer". Forschung auf dem Gebiete des Ingeniurwesens. Vol. 13, 1942 pp. 226 - 235.

2. C. BATHO: Proc. Inst. Civil Engrs. Vol. 174 Part 4, 1907.

3. J. BIALOKOZ; "Heat Transfer to a Fully Developed Turbulent Airstream Flowing in a Duct at Subsonic and Supersonic Speeds". Paper received from the Mechanical Engineering Research Laboratory of the Department of Scientific and Industrial Research.

4. H. BLASIUS; "Grenzschichten in Flussigkeiten mit kleiner Reibung" Zeitschr. f. Math. u. Physik. Bd. 56, 1908 pp. 1 - 37.

5. L.M.K. BOELTER, R.C. MARTINELLI, T. JONASSEN; "Remarks on Analogy between Heat Transfer and Momentum Transfer" Trans. Am. Soc. Mech. Engrs. Vol. 63, 1941 pp. 447 - 455.

6. L.M.K. BOELTER, G. YOUNG, H.W. IVERSON; "Distribution of Heat Transfer Rate in Entrance Section of Circular Tube" N.A.C.A. Tech. Note 1451, 1948.

7. J.G. BRAINERD, H.W. EMMONS; "Effect of Variable Viscosity on Boundary Layers with a Discussion on Drag Measurements" Trans. Am. Soc. Mech. Engrs. Vol. 64, 1942.

8. W.B. BROWN; Contribution to the Discussion on paper by Kaye, Keenan and McAdams. Trans. Am. Soc. Mech. Engrs. Vol. 73, 1951 pp. 277 - 278.

9. E. BRUN and M. JAMPY; "Convection forcee aux grandes vitesses". Bulletin bi-mensual, Societe Francaise de Physique. 15 Mai 1936 No. 389 p. 87.

10. A. BUSEMANN; "Laminar Flow of a Gas along a Plate" Zeitschrift fur. Angewandte Mathematik and Physik. Vol. 5, 1938 pp. 227 - 232.

11. P.G. CARPENTER, A.P. COLBURN, E.M. SCHOENBORN and A. WURSTER; "Heat Transfer and Friction of Water in an Annular Space" Trans. Am. Inst. of Chem. Engrs. Vol. 42, 1946 p. 165.

12. A. CHOLETTE; "Heat Transfer - Local and Average Coefficients for Air Flowing inside Tubes" Chem. Engr. Progress. Vol. 44 No. 1, 1948 pp. 81 - 88.

13. A.P. COLBURN; Trans. Am. Inst. Chem. Engrs. Vol. 29, 1933 p. 174.

14.   A.P. COLBURN: Engg. Bull. Pardue University, Vol. 26 No. 1, 1942.

15.   A.P. COLBURN: and C.A. COGHLAN: "Heat Transfer to Hydrogen-Nitrogen Mixtures inside Tubes". Trans. Am. Soc. Mech. Engrs. Vol. 63, 1941 pp. 561 - 566.

16.   W.F. COPE: "The Friction and Heat Transfer Coefficients of Rough Pipes". Proc. Inst. Mech. Engrs. Vol. 137, 1941 pp. 99 - 105.

17.   W.F. COPE: "Heat Transfer at High Speeds" Proc. Seventh International Congress of Applied Mechanics Vol. 3, 1948 p. 120.

18.   L. CROCCO: "Transmission of Heat from a Flat Plate to a Fluid Flowing at a High Velocity". N.A.C.A. Tech. Memo. 690, 1932.

19.   L. CROCCO: "Boundary Layer of Gases Along a Flat Plate" Seminario Matematico Rendiconti, University of Roma, Rome, Italy. Vol. 2, 1941 p. 138.

20.   E.S. DAVIS: Trans. Am. Soc. Mech. Engrs. Vol. 65, 1943 p. 755.

21.   R.G. DEISSLER: "Investigation of Turbulent Flow and Heat Transfer in Smooth Tubes, Including the Effects of Variable Fluid Properties" Trans. Am. Soc. Mech. Engrs. Vol. 73, 1951 p. 101.

22.   L.G. DESMOND and E.W. SAMS: "The Correlation of Forced Convection Heat Trasnfer Data for Air Flowing in a Smooth Platinum Tube with Long Approach Entrance at High Surface and Inlet Air Temperatures". N.A.C.A. R.M. E50 H23 1950.

23.   G. EBER: "Experimental Research on Friction Temperature and Heat Transfer for Simple Bodies at Supersonic Velocities" German Archive Report 66/57 Part 1 Nov. 1941.

24.   E. ECKERT: "Heat Transmission of Bodies in Rapidly Flowing Gases" Intelligence T.2, Air Documents Office, Foreign Exploitation Section - Wright Field, Dayton, Ohio, 1946.

25.   E. ECKERT and O. DREWITZ: "Heat Transfer to a Plate in Flow at High Speed". Forschung auf dem Gebeite des Ingenieurwesens. Vol. 11. No. 3, 1940 pp. 116 - 124. Translated in N.A.C.A. Tech. Memo. 1045, 1943.

26.   E. ECKERT and W. WEISE: "Temperature of Unheated Bodies in a High Speed Gas Stream" Forschung auf dem Gebeite des

Ingenieurwesens. Vol. 12 No. 1, 1941 pp. 40 - 50.
Translated in N.A.C.A. Tech. Memo. 1000 - 1941.

27. E. ECKERT and W. WEISE: "Measurement of Temperature Distribution on Surface of Unheated Bodies in High Velocity Flow" Forschung auf. dem Gebeite des Ingenieurwesens. Vol. 13, 1942 p. 246.

28. E. ECKERT: "Temperature Recording in High Speed Gases" Zeitschrift des Vereines Deutscher Ingenieure. Vol. 84 No. 43, 1940 pp. 813 - 17. Translated in N.A.C.A. Tech. Memo. 983, 1941.

29. H.W. EMMONS and J.G. BRAINERD: "Temperature Effects in a Laminar Compressible Fluid Boundary Layer along a Flat Plate" Trans. Am. Soc. Mech. Engrs. Vol. 63, 1941 pp. A105 - 110.

30. A. EUCKEN: Physik Zeitschrift Vol. 12 pp. 1101 - 1107, 1911 Vol. 14 p. 324, 1913.

31. W.W. FISCHER and R.H. NORRIS: "Supersonic Convective Heat Transfer Correlation from Skin Temperature Measurements on a V-2 Rocket in Flight". Trans. Am. Soc. Mech. Engrs. Vol. 71, 1949 pp. 457 - 469.

32. W. FROSSEL: "Stromung in glatten Rhoren mit Uberund Unterschallgeschwindigkeit". Forsch. Geb. Ing. Wes. 1936 pp. 75 - 84. Translated in N.A.C.A. Tech. Memo. 844, 1938.

33. S. GOLDSTEIN: "Modern Developments in Fluid Dynamics" Oxford University Press 1938.

34. W.J. GOUDIE: "Steam Turbines" Longmans, Green & Company, 1922.

35. L. GRAETZ: Ann. Physik. Vol. 18, 1889 pp. 79 - 94.
Vol. 25, 1895 pp. 337 - 357.

36. A. GUCHMAN, N. ILJUCHIN. W. TAASSOWA and G. WARSCHAWSKI: "Untersuchung des Warmeuberganges bei Bewegung eines Gases mit sehr grosser Geschwindigkeit". Tech. Physics of the U.S.S.R. 2, 1935 pp. 375 - 413.

37. H. HAUSEN: Z. Ver. deut. Ing., Beiheft Verfuhrenstechnik No. 4, 1943 pp. 91 - 98.

38. G.A. HAWKINS, W.L. SIBBIT, H.L. SOLBERG: Trans. Am. Soc. Mech. Engrs. Vol. 70, 1948 pp. 19 - 23.

39. G.A. HAWKINS, H.L. SOLBERG and A.A. POTTER: Trans. Am. Soc. Mech. Engrs. Vol. 62, 1940 pp. 677 - 88.

40.   H. HELMHOLTZ: Annal. De. Physique, N.F. 32, 1887, 1.

41.   W.F. HILTON: "Thermal Effects on Bodies in an Air Stream"
        Proc. of Royal Soc. Series A Vol. 168, 1938 pp. 43 - 57.

42.   E. HOFFMANN: Z. Ver. deut. Ing. Vol. 82, 1938 pp. 741 - 782.

43.   L.V. HUMBLE, W.H. LOWDERMILK and M.D. GRELE: "Heat Transfer
        Coefficients and Friction Factors for Air Flowing in a Tube
        at High Surface Temperatures" Heat Transfer and Fluid
        Mechanics Institute, Berkeley, California 1949 p. 165.

44.   N.V. ILJUCHIN: "Investigations of Heat Transfer and Frictional
        Resistance in Steady Gas Flow at very High Velocities" Bulletin
        of the Academy of Science of U.S.S.R. 1946 No. 5.

45.   M. JAKOB: "Heat Transfer" John Wiley & Sons, N.Y. 1949.

46.   M. JAKOB and W.M. DOW: "Heat Transfer from a Cylindrical
        Surface to Air in Parallel Flow with or without Unheated
        Starting Sections".   Trans. Am. Soc. Mech. Engrs.   Vol. 68,
        1946 pp. 124 - 134.

47.   H.A. JOHNSON and M.W. RUBESIN: "Aerodynamic Heating and
        Convective Heat Transfer - Summary of Literature Survey".
        Trans. Am. Soc. Mech. Engrs.   Vol. 71, 1949 pp. 447 - 456.

48.   J.E. JOHNSON and R.J. MONAGHAN: "Measurements of Heat Transfer
        and Skin Friction at Supersonic Speeds".   R.A.E. Tech. Note
        1994, 1949.

49.   V. JOUKOWSKY: "On the Measurement of the Temperature of
        Gases Flowing at very High Speeds".   Tech. Physics of the
        U.S.S.R.   Vol. 5, 1938 pp. 968 - 994.

50.   T. VON KARMAN: "Analogy between Fluid Friction and Heat
        Transfer".   Trans. Am. Soc. Mech. Engrs.   Vol. 61, 1939
        pp. 705 - 710.

51.   T. VON KARMAN and H.S. TSIEN: "Boundary Layer in Compressible
        Fluids".   Journal of Aeronautical Sciences, Vol. 5, 1938 pp.
        227 - 232.

52.   J. KAYE, J.H. KEENAN, K.K. KLINGENSMITH, J.M. KETCHUM and
        T.Y. TOONG: "Measurements of Recovery Factors and Friction
        Coefficients for Supersonic Flow of Air in a Tube I - Apparatus
        Data and Results based on a simple one-dimensional flow model"
        Trans. Am. Soc. Mech. Engrs.   Vol. 74, 1952 p. A77.

53. J. KAYE, T.Y. TOONG and R.H. SHOULBERG: "Measurement of Recovery Factors etc. II - Results based on a Two-dimensional Model for Entrance Region". Trans. Am. Soc. Mech. Engrs. Vol. 74, 1952 p. A185.

54. J. KAYE, J.H. KEENAN and W.H. McADAMS: "Report of Progress on Measurements of Friction Coefficients, Recovery Factors, and Heat Transfer Coefficients for Supersonic Flow of Air in a Pipe". Heat Transfer and Fluid Mechanics Institute, Berkeley, California, 1949 p. 147.

55. J. KAYE, J.H. KEENAN and R.H. SHOULBERG: "Measurement of Recovery Factors and Friction Coefficients for Supersonic Flow of Air in a Tube". General Discussion on Heat Transfer, London Conference, 1951.

56. J.H. KEENAN: "Thermodynamics". John Wiley & Sons, Inc. 1941.

57. J.H. KEENAN: Contribution to Discussion on paper by Yellot Trans. Am. Soc. Engrs. Vol. 56, 1934 pp. 411 - 430.

58. J.H. KEENAN: "Friction Coefficients for the Compressible Flow of Steam". Trans. Am. Soc. Mech. Engrs. Vol. 61, 1939 p. A11.

59. J.H. KEENAN and F.G. KEYES: "Thermodynamic Properties of Steam" John Wiley & Sons, Inc. 1936.

60. J.H. KEENAN and E.P. NEUMANN: "Measurements of Friction in a Pipe for Subsonic and Supersonic Flow of Air". Trans. Am. Soc. Mech. Engrs. Vol. 68, 1946 p. A91.

61. LORD KELVIN: Proc. Royal Soc. of Edinburgh. Vol. 7, 1870 p. 63.

62. F.G. KEYES: "Viscosity and Heat Conductivity of Steam" J. Am. Chem. Soc. Vol. 72, 1950 p. 438.

63. F.G. KEYES and D.J. SANDELL: Trans. Am. Soc. Mech. Engrs. Vol. 72, 1950 p. 767.

64. W. KERR, A.W. SCOTT and M.A. SOROUR: "Determination of the Reversion Point in the Supersonic Supersaturated Expansion of Steam" General Discussion on Heat Transfer, London Conference, 1951.

65. KRAUS: "Braking Temperature Measurements on a Tubular Probe Paralleling the Airflow at Sub and Supersonic Velocities" German Archive 66/170 March, 1945.

66. H.L. LANGHAAR: "Steady Flow in the Transition Length of a Straight Tube". Trans. Am. Soc. Mech. Engrs. Vol. 64, 1942 p. A55.

67. H. LATZKO: Zeitschr. f Angew. Math. u. Mech. Vol. 1, 1921 p. 268.

68. E.F. LEIB: Combustion. Vol. 12, 1940 p. 45.

69. V.L. LELCHUCK: "Heat Transfer and Hydraulic Flow Resistance for Streams of High Velocity". J. of Tech. Physics of U.S.S.R. Vol. 9, 1939 pp. 808 - 818. Translation in N.A.C.A. Tech. Memo 1054, 1943.

70. H.M. MARTIN: Engineering 1918 pp. 53, 161, 189, 245.

71. J.C. MAXWELL: "Collected Works". Vol. II Cambridge 1890 p. 1.

72. W.H. McADAMS: "Heat Transmission". McGraw-Hill 2nd Ed. 1942.

73. W.H. McADAMS, W.E. KENNEL and J.N. ADDOMS: "Heat Transfer to Superheated Steam at High Pressures". Trans. Am. Soc. Mech. Engrs. Vol. 72, 1950 pp. 421 - 428.

74. W.H. McADAMS, L.A. NICOLAI, and J.H. KEENAN: "Measurements of Recovery Factors and Coefficients of Heat Transfer in a Tube for Subsonic Flow of Air". Trans. Am. Inst. of Chem. Engrs. Vol. 42, 1946 p. 907.

75. A.L. MELLANBY and W. KERR: "Pressure Flow Experiments on Steam Nozzles". Inst. of Engrs. and Shipbuilders in Scotland, 1921.

76. T. MIZUSHINA: "Analogy between Fluid Friction and Heat Transfer in Annuli". General Discussion on Heat Transfer, London, 1951 p. 191.

77. C.C. MONRAD and J.F. PELTON: Trans. Am. Inst. of Chem. Engrs. Vol. 38, 1942 p. 593.

78. F. MULLER: "Uber die Ermittlung des Temperaturverlaufes von Gasen oder Dampfen in einer Lavalduse". Dissertation Oldenbourg, 1919. Also, reference 93 Vol. II p. 1054.

79. J.W. MURDOCK and E.F. FIOCK: "Measurement of Temperatures in High Velocity Steam". Trans. Am. Soc. Mech. Engrs. Vol. 72, 1950 p. 1155.

80. W. NUSSELT: Z. Ver-deut. Ing. Vol. 54, 1910 pp. 1154 - 1158.

81.   E. OWER: "The Measurement of Air Flow".   Chapman & Hall
        Ltd., 1949.

82.   L. PRANDTL: Ergebnisse der aerodynamischen Versuchsanstalt
        Gottingen, Bd. 3, 1927 p. 4.

83.   L. PRANDTL: Z. Physik.   Vol. 29, 1928 p. 487.

84.   E. POHLHAUSEN: Zeitschr. f Angew. Math. u. Mech. Vol. 1,
        1921 p. 115.

85.   O. REYNOLDS: Proc. Manchester Lit. Phil. Soc.   Vol. 8, 1874.

86.   R.R. ROTHFUS, C.C. MONRAD and V.E. SENECHAL: Industrial and
        Engineering Chemistry.   Vol. 42, 1950 p. 2511.

87.   M.W. RUBESIN and H.A. JOHNSON: "A Review of Skin Friction
        and Heat Transfer Solutions of the Laminar Boundary Layer of
        a Flat Plate".   Trans. Am. Soc. Mech. Engrs.   Vol. 71, 1949
        pp. 383 - 388.

88.   F.L. RUBIN: "The Prandtl Number for Steam".   Chem. Engr.
        Progress.   Vol. 57. No. 10, 1951 p. 541.

89.   O.A. SAUNDERS and P.H. CALDER: "Heat Transfer in a Nozzle at
        Supersonic Speeds".   Proc. B. Inst. Mech. Engrs.   Vol. 1B
        No. 6, 1952.

90.   M. SCHIROKOW: "The Influence of the Laminar Boundary Layer on
        Heat Transfer at High Velocities".   Tech. Physics of U.S.S.R.
        Vol. 3, 1936 pp. 1020 - 1027.

91.   E.N. SIEDER and G.E. TATE: Ind. Eng. Chem. Vol. 28, 1936
        p. 1429.

92.   M.A. SOROUR: "Investigations on Supersaturation in Nozzle
        Flow".   Ph.D. Thesis.   University of Glasgow, 1950.

93.   STODOLA-LOWENSTEIN: "Steam and Gas Turbines".   McGraw-Hill,
        1927.

94.   G.I. TAYLOR: Brit. Adv. Comm. Aeronaut. R. & M. 272, 1916
        pp. 423 - 429.

95.   TUCKER and MASLEM: "Turbulent Boundary Layer Temperature
        Recovery Factor in Two-dimensional Supersonic Flow".
        N.A.C.A. Tech. Note 2296, 1951.

96.   J.H. WIEGAND: Trans. Am. Inst. Chem. Engrs.   Vol. 41, 1945
        p. 147.

APPENDIX.

Table 1a - Calculated values of Recovery Factor - Results of Part II

Test	Nozzle Section.									
	a	b	Throat	c	d	e	f	g	h	j
PA1	.863	.902	.921	.933	.937	.938	.937	.935	.922	.867
PA2	.913	.927	.944	.944	.944	.941	.936	.931	.914	.856
PA3	.916	.921	.941	.945	.943	.939	.936	.930	.918	.857
PA4	.840	.890	.921	.926	.928	.926	.923	.918	.909	.862
PA5	.882	.904	.932	-	-	-	-	-	-	-
PA6	.870	.898	.919	-	-	-	-	-	-	-
PB1	.887	.926	.937	.940	.943	.943	.940	.898	.848	.722
PB2	.876	.921	.940	.942	.942	.940	.936	.886	.820	.716
PB3	.920	.926	.947	.950	.951	.951	.939	.885	.832	.710
PB4	.855	.877	.934	.936	.933	.927	.915	.887	.810	.708
PC1	.861	.931	.955	.952	.947	.916	.855	.718	.701	.730
PD1	.926	.938	.941	.944	.944	.942	.938	.933	.926	.913
PD2	.937	.944	.946	.951	.948	.944	.940	.935	.928	.915
PD3	.900	.926	.930	.943	.941	.937	.932	.926	.920	.908
PD4	.936	.942	.944	.939	.932	.930	-	-	-	-
PD5	.928	.931	.928	-	-	-	-	-	-	-
PD6	.915	.931	.916	-	-	-	-	-	-	-

Table 2a - Calculated values of Recovery Factor, Diameter Reynolds number and Length Reynolds number - Results of Part III.

Test Section	RA1			RA2			RA3		
	r	Re_d	Re_l	r	Re_d	Re_l	r	Re_d	Re_l
a	.969	1.028	2.281	.932	1.213	2.69	.922	1.259	2.793
b	.959	1.032	4.58	.912	1.226	5.435	.903	1.267	5.62
c	.929	1.038	6.91	.894	1.23	8.179	.89	1.272	8.46
d	.914	1.041	9.24	.886	1.238	10.97	.884	1.277	11.32
e	.914	1.05	11.64	.876	1.242	13.76	.876	1.285	14.25
f	.91	1.057	14.07	.872	1.251	16.63	.869	1.294	17.21
g	.907	1.06	16.46	.865	1.26	19.54	.863	1.299	20.15
h	.907	1.07	18.99	.863	1.268	22.48	.861	1.308	23.2
j	.904	1.08	21.56	.864	1.281	25.55	.854	1.322	26.37
k	.903	1.098	24.35	.865	1.299	28.79	.850	1.345	29.83
l	.901	1.12	27.3	.862	1.337	32.57	.850	1.375	33.52

Test Section	RA4			RA5			RA6		
	r	Re_d	Re_l	r	Re_d	Re_l	r	Re_d	Re_l
a	.874	1.298	2.879	.872	1.322	2.93	.863	1.349	2.99
b	.852	1.307	5.79	.844	1.327	5.88	.843	1.349	5.98
c	.838	1.312	8.73	.833	1.331	8.85	.825	1.353	9.0
d	.825	1.317	11.68	.824	1.34	11.89	.817	1.364	12.09
e	.822	1.326	14.69	.819	1.35	14.97	.813	1.374	15.21
f	.818	1.335	17.76	.814	1.36	18.1	.812	1.384	18.4
g	.817	1.344	20.86	.81	1.37	21.25	.807	1.394	21.63
h	.820	1.354	24.04	.809	1.38	24.47	.8	1.404	24.9
j	.817	1.369	27.34	.808	1.395	27.85	.794	1.420	28.32
k	.813	1.389	30.85	.807	1.411	31.3	.787	1.437	31.84
l	.799	1.411	34.4	.802	1.438	35.08	.786	1.471	35.82

Table 2a (Contd.)

	RB1			RB2			RB3		
	r	Re_d	Re_l	r	Re_d	Re_l	r	Re_d	Re_l
a	.973	1.078	2.39	.930	1.27	2.815	.945	1.33	2.945
b	.953	1.089	4.83	.916	1.28	5.68	.913	1.335	5.91
c	.938	1.094	7.28	.90	1.284	8.54	.898	1.342	8.915
d	.926	1.1	9.76	.887	1.288	11.43	.882	1.347	11.92
e	.914	1.107	12.27	.88	1.296	14.37	.879	1.362	15.08
f	.903	1.113	14.80	.87	1.303	17.35	.874	1.367	18.17
g	.898	1.118	17.36	.867	1.312	20.36	.864	1.372	21.25
h	.898	1.127	19.99	.865	1.323	23.48	.860	1.379	24.45
j	.896	1.137	22.68	.868	1.337	26.67	.864	1.397	27.85
k	.891	1.153	25.55	.873	1.352	30.00	.867	1.41	31.24
l	.887	1.176	28.65	.872	1.383	33.75	.869	1.438	35.00

	RB4			RB5			RC1		
	r	Re_d	Re_l	r	Re_d	Re_l	r	Re_d	Re_l
a	.916	1.464	3.247	.889	1.596	3.54	.917	1.665	3.69
b	.893	1.473	6.53	.857	1.612	7.15	.897	1.675	7.43
c	.877	1.483	9.86	.839	1.618	10.76	.876	1.68	11.18
d	.866	1.492	13.17	.827	1.623	14.41	.866	1.684	14.94
e	.855	1.498	16.6	.824	1.635	18.13	.857	1.695	18.79
f	.845	1.507	20.05	.822	1.646	21.92	.849	1.706	22.68
g	.838	1.517	23.55	.822	1.658	25.74	.845	1.717	26.64
h	.833	1.527	27.07	.814	1.670	29.63	.849	1.732	30.74
j	.832	1.542	30.77	.806	1.68	33.56	.850	1.749	34.9
k	.834	1.563	34.47	.803	1.712	37.95	.847	1.778	39.4
l	.842	1.597	38.92	.817	1.743	42.55	.849	1.812	44.15

Table 2a (Contd.)

	RD1			RE1			RF1		
	r	Re_d	Re_1	r	Re_d	Re_1	r	Re_d	Re_1
a	.887	2.008	4.456	.973	.972	2.157	.972	.872	1.932
b	.852	2.025	8.985	.961	.978	4.34	.955	.872	3.865
c	.834	2.033	13.52	.949	.983	6.55	.94	.874	5.81
d	.822	2.045	18.14	.939	.987	8.76	.925	.874	7.75
e	.815	2.057	22.82	.928	.989	10.97	.913	.877	9.715
f	.81	2.07	27.55	.921	.993	13.21	.902	.879	11.68
g	.809	2.09	32.45	.912	.998	15.49	.892	.882	13.68
h	.81	2.11	37.46	.908	1.004	17.83	.886	.884	15.68
j	.812	2.136	42.65	.903	1.011	20.17	.882	.887	17.69
k	.817	2.163	48.00	.897	1.013	22.48	.878	.889	19.72
l	.822	2.208	53.9	.893	1.023	24.96	.873	.895	21.8

	RF2			RG1			RH1		
	r	Re_d	Re_1	r	Re_d	Re_1	r	Re_d	Re_1
a	.977	.8875	1.967	.938	1.287	2.853	.978	1.236	2.743
b	.955	.89	3.945	.911	1.295	5.74	.934	1.236	5.485
c	.945	.8925	5.93	.896	1.299	8.635	.899	1.236	8.225
d	.917	.895	7.935	.889	1.303	11.54	.883	1.236	10.97
e	.904	.895	9.915	.883	1.311	14.53	.867	1.24	13.75
f	.90	.898	11.93	.878	1.316	17.49	.856	1.24	16.52
g	.895	.90	13.96	.872	1.319	20.47	.847	1.244	19.32
h	.891	.903	16.01	.867	1.328	23.53	.84	1.247	22.15
j	.887	.903	18.0	.868	1.336	26.64	.838	1.251	25.00
k	.884	.908	20.12	.868	1.344	29.78	.834	1.255	28.74
l	.884	.914	22.25	.868	1.357	33.07	.833	1.259	31.7

Table 2a (Contd.)

	RD1			RE1			RF1		
	r	Re_d	Re_l	r	Re_d	Re_l	r	Re_d	Re_l
a	.887	2.008	4.456	.973	.972	2.157	.972	.872	1.932
b	.852	2.025	8.985	.961	.978	4.34	.955	.872	3.865
c	.834	2.033	13.52	.949	.983	6.55	.94	.874	5.81
d	.822	2.045	18.14	.939	.987	8.76	.925	.874	7.75
e	.815	2.057	22.82	.928	.989	10.97	.913	.877	9.715
f	.81	2.07	27.55	.921	.993	13.21	.902	.879	11.68
g	.809	2.09	32.45	.912	.998	15.49	.892	.882	13.68
h	.81	2.11	37.46	.908	1.004	17.83	.886	.884	15.68
j	.812	2.136	42.65	.903	1.011	20.17	.882	.887	17.69
k	.817	2.163	48.00	.897	1.013	22.48	.878	.889	19.72
l	.822	2.208	53.9	.893	1.023	24.96	.873	.895	21.8

	RF2			RG1			RH1		
	r	Re_d	Re_l	r	Re_d	Re_l	r	Re_d	Re_l
a	.977	.8875	1.967	.938	1.287	2.853	.978	1.236	2.743
b	.955	.89	3.945	.911	1.295	5.74	.934	1.236	5.485
c	.945	.8925	5.93	.896	1.299	8.635	.899	1.236	8.225
d	.917	.895	7.935	.889	1.303	11.54	.883	1.236	10.97
e	.904	.895	9.915	.883	1.311	14.53	.867	1.24	13.75
f	.90	.898	11.93	.878	1.316	17.49	.856	1.24	16.52
g	.895	.90	13.96	.872	1.319	20.47	.847	1.244	19.32
h	.891	.903	16.01	.867	1.328	23.53	.84	1.247	22.15
j	.887	.903	18.0	.868	1.336	26.64	.838	1.251	25.00
k	.884	.908	20.12	.868	1.344	29.78	.834	1.255	28.74
l	.884	.914	22.25	.868	1.357	33.07	.833	1.259	31.7

Table 3a. Values of Recovery Factor and Ratio of Stream Temperature to Saturation Temperature – Results of Part III.

Test	$Re_1 = 5 \times 10^5$		$Re_1 = 10 \times 10^5$		$Re_1 = 15 \times 10^5$		$Re_1 = 20 \times 10^5$	
	r	T_s/T_{sat}	r	T_s/T_{sat}	r	T_s/T_{sat}	r	T_s/T_{sat}
RA1	.945	1.14	.92	1.133	.91	1.127	.906	1.121
RA2	.913	1.038	.887	1.034	.872	1.03	.867	1.026
RA3	.907	1.019	.885	1.016	.872	1.013	.865	1.01
RA4	.857	.993	.833	.99	.82	.987	.817	.981
RA5	.853	.978	.829	.973	.818	.969	.81	.965
RA6	.846	.962	.822	.962	.812	.958	.81	.953
RB1	.953	1.258	.923	1.252	.904	1.249	.898	1.246
RB2	.919	1.127	.893	1.126	.874	1.124	.864	1.12
RB3	.924	1.106	.892	1.103	.875	1.1	.865	1.097
RB4	.903	1.049	.876	1.046	.86	1.044	.845	1.042
RB5	.877	.99	.844	.989	.826	.988	.82	.987
RC1	.908	1.068	.881	1.069	.856	1.068	.853	1.067
RD1	.889	1.037	.855	1.037	.838	1.036	.828	1.033
RE1	.955	1.157	.933	1.156	.913	1.154	.899	1.149
RF1	.945	1.192	.909	1.191	.888	1.19	.875	1.185
RF2	.94	1.17	.907	1.168	.891	1.166	.885	1.163
RG1	.916	1.102	.891	1.1	.882	1.099	.873	1.098
RH1	.938	1.082	.888	1.083	.859	1.085	.843	1.086
RAO	.98	1.427	.93	1.418	.92	1.405	.92	1.375
RBO	.981	1.416	.941	1.413	.921	1.405	.913	1.397

Table 3a (Contd.)

Test	$Re_1 = 25 \times 10^5$		$Re_1 = 30 \times 30^5$		$Re_1 = 35 \times 10^5$		$Re_1 = 40 \times 10^5$	
	r	T_s/T_{sat}	r	T_s/T_{sat}	r	T_s/T_{sat}	r	T_s/T_{sat}
RA1	.903	1.112	-	-	-	-	-	-
RA2	.865	1.022	.864	1.01	-	-	-	-
RA3	.857	1.007	.85	.994	-	-	-	-
RA4	.82	.976	.815	.97	-	-	-	-
RA5	.809	.961	.807	.953	.805	.944	-	-
RA6	.801	.948	.794	.942	.786	.935	-	-
RB1	.894	1.235	-	-	-	-	-	-
RB2	.866	1.115	.873	1.105	-	-	-	-
RB3	.861	1.093	.864	1.09	.869	1.076	-	-
RB4	.833	1.039	.831	1.033	.836	1.026	-	-
RB5	.822	.983	.814	.98	.803	.977	.808	.967
RC1	.849	1.064	.849	1.06	.849	1.055	.848	1.048
RD1	.823	1.030	.82	1.027	.819	1.024	.82	1.02
RE1	.894	1.144	-	-	-	-	-	-
RF1	-	-	-	-	-	-	-	-
RF2	-	-	-	-	-	-	-	-
RG1	.867	1.094	.867	1.09	.867	1.086	-	-
RH1	.838	1.085	.834	1.083	-	-	-	-
RA0	-	-	-	-	-	-	-	-
RB0	.910	1.363	-	-	-	-	-	-

Table 4a. Values of Heat Transfer Coefficient, Stanton Number, Length and Diameter Reynolds Numbers:- Results of Part IV.

Section	Test HA1				Test HA2			
	h BTU/hr ft² °F	$St \times 10^2$	$Re_d \times 10^{-5}$	$Re_1 \times 10^{-5}$	h BTU/hr ft² °F	$St \times 10^2$	$Re_d \times 10^{-5}$	$Re_1 \times 10^{-5}$
a	92.8	.0927	.885	1.963	111	.108	1.019	2.26
b	99	.0989	.89	3.947	116	.113	1.028	4.53
c	120.5	.1214	.892	5.94	164	.159	1.033	6.885
d	153	.154	.895	7.935	204	.198	1.038	9.21
e	190	.193	.899	9.97	234	.227	1.044	11.57
f	203	.207	.905	12.03	235	.231	1.047	13.93
g	198	.202	.91	14.11	234	.229	1.053	16.36
h	197	.200	.92	16.31	228	.224	1.063	18.87
j	193	.196	.93	18.57	230	.228	1.073	21.42
k	189	.192	.94	20.84	221	.219	1.089	24.16
l	186	.189	.959	23.38	162	.161	1.107	27

Section	Test HA3				Test HA4			
	h BTU/hr ft² °F	$St \times 10^2$	$Re_d \times 10^{-5}$	$Re_1 \times 10^{-5}$	h BTU/hr ft² °F	$St \times 10^2$	$Re_d \times 10^{-5}$	$Re_1 \times 10^{-5}$
a	88.3	.084	1.118	2.48	114	.1043	1.213	2.69
b	99.5	.0945	1.126	4.99	142.3	.1302	1.221	5.415
c	138	.131	1.128	7.51	198	.1814	1.229	8.175
d	174	.165	1.136	10.07	276	.2525	1.237	10.98
e	204	.196	1.14	12.63	256	.234	1.242	13.77
f	211	.202	1.147	15.25	247	.228	1.25	16.63
g	211	.202	1.155	17.91	234	.216	1.258	19.53
h	198	.192	1.165	20.68	234	.219	1.267	22.47
j	190	.184	1.177	23.5	226	.211	1.28	25.55
k	195	.191	1.192	26.45	221	.209	1.297	28.8
l	192	.188	1.218	29.7	219	.207	1.326	32.35

Table 4a (Contd.)

Section	Test HA5				Test HA6			
	h BTU/hr ft²°F	St x 10²	Re_d x10⁻⁵	Re_l x 10⁻⁵	h BTU/hr ft²°F	St x 10²	Re_d x 10⁻⁵	Re_l x 10⁻⁵
a	72	.066	1.213	2.69	73.5	.0674	1.213	2.69
b	988	.907	1.221	5.415	90	.0825	1.221	5.415
c	-757	-.694	1.229	8.175	110	.1007	1.229	8.175
d	-319	-.292	1.237	10.98	218	.1996	1.237	10.98
e	-395	-.35	1.242	13.77	177	.162	1.242	13.77
f	-766	-.71	1.25	16.63	209	.193	1.25	16.63
g	-575	-.53	1.258	19.53	184	.170	1.258	19.53
h	1026	.96	1.267	22.47	196	.183	1.267	22.47
j	681	.64	1.28	25.55	193	.180	1.28	25.55
k	1214	1.15	1.297	28.8	183	.173	1.297	28.8
l	1778	1.68	1.326	32.35	175	.165	1.326	32.35

Section	Test HB1				Test HB2			
	h BTU/hr ft²°F	St x 10²	Re_d x10⁻⁵	Re_l x 10⁻⁵	h BTU/hr ft²°F	St x10²	Re_d x 10⁻⁵	Re_l x10⁻⁵
a	122	.101	.937	2.076	129.5	.0978	1.183	2.625
b	116	.096	.943	4.18	150.5	.1133	1.188	5.265
c	133	.1103	.945	6.3	205	.156	1.19	7.91
d	160	.133	.95	8.43	261	.199	1.193	10.59
e	174	.144	.954	10.57	273	.208	1.2	13.3
f	205	.170	.959	12.76	274	.2085	1.207	16.06
g	200	.166	.965	15.0	-	-	-	-
h	197	.163	.973	17.27	-	-	-	-
j	194	.161	.983	19.63	-	-	-	-
k	187	.155	.997	22.1	-	-	-	-
l	173	.145	1.017	24.8	-	-	-	-

Table 4a (Contd.)

Section	Test HB3				Test HB4			
	h BTU/hr ft² °F	$St \times 10^2$	$Re_d \times 10^5$	$Re_l \times 10^5$	h BTU/hr ft² °F	$St \times 10^2$	$Re_d \times 10^5$	$Re_l \times 10^5$
a	120	.093	1.183	2.625	46	.033	1.321	2.925
b	142	.111	1.188	5.265	151	.1095	1.328	5.88
c	193	.144	1.19	7.91	212	.154	1.337	8.89
d	259	.194	1.193	10.59	248	.180	1.34	11.89
e	262	.1966	1.2	13.3	261	.1896	1.348	14.94
f	263	.197	1.207	16.06	259	.188	1.356	18.04
g	256	.192	1.217	18.9	263	.191	1.364	21.16
h	247	.185	1.227	21.79	258	.189	1.372	24.35
j	245	.185	1.242	24.8	248	.184	1.389	27.73
k	235	.1775	1.256	27.85	230	.171	1.41	31.26
l	223	.170	1.286	31.35	221	.166	1.441	35.15

Section	Test HB5				Test HB6			
	h BTU/hr ft² °F	$St \times 10^2$	$Re_d \times 10^5$	$Re_l \times 10^5$	h BTU/hr ft² °F	$St \times 10^2$	$Re_d \times 10^5$	$Re_l \times 10^5$
a	164.6	.115	1.52	3.37	229	.160	1.52	3.37
b	180.8	.1256	1.529	6.78	408	.285	1.529	6.78
c	282.5	.1972	1.534	10.21	1976	1.377	1.534	10.21
d	326	.230	1.539	13.66	2000	1.396	1.539	13.66
e	324.4	.229	1.55	17.19	1530	1.08	1.55	17.19
f	309.3	.220	1.56	20.76	1090	.778	1.56	20.76
g	326	.232	1.57	24.4	768	.548	1.57	24.4
h	304	.216	1.58	28.05	700	.5	1.58	28.05
j	320	.228	1.602	31.99	770	.55	1.602	31.99
k	322	.229	1.623	36	395	.285	1.623	36
l	287	.207	1.663	40.6	638	.46	1.663	40.6

Table 4a (Contd.)

Section	Test HB7 h BTU/hr.ft.°F	$St \times 10^2$	$Re_d \times 10^{-5}$	$Re_1 \times 10^{-5}$	Test HC1 h BTU/hr.ft.°F	$St \times 10^2$	$Re_d \times 10^{-5}$	$Re_1 \times 10^{-5}$
a	75	.0524	1.52	3.37	148	.0896	1.483	3.287
b	109	.076	1.529	6.78	185	.112	1.491	6.61
c	180	.1255	1.534	10.21	276	.169	1.499	9.97
d	223	.157	1.539	13.66	319	.195	1.512	13.42
e	270	.190	1.55	17.19	370	.226	1.516	16.81
f	347	.247	1.56	20.76	333	.206	1.525	20.31
g	317	.226	1.57	24.4	315	.195	1.533	23.8
h	319	.226	1.58	28.05	317	.198	1.547	27.43
j	253	.180	1.602	31.99	306	.191	1.56	31.13
k	268	.193	1.623	36	298	.186	1.588	35.18
l	245	.176	1.663	40.6	274	.171	1.62	39.5

Section	Test HC2 h BTU/hr.ft.°F	$St \times 10^2$	$Re_d \times 10^{-5}$	$Re_1 \times 10^{-5}$	Test HC3 h BTU/hr.ft.°F	$St \times 10^2$	$Re_d \times 10^{-5}$	$Re_1 \times 10^{-5}$
a	146	.0845	1.632	3.622	143	.0805	1.795	3.978
b	189	.109	1.643	7.28	199	.112	1.806	8.0
c	270	.158	1.65	10.98	274	.156	1.818	12.08
d	336	.196	1.662	14.73	310	.176	1.829	16.22
e	322	.189	1.671	18.53	327	.186	1.835	20.34
f	331	.195	1.682	22.37	306	.176	1.847	24.55
g	312	.185	1.692	26.25	296	.17	1.859	28.83
h	308	.184	1.702	30.18	285	.165	1.871	33.15
j	298	.178	1.717	34.27	272	.158	1.889	37.67
k	294	.177	1.743	38.7	265	.155	1.921	42.6
l	282	.170	1.783	43.4	244	.143	1.967	47.9

Table 4a (Contd.)

Section	Test HC4				Test HC5			
	h B.T.U/hr.ft.°F	$St \times 10^2$	$Re_d \times 10^{-5}$	$Re_1 \times 10^{-5}$	h B.T.U/hr.ft.°F	$St \times 10^2$	$Re_d \times 10^{-5}$	$Re_1 \times 10^{-5}$
a	209	.118	1.795	3.978	110	.062	1.795	3.978
b	505	.284	1.806	8.0	147	.083	1.806	8.0
c	1647	.937	1.818	12.08	400	.227	1.818	12.08
d	3360	1.910	1.829	16.22	739	.42	1.829	16.22
e	2250	1.28	1.835	20.34	1111	.631	1.835	20.34
f	934	.537	1.847	24.55	1295	.744	1.847	24.55
g	724	.418	1.859	28.83	980	.564	1.859	28.83
h	851	.495	1.871	33.15	958	.556	1.871	33.15
j	658	.382	1.889	37.67	1088	.63	1.889	37.67
k	409	.239	1.921	42.6	2100	1.232	1.921	42.6
l	147	.087	1.967	47.9	640	.376	1.967	47.9

Section	Test HD1				Test HD2			
	h B.T.U/hr.ft.°F	$St \times 10^2$	$Re_d \times 10^{-5}$	$Re_1 \times 10^{-5}$	h B.T.U/hr.ft.°F	$St \times 10^2$	$Re_d \times 10^{-5}$	$Re_1 \times 10^{-5}$
a	187	.087	2.093	4.64	296	.1374	2.093	4.64
b	272	.1263	2.114	9.37	403	.187	2.114	9.37
c	403	.187	2.12	14.1	558	.259	2.12	14.1
d	419	.1965	2.133	18.93	614	.288	2.133	18.93
e	391	.183	2.146	23.77	410	.192	2.146	23.77
f	389	.188	2.16	28.73	372	.176	2.16	28.73
g	354	.168	2.175	33.72	304	.144	2.175	33.72
h	348	.1665	2.193	38.93	329	.158	2.193	38.93
j	326	.156	2.215	44.2	241	.115	2.215	44.2
k	309	.149	2.253	49.9	257	.124	2.253	49.9
l	298	.146	2.306	56.15	265	.129	2.306	56.15

Table 4a (Contd.)

Section	Test HD3				Test HJ1			
	h BTU/hr ft² °F	$St \times 10^2$	$Re_d \times 10^5$	$Re_1 \times 10^5$	h BTU/hr ft² F	$St \times 10^2$	$Re_d \times 10^5$	$Re_1 \times 10^{-5}$
a	157	.073	2.093	4.64	155	.0623	2.365	5.25
b	207	.096	2.114	9.37	220	.0884	2.387	10.58
c	393	.182	2.12	14.1	286	.115	2.402	15.97
d	1040	.488	2.133	18.93	313	.1258	2.41	21.38
e	2520	1.18	2.146	23.77	294	.1193	2.424	26.88
f	1740	.824	2.16	28.73	286	.1161	2.448	32.55
g	2550	1.209	2.175	33.72	289	.1173	2.462	38.2
h	3845	1.838	2.193	38.93	273	.1127	2.485	44.1
j	1584	.758	2.215	44.2	256	.105	2.508	50.1
k	2835	1.37	2.253	49.9	255	.1056	2.556	56.7
l	840	.41	2.306	56.15	224	.0937	2.625	64.1

Table 5a. Values of $Y = St. \, Pr^{2/3} \dfrac{1}{1 + 2.5 \frac{D}{x}}$ and $Y^1 = St. \, Pr^{2/3} \left(\dfrac{x}{D}\right)^{1/13}$

and Diameter Reynolds Number.

Section	d			e			f		
x/De	8.868			11.085			13.302		
	Y	Y^1	$Re_d \times 10^{-5}$	Y	Y^1	$Re_d \times 10^{-5}$	Y	Y^1	$Re_d \times 10^{-5}$
HA1	.120	.182	.895	.158	.232	.899	.174	.252	.905
HA2	.155	.235	1.038	.185	.273	1.044	.194	.282	1.047
HA3	.129	.195	1.136	.160	.236	1.14	.170	.247	1.147
HA4	.197	.299	1.237	.191	.281	1.242	.192	.278	1.25
HA6	.156	.236	1.237	.132	.195	1.242	.163	.235	1.25
HB1	.104	.157	.95	.1175	.173	.954	.143	.207	.959
HB2	.155	.235	1.193	.170	.250	1.2	.1755	.254	1.207
HB3	.151	.226	1.193	.159	.232	1.2	.164	.236	1.207
HB4	.140	.213	1.34	.155	.228	1.348	.158	.229	1.356
HB5	.179	.272	1.539	.187	.276	1.55	.185	.268	1.56
HB7	.123	.186	1.539	.155	.229	1.55	.208	.301	1.56
HC1	.152	.231	1.512	.185	.272	1.516	.173	.251	1.525
HC2	.153	.232	1.662	.154	.227	1.671	.164	.238	1.682
HC3	.137	.208	1.829	.152	.224	1.835	.148	.215	1.847
HD1	.153	.232	2.133	.149	.220	2.146	.158	.229	2.16
HD2	.225	.340	2.133	.157	.231	2.146	.148	.215	2.16
HJ1	.098	.149	2.41	.0975	.144	2.424	.098	.142	2.448

Table 5a (Contd.)

Section	g			h			j		
x/Do	15.519			17.736			19.953		
	γ	γ^1	$Re_d \times 10^{-5}$	γ	γ^1	$Re_d \times 10^{-5}$	γ	γ^1	$Re_d \times 10^{-5}$
HA1	.174	.249	.91	.175	.249	.92	.174	.247	.93
HA2	.197	.283	1.053	.196	.279	1.063	.203	.287	1.073
HA3	.174	.249	1.155	.168	.240	1.167	.164	.232	1.177
HA4	.186	.267	1.258	.192	.273	1.267	.188	.266	1.28
HA6	.146	.210	1.258	.160	.228	1.267	.160	.227	1.28
HB1	.143	.205	.965	.143	.203	.973	.143	.203	.983
HB2	-	-	-	-	-	-	-	-	-
HB3	.163	.232	1.217	.160	.226	1.227	.162	.228	1.242
HB4	.164	.236	1.364	.166	.236	1.372	.164	.232	1.389
HB5	.20	.286	1.57	.184	.261	1.58	.203	.287	1.602
HB7	.195	.279	1.57	.198	.282	1.58	.160	.227	1.602
HC1	.168	.241	1.533	.173	.247	1.547	.170	.241	1.56
HC2	.159	.228	1.692	.161	.229	1.702	.158	.224	1.717
HC3	.146	.210	1.859	.145	.206	1.871	.141	.199	1.889
HD1	.145	.207	2.175	.146	.208	2.193	.139	.196	2.215
HD2	.124	.178	2.175	.139	.197	2.193	.102	.145	2.215
HJ1	.101	.145	2.462	.099	.141	2.485	.093	.132	2.508

Table 5a (Contd.)

Section	k			l		
x/De	22.17			24.387		
	Y	Y'	$Re_d \times 10^{-5}$	Y	Y'	$Re_d \times 10^{-5}$
HA1	.172	.244	.94	.170	.241	.94
HA2	.197	.278	1.089	.146	.206	1.107
HA3	.172	.242	1.192	.171	.240	1.218
HA4	.188	.265	1.297	.188	.264	1.326
HA6	.155	.219	1.297	.150	.211	1.326
HB1	.139	.197	.997	.132	.185	1.017
HB3	.142	.200	1.256	.136	.192	1.286
HB4	.154	.217	1.41	.151	.212	1.441
HB5	.206	.290	1.623	.188	.264	1.663
HB7	.173	.245	1.623	.160	.225	1.663
HC1	.167	.236	1.588	.155	.219	1.62
HC2	.159	.225	1.743	.154	.217	1.783
HC3	.139	.197	1.921	.130	.183	1.967
HD1	.134	.189	2.253	.133	.187	2.306
HD2	.111	.157	2.253	.117	.165	2.306
HJ1	.095	.134	2.556	.085	.120	2.625

Table 6a.   Values of Friction Factors - $f \times 10^2$.

Section	HA1	HA2	HA3	HA4,5,6	HB1	HB2,3	HB4
a - b	.621	.620	.613	.707	.612	.682	.546
b - c	.601	.519	.465	.456	.488	.494	.445
c - d	.553	.551	.58	.574	.553	.537	.492
d - e	.482	.521	.511	.426	.493	.471	.466
e - f	.412	.466	.461	.445	.432	.46	.38
f - g	.446	.453	.435	.452	.436	.406	.395
g - h	.479	.486	.443	.476	.447	.378	.398
h - j	.476	.498	.517	.499	.432	.451	.367
j - k	.429	.470	.456	.458	.458	.449	.378
k - l	.347	.375	.347	.344	.392	.367	.296

Section	HB5,6,7	HC1	HC2	HC3,4,5	HD1,2,3	HJ1
a - b	.596	.643	.671	.72	.645	.671
b - c	.468	.498	.482	.524	.502	.515
c - d	.582	.511	.545	.567	.496	.508
d - e	.519	.525	.521	.475	.536	.473
e - f	.421	.497	.441	.403	.462	.508
f - g	.437	.398	.398	.425	.387	.369
g - h	.418	.401	.422	.476	.411	.381
h - j	.418	.431	.416	.445	.421	.415
j - k	.45	.471	.449	.435	.429	.439
k - l	.373	.368	.359	.345	.334	.318

<u>SYNOPSIS</u>

1. <u>Introduction</u>

The aim and the nature of the work stated. The present day crisis of the individual. The need for the existential decision for God. The failure of the "conceptualist" theological thinking to offer adequate categories for the formulation of the theology to a man in existential crisis. The search for the personalistic thinking, in theology, which is also the quest for the Christian Doctrine of the Holy Spirit.

<u>PART I.</u>

2. <u>The New Testament Doctrine of the Holy Spirit</u>

(a) The teaching of the Synoptics concerning the problem Jesus and the Holy Spirit. The understanding of the person of Jesus The Christ. The unique possession of the Holy Spirit by Jesus. This reveals that his human existence veils within itself the Incarnate Word of God, with whom the Father through the Holy Spirit reveals the one-ness of Being. This is not <u>the Incarnation of the Holy Spirit in Jesus</u>, but the revelation of the Word in Jesus by the Holy Spirit, who also reveals Jesus to Himself as the Christ.

(b) The teaching of the IVth Evangelist concerning the Comforter. The Johannine contribution towards the understanding of the relationship of Jesus the Christ and the Holy Spirit. This in turn reveals the nature and character of God which implicitly destroys the Jewish Unitarian conception of Him.

(c) The teaching of the Acts of the Apostles, the Pauline Epistles and the other New Testament writings concerning the Holy Spirit. The Revelation of the Holy Spirit as the present Reality in the Church according to the Promise of Christ. The revelation of Christ through and in the Holy Spirit as the Lord (Kyrios) who is and who is still to come. (The words Maranatha spoken in the Church reveal that Christ is present in the Holy Spirit in the Church. Other aspects of the Doctrine of the Holy Spirit expounded.

The/

The data of the New Testament doctrine of the Holy Spirit present themselves as the quest for the understanding of the Christian Doctrine of God and serve as the Prolegomena of this Doctrine.

PART II.

The Christian Doctrine of God.

Chapter One.

The problem stated. The Birth of Christianity inside Judaism. The parting of the ways between Jewish Unitarianism and Christian Triniterianism. Two different conceptions of Monotheism.

(a) The development of the Christian Doctrine of God from the New Testament period onwards until the IVth century. Tertullian and Origen. St. Athanasius and the Cappadocian Fathers.

(b) A re-statement of the Christian Doctrine of God in terms of Analogia amoris.

Chapter Two.

The justification of the Christian Doctrine of God on the basis of the structure of personality. Personality, Divine and Human.

Chapter Three.

The Doctrine of Filioque. A conceptualistic theological thinking engenders this Doctrine while a personalistic (existential) theological thinking denies the Doctrine of Filioque.

PART III.

Eastern Orthodox, Roman Catholic and Reformed teaching concerning the Holy Spirit.

(a) The Concept of Sobornost in E. Orthodoxy.
(b) The Concept of the Juridical Mission of Christ in Roman Catholicism.
(c) The concept of the Scripture as the sole norm of the Church, its faith and life in the Reformer Church.

APPENDIX A.

The old Testament ideas concerning the Spirit of
God.   The problem stated in relation to the creation,
moral order and history which is the stage of God's
action in the world.

APPENDIX B.

Some theological, historical sketches of the
German theology in connection with the problems raised
in the theology of Rudolf Bultmann.